

**Integrated Solid Phase, Aqueous Phase and Numerical Investigation of Plume
Geochemistry at an Oil Sand Mining Facility**

by

Alexander Avraham Louis Oiffer

A thesis
presented to the University of Waterloo
in fulfillment of the
thesis requirement for the degree of
Master of Science
in
Earth Sciences

Waterloo, Ontario, Canada, 2006
© Alexander Avraham Louis Oiffer 2006

AUTHOR'S DECLARATION FOR ELECTRONIC SUBMISSION OF A THESIS

I hereby declare that I am the sole author of this thesis. This is a true copy of the revisions, as accepted by my examiners.

I understand that my thesis may be made electronically available to the public

ABSTRACT

A plume of process-affected groundwater was identified in a shallow sand aquifer adjacent to a tailings impoundment at Syncrude Canada Ltd. Quantitative and qualitative Naphthenic Acid (NA) analyses were performed on groundwater samples to investigate NA fate and transport properties in the subsurface. Analysis of dissolved organic and inorganic components was undertaken to identify, quantify and assess the mobility of other dissolved components of environmental significance. NAs at concentrations up to 87 mg L^{-1} were found to represent the major contributor to aquatic toxicity. Attenuation of NAs by biodegradation is not observed based on screening techniques developed to date. Retardation of NAs observed at the field scale, is consistent with weak sorption observed in the laboratory by other authors. Concentrations of NH_4^+ approached 4 mg L^{-1} in the plume, however mobility is limited by cation exchange. Aromatics and trace metals are present in low quantities (i.e. $<10 \text{ } \mu\text{g L}^{-1}$) and are only detected in groundwater immediately adjacent to the toe of the tailings impoundment. Cl and Na are found at concentrations of up to 282 and 579 mg L^{-1} respectively. Dissolved oxygen is typically $< 1 \text{ mg L}^{-1}$ within the plume, while redox indicators Mn(II), Fe(II) and CH_4 are detected between $<0.1 - 2.6$, $0.2 - 3.5$ and $<0.1 - 2.1 \text{ mg L}^{-1}$ respectively within the plume. Solid phase geochemistry, determined through solid phase extractions, was coupled with aqueous geochemistry and reactive transport modeling to identify the dominant geochemical processes occurring within the plume. Based on scenarios evaluated using reactive transport modeling, the most likely origin for the presently observed, weakly reducing conditions in the plume appears to be the presence of a small amount of dissolved, degradable organic carbon. The dominant terminal electron acceptors appear to be Fe(III) and Mn(III/IV) in the plume core and $\text{O}_{2(\text{aq})}$ at the plume fringe. Dissolved Fe and Mn are observed to enter the domain at the upgradient boundary at maximal concentrations of 4.2 and 0.7 mg L^{-1} respectively. Trace metal geochemistry of the aquifer material was also assessed using solid phase extractions. The potential for trace metal release via reductive dissolution of the native geologic material is considered minimal in this case, based on the weakly reducing nature of the plume and a lack of excessive trace metal content in the aquifer material.

ACKNOWLEDGEMENTS

First and foremost, I would like to thank Shannon, for agreeing to leave Alberta for the hot and humid climate of Southern Ontario. Her enduring support and intermittent role as sugar-momma throughout our time in Waterloo is only superseded by her patience with my absenteeism in the final throes of preparing this thesis, while in Ft. McMurray and during my summer in Vancouver. Perhaps for this reason she insisted on having roommates, Jean Jacque and Karlee, whose friendly company was always appreciated. My time at Waterloo was always made immensely more enjoyable by the other grad students in the department. However, I hesitate to specifically mention each of the grad students who I've had the pleasure to meet over course of my studies, due to the fear of forgetting someone. Rest assured that I will always look back with enjoyment regarding my time in Waterloo.

The work of Francoise Gervais regarding Naphthenic Acids in groundwater formed the basis for my work. For this reason I am grateful to her, for this contribution to my thesis. I would like to thank my supervisors, Drs. Jim Barker and Uli Mayer and committee members, Drs. Carol Ptacek and Dave Rudolph for their direction and insights into my thesis despite their often hectic schedules. Specifically, I would like to thank Jim for allowing me the flexibility to pursue my own hypotheses throughout the project. A big thank you must be given to Shirley Chatten and Marianne vanderGriendt, who were always available to answer my questions and who analyzed numerous groundwater and soil samples, without which this thesis would not be possible. From Syncrude, those who have helped and added considerably to this project through advice, field support, analytical support and providing historical information have included: Barry Esford, Grey Kampala, Karen Chovan, Mike MacKinnon, Steve Carroll, Lori Cyprien and Gord Flasha. As well, the Syncrude Research Department in Edmonton, Alberta provided numerous groundwater analyses for the project. Field work was always made more interesting and easier by the willing hands of Naoki Yasuda and bug jacket clad Lindsay Oiffer. Although this may be construed as an oxymoron, I would also like to thank Mike Gunsinger for introducing me to and his help with the extractions. As well, I would like

to thank Ed Cey and Matt Lindsay for helpful technical discussions and Wayne Noble for analytical support. Data and helpful discussions with Bill Marsh at the University of Alberta are also acknowledged. Last but not least I would also like to express my thanks to the hydro students at the University of British Columbia for their hospitality and most notably Rich Amos for enduring my numerous and sometimes repetitive questions.

DEDICATION

This thesis is dedicated to my Parents, for all their encouragement and support.

TABLE OF CONTENTS

ABSTRACT.....	iii
ACKNOWLEDGEMENTS.....	iv
DEDICATION.....	vi
TABLE OF CONTENTS.....	vii
LIST OF FIGURES.....	xi
1.0 Introduction.....	1
1.1 Setting.....	3
2.0 Conceptual Framework/Background.....	6
2.1 Oil Sand Extraction Process.....	6
2.2 Process Water Chemistry.....	6
2.3 Naphthenic Acids.....	7
3.0 Methods.....	10
3.1 Drilling and Coring.....	10
3.2 Physical Properties.....	10
3.3 Pore Water Sampling and Analysis.....	10
3.4 Solid Phase Analysis.....	12
3.5 Speciation Modeling.....	13
3.6 Reactive Transport Modeling.....	13
4.0 Results and Discussion.....	14
4.1 Physical Hydrogeology and Physical Properties.....	14
4.2 Naphthenic Acids.....	18
4.2.1 Biodegradation of Naphthenic Acids.....	19
4.2.2 Sorption of Naphthenic Acids.....	22
4.3 Plume Chemistry and Redox Conditions.....	23
4.3.1 Aqueous Geochemistry.....	23
4.3.2 Solid Phase Geochemistry.....	25
5.0 Reactive Transport Modeling.....	31
5.1 Modeling Approach.....	31
5.2 Flow System and Physical Hydrogeology.....	31
5.3 Aqueous Boundary and Initial Conditions.....	34

5.4	Initial Solid Phase Geochemistry.....	35
5.5	Reactions Common to Both Conceptual Models.....	37
5.6	Conceptual Model 1 – Advection and Oxidation of Inorganic Components and CH _{4(aq)}	38
5.6.1	<i>Model Specific Parameters</i>	38
5.6.2	<i>Results and Discussion</i>	39
5.7	Conceptual Model 2 – Advection of Reduced Inorganic Components and Oxidation of CH ₂ O	43
5.7.1	<i>Specific Model Parameters</i>	43
5.7.2	<i>Results and Discussion - 1D Simulations</i>	46
5.7.3	<i>Results and Discussion - 2D Simulations</i>	49
5.8	Model Sensitivity and Error.....	55
5.8.1	<i>Model Sensitivity</i>	55
5.8.2	<i>Mass Balance</i>	57
5.9	Implications of Reactive Transport Modeling.....	59
6.0	Implications for Metal Release and Mobility	61
7.0	Implications for Aquatic Toxicity.....	63
8.0	Conclusions.....	64
	TABLES	66
	FIGURES.....	84
	REFERENCES	110
	APPENDIX A.....	121
	APPENDIX B.....	124
	APPENDIX C.....	161
	APPENDIX D.....	188
	APPENDIX E	239

LIST OF TABLES

Table 3-1	Summary of Laboratory Analysis.....	67
Table 3-2	Summary of Analytical Methods for Inorganic Parameters.....	68
Table 3-3	Overview of Solid Phase Extractions.....	69
Table 4-1	Summary of Previous Studies on Sorption of Oil Sands Naphthenic Acids.	70
Table 4-2	Criteria for Determining Dominant Redox Process (Based on Lyngkilde et al., 1992).....	71
Table 4-3	Dissolved Monoaromatic Concentrations (June 2005).....	72
Table 5-1	Physical Parameters Used during Reactive Transport Simulations.....	73
Table 5-2	Inflow and Initial Aqueous Geochemistry (Concentrations in mg L ⁻¹).....	74
Table 5-3	Initial Mineral Volume Fractions (expressed as fraction of bulk porous medium).....	75
Table 5-4	Summary of Cation Exchange Parameters.....	76
Table 5-5	Conceptual Model 1 – Intra-Aqueous and Mineral Dissolution/Precipitation Reactions.....	77
Table 5-6	Conceptual Model 2 – Rate and Half Saturation Constants for Reactions in Table 5-5.....	77
Table 5-7	Conceptual Model 2 – Intra-Aqueous and Mineral Dissolution/Precipitation Reactions.....	78
Table 5-8	Conceptual Model 2 – Rate and Half Saturation Constants for Reactions in Table 5.7.....	78
Table 5-9	Analysis of Contributors to Biochemical Oxygen Demand (BOD).....	79
Table 5-10	Total Sources and Sinks for dissolved Fe(II) in Plume.....	80
Table 5-11	Total Sources and Sinks for dissolved Mn(II) in Plume.....	80
Table 5-12	Total Mass of CH ₂ O Oxidized via each TEAP.....	81
Table 6-1	Summary of Dissolved Trace Metal Concentrations in Plume (mg L ⁻¹).....	82

Table 6-2 Trace Metal Content in 0.5M HCl Extraction Supernatant (mg g^{-1})..... 83

Table 6-3 Trace Metal Content in 5.0M HCl Extraction Supernatant (mg g^{-1})..... 83

LIST OF FIGURES

Figure 1-1	Location of study area (Top) and location of transect (Bottom).....	85
Figure 2-1	Illustration of GS-MS profile obtained using the characterization method for naphthenic acid mixtures of St. John et al. (1998), Holowenko et al. (2002) and Clemente (2003).....	86
Figure 4-1	Water table surface as measured in November 2005 (Top) and illustration of monitoring well transect (Bottom). All elevations are meters above sea level (mASL). Flowpath represented by transect shown by arrow in top diagram.....	87
Figure 4-2	Transects showing Chloride (A) and Sodium (B) Distributions, Ratios of Sodium to Chloride in the Plume (C) and Hydraulic Conductivity measurements (D). All concentrations are in mg L^{-1} where the values represent the arithmetic average of all measured concentrations. The hydraulic conductivity measurements are in m s^{-1} and represent the arithmetic average of all slug tests performed at a given monitoring well. The ratio of Sodium:Chloride is determined in terms of meq L^{-1} . The location of the transect is shown in Figure 4-1. The roman numerals along the top of the top two figures represent the monitoring well nest number. The dotted line, with the inverted triangle represents the approximate location of the water table. The dotted line with the question mark represents the estimated front of the plume. The crosshatched area represents the aquitard.....	88
Figure 4-3	Non-quantitative flownet for dyke drainage. Shown are two hypothesized flowpaths and 5 hypothesized equipotential lines. The dashed line with the inverted triangle represents the hypothesized water table.....	89
Figure 4-4	Change in Ionic Composition of Process Water Contained in the MLSB (Syncrude 2003).....	90
Figure 4-5	Transects showing naphthenic acid distribution (A), November 2005 field measured pH (B) and alkalinity (C). Naphthenic acid concentrations are in mg L^{-1} and represent the arithmetic average of all measured concentrations. Alkalinity is shown as HCO_3 equivalent concentrations in mg L^{-1} based on measurements made during June 2005. The location of the transect is shown in Figure 4-1. The roman numerals at the top of the figure, refer to the well nest number. The dotted line, with the inverted triangle represents the approximate location of the water table. The crosshatched area represents the aquitard.....	91

Figure 4-6	Comparison of aqueous naphthenic acid to sodium (A) and chloride (B) concentrations. All concentrations are based on arithmetically averaged values from September 2004 and June 2005 sampling events. Error bars represent one standard deviation.....	92
Figure 4-7	Naphthenic acid signatures versus distance from toe of tailings impoundment to plume front(A) and distance from water table (B) Group 1 (Circles), Group 2 (Triangles), Group 3 (Squares). Note, location of flowpath is shown in Figure 4-1.....	93
Figure 4-8	Transects showing dissolved oxygen (A), dissolved manganese (B), dissolved iron (C), dissolved sulfate (D), dissolved methane (E) distributions and interpreted redox zonation (F). Dissolved oxygen measurements were made on November 2005. Values shown for Manganese, Iron, Sulphate and Methane represent arithmetically averaged values based on samples collected during September 2004 and June 2005. All concentrations are shown in mg L ⁻¹ . Redox zones shown in (F) were assigned based on the criteria in Table 4-2. The location of the transect is shown in Figure 4-1. The roman numerals along the top figures refer to the monitoring well nests. The dotted line, with the inverted triangle represents the approximate location of the water table. The crosshatched area represents the aquitard.....	94
Figure 4-9	Carbonate Saturation Indices, Calcite (A), Siderite (B) and Rhodochrosite (C) calcium, iron and manganese concentrations used during saturation index calculations are averaged values from the September 2004 and June 2005 sampling events. Alkalinity used during saturation index calculations is based on field measured values obtained June 2005. The location of the transect is shown in Figure 4-1. The roman numerals along the top of the uppermost figure refer to the well nest number. The dotted line, with the inverted triangle represents the approximate location of the water table. The crosshatched area represents the aquitard.....	95
Figure 4-10	Soil coring locations. The area shown above is the same as that shown in Figure 4-1.....	96
Figure 4-11	Solid phase extraction data. Components shown in each case are listed in each plot. Abbreviations for the specific extraction method used are listed in the text. Shaded areas represent grey colored sand whereas white areas represent red colored sand. The cross-hatched area represents the aquitard. The dotted line represents the water table. Refer to Figure 4-9 for the location where each soil core (A,B,C) was obtained.....	97

- Figure 4-12 Distribution of extractable Fe along flowpath Extractions shown above are: 0.5 M HCl (A), 5.0 M HCl (B) and Na-Ascorbate (C). Data points shown above represent only sampling locations from the red coloured sand. Note that two sampling points are shown in (A) and (B) for both Fe(II) and Fe(III) at each position on the flowpath, however in many cases they are very similar and plot on top of one another. Note also that there are 5 data points in (C) however the two data points on both the left and right side are identical. Refer to Figure 4-10 for soil coring locations.....98
- Figure 5-1 Illustration of Geologic Model (A), Domains and Boundary Conditions used for 2-Dimensional (B) and 1-Dimensional Simulations (C). The shaded portion the geologic model (A) represents the area considered during the simulations. The roman numerals in the top diagram (A), refer to the well nest number. Arrows in middle diagram (B) refer to different recharge boundary fluxes, 250 mm year-1 (1), 63 mm year-1 (2), 40 mm year-1 (3). Divisions in the bottom (C) diagram represent zones of constant effective porosity in the 1-Dimensional domain.....99
- Figure 5-2 Illustration of the distribution of red and grey sand at the field site (top). Conceptualization of the distribution of red and grey sand in the 2D Domain (bottom). In the top illustration, the solid line represents the interface between the red and grey sand defined based on borehole data. The dotted line with question marks, indicates the predicted location of this interface. Roman numerals in the uppermost figure refer to the well nest number. Furthermore in the uppermost figure, the dashed line with the inverted triangle represents the approximate location of the water table and the crosshatched area represents the aquitard..... 100
- Figure 5-3 Comparison of field to predicted results based on conceptual model 1 after 27 years. All plots consider aerobic oxidation of Fe(II) and Mn(II) in addition to: CEC (high estimate) (A), CEC (low estimate) (B), CEC (high estimate) and oxidation of MnO₂ (high rate) (C), CEC (low estimate) and oxidation of MnO₂ (high estimate) (D), CEC (low estimate) and oxidation of MnO₂ (low rate) (E) and a comparison of field to predicted CH_{4(aq)} if a constant flux or a 14 year lag is observed prior to CH_{4(aq)} ingress into the domain (F). Refer to the text for specific CEC and rate constants used in each case. Field data is based on the arithmetic average of September 2004 and June 2005 Sampling Events..... 101
- Figure 5-4 Transect showing biological oxygen demand measurements. Biological oxygen demand measurements are expressed as mg L⁻¹. Each measurement represents the laboratory derived biological oxygen demand measurement. No correction has been performed for the effect of reduced inorganic or organic constituents. The roman numerals refer to the well nest number. The dotted line with the inverted triangle represents the water table and the cross-hatched area represents the underlying aquitard..... 102

- Figure 5-5 Results from conceptual model 2 using 1D simulations after 27 years. Plots represent the following: Total dissolved Fe(II), Mn(II) and O_{2(aq)} (A), Intra-Aqueous Reaction Rates (B), Mineral Dissolution-Precipitation Reaction Rates (C) and Mineral Volume Fractions (D). Dots represent field measured or experimentally derived values. Lines represent values determined using MIN3P. Concentrations of Fe(II) and Mn(II) are based on the arithmetic average of September 2004 and June 2005 Sampling Events. Dissolved oxygen concentrations are based on the arithmetic average of September 2004 and November 2005 measurements. Extractable Fe and Mn data is based on values determined using the Na-Ascorbate extraction..... 103
- Figure 5-6 Distributions of redox sensitive components, HCO₃ and pH based on Conceptual Model 2 using 2D Simulations after 27 years. Concentrations are in mg L⁻¹, with the exception of pH, which is in pH units. Plots shown are: O_{2(aq)} (A), Mn(II) (B), Fe(II) (C), SO₄ (D), CH_{4(aq)} (E), NH₄⁺ (F), HCO₃ (G) and pH (H). Blacked-out area represents the unsaturated zone and the underlying aquitard, which were not considered during simulations..... 104
- Figure 5-7 Intra-aqueous reaction rates and mineral volume fractions based on conceptual model 2 using 2D simulations after 27 years. Intra-aqueous reaction rates are expressed as mol L⁻¹(H₂O) s⁻¹. Plots shown are: Aerobic Degradation Rates (A), Sulphate Reduction Rates (B), Methanogenesis Rates (C), Pyrolusite Volume Fraction (D), Goethite Volume Fraction (E), Siderite Volume Fraction (F), Rhodochrosite Volume Fraction (G) and Calcite Volume Fraction (H). Blacked-out area represents the unsaturated zone and the underlying aquitard, which were not considered during simulations..... 105
- Figure 5-8 Distributions of chloride and major cations based on conceptual model 2 using 2D simulations after 27 years. Plots shown are: Chloride (A), Calcium (B), Magnesium (C) and Sodium (D). Concentrations are in (mg L⁻¹). Blacked-out area represents the unsaturated zone and the underlying aquitard, which were not considered during simulations..... 106
- Figure 5-9 Transects showing field measured values of Calcium (A), Magnesium (B) and Ammonium (C). The value shown in each case is the arithmetic average of analysis performed on groundwater samples collected during September 2004 and June 2005. The location of the transect is shown in Figure 4-1. The roman numerals along the top of the uppermost diagrams, refer to the well nest number. The dotted line, with the inverted triangle represents the approximate location of the water table. The crosshatched area represents the aquitard..... 107

Figure 5-10 Sensitivity analysis of various geochemical parameters. Solid lines represent dissolved Fe(II), while dashed lines represent dissolved Mn(II). Plots are as follows: Sensitivity to FeOOH dissolution rates (A), Sensitivity to MnO₂ dissolution rates (B), Sensitivity to FeCO₃ dissolution/precipitation rates (C), Sensitivity to MnCO₃ dissolution/precipitation rates (D), Sensitivity to an increase in background dissolved Fe(II) and Mn(II) (E), Sensitivity to cation exchange capacity (F) and Sensitivity to a decrease in CH₂O, in the plume (G)..... 108

Figure 7-1 Correlation of toxic response to Ammonium (A) and Naphthenic Acid concentrations. Note all concentrations are in mg L⁻¹. Naphthenic acid and ammonium concentrations were determined based on samples collected in June 2005. Labels adjacent to each point refer to the monitoring well at which each sample was collected (see Figure 4-1 for locations)..... 109

1.0 Introduction

The Canadian Athabasca Oil Sands deposit is a vast resource, with estimates of proven crude oil reserves at 174 billion barrels (Alberta Government, 2005). Recently, increased interest and investment directed towards the Athabasca oil sands deposit has highlighted the need for a greater understanding of the environmental impacts involved in the exploitation of this resource. Among the oil companies currently operating in this area, the largest, Syncrude Canada Ltd (Syncrude), produces approximately 230,000 barrels of oil per day (Syncrude, 2003) at their Mildred Lake Mine. Syncrude maintains a “Zero Discharge Policy”, whereby saturated tailings produced during processing of oil sand ore are contained onsite in abandoned open pit mines or above grade tailings impoundments.

Tailings consist of a liquid phase and clastic material derived from the oil sand reservoir. The liquid phase consists mainly of a mixture of oil sand connate water, relatively fresh river water, recycled process water and caustic (NaOH) used during the extraction process (MacKinnon, 1989, Kasperski, 1992) and are herein termed process waters. The primary source of aquatic toxicity in process water is a complex mixture of methyl substituted, aliphatic and cycloaliphatic organic acids termed naphthenic acids (MacKinnon and Boerger, 1986). Naphthenic acids are ubiquitous in petroleum deposits, but are of particular concern in this case, as they become concentrated in the process waters during bitumen extraction (Schramm 2000).

To date, much of the research regarding the environmental fate of naphthenic acids (NAs) has been confined to surface water (MacKinnon and Boerger, 1996) or laboratory investigations (Herman et al., 1993, Herman et al., 1994, Lai et al., 1994, Zou et al., 1997, Headley et al., 2002, Holowenko et al., 2001, Peng et al., 2002, Clemente et al., 2003, Clemente et al., 2004 & Scott et al., 2005). Research regarding the fate of NAs in the subsurface is limited to the recent work of Gervais (2004) and MacKinnon et al. (2004). The investigation of Gervais (2004) consisted of three components: laboratory batch sorption experiments, laboratory microcosm experiments and field based

investigations of existing NA plumes in the Athabasca Oil Sands. MacKinnon et al. (2004) evaluated the attenuation of NAs and inorganic components present in process affected water based on water samples collected from surface water bodies and groundwater discharge from hillsides near to tailings impoundments.

To date, numerous laboratory microcosm experiments have demonstrated some degree of aerobic degradation using NAs extracted from oil sand process water (Herman et al., 1994, Clemente et al., 2003, Gervais, 2004 and Scott et al., 2005). However, attempts at stimulating anaerobic degradation of these same NAs have been unsuccessful (Holowenko et al., 2001 and Gervais, 2004). Field evidence of anaerobic NA degradation was suggested by Gervais (2004) in a NA plume at the Syncrude site, based on lower than expected NA and dissolved SO_4 concentrations coupled with the presence of $\text{CH}_{4(\text{aq})}$. Thus, the current study further examines this possibility and also further relates the results of previous laboratory studies to the field scale. As well, to further clarify which processes may contribute to NA attenuation, this study was conducted within the broader context of considering the overall geochemical evolution of process water in the subsurface. Beyond the electron accepting potential of $\text{O}_{2(\text{aq})}$ in NA degradation, of interest was the relative contribution of other electron acceptors, Mn(III/IV), Fe(III) and CO_2 to NA degradation. The broader approach of the study also provided the opportunity to consider additional potential environmental impacts of seepage from oil sands tailings impoundments.

Groundwater monitoring by Syncrude and at other Oil Sand mines has established that process water discharged to tailings impoundments may contain additional components of environmental significance, such as NH_4^+ , As and salinity in the form of dissolved Na and Cl. Based on the presence of residual bitumen in the tailings stream, it is also hypothesized that dissolved aromatic compounds may exist in the process water. In addition to components introduced to groundwater via seepage from the tailings impoundments, the potential for the mobilisation of trace metals via reductive dissolution reactions mediated by electron donors in the plume was considered. Release of trace

metals has been observed in reducing plumes at landfill sites (Keimowitz et al., 2005); however, this possibility has not been evaluated in the Oil Sands setting.

In order to realize these objectives a field study was initiated. Groundwater characterization was used to identify and define the expected range of concentrations at which components of environmental concern occur in groundwater affected by seepage of process affected water adjacent to tailings impoundments. Because many of these components are redox sensitive and subject to interactions with the solid phase, solid phase extractions (extractions) were performed on core samples of the aquifer to aid in the assessment of redox processes and overall plume geochemistry. The coupling of solid phase and aqueous phase geochemistry has been shown to provide a better understanding of redox processes, because the occurrence and magnitude of terminal electron accepting processes may be masked by sequestration of Fe(II), Mn(II) and H₂S by the solid phase (Baedecker et al., 1993, Hunter et al., 1998 and van Breukelen et al., 2003). Using both solid and aqueous phase geochemical data, the reactive transport code MIN3P (Mayer et al., 2002) was used as an interpretative aid, when considering the various processes giving rise to the geochemical conditions presently observed in the plume. These results, coupled with estimations of trace metal content using the extractions, were used to generalize the potential for the release of naturally occurring trace metals from the solid phase.

1.1 Setting

The Syncrude Mildred Lake Site is located approximately 35 km north of the town of Fort McMurray Alberta (Fig. 1-1 setting). Regionally, the terrain is relatively flat and slopes gradually to the north. Topographic lows are associated with major drainage features, namely the Athabasca and Clearwater Rivers, as well as their tributaries. With the exception of these areas, Oil Sand-bearing, Cretaceous bedrock is typically overlain by till deposits (Syncrude, 1991). Depending on erosional intensity, till or bedrock is overlain by glaciolacustrine deposits of Glacial Lake McMurray or fluvial deposits associated with a paleoflood originating from Glacial Lake Agassiz (Fisher et al., 1993 and Smith et al., 1993). Fisher et al. (1993) indicates that aggregate deposits within the

Syncrude Mildred Lake Site are derived mainly from the latter. The climate of the area is continental, with the bulk of the precipitation occurring in the summer months (Strong et. al. 1981) and mean annual precipitation from 1994 to 2004 was 405 mm (Environment Canada, 2005). Average daily summer temperatures range from 10.5 to 14.0 °C, while average daily December-February temperatures range from -11.5 to -23.5 °C (Strong et. al., 1981).

The oldest tailings impoundment on the Syncrude Mildred Lake site is the Mildred Lake Settling Basin (MLSB). Begun in 1978, the MLSB extends over approximately 22 km², with dykes rising approximately 35-75 m above grade (MacKinnon 1989, Syncrude 2004). Herein, all material contained within this feature and the dyke structures which form its perimeter, have been collectively referred to as the tailings impoundment.

Adjacent to the eastern side of the MLSB, routine groundwater compliance monitoring by Syncrude has identified areas of seepage. One such area was selected by Gervais (2004) for groundwater sampling from existing monitoring wells and for sampling using the Waterloo Profiling tool (Pitkin et al., 1999). Gervais (2004) collected groundwater samples along two transects, one parallel and one perpendicular to the MLSB. Based on profiling locations within the second transect, a similar, extended transect consisting of monitoring wells was selected for the current study (Fig. 1-1).

The study area shown in Figure 1-1 begins at the edge of the tailings impoundment and as such, the mechanism for seepage of process waters into the aquifer was not evaluated. Based on studies performed in a similar setting, it is suggested that fluids contained within tailings impoundments are poorly connected to the adjacent dyke structures and underlying natural deposits (Hunter, 2001). This occurs for two reasons, firstly, clay and silt sized tailings accumulate at the bottom of the tailings impoundment and act to minimize seepage (Hunter, 2001). Secondly, permeability is reduced as residual bitumen from the tailings stream forms bitumen mats in the beaches of coarser grained tailings along the edges of the tailings impoundment (Hunter, 2001). Due to the

presence of these features, seepage is thought to originate primarily from drainage of the dyke structures because they are emplaced as saturated sand tailings.

2.0 Conceptual Framework/Background

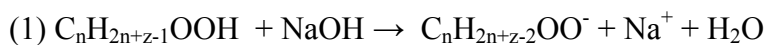
2.1 Oil Sand Extraction Process

Oil sand in its natural state is a combination of mineral matter, connate water and bitumen coexisting in an approximate 70:10:20 volumetric ratio. At Syncrude, bitumen is separated from the oil sand using the Clark hot water process, whereby oil sand is aerated while mixing with warm water and caustic (NaOH) (Schramm, 2000). The production of 0.16 m³ (1 US barrel) of bitumen yields approximately 2.55m³ of water saturated mineral matter, collectively referred to as tailings (Scott and Dusseault, 1985). Further information regarding the extraction process is provided in Schramm (2002).

2.2 Process Water Chemistry

Dissolved inorganic components in process water are derived mainly from those that occur naturally in oil sands connate water. Although the composition of connate water is spatially variable, Syncrude connate water imparts much of the Na and Cl dissolved in process water (Kaperski et al., 1992). Furthermore if porewater collected from the non-oil bearing portion of the reservoir may be used to approximate porewater composition within the overlying oil bearing portion, connate water may also impart HCO₃⁻, NH₄⁺ and low quantities of trace metals (porewater chemistry from Lake and Rogers, 1979). Another origin for NH₄⁺ may be via process chemicals added to the pond (MacKinnon, 1989). SO₄ may arise from Al₂(SO₄)₃ or H₂SO₄ used for treatment of waters prior to bitumen extraction or the production of sour water from bitumen upgrading (Kaperski et al., 1992). Lastly, Na in process water is further increased through the addition of NaOH during extraction (Schramm, 2000).

The use of NaOH as a process aid has two notable effects on process water chemistry. Firstly, the increased pH causes increased alkalinity through both CO₂ dissolution during aeration (Dai et al., 1992) and dissolution of carbonate minerals (Smith et al., 1992). Secondly, the dissociation and subsequent release of Naphthenic Acids (NAs) from the bitumen into the aqueous phase is enhanced via reaction 1 (Schramm, 2000).



2.3 *Naphthenic Acids*

NAs will remain in their more soluble ionized form in aqueous solutions at circumneutral pH, due to estimated acid disassociation constants (pKa) of approximately 5 - 6 (Havre et al., 2003, Headley et al., 2004 and Clemente et al., 2005). Loss of NAs to the vapour phase is minimal due to low volatility (Headley et al., 2004 and Clemente et al., 2005).

The definitions for NAs differ slightly depending on the application. The convention commonly used in oil sands research is followed herein, whereby NAs are defined as complex mixture of acyclic and aliphatic carboxylic acids, with the general chemical formula $\text{C}_n\text{H}_{2n+z}\text{O}_2$, where n refers to the number of carbon atoms and Z to the hydrogen atom deficiency caused by ring formation (Holowenko et al., 2002). NAs are common constituents of Oil Sand, such that concentrations of a few mg L^{-1} are often observed in surrounding surface water bodies, un-impacted by process water (Schramm, 2000). NAs discussed in the literature may consist of individual surrogate compounds (SNA), commercially available mixtures (CNA) or Oil Sands derived NAs (OSNA). Considering each of these three groupings has different properties, NAs discussed herein have been qualified using these genetic prefixes.

Microcosm studies of SNAs, CNAs and OSNAs may be viewed under the general pretexts of aerobic or anaerobic conditions. Aerobic degradation of NAs has been observed to yield an *aerobic signature* (Gervais 2004), whereby lower molecular weight components of the NA mixture are preferentially utilized (Clemente et al., 2004, Gervais, 2004, Scott et al., 2005). Conversely in anaerobic conditions, such as those prevalent in groundwater, a signature has not been defined due to the recalcitrance of mixture-based CNAs and OSNAs in these conditions (Holowenko et al., 2001, Gervais, 2004). If the longer time scales afforded by the current study were to yield anaerobic degradation, it is conceivable that a signature similar to that associated with aerobic degradation would occur. However, it is worthwhile to note that the opposite has been observed in an

alkylcyclohexane mixture, which showed preferential removal of higher molecular weight components during anaerobic degradation at Bemidji, Minnesota (Hostettler et al., 2002). In this case cleavage of larger molecular weight compounds occurred, yielding lower molecular weight alkylcyclohexanes (Hostettler et al., 2002).

When assessing biodegradation signatures, rather than attempt to identify a decrease in each component of the NA mixture, Clemente et al. (2003) suggested dividing the mixture in three groups based on natural divisions observed in the GC-MS profile (Fig. 2-1). Each group is then defined based on stoichiometric carbon content, whereby Group 1 contains NAs with 5 – 13 Carbon atoms, while Group 2 represents members having 14 - 21 Carbon atoms and finally Group 3 contains those with more than 22 Carbon atoms. Based on these groupings, Clemente et al. (2003) suggested a quantitative test to assess biodegradation. The test is implemented such that the distribution of individual members within an NA group, in a given sample, is compared to the distribution in the same group, in all other samples.

In contrast to biodegradation studies, using the statistical test of Clemente et al. (2003), Gervais (2004) noted no change in signature during batch sorption studies using OSNAs and sandy soils. The apparent homogeneous sorption of all components in OSNAs may be related to the low sorption characteristic of OSNAs in sandy soils (Gervais, 2004 and Schramm, 2000). In these instances, preferential sorption may be too small for identification by current analytical methods, due to the low total amount of sorption.

Other organic pollutants are generally present only in trace quantities or below detection limits within the tailings water (MacKinnon, 1989). For example, concentrations of phenols are generally below $100 \mu\text{g L}^{-1}$, while polycyclic aromatic hydrocarbons have been detected at concentrations of approximately $1 \mu\text{g L}^{-1}$ (MacKinnon, 1989).

Please see Appendix A for additional information on tailings geochemistry, tailing impoundment construction and seepage mechanisms.

3.0 Methods

3.1 *Drilling and Coring*

An M5T- tracked drilling rig supplied and operated by Mobile Augers Ltd. of Edmonton, Alberta was employed for monitoring well installations, soil coring and test hole drilling. Test hole drilling using 0.15 m solid stem augers was performed prior to the installation of each nest of monitoring wells to determine placement of the well intakes. Monitoring wells were installed by driving hollow steel casing with a disposable stainless steel tip using a percussion hammer. Monitoring wells constructed of 2.0 cm ID/2.7 cm OD, Schedule 40 PVC, with 75 cm bentonite sleeves and 15 cm Prepak™ intakes, purchased from Geosight of Las Cruces, NM, were then inserted into the steel casing and the casing withdrawn. Following installation, locking steel protective casings were installed at surface and secured using bentonite and drill cuttings.

Core samples were collected using the Geoprobe Macro-Core Soil Sampler (TM). This method is similar to the piston coring device described by Starr and Ingleton (1992). Cores collected in clear 44 mm wide, 1.2 m long plastic liners, were capped and frozen in the field using dry ice. In order to facilitate the use of the coring tool, the interval above the sampling interval was pre-drilled using solid stem augers.

3.2 *Physical Properties*

In-situ estimates of hydraulic conductivity were conducted by slug testing of monitoring wells, using the interpretative method of Hvorslev (1951). Slug testing was performed in triplicate at all monitoring wells shown in Figure 4-1, except for wells 5B and 6.

3.3 *Pore Water Sampling and Analysis*

All samples were collected using peristaltic pumps, operating at flowrates of 0.15-0.25 L min⁻¹. Flexible silicon tubing was used in the pump head housing with polyethylene tubing inserted down the monitoring well. Prior to sampling, monitoring wells were purged until three successive measurements of temperature, pH and electrical conductivity or temperature, pH and dissolved oxygen were within the criteria for field

measurements described in USGS (2005). Due to the small diameter of the monitoring wells, purge volumes often amounted to three or more well volumes. With the exception of alkalinity, field measurements were performed on unfiltered samples. pH was measured using either a gel filled Thermo Orion low maintenance triode (Model 9107) or a refillable Thermo Orion combination pH electrode (Model 9156). pH probes were calibrated using standard pH 7 and 10 buffers. Eh was measured using a Cole Parmer general purpose pH/ORP electrode (59001-77). Eh measurements were standardized using an Orion ORP Standard application solution. Alkalinity was measured in the field using a Bromocresol Green-Methyl Red indicator solution and titrating groundwater samples with 0.1M HCl. An Orion (835) dissolved oxygen (DO) meter was used to measure DO in the field.

An overview of the various groundwater sampling sessions and laboratories used in each case is shown in Table 3-1. The analytical methods employed by each laboratory for the analysis of inorganic components are shown in Table 3-2. Generally, following sample collection, groundwater samples were stored and shipped in coolers with ice packs. Samples for trace metal analysis (see Table 3-2 for cations grouped under Trace Metals) were field-filtered immediately after sample collection using 0.45 µm Aqua-Prep™ filters. Trace metal and NH₃-N samples were preserved with HCl and H₂SO₄ respectively. Biological oxygen demand testing, using a standard 5-day test was begun within 48 hours of sample collections. Samples for Microtox toxicity testing were collected in glass bottles, stored in coolers and testing was begun within 24 hours of sample collection.

Samples for analysis of organic compounds were collected unfiltered in glass bottles with no headspace. Sodium azide preservative was used in samples collected for acetate, formate, PAH and BTEX analysis. Fatty acid analysis was performed using ion chromatography (IC). Upon arrival at the laboratory, samples for fatty acid analysis were frozen until analysis. BTEX, PAH and dissolved CH₄ analyses were performed using a gas chromatograph with a flame ionization detector (GC-FID) and equipped with a 0.25 mm x 30 m DB5 capillary column with a film thickness of 0.25 µm. BTEX and PAH

compounds were analyzed using the method of Henderson et al. (1976). Sample bottles for CH_{4(aq)} were refrigerated and analyzed within 2 weeks of sample collection, using a method based on RSK-175 (R. S. Kerr Laboratory) and Kampbell et al. (1998). The method has been further modified to allow automatic sample injection. Total (quantitative) NA content was analyzed based on the method of Jivraj et al. (1995). Detailed (qualitative) naphthenic acid characterization was performed using the gas chromatography – mass spectrometry (GC-MS) method of St. John et al. (1998) and Holowenko et al. (2002).

3.4 Solid Phase Analysis

Frozen core samples were cut in half and transferred to an anoxic glovebox (Coy Laboratory Products), where subsamples were collected for solid phase extraction. A summary of solid phase extractions (extractions) employed for this study and the target phase of each is presented in Table 3-3.

Fractional organic carbon analysis was performed using the method of Churcher et al. (1987). Quantification of calcite and dolomite content was performed using the method of Dreimanis et al. (1962).

Selective extractions were used to distinguish the Fe and Mn containing phases which may be susceptible to reductive dissolution reactions and to determine the trace metal content of these phases. Reagents for selective extractions were added to capped 0.60 L glass vials in an anaerobic glove box. Sealed glass vials were taken from the glove box and shaken in the dark for 21 days for the 5.0 M HCl extraction and 24 hours for the 0.5 M HCl and Na-Ascorbate extractions. Samples were then returned to the anaerobic chamber, filtered using 0.45 µm cellulose acetate filters, bottled and if necessary preserved with HCl for major cation and trace metal analysis (see Table 3-2 for cations included in these groupings). Extractant supernatant from the Na-Ascorbate extraction was analyzed for major cations and trace metals using ICP-OES at ALS Laboratories (Vancouver, British Columbia), while supernatant from the 0.5M HCl and 5.0 M HCl extractions was analyzed in a similar fashion by National Laboratory for

Environmental Testing, Environment Canada, Burlington, Ontario. Fe in supernatant from the 0.5M HCl and 5.0M HCl extractions, was speciated using the Ferrozine method (Gibbs 1979).

3.5 Speciation Modeling

MINTEQA2 (Allison et al., 1999) was used for the determination of aqueous speciation and saturation indices for groundwater samples. The MINTEQA2 (Allison et al., 1991) database was modified to be consistent with the WATEQ4F database (Ball and Nordstrom 1991). This was performed by updating values from the MINTEQA2 database with those from the WATEQ4F database, in cases where the latter were available. Field measured Eh-values for each sampling location were used to specify redox conditions. As shown by Lindberg and Runnels (1984), redox couples are often in a state of disequilibrium, thus measured Eh values cannot be assumed as representative of the true redox conditions of the system. For this reason, saturation indices calculated where measured Eh values are used as input, may only be used to provide general guidance with respect to the precipitation-dissolution dynamics in a system.

3.6 Reactive Transport Modeling

The multicomponent reactive transport code MIN3P (Mayer, 2002) was used to explore hypotheses regarding the origin of the geochemical conditions and component distributions observed in the study area. Specifically MIN3P was used to simulate advective-dispersive transport, aqueous complexation, cation exchange, sorption, mineral dissolution/precipitation and redox reactions. For this study, intra-aqueous redox reactions and reductive dissolution reactions were represented using a multiplicative Monod approach (Mayer et al., 2002). The thermodynamic database of MIN3P is based on those of WATEQ4F (Ball and Nordstrom, 1991) and MINTQA2 (Allison et al., 1991).

4.0 Results and Discussion

4.1 *Physical Hydrogeology and Physical Properties*

Test hole drilling identified an unconfined sand aquifer extending throughout the study area, ranging from 4.8 to 11.6 m thickness. In all test holes, a clay-till aquitard was found to underlie the aquifer. Only one test hole completely penetrated the clay-till aquitard, where it was found to be 5.1 m thick. Low grade oil sand was encountered below the aquitard and visually identified in the field with the help of Syncrude geologists (G. Kampala pers. comm. 2004). Figure 4-1 illustrates the stratigraphy of the study area and phreatic surface in the aquifer.

The transect illustrated in Figure 4.1 represents a general flowpath for groundwater exiting the dyke system. The sand dyke, where the transect begins, forms a hydraulic high. Farther from the dyke, the flowpath gradually assumes a more northward direction based on the increasing influence of the natural flow regime. Additionally, the northward direction assumed by the flowpath may also be related to preferential flow pathways within the surficial aquifer. Based on the work of Fisher et al. (1993) and Smith et al. (1993) the genesis of the sand aquifer is thought to be related to a north-south trending fluvial deposit. Thus, the orientation of the sedimentary deposits associated with this feature may contribute to the northward deviation of the flowpath.

This northward deviation in the flowpath was unexpected, because originally monitoring wells were installed in a linear transect, perpendicular to the edge of the tailings dyke. For this reason the most downgradient monitoring point 7, intended to represent background conditions, did not fall on the flowpath. Thus, when defining the hydraulic gradient, monitoring point 6, previously installed by Syncrude Canada Ltd was used (Fig. 4-1). The borehole record and completion details provided by Syncrude for monitoring well 6 are shown in Appendix C.

Hydraulic conductivity (K) measurements, determined by slug testing, ranged from 5.9×10^{-6} to $1.4 \times 10^{-4} \text{ m s}^{-1}$ with an arithmetic average of $5.2 \times 10^{-5} \text{ m s}^{-1}$ (Fig. 4-

2d). Elevated K is observed in the western half of the transect (Fig. 4-2d), however it is not known how representative the lower K's noted monitoring well nest 5 are of this portion of the aquifer. Some support for the distribution of K defined by slug testing is provided by borehole drilling. At monitoring well location 3, some intervals of the sand aquifer were noted to be coarser than those generally encountered during borehole drilling at this and other monitoring well locations along the transect (Appendix C).

The horizontal hydraulic gradient of the transect, calculated using water level measurements made during November 2005, is 0.004. Vertical gradients could not be resolved based on field data, because in each case 0.04 m or less separates water levels measured in the highest, versus the lowest monitoring well in each nest. It is not practical to define a vertical gradient based on these differences, as the error incurred in measuring water levels and surveying monitoring well elevations is of a similar magnitude.

Using Darcy's equation, with an estimated effective porosity of 0.30, a hydraulic gradient of 0.004 and using the minimum, maximum and average slug test hydraulic conductivities reported above, the estimated average linear groundwater velocity for the study area is 2, 59 and 22 m year⁻¹ respectively.

Cl in the plume provides a useful tracer, based on conservative transport properties at circumneutral pH and its relative abundance in process water compared to natural groundwater found at the site (Fig. 4-2a). The use of Cl as a tracer for process affected waters was previously noted by Baker (1999), MacKinnon et al. (2004) and Gervais (2004). The plume length is estimated to be 594 m using an average linear groundwater velocity of 22 m year and assuming this velocity has remained constant over the 27 year lifetime of the tailings impoundment/dyke system. Field data indicate that the leading edge of the Cl plume is between wells 5 and 6, between 475 and 900 m from the tailings dyke (Fig. 4-2a), which is consistent with the Darcy estimate of the length. Contour plots of Cl and other components shown in later sections are often based on arithmetically averaged concentrations obtained from up to three sampling events. In each case, the sampling events from which contour data was derived are shown within

the caption beneath the figure. This was performed to lessen the impact of outliers on interpretation and to provide a range of concentrations for each component. All sampling was performed approximately within the period of a year (September 2004 – November 2005), which is much shorter than the 27 year lifespan of the plume. Furthermore, the effect of advective transport between sampling sessions on component concentrations is felt to be minimal.

Fig 4-2a and b indicate that Na and more notably Cl concentrations are elevated in the lower half of the plume relative to the upper half. When interpreting the origin of this stratification, it is assumed that because tailings discharged to the tailings impoundment are also used in dyke construction, temporal changes in aqueous chemistry of each will be comparable. Based on this assumption SO_4 , whose concentration in the free water zone of the MLSB has been observed to remain constant over the lifetime of the MLSB (Syncrude, 2003), is also observed to be regularly distributed in sampling points along the upgradient boundary of the domain (Fig 4-8d). If dilution by meteoric recharge were causing the stratification observed in the plume, lower SO_4 concentrations would be expected in sampling points in the upper portion of the plume relative to those in the lower portion of the plume. It should be noted that lower SO_4 concentrations observed in monitoring well 1B are thought to be related to anaerobic CH_4 oxidation and are discussed in Section 5.6.2.

Historical monitoring by Syncrude indicates that the Cl content of the waters in the MLSB increased nearly five fold during the mid 1990's, while the Na content roughly doubled during that time (Fig. 4-4). Using the ratio of dissolved (meq L^{-1}) Na to Cl, an indication of the age of the process water may be obtained (M. MacKinnon pers. comm. 2004). A ratio of approximately 2 is characteristic of post-1995 dyke construction water and 5 or higher of pre-1990 water (Fig. 4-4). Calculating similar ratios for the plume, indicates that water entering near the top of the upgradient boundary has ratios characteristic of pre-1990 construction water (Fig. 4-2c). Conversely, ratios determined at sampling points closer to the bottom of the input boundary have distinctly lower ratios, characteristic of younger construction waters. Such an observation is also not supportive

of dilution by meteoric recharge as an origin for the stratification, as this would not change the Na:Cl ratio. If the waters in the plume represent different ages of process water, it is not clear how such a relationship would arise, whereby younger waters are observed to underlie older waters. A possible conceptualization is shown in Figure 4-3. Based on Figure 4-3, a shallow flowpath is assumed to originate nearer to the toe of the tailings dyke which was constructed first, in the late 1970's (construction date from K. Chovan pers. comm. 2005). To accommodate greater volumes of tailings, the height of the dyke was increased over time, thus fluids entrained higher in the tailings dyke were emplaced at a later time. Because dyke construction concluded in the 1990's, pore water entrained at this time in the upper portion of dyke is expected to be representative of tailings pond waters sampled during this period. Thus, it is hypothesized that younger fluids draining from the upper portion of the dyke follow a deeper flowpath (Fig 4-3). The geochemical data currently available is supportive of this hypothesis, however the flow dynamics, which could give rise to such conditions are unclear. Furthermore, because this hypothesis is based only on a small number of data points, a more detailed investigation, including the assessment of drainage and flow within the dyke structure would be required to confirm if in fact Fig 4-3 is realistic.

Although the origin of the geochemical stratification cannot be confirmed, its presence indicates that the plume entering the aquifer cannot be assumed chemically homogeneous. Generally, the plume has been divided into two zones: an upper zone with lower Na and Cl concentrations and a lower zone with elevated Na and Cl concentrations. Adjacent to the upgradient boundary this grouping was performed based on the ratio of Na:Cl. However, cation exchange of Na during lateral migration of the plume and possible vertical shifting at the plume fringe is expected to naturally reduce the Na:Cl ratio. Thus, monitoring wells farther downgradient from the upgradient boundary were grouped based on overall Cl and Na concentrations. For this reason, despite lower Na:Cl ratios, monitoring wells 3A, 4A, 4B, 5A, 5B and 5C were included in the upper-plume.

4.2 *Naphthenic Acids*

Groundwater samples were screened for evidence of NA attenuation by comparison to conservative tracers. Processes affecting attenuation may include sorption, biodegradation and variable input into the domain. Generally, Cl has reached Well 5, 500m downgradient (Fig. 4-2a), while NA has not (Fig. 4-5a), thus NA is attenuated to some degree relative to Cl. This relationship may be quantified using the ratio of the advective displacements of NA versus Cl, where the advective fronts are defined as half of the maximum aqueous concentration ($0.5C_{\max}$) for each component. However, the advective front of the Cl plume is poorly constrained by the field data, thus only the range of attenuation may be determined based on the sampling points constraining the latter. Assuming monitoring well nest 4 approximates the advective front of the NA plume, the Cl plume has moved between 1.3 to 2.4 times faster than the NA plume through the aquifer. This screening technique, whereby the advective fronts of two components are compared, is useful when considering attenuation via linear sorption. When other attenuation mechanisms are significant, such as non-linear sorption or biodegradation this mechanism may not be as effective. For example, the self-sharpening nature of a reactive plume front suggests that attenuation may not be detected if only the positions of the advective fronts are considered. The applicability of the degree of attenuation determined by comparing the advective fronts of Cl and NA is assessed in the proceeding sections.

As employed by Gervais (2004), a second method for assessing attenuation, is a direct comparison of NA concentrations to those of either a conservative tracer, Cl, or a weakly retarded tracer, Na. The comparison of NA concentrations to Na serves to provide some indication of the degree of attenuation. In order to account for the variable concentration of Cl and Na entering the domain (Fig. 4-2c), comparisons presented herein were performed using only samples collected from the upper-plume (Fig. 4-6), because of the larger number of these samples. Due to the paucity of lower-plume samples, it was elected not to perform the comparison in these cases. It is assumed that concentrations of Cl and Na in waters giving rise to the upper-plume (Fig. 4-2c), have remained relatively

constant. A similar assumption has also been made regarding NA, although concentrations of NA near the upgradient boundary, appear less variable (Fig. 4-5a).

Figure 4.6b demonstrates a poor correlation between NA and Cl however Figure 4-6a shows a strong correlation between NA and Na concentrations. The strong correlation between the distribution of NA and Na, supports some degree of NA attenuation. If it is assumed that Na attenuation in sandy soils arising from cation exchange is weak, by correlation, it may be generalized that NA attenuation is similarly weak. Potential mechanisms giving rise to this attenuation are explored below.

4.2.1 Biodegradation of Naphthenic Acids

The primary evidence for microbial degradation in groundwater is a decrease in concentration beyond that attributable to dispersive mixing and retardation. Confidently attributing the relatively small amount of NA attenuation to biodegradation is hampered by uncertainty regarding the relative effects of other processes: sorption, temporal variations in source concentrations and flow system dynamics. Thus, it is worthwhile to consider previous laboratory experiments, where greater certainty is afforded by more controlled conditions (Lai et al., 1994; Herman et al., 1993; Herman et al., 1994; Headly et al., 2002; Holowenko et al., 2001; Clemente et al., 2004; Gervais et al., 2004; Scott et al., 2005).

Aerobic microcosm studies of OSNAs by Gervais (2004) showed that, relative to a sterile control, the proportion of Group 1 NAs in the mixture decreased approximately 20% over 140 days. More striking examples are observed in aerobic degradation of CNAs, where in one case Group 1 NAs were observed to decrease from 27% to 11% of the mixture over 18 days, while in a second case almost complete removal of Group 1 NAs was observed (Clemente et al., 2004). For comparison, Figure 4-7 illustrates the relative proportion of each group, first versus its position along the flowpath (Fig. 4-7a) and secondly relative to distance from the water table (Fig. 4-7b). The data points shown in these figures represent NAs entrained only within the plume, because NA concentrations in background samples are too low for GC-MS characterization.

A visual appraisal of Figure 4-7a and Figure 4-7b, indicates that a distinct change in signature is absent throughout the plume. The apparent homogeneity of the NA mixture is further illustrated by the statistical method of Clemente et al. (2003) (Appendix B). This analysis indicated that with some exceptions regarding Group 3, no significant difference occurred between any two groups (Appendix B). Typically, because Group 3 comprises the smallest proportion of the mixture (10-15 %), small changes are reflected to a greater degree. Thus a statistically significant difference between the distributions of Group 3 NAs is not regarded as sufficient evidence for naphthenic acid degradation. In anaerobic microcosms, Gervais (2004) also noted statistically significant differences between Group 3 OSNAs, but observed no decrease in total OSNA concentration. In OSNAs extracted directly from tailings water contained in the MLSB, the relative proportions of groups 1, 2 and 3 were 27%, 60% and 13% respectively (Clemente et al., 2003). These values are comparable to the range observed in samples shown in Figures 4-7a,b 33-42 % (Group 1), 44-57 % (Group 2) and 10-14 % (Group 3), suggesting that the character of the NA mixture has not changed extensively since initial release.

MacKinnon et al. (2004) indicated that the NA mixture in samples collected from hillside groundwater discharge areas, relative to the mixture characteristic of tailings pond or seepage collection ditch waters, reflects a change characteristic of aerobic degradation. In the case at hand, in areas more likely to encounter aerobic conditions near the water table, an aerobic biodegradation signature is not observed (Fig. 4-7b). The lack of a signature may be related to a number of factors, such as: low rates of meteoric recharge, the presence of a more reactive electron donor, able to consume dissolved oxygen entrained in meteoric recharge or low transverse vertical dispersivity. Additionally, relative to laboratory conditions, those in the subsurface are kinetically, less supportive of NA degradation. For example, laboratory studies which have demonstrated aerobic biodegradation of NAs, are performed at ambient temperatures and amended with additional nutrients. Headley et al. (2002) observed that half lives decreased 2 - 13 times for SNAs when temperatures were decreased from 30°C to a temperature of 10°C more

representative of groundwater. In microcosm studies performed by Herman et al. (1994) using unamended tailings water from Syncrude's Mildred Lake Settling Basin, minimal microbial degradation of OSNAs was noted until supplemental nutrients were added. For example microcosm studies are often supplemented with Bushnell Haas medium containing among other additives: 1 g L⁻¹ of K₂HPO₄, KH₂PO₄ and NH₄NO₃ (Gervais, 2004). For comparison, maximum HPO₄, NO₃-N and NH₃-N concentrations observed either in background or impacted waters are low, generally less than < 1, < 0.2 and < 4.0 mg L⁻¹ respectively.

Overall, support for NA biodegradation in the study area, via a change in signature, was not observed. However, because anaerobic degradation of mixture based CNAs or OSNAs has not been documented in this or previous studies, it is unknown if indeed a signature will arise under these conditions. For this reason, the absence of such a change cannot be used to refute the occurrence of anaerobic biodegradation. Logically, based on the anoxic conditions observed in the plume (Fig. 4-8a), recalcitrance of NAs would be consistent with the observations in anaerobic microcosms by other researchers: reduced degradation of SNAs (Lai et al., 1996) and the absence of both CNA (Holowenko et al., 2001) and OSNA degradation (Holowenko et al., 2001 & Gervais 2004).

Groundwater samples hypothesized by Gervais (2004) to show NA biodegradation were collected near monitoring wells 3B, 3C and 4B. Gervais (2004) employed one of two methods to assign the possibility of biodegradation. In the first, when NA concentrations were plotted versus those of Cl and Na, the NA concentration associated with a given data point should be distinctly below that predicted by linear regression through all data points. This scatter plot method, developed by Gervais (2004), was also employed in the current study (Fig. 4-6). However, sufficient data was not available to Gervais (2004) at the time of the study regarding the stratification of the plume, thus varying initial concentrations of Cl and Na were not considered. For example, 2 of the 3 sampling locations highlighted by Gervais (2004) using this method occur within the area around monitoring well 3B, where Cl and Na concentrations are

elevated relative to other locations due to the association with the lower plume. The third sampling point highlighted by Gervais (2004) using this method, falls within the sampling points discussed below.

Using a second method, Gervais (2004) declared NAs as potentially biodegraded if NA concentrations distinctly below those in the core of the plume were coupled with distinctly lower SO_4 concentrations and the presence of $\text{CH}_{4(\text{aq})}$. Four points were identified that fall in this category and generally were located near the base of the aquifer, near monitoring well 3C and below monitoring well 4B. It should be noted that anomalously low SO_4 was also noted during the current study in monitoring well 3C. However, the current study found Cl and Na concentrations are also lower in this area. This was felt to be related to irregularities in the flow field in this area, which may arise from increased geologic heterogeneity near the aquifer/aquitard boundary or reduced permeability due to mixing of the aquifer material with finer grained sediments from the underlying aquitard. For example K in monitoring well 3C is almost an order of magnitude lower than that in monitoring well 3A and 3B. A similar explanation is offered for anomalies noted by Gervais (2004) below well 4B. Although K was not measured in this area, the sediments were noted to become increasingly fine grained during test drilling (see monitoring well completion details in Appendix C).

Characterization of NAs in the samples discussed above was not permitted by the sample volumes collected by Gervais (2004). However, no change in signature was observed at these locations in the current study.

4.2.2 Sorption of Naphthenic Acids

If the attenuation of NAs relative to Cl observed at the site is not related to biodegradation, it is necessary that it be entirely attributable to sorption. Using a bulk density (ρ_b) of 1.85 g cm^{-3} and a porosity (n) of 30 %, NA soil/water distribution coefficients (K_d 's) are estimated using (Fetter, 1994):

$$(2) \quad R = 1 + \left(\frac{\rho_b}{n} \right) (K_d)$$

This approach for estimating K_d is deemed reasonable because biodegradation is not considered significant (Section 4.2.1) and sorption of OSNAs is assumed linear in sandy soils based on batch sorption studies performed by Gervais (2004). In conjunction with the ratios of the NA versus the Cl advective lengths determined in Section 4.2, NA K_d 's of 0.05 and 0.22 mL g⁻¹ are required to explain the possible range of NA versus Cl retardation. Based on sorption of NAs in sandy porous media, previously documented in laboratory batch experiments by other authors (Table 4-1), this would appear reasonable. Furthermore these studies support the correlation between NA and Na concentrations (Fig. 4-6a). Gervais (2004) indicated that a change in OSNA signature was not observed during batch sorption studies, which is consistent with NA characterization performed during this study.

Low sorption of OSNA is promoted by the circumneutral pH characteristic of the plume (Fig. 4.5b), whereby at pH's greater than $pK_a + 2$, organic acids will generally be in their more mobile ionized form (Dellesite, 2001). Sorption is further limited by the low organic carbon content (foc), generally below 0.1 wt% (Appendix C) and low clay content, generally below 2.0 wt% (Marsh, 2006) of the aquifer. While it is generally accepted that soil organic carbon facilitates sorption of organic compounds (Dellesite 2001, Schwarzenbach, 2003), to date, research regarding the specific role of soil organic carbon on NA sorption is limited. Conversely, studies using clay minerals have attributed NA sorption to physical and electrostatic interactions with inorganic soil minerals (Peng et al., 2002, Zou et al., 1997). Where the sorbent consists solely of clay minerals, sorption of NAs has been observed to be many times greater than in sandy soils (Zou et al., 1997, Schramm 2000). Thus in clay-mineral-rich aquifers NA sorption may have a more significant attenuative effect than in this organic-carbon and clay-mineral-poor aquifer.

4.3 Plume Chemistry and Redox Conditions

4.3.1 Aqueous Geochemistry

An assessment of redox conditions was conducted in order to provide a better understanding of plume geochemistry and the processes governing the fate of other

harmful components (i.e. NH_4^+ and dissolved metals) entrained in the plume. Based on criteria presented by Lyngkilde et al. (1992), (Table 4-2) was created and used in order to identify the dominant redox processes within the plume (Fig. 4-8f). The criteria of Lyngkilde et al. (1998) were modified to remove entries for N_2O and S^{2-} , for which data was not available. Furthermore, the threshold concentration of dissolved Fe required for iron reducing conditions was reduced from 1.5 to 1.0 mg L^{-1} , so that each portion of the aquifer would fall under one of the classifications. Aqueous geochemistry data, to which the criteria were applied, is also shown in Figure 4-8. Raw aqueous geochemistry data is provided in Appendix D.

Most areas of the transect were amenable to classification using the criteria shown in Table 4-2. Although $\text{CH}_{4(\text{aq})}$ exceeds 1 mg L^{-1} in areas near the upgradient boundary, SO_4 concentrations exceeded 40 mg L^{-1} , thus these zones were not classified as methanogenic. A detailed discussion regarding $\text{CH}_{4(\text{aq})}$ in these areas is provided in section 5.6.2. The upper west corner of the transect was not amenable to classification using Table 4-2. This is believed to be related to temporally variable recharge entering this area via the drainage ditch (see Figure 4-1 for drainage ditch location). Currently, water entering the drainage ditch in this area is derived primarily from surface runoff during rainfall events (Gervais, 2004 and observations by author). As a result, during these events, increased recharge may cause this area to become temporarily aerobic.

All other areas of the plume were found to be anaerobic. Within these areas, $\text{CH}_{4(\text{aq})}$ is present only in low concentrations, below 0.5 mg L^{-1} , with the exception of values between 1-2 mg L^{-1} observed near the upgradient boundary (Fig. 4-8e). For comparison, this is similar to the levels of $\text{CH}_{4(\text{aq})}$ observed in groundwater samples collected by Gervais (2004) from the same area. $\text{CH}_{4(\text{aq})}$ observed adjacent to the upgradient boundary is believed to originate upgradient of the transect, because it is generally accepted that methanogens are inhibited in the presence of SO_4 (Lovely et al., 1986). Particularly, in regards to the setting at hand, Fedorak et al. (2002) indicated that in microcosms using oil sand tailings, SO_4 concentrations were observed to decrease below approximately 20 mg L^{-1} prior to initiation of methanogenesis. Similarly, low

concentrations of NO_3 , typically less than 1 mg L^{-1} in background water and below detection limits in the plume (Appendix D), indicate that NO_3 reduction is not significant.

Based on criteria in Table 4-2, Fe(III) and Mn(III/IV) reduction are indicated to occur in the plume (Fig. 4-8f). However, determining the magnitude of Fe(III) and Mn(III/IV) reduction is not possible using only aqueous phase geochemical data, because precipitation of secondary mineral phases can buffer the occurrence of dissolved redox indicators (Baedecker et al., 1993, Hunter et al., 1998 and van Breukelen et al., 2003). For example, saturation indices calculated using MINTEQA2 (Allison et al., 1999) and shown in Figures 4-9b,c indicate the majority of the plume is oversaturated with respect to rhodochrosite (MnCO_3) and siderite (FeCO_3). Although analysis of H_2S was not performed, in the presence of SO_4 reduction, rapidly precipitating Fe-Sulfides (Rickard, 1995) may also act as another possible sink for dissolved Fe(II). To further identify the abundance of terminal electron acceptors, Fe(III) and Mn(III/IV) and the fate of redox indicators, solid phase extractions (discussed in the next section) were employed in conjunction with aqueous phase sampling.

Despite the observation of anaerobic conditions and small quantities of dissolved Mn(II) and Fe(II) in the plume, the electron donor(s) capable of producing such conditions is/are unknown. As discussed above, NAs which form the major component of dissolved organic carbon appear recalcitrant. Attempts at identifying alternative electron donors within the plume were unsuccessful. Concentrations of fatty acids, formate and acetate, were below the method detection limit of 0.5 mg L^{-1} (data not shown). Concentrations of polycyclic aromatic hydrocarbons (PAH) and monoaromatics were typically below quantitation limits ($3 \times$ Method Detection Limit) and in all cases below $10 \text{ } \mu\text{g L}^{-1}$ (Table 4-3 and Appendix D).

4.3.2 Solid Phase Geochemistry

If reductive dissolution reactions are, or have been significant, an impact should be reflected in the distribution of Fe(III) in the solid phase. Using solid phase extraction techniques (extractions), other authors have noted that reducing plumes often yield a

systematic depletion or decline of Fe(III), in an upgradient direction, towards a reduced contaminant source (Tuccillo et al., 1999, Amirbahman et al., 1998 and Heron et al., 1995). To assess this possibility, three locations were selected for aquifer core collection, one in an unimpacted (background) portion of the aquifer, one near the front of the plume and one near the edge of the tailings dyke (Fig. 4-10).

Visual inspection of cores A and B indicated that a layer of red coloured (red) sand overlies a layer of grey coloured (grey) sand (Fig. 4-11). The colour contrast between the layers was assumed to result from an abundance of Fe(III)-containing grain coatings in the red sand and the relative scarcity of such coatings with respect to the grey sand (Heron et al., 1994). For this reason, within each layer, a discernable trend in the solid phase associations of extractable Fe was expected. Figure 4-11 indicates that the proportion of Fe(III) relative to Fe(II) removed by the 0.5M HCl extraction is greater in the red sand, while the opposite is true in the grey sand (Fig. 4-11). The expectation of higher 0.5M HCl and 5.0M HCl (acid) extractable Fe(III) in the red sand versus the grey sand was observed with the exception of 0.5M HCl extractable Fe(III) in Core A (Fig. 4-11). In this case, a rise in 0.5M HCl extractable Fe(III) with depth may be related to some dissolution of clay minerals (Kostka et al., 1994). The release of Fe(II) from cation exchange sites is not expected to significantly impact the acid extractions based on the low cation exchange capacity of the sand aquifer. The arithmetic average of all cation exchange determinations performed by Marsh (2006) on samples of the aquifer was $0.64 \text{ meq } 100 \text{ g}^{-1}$. Even if all the exchange sites were populated by Fe(II), this would translate into $0.2 \text{ mg-Fe(II) g}^{-1}$, whereas the changes in acid extractable Fe(II) within each core are an order of magnitude larger. Similarly, Heron et al. (1995) noted that cation exchangeable Fe(II) was less than 0.1 mg g^{-1} using a 1M CaCl_2 extraction of sandy aquifer sediments.

An origin for the layering, independent of the ingress of the plume, is supported by the horizontal as opposed to a vertical orientation of the stratification. Additionally, no correlation is observed between either SO_4 or dissolved Fe with the colour of the aquifer (Fig. 4-11). If reductive dissolution reactions driven by the plume were causing

the release of Fe(II) into the aqueous phase, increased dissolved Fe(II) is not observed relative to the red sand. Furthermore the potential for monosulfides (FeS) to act as a sink for dissolved Fe(II) appears unlikely due to the low AVS content, operationally defined as FeS, relative to the change in Fe(III) extracted from the red and grey portions of each core (Fig. 4-11). Based on Figure 4-9b, FeCO₃ may act as a sink of dissolved Fe(II). However sluggish precipitation kinetics for FeCO₃ (Jensen et al., 2002), suggest that pore water in the grey sand would remain elevated in dissolved Fe(II) relative to that of the red sand. Although Gervais (2004) was unable to directly observe the aquifer material, pore water was noted to have a red colour in the upper portion of the aquifer and a grey colour in the lower portion of the aquifer. Assuming a correlation between porewater and sand colour may be made, Gervais' (2004) observation of grey porewater in an area south of the transect, unimpacted by the plume, suggests the plume is not responsible for the change from red to grey sand.

The literature indicates that layering such as this, termed a redoxcline (Postma et al., 1991, Robertson et al., 1995) or soil gleying (Lovley, 1991), has been interpreted to occur naturally, representing a contrast between weathered and unweathered soils (Robertson et al., 1995). Accordingly, the absence of grey sand in the background location (Core C), may be related to a thinner saturated thickness and increased proximity to ground surface of the aquifer in this area (Fig. 4-11). Because the layer of grey sand is not present in Core C, when comparing extractable Fe in each of the three coring locations, only samples of the red sand were considered.

Figure 4-12 illustrates the change in extractable Fe content in the red sand, relative to position on the flowpath. Generally, lower amounts of acid extractable Fe(III) are noted nearer to the tailings dyke (Fig. 4-12). However, of the two acid extractions, the 0.5M HCl extraction is more selective in targeting easily reducible solid phases (Heron et al., 1994) and is deemed more sensitive to changes in Fe(III) caused by reductive dissolution reactions. At first glance, an upgradient decrease in 0.5M HCl extractable Fe(III), is punctuated by an elevated measurement (4.2 mg g⁻¹), in the background location. Based on the observations of Tuccillo et al. (1999), if 4.2 mg g⁻¹

represented the initial 0.5M HCl extractable Fe(III) throughout the aquifer, lower 0.5M HCl extractable Fe(III) noted within the plume should be coupled with elevated dissolved or 0.5M HCl extractable Fe(II) relative to the background location. Based on dissolved Fe below 5 mg L⁻¹ (Fig. 4-8c) and the absence of a significant increase of 5.0M HCl or 0.5M HCl extractable Fe(II) within the plume, relative to the background location, the elevated measurement noted above is considered to be anomalous. If this data point is ignored, the difference in extractable iron between the locations most proximal and distal to the tailings dyke is approximately 0.8 mg g⁻¹. Decreases in 0.5M HCl Fe(III) of similar magnitude have been previously related to the ingress of reducing plumes (Tuccillo et al., 1999 and Heron et al., 1995). However, based on the discussion above, it is questionable to relate the difference at hand to reductive dissolution caused by the ingress of the plume, because geologic heterogeneity has been related to changes many times greater.

Compared to the acid extractions discussed above, the Na-Ascorbate extractant is a weak reductant, used to target hydroxide phases and is not expected to significantly dissolve carbonates (Amirbahman et al., 1998). Furthermore, based on extractions of standard minerals, the Na-Ascorbate extraction will not significantly dissolve oxide or clay phases (Kostka et al., 1994). Thus the Fe extracted by the Na-Ascorbate extractant is primarily Fe(III), with the exception of Fe(II) liberated from monosulfides (Kostka et al., 1994) and cation exchange sites.

In the red coloured sand, the extractable Na-Ascorbate Fe(total) at the upgradient (Core A) and background locations (Core C) was almost identical at 0.3 mg g⁻¹, while Core B had a slightly elevated value of 0.4 mg g⁻¹ (Fig. 4-12). Duplicate samples taken from a given interval for the Na-Ascorbate extraction, returned identical values when rounded to the nearest 0.1 mg g⁻¹ (Appendix C). For comparison, Amirbahman et al. (1998) noted a decreasing trend coupled with a drop in Na-Ascorbate extractable Fe from approximately 0.6 to 0.2 mg g⁻¹, between samples taken from an oxic portion of an aquifer and those beneath a landfill. In this case, a smaller range is noted, no clear trend in Na-Ascorbate extractable Fe is observed along the flowpath and values are identical in

the background and most upgradient locations. This suggests that the difference between the maximum and minimum Na-Ascorbate extractable Fe is more likely related to geologic heterogeneity or varying amounts of Fe(II) released from cation exchange sites. It should be noted that the AVS extraction indicates that monosulfides are not present in sufficient quantities to significantly affect results (Fig. 4-11).

Even if some uncertainty is associated with the effect of geologic heterogeneity, collectively, the distribution of Fe(III) determined by the extractions does not provide credible evidence for a strongly reducing plume. Evidence of sinks for dissolved Fe and Mn, which would indicate that reductive dissolution reactions are in fact more significant than suggested by concentrations of each, below 5 mg L^{-1} , is limited. Cation exchange of Fe(II) and Mn(II) may decrease dissolved concentrations to some degree. However as shown above, the maximum amount of Fe(II) or Mn(II) capable of being stored in the solid phase, relative to that observed at other sites to be released by strongly reducing plumes (Tuccillo et al., 1999, Heron et al., 1995) is approximately an order of magnitude lower. The precipitation of monosulfides (FeS) occurs rapidly (Rickard et al., 1995) in the presence of dissolved S^{2-} and may act as a Fe sink. However the strong correlation of FeS with the grey sand, suggests its origin is natural and not related to the arrival of the plume. In the absence of monosulfides, saturation indices suggest that FeCO_3 and MnCO_3 may act as the solubility controlling solids for dissolved Fe and Mn respectively (Fig. 4-9b,c). However, as mentioned above, the precipitation rates of these phases are sluggish (Jensen et al., 2002). Thus it is reasoned, if release of Fe into the aqueous phase based on the changes in 0.5M HCl extractable Fe observed by Tuccillo et al. (1999) and Heron et al. (1995) occurred, Fe and Mn concentrations significantly above those presently observed in the aqueous phase would be expected.

Weakly reducing conditions are implied by low concentrations, $< 5 \text{ mg L}^{-1}$, of dissolved Fe and Mn observed in groundwater samples from the study area and the absence of $\text{O}_{2(\text{aq})}$ throughout much of the plume. This is consistent with the absence of a decreasing trend in extractable Fe(III) and the absence of an increasing trend in extractable Fe(II) in the upgradient direction. Other terminal electron accepting

processes such as methanogenesis and SO_4 reduction are not believed to be significant. Although $\text{CH}_{4(\text{aq})}$ concentrations may approach 2 mg L^{-1} , concentrations of this magnitude are highly localized. Furthermore the presence of SO_4 in concentrations exceeding 40 mg L^{-1} suggests that $\text{CH}_{4(\text{aq})}$ production will be inhibited and is not significant in the study area. Extractable AVS concentrations are low and the apparent association of these phases with the grey sand suggests an origin unrelated to the plume. To evaluate possible processes which may give to the presently observed weakly reducing conditions, reactive transport modeling was used.

5.0 Reactive Transport Modeling

5.1 Modeling Approach

The field investigation provides useful information about the current groundwater chemistry and the extractable chemistry of the solids, but does not identify the interactions between the components and the processes giving rise to the present geochemical conditions. Thus reactive transport modeling was used to consider two conceptual models thought capable of explaining the weak redox zonation observed at the site:

1. Redox zonation arises from the advection into the domain and oxidation of reduced components, $\text{CH}_4(\text{aq})$, Fe(II), Mn(II) dissolved in the plume; or
2. Redox zonation arises from the oxidation of a small amount of degradable organic carbon dissolved in the plume and the advection into the domain and oxidation of dissolved components, $\text{CH}_4(\text{aq})$, Fe(II), Mn(II).

Provided the particular conceptual model was able to sufficiently represent the redox zonation, the scope of the simulations was expanded to evaluate fate and transport properties of other dissolved components, i.e. Ca, Cl, Mg, Na, NH_4^+ . Numerical simulations were run for 27 years, representing the lifetime of the tailings impoundment (1978-2005). An overview of the framework common to both conceptual models follows, while individual aspects are described separately, prior to the discussion of each model.

5.2 Flow System and Physical Hydrogeology

Both 1-dimensional (1D) and 2-dimensional (2D) representations of the flow domain were employed during numerical simulations. The lower computation times for 1D simulations present an efficient method for narrowing the range of potential input parameters and screening different conceptual models. 2D simulations are capable of including the effect of site geometry and recharge along the flowpath and may provide more realistic results for scenarios selected based on the preliminary 1D simulations. A detailed overview of the methodology used to create the 2D domain is discussed first,

followed by an overview of the simplifications made to the latter in creating the 1D domain.

A fully saturated 2D domain was created to approximate the groundwater flow system in the unconfined aquifer (Fig. 5-1). Because the potential for contaminant transport is primarily through the aquifer, areas of the domain representing the underlying aquitard and overlying unsaturated zone were not considered and assigned low hydraulic conductivity (K) values ($1 \times 10^{-50} \text{ m s}^{-1}$). A single K value (Table 5-1) was applied to the aquifer, initially estimated based on slug test results and refined using model calibration. A longitudinal dispersivity of 1.0 m was used for the simulations, which is consistent with dispersivities derived by Sudicky (1986) and Garabedian et al. (1991) and used by other authors for similar scales (Mayer et al., 2001 and van Breukelen et al., 2004). A vertical transverse dispersivity of 5 mm was found to best fit the data. Once again this is similar to the range calculated by Garabedian et al. (1991) and used by other researchers at similar scales (Robertson et al., 1991, Mayer et al., 2001).

Average annual precipitation in the area, for the period 1994-2004, is approximately 405 mm year^{-1} (Environment Canada, 2005). Much of the domain is forested and within these areas, meteoric recharge (recharge) was estimated via model calibration to be approximately 40 mm year^{-1} . Notably, recharge was estimated to be higher beneath the drainage ditch (250 mm year^{-1}) and beneath un-vegetated areas near the edge of the tailings impoundment (63 mm year^{-1}) (Fig. 5-1). Because the unsaturated zone is not considered, recharge flux was applied directly to the aquifer via nodes located at the water table. Inflow and outflow boundaries at the horizontal extents of the domain were defined using constant head boundaries, based on water level measurements made during November 2005 (Fig. 5-1).

Transient head boundary conditions may be more appropriate for the inflow boundary given the potential decline of dyke drainage over time. However, data detailing temporal changes in the saturation state of the dyke are limited and a detailed evaluation of this phenomenon was beyond the scope of this work. Hunter (2001) provides such an

analysis for a different, older tailings impoundment at the Suncor Energy Inc. site. Furthermore, with the exception of runoff generated during periods of intense rainfall, the drainage ditch, which collects water from perforated drainage pipes installed in the dyke, is dry in this area (based on field observations). Syncrude historical records beginning in 1982, indicate that flow from drainage pipes discharging into portions of the drainage ditch immediately adjacent to and upstream of the transect has generally been absent or limited to dripping (Karen Chovan, pers. comm. 2005). Because discharge from the drainage pipes is minimal, recharge via seepage through the ditch was not considered to represent an additional input of tailings water into the domain. However, collection of surface runoff in the drainage ditch is expected to yield elevated recharge of meteoric waters, which is consistent with calibration exercises described above. Additional physical parameters used during reactive transport simulations are shown in Table 5-1.

The 1D domain was generated based on the geometry of the 2D domain. To reflect the variable transmissivity of the aquifer and flow velocities, the 1D domain was divided into 7 zones and the porosity was proportionally adjusted in each to reflect the thickness of a given zone relative to the average thickness of all zones (Fig. 5-1). Accordingly, mineral volume fractions and cation exchange capacity were adjusted in a similar manner. Because the simulations only consider 1D, a top boundary condition, i.e. meteoric recharge, cannot be considered. Thus, hydraulic conductivity was reduced, globally, to maintain flow velocities consistent with the 2D simulations. Accounting for groundwater recharge using this approach, rather than additional adjustments of porosity was chosen due to the relative ease of calibrating one value, versus seven values. Because most of the domain is subject to the same groundwater recharge flux (Fig. 5-1), the representation of the latter by varying a single value was deemed acceptable. Additional physical properties were similar to those described for the 2D domain (Table 5-1).

5.3 *Aqueous Boundary and Initial Conditions*

Boundary and initial aqueous geochemistry are defined based on sampling points located at the upgradient (inflow) and downgradient (outflow) boundaries of the transect respectively (Table 5-2).

Major ion chemistry from well 7 compared closely to that of monitoring well 6A (Appendix D). Although monitoring well 6A is sampled by Syncrude personnel, a complete dataset including parameters such as field alkalinity and dissolved oxygen was not available. Thus, during sampling sessions for the current study, although monitoring well 7 was not located on the cross section, it was much easier to sample than monitoring well 6 and therefore it was used to provide background groundwater chemistry (See Fig. 4-1 for locations).

Composition of the plume upon initial ingress was assumed similar to groundwater most recently collected from sampling points in the upper half of the upgradient boundary, monitoring wells 1A and 1B (see Fig. 4-1 for locations). At later times, a transient input function provided a better representation of plume chemistry, for example, the stratification of Na and Cl noted in Section 4.1. At later time, the composition of the plume entering through the lower half of the inflow boundary was based on groundwater chemistry at monitoring well 2C. The time at which the transition in plume chemistry began was adjusted during simulations, until results matched the elevated Cl concentrations near the lower portion of the inflow boundary. In support of the hypothesized flowpaths shown in Figure 4-3, the adjusted time of 15 years is comparable to the date at which the transition in Na:Cl ratios was observed in the tailings impoundment, 1990 (Fig. 4-4).

Because Fe(III) and Mn(III/IV) are not significantly soluble at circumneutral pH, it was assumed that field measured concentrations of total dissolved Fe and Mn were analogous to those of dissolved Fe(II) and Mn(II). As noted above, dissolved oxygen (DO) in monitoring well 1A is thought to be related to groundwater recharge. Thus, the plume itself was deemed anaerobic as it enters the domain, based on low concentrations,

<0.5 mg L⁻¹, of dissolved oxygen (DO) measured at deeper points near the upgradient boundary. Trace quantities of DO detected at these locations are considered sampling artefacts, because CH_{4(aq)} and Fe(II) also detected, are not expected to co-exist with dissolved oxygen.

As noted above, a clear indication of the redoxcline is absent in the area where the background well (Monitoring Well 7) is installed. Thus background geochemical data is not available for the lower portion of the aquifer characterized by grey sand. Initially the grey sand was assumed to be anaerobic, with major ion, aqueous geochemistry similar to that in the red sand. Concentrations of dissolved Fe(II) and Mn(II) initially present in the grey sand are unknown; the impact of this uncertainty is approached through model sensitivity analysis. Meteoric recharge entering the domain was assigned a constant chemical composition similar to that of background groundwater.

1D simulations were conducted for a shallow flowpath located in the red sand unit and initial geochemical conditions, representative of the red sand were assigned. Furthermore, the geochemistry of the plume entering the 1D domain was not considered transient and component concentrations were set equal to those defined for the upper inflow boundary. A 1D simulation, based on a flowpath extending through the grey sand unit was not performed because the 1D simulations were only used as a general screening tool. The use of 1D simulations also provided justification for neglecting the effect of meteoric recharge. For cases where the 1D simulations were deemed to reasonably represent the overall geochemistry observed in the study area, the conceptual model was more rigorously evaluated using the 2D simulations, which accounted for the presence of the grey sand.

5.4 Initial Solid Phase Geochemistry

Detailed stratigraphic information regarding the location of the red-grey sand interface was not available for monitoring well 6. The location of the interface in the downgradient portion of the domain was approximated using its distance from the water table in test holes drilled near monitoring wells 1, 2, 3 and 4 for guidance. Figure 5-2 illustrates the

distribution of the red and grey sand based on borehole data and that defined for the domain.

The initial calcite (CaCO_3) content of the aquifer is estimated based on the arithmetic average of the measured results (Fig. 4-11). In each case a bulk density (ρ_b) of 1.85 g cm^{-3} was assumed. Data regarding the volume fraction of secondary mineral phases, siderite (FeCO_3) and rhodochrosite (MnCO_3), is unavailable, thus they were assumed absent prior to the ingress of the plume.

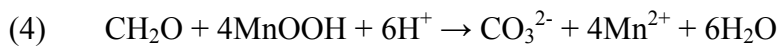
The volume fractions of bioavailable Fe(III) and Mn(III/IV) mineral phases (Table 5-3) are based on the Na-Ascorbate extractions. Although the grey colour of the sand found lower in the aquifer suggests a deficiency of solid phase Fe(III), Na-Ascorbate extractable Fe was relatively constant across the redoxcline. Similarly, Postma et al. (1991) defined a redoxcline based on the disappearance of dissolved oxygen in vertical profiles of a sand aquifer. Below the redoxcline, Fe-oxides and Fe-(oxy)hydroxides were identified based on dithionite-citrate-bicarbonate and ammonium oxalate extractions (Postma et al., 1991). In the current study, the grey sand was considered to contain reducible Fe(III)-solid phases in quantities consistent with the Na-Ascorbate extraction despite its colour.

To prevent the over or underestimation of reducible Fe(III) or Mn(III/IV), extraction results for the entire domain were averaged when estimating the above mentioned volume fractions. Implied in this estimate is the assumption that current mineral volume fractions are roughly equivalent to those present prior to the arrival of the plume. Essentially changes in the solid phase caused by the plume are not assumed significant. Based on the discussion in Section 4.3.2, though not shown definitively, the aqueous and solid phase extraction results suggest that the plume does not impart a significant effect on solid phase composition. The conceptual models evaluated below intend to evaluate whether the reductive capacity of the plume is in fact this low.

For simplicity and because detailed mineralogical information is not available, two surrogate phases were used: an Fe-bearing, (FeOOH) and a Mn-bearing, (MnO₂) phase. Thus dissolution rates of these phases represent the collective rate at which Fe(II) and Mn(II) are released into the aqueous phase. Consideration must be given when selecting the Mn-bearing surrogate, because both the Mn(III) and Mn(IV) valence states may be expected in soils (Postma et al., 2000). Field data indicates that dissolved Mn(II) increases in concentration, downgradient of the input boundary (Fig. 4-8b). Thus, as one role of the conceptual models is to produce Mn(II) within the domain, the results are deemed more credible if the latter is achieved by a conservative prediction of Mn(II) production using MnO₂:



rather than the less conservative prediction using MnOOH:



5.5 *Reactions Common to Both Conceptual Models*

Reactions common to both conceptual models include aqueous complexation reactions, CaCO₃ precipitation/dissolution and ion exchange. Based on circumneutral pH throughout the domain (Fig. 4-5b), anion exchange was not considered significant (van Breukelen et al., 1998, Carlyle et al., 2004, Appelo 1994). Similarly, the relatively constant pH conditions also permits the use of a simple cation exchange model (Dance et al., 1983). Cation exchange is defined using the classic single-site Gaines-Thomas model and is considered both instantaneous and reversible. Cation exchange capacity (CEC) and selectivity coefficients are assumed constant. Despite its simplicity, the single site Gaines-Thomas model has been shown to reasonably represent cation exchange processes at bench scale (Valava et al., 2002) and field scale (Valocchi et al., 1981, Carlyle et al., 2004).

Exchangeable cations considered during simulations include: Ca, Fe(II), K, Mg Mn(II), Na and NH_4^+ . Na is the dominant cation in the plume, while Ca, Mg and to a lesser degree K are the dominant cations initially present in the porewater and on ion exchange sites prior to the ingress of the plume. Although present in low quantities, ion exchange of NH_4^+ was considered due to its potential environmental significance at low concentrations. To properly predict Fe(II) and Mn(II) distributions, exchange of the latter was also considered.

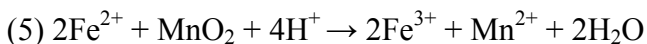
Selectivity coefficients were estimated based on the range listed in Appelo and Postma (1998) and adjusted based on model calibration (Table 5-4). Cation exchange capacity (CEC) was determined experimentally on aquifer cores collected from the study area (Marsh 2006). Excluding measurements made on samples of the underlying aquitard and areas of elevated clay content near the aquifer-aquitard boundary, CEC ranged from 0.36 to 0.96 meq 100 g^{-1} , with an arithmetic average of 0.64 meq 100 g^{-1} . Based on the narrow range of CEC measurements, assigning the average CEC to the aquifer for numerical simulations was deemed appropriate.

5.6 Conceptual Model 1 – Advection and Oxidation of Inorganic Components and $\text{CH}_{4(aq)}$

5.6.1 Model Specific Parameters

A summary of the input parameters used for the 1D simulations are provided in Table 5-2. Central to this conceptual model is the assumption that migration and oxidation of reduced compounds initially present in the plume, at the upgradient boundary, give rise to the distribution of redox sensitive species observed in the study area. Accordingly, reactions considered in this conceptual model involved the aerobic oxidation of inorganic components Fe(II) and Mn(II). Furthermore, simulations were also performed that considered oxidation of Fe(II) via reductive dissolution of MnO_2 , as noted in microcosm experiments of Lovley et al. (1988). Simulations were performed sequentially to determine the relative impact of the various processes on model output. Initial simulations were performed using only cation exchange processes, followed by

simulations also considering aerobic oxidation of Fe(II) and Mn(II) and finally simulations considering these reactions and reductive dissolution of MnO₂:



While aerobic oxidation of CH₄ in aquatic environments is well established (Hanson et al., 1996) and commonly accepted to occur quite quickly (Whalen et al., 1990), anaerobic oxidation of CH_{4(aq)} is less well established. Thus simulations have included only the aerobic oxidation of CH_{4(aq)}. Anaerobic CH_{4(aq)} oxidation was not directly considered during simulations, however a discussion is provided in section 5.6.2. An overview of reactions and reaction constants is provided in Tables 5-5 and 5-6.

5.6.2 Results and Discussion

Distribution of Dissolved Fe(II) and Mn(II)

When only simple advection and cation exchange of dissolved Fe(II) and Mn(II) are considered, concentrations of the latter are underpredicted relative to field measured values (Fig. 5-3). This is notable because this conceptual model represents a relatively conservative approach. Namely precipitation of Fe and Mn-carbonates has not been considered. Although it is known that FeCO₃ and MnCO₃ precipitation is slow and kinetically controlled (Jensen et al., 2002), specific reaction rates are not well defined and thus cannot be defined a priori. Alternatively, estimation via calibration is not feasible, as predicted dissolved Fe(II) and Mn(II) concentrations are generally below field measured values. Thus, although supersaturation with respect to FeCO₃ and MnCO₃ is observed (Fig. 4-9b,c), precipitation of these phases was not considered.

Aerobic oxidation of Fe(II) and Mn(II) at the plume front is likely not significant because Fe(II) and Mn(II) are retarded by cation exchange and accordingly predicted to remain behind the oxic/anoxic interface as noted for a landfill leachate plume by van Breukelen et al. (2004). Output from 1D simulations considering cation exchange and aerobic oxidation of Fe(II) and Mn(II) were identical to those considering only cation exchange (results not shown).

Overall, peaks of dissolved Fe(II) observed in the field data immediately proceeding the input boundary and that of Mn(II) observed downgradient in monitoring wells 3A and 4B are not well represented by simulations (Fig. 5-3a,b). The magnitude of dissolved Fe(II) concentrations measured in groundwater samples are not well replicated using this conceptual model. However, it is not reasonable to match the distribution of the peaks in dissolved Fe(II) observed in the field data, because analytically derived Fe(II) was observed to fluctuate considerably relative to its average value (e.g. error bars in Fig. 5-3a). Conversely, on average, analytical results for dissolved Mn(II) were much more reproducible. These results suggest that the peak of dissolved Mn(II) observed based on field data may be considered more representative of field conditions and is not a result of short term fluctuations in groundwater chemistry or analytical error. To better replicate the peak of dissolved Mn(II) observed in the study area, simulations were modified to include reduction of Mn-Oxides by dissolved Fe(II) (Table 5-5). Reduction of Mn-Oxides by dissolved Fe(II) was observed by Lovley et al. (1988) and has been suggested as a possible origin for dissolved Mn(II) at other sites (Bjerg et al., 1995, van Breukelen et al., 2004).

When MnO₂ reduction is considered (Fig. 5-3c), results predict a peak of dissolved Mn(II), however it occurs nearer to the input boundary than observed in the field. Also, reductive dissolution of MnO₂ serves to further attenuate dissolved Fe(II), in this case within a few 10's of meters of the input boundary. Lowering the CEC to be consistent with the lowest measured value by Marsh (2006), 0.36 meq 100 g⁻¹, did not significantly alter results (Fig. 5-3b,d). Similarly decreasing the reaction rate for reductive dissolution of MnO₂ by one order of magnitude (1×10^{-11} mol L⁻¹ bulk⁻¹ s⁻¹) in combination with a lower CEC, did not significantly affect results (Fig. 5-3e). It was hypothesized that a heterogeneous distribution of Mn(III/IV) bearing mineral phases may yield the distribution of Mn(II) observed in the domain. This possibility was evaluated by slightly altering the domain, such that MnO₂ was absent from the first 250 m of the aquifer. Results (not shown) predicted that dissolved Fe(II) would be attenuated by

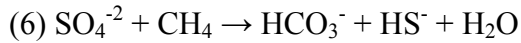
cation exchange prior to arriving in the MnO₂ bearing portion of the aquifer, preventing the formation of a peak in dissolved Mn(II).

To some degree the processes used in Conceptual Model 1 to generate dissolved Fe and Mn may be occurring in the study area, yet dissolved Mn(II) and Fe(II) were regularly underestimated in this conceptual model (Fig. 5-3a,b,c,d,e). The potential that dissolved Fe(II) and Mn(II) concentrations entering the domain were considerably larger in the past is unlikely, based on the overall deficiency of dissolved Fe (<1 mg L⁻¹) and Mn (<0.1 mg L⁻¹) in samples taken from the sediment and free water zones of the tailings impoundment (MacKinnon, 1989). It appears more reasonable that in order to better match the field data, a mechanism for generating dissolved Fe(II) within the domain is necessary. Because this conceptual model was not able to produce results consistent with those observed in the field using 1D simulations, 2D simulations were not pursued.

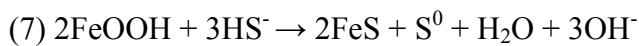
Distribution of Dissolved CH_{4(aq)}

To account for uncertainty regarding when CH_{4(aq)} began entering the domain, simulations considered both the possibility that CH_{4(aq)} was either initially present or initially absent from the plume. With regards to the latter, a lag time of 14 years prior to CH_{4(aq)} inflow was used, based on the first observation of CH₄ bubbles at the tailings impoundment surface (Holowenko et al., 2000). However, under both scenarios, the predicted plume of CH_{4(aq)} extended beyond that observed in the field (Fig. 5-3f), suggesting that either the lag time was greater than predicted or an attenuation process such as anaerobic methane oxidation (AMO) was occurring. Because the primary intention of the simulations was to evaluate the overall geochemistry of the domain, due to the localized occurrence of elevated CH_{4(aq)} (1-2 mg L⁻¹) at the input boundary, AMO was not considered during simulations. Evaluation of this process is limited to discussion based on field data and conservative simulations of CH_{4(aq)}.

Current understanding indicates that AMO is coupled to SO₄ reduction, yielding the net reaction (Valentine et al., 2000):



Consistent with (6), when compared to conservative Cl, lower relative SO_4 concentrations were noted in areas of elevated $\text{CH}_{4(\text{aq})}$ (Fig. 4-8d). Although H_2S was not measured in the field, it is expected that dissolved Fe(II) is effective at removing H_2S via rapid precipitation of monosulfides (Rickard, 1995). Alternatively, in the absence of dissolved Fe(II), H_2S may also be attenuated via reactions with Fe(III)-bearing solid phases (Appelo and Postma, 1999):



An assessment of monosulphide content via the AVS extraction indicates that slightly elevated values are present in areas of elevated dissolved methane (Fig. 4-11). However, while some support for AMO is available, it is important that evidence presented above be kept in context. Firstly, because significant concentrations of $\text{CH}_{4(\text{aq})}$, i.e. amounts greater than 1 mg L^{-1} , were only observed at two sampling locations, the amount of supporting evidence is sparse. Additionally, increased AVS content appears related to geologic heterogeneity or local stratigraphy. For example, AVS is also noted to increase in the grey sand unit of coring location B (Fig. 4-11), where concentrations of $\text{CH}_{4(\text{aq})}$ are two orders of magnitude lower relative to those at coring location A (Fig. 4-8e).

$\text{CH}_{4(\text{aq})}$ oxidation via reductive dissolution of Fe(III)-bearing mineral phases has not been observed under laboratory conditions (Gal'chenko 2004). With regards to the case at hand, a reduction in Na-Ascorbate extractable Fe(tot) in those areas of elevated $\text{CH}_{4(\text{aq})}$, is not observed (Fig. 4-11), while Fe(II) is distributed ubiquitously throughout the domain and does not appear more abundant in areas of elevated $\text{CH}_{4(\text{aq})}$ (Fig. 4-8c,e). Therefore a correlation between $\text{CH}_{4(\text{aq})}$ oxidation and reductive dissolution of Fe(III)-bearing phases is not supported by field data.

Overall, this conceptual model appears to provide a reasonable representation of the $\text{CH}_{4(\text{aq})}$ concentrations observed in the field, provided AMO or a significant lag time

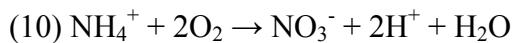
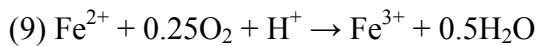
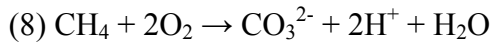
prior to $\text{CH}_{4(\text{aq})}$ inflow into the domain are invoked. As noted in section 4.3.1 it is likely that $\text{CH}_{4(\text{aq})}$ is produced upgradient of the domain; however, direct investigation of the mechanisms responsible for the latter were beyond the scope of this study. Previously, in microcosms containing oil sand fine tailings collected from the MLSB, Holowenko et al. (2001), suggested that residual bitumen not captured during the extraction process, may act as an electron donor capable of stimulating methanogenesis. Thus, within the tailings sand, it is conceivable that oxidation of residual bitumen first depletes SO_4 , followed by the production of $\text{CH}_{4(\text{aq})}$. Subsequent transport of dissolved $\text{CH}_{4(\text{aq})}$ towards the domain may lead to mixing with groundwater containing SO_4 , giving rise to the coexistence of the latter two components, as observed in the study area.

5.7 Conceptual Model 2 – Advection of Reduced Inorganic Components and Oxidation of CH_2O

5.7.1 Specific Model Parameters

Based on the shortcomings of the previous conceptual model in describing the distribution of dissolved Fe(II) and Mn(II) in the domain, it was hypothesized that in addition to Fe(II) and Mn(II) entering the domain, a source of degradable organic carbon is present within the plume. Support for this line of reasoning is a decreasing trend in biological oxygen demand (BOD) downgradient from the tailings impoundment, from 18 mg L^{-1} in monitoring well 1B to $<2 \text{ mg L}^{-1}$ in monitoring well 4B (Fig. 5-4). To validate the relationship between BOD and the presence of degradable organic carbon, the BOD exerted by $\text{CH}_{4(\text{aq})}$ and dissolved inorganic components, Fe(II), Mn(II), NH_4^+ must be accounted for (Table 5-9). Some uncertainty with regards to the significance of these components on BOD measurements is acknowledged, for example, it is not clear that each component is completely oxidized during the 5 day test. Furthermore, $\text{CH}_{4(\text{aq})}$ may be volatilized during sample preparation and dissolved Mn(II) and Fe(II) may be oxidized because a preservative is not used. Despite these uncertainties, a conservative estimate of the amount of organic carbon owing to BOD, termed residual BOD, was performed assuming all inorganic constituents are completely oxidized based on reactions 8, 9 and 10. This analysis was performed on samples collected near the upgradient boundary of the domain (monitoring wells 1B and 2C), in order to provide an estimate of the inflow

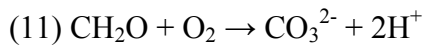
concentration of degradable organic carbon. The concentrations of reduced inorganic components, $\text{NH}_4^+(\text{aq})$, $\text{Fe}(\text{II})$ and $\text{CH}_{4(\text{aq})}$, were based on the maximum previously recorded concentrations at each sampling point.



The effect of dissolved $\text{Mn}(\text{II})$ on these calculations was assumed negligible, because maximum recorded concentrations at sampling points described in Table 5-9 were less than 0.1 mg L^{-1} in all cases. Although the absolute values of BOD are similar at the two sampling points, Table 5-9 indicates that potentially all the BOD in monitoring well 1B could be attributable to $\text{CH}_{4(\text{aq})}$ and inorganic components. This is in contrast to monitoring well 2C, where less than half of measured BOD is attributable to oxidation of $\text{CH}_{4(\text{aq})}$ and inorganic components. This serves to highlight the uncertainty regarding the contribution of $\text{CH}_{4(\text{aq})}$ and dissolved inorganic components to BOD. This exercise also indicates that if present, the quantity of reduced organic carbon is small, because it is easily occluded by the presence of low concentrations of $\text{CH}_{4(\text{aq})}$ and other dissolved inorganic components. In order to proceed with Conceptual Model 2, monitoring well 2C, where $\text{CH}_{4(\text{aq})}$ and reduced inorganic components are less prolific, was selected to estimate reduced organic carbon ($\text{C-CH}_2\text{O}$) for the entire input boundary. By applying the estimate obtained from monitoring well 02C to the entire input boundary, the amount of $\text{C-CH}_2\text{O}$ entering via the upper portion of the input boundary is uncertain and may in reality be largely absent. Furthermore the application of BOD measurements for defining the concentration of reducible, dissolved components should be viewed only as an estimate. Simply this method assumes that all reducible components are capable of being completely oxidized within the 5 day timeframe of the BOD test. Although the BOD test suggests that small concentrations of reducible components are dissolved in the

plume, additional analysis is necessary to properly define the flux and nature of reducible components entering the domain.

Based on the residual BOD calculated for monitoring well 2C, an inflow concentration of 4 mg L^{-1} C-CH₂O ($9 \text{ mg-CH}_2\text{O L}^{-1}$) was calculated using (11) (Table 5-9).



Anaerobic CH_{4(aq)} oxidation is thought to preclude reductive dissolution reactions (Gal'chenko, 2004) and because its occurrence is relatively isolated along the input boundary, CH_{4(aq)} is not included in the input function for conceptual model 2 or included in the estimate of CH₂O-C. Not considering CH_{4(aq)} input via the plume also provides the opportunity to determine if CH_{4(aq)} observed near the upgradient boundary, could be produced within the domain. The remaining component concentrations for both input boundaries and initial conditions are listed in Table 5-2.

The concentrations of Fe(II) and Mn(II) entering the domain via the plume described in Conceptual Model 1 are also implemented in this case. Generally the composition of the process water entering the domain in Conceptual Models 1 and 2 is identical with the exception that dissolved CH₂O is incorporated in Conceptual Model 2. With the exception of NO₃, which is not detected within the domain, the potential for CH₂O oxidation via commonly observed terminal electron accepting processes (TEAPs), O₂, Fe(III), Mn(III/IV), SO₄ and CO₂ utilization was considered (Table 5-7). Secondary mineral precipitation-dissolution reactions were represented as reversible, equilibrium driven, kinetic reactions for FeCO₃, MnCO₃, and CaCO₃ (Table 5-7). Rate constants, half saturation and inhibition constants for each reaction have been calibrated or estimated using values from the literature as guidelines (Table 5-8).

5.7.2 Results and Discussion - 1D Simulations

Redox Sensitive Components

Although, the simulation predicts that each TEAP will occur to some degree at all points in the domain, inhibition terms and differing reaction rates give rise to dominant TEAP(s), similar to that documented by Ludvigsen et al. (1998). Specifically, proliferation of Fe(III) and Mn(IV) reduction are predicted at the expense of SO_4 reduction and methanogenesis (Fig. 5-5b). Numerically this arises from inhibition terms embedded in the Monod equation (Table 5-8), whereas physically, this could represent competitive exclusion between bacterial populations mediating the different TEAPs. Competitive exclusion of this form, has been well documented by Lovley et al. (1986) and Lovley et al. (1987) and is consistent with the conceptual model. Particularly, that dissolved Fe(II) and Mn(II) are produced in the domain, while $\text{CH}_{4(\text{aq})}$ originates upgradient of the domain. Accordingly, lower than expected SO_4^{-2} in monitoring well 1B appears more plausibly related to the oxidation of $\text{CH}_{4(\text{aq})}$, rather than oxidation of CH_2O .

Simulations indicate that aerobic degradation rates will increase near the front of the plume (Fig. 5-5b). However, in reality degradation in these areas may be unreasonable, because during numerical simulations, CH_2O mobility is not restricted by sorption. Given that the actual form of reduced organic carbon is unknown, it is not possible to reliably define sorption parameters. The major consequences of increased CH_2O mobility are shifting of the oxic/anoxic interface and extending the dissolved Mn(II) and Fe(II) plumes downgradient. In terms of evaluating the overall applicability of the conceptual model, this effect was not considered significant.

Due to low absolute reaction rates associated with the reduction of dissolved electron acceptors, $\text{O}_{2(\text{aq})}$, SO_4 and $\text{CO}_{2(\text{aq})}$, Fe(III) and Mn(III/IV) are predicted by the simulations to become the primary electron acceptors (Figs 5-5b,c). Of note, the low absolute reaction rates associated with methanogenesis support an origin for $\text{CH}_{4(\text{aq})}$ upgradient of the domain, as employed in Conceptual Model 1. Overall, the major trends in dissolved Fe(II) and Mn(II) observed in the field data are well replicated using this

conceptual model (Fig. 5-5a). The general sequence, whereby a peak in dissolved Mn(II) is observed near the front of the plume, followed by a Fe(II) peak upgradient, is relatively well mirrored in the simulations and conforms to the commonly predicted (Chapelle, 2001) and observed (Bjerg et al., 1995) succession of redox zones in reducing plumes (Figs 4-8b,c and 5-5a).

Due to the limited quantity of the electron donor, reductive dissolution of FeOOH and MnO₂ is not predicted to lead to significant depletion of these phases (Fig. 5-5d). This is consistent with the initial assumption when creating the domain, that volume fractions of FeOOH and MnO₂ defined by the extractions are similar to those prior to the arrival of the plume. Generally the maximum effective reaction rates for the reductive dissolution of FeOOH and MnO₂ obtained by calibration are 1 to 3 orders of magnitude lower than those reviewed in Mayer et al. (2001) (Table 5-8). Although little is known regarding the identity of the electron donor, it is possible that the lower reaction rates may be related to recalcitrance of this/these component(s). Despite the slow reaction rates specified during simulations, Fe(III) and Mn(IV) reduction occurs concomitantly throughout the modeling domain, with Mn(IV) reduction occurring more quickly due to its higher maximum effective reaction rate (Table 5-8 and Fig. 5-5b). Although inhibition of Fe(III) reduction in the presence of MnO₂ is not expected (Lovley et al., 1988), simulations required higher reaction rates for Mn(IV) relative to Fe(III) reduction to more closely match the field data. This requirement may not necessarily reflect inhibition or a difference in kinetics between the two reactions. Rather it may be a consequence of additional MnO₂ reduction by dissolved Fe(II) (Lovley et al., 1988). Regardless of this possibility, the net quantity of Fe(II) and Mn(II) produced is expected to be similar whether a kinetic advantage or reduction by dissolved Fe(II) is in fact causing the observed concentrations. For simplicity MnO₂ reduction by Fe(II) was not incorporated into simulations.

Decreasing concentrations of dissolved Mn(II), as noted in the upgradient portion of the plume, are represented using MnCO₃ precipitation in simulations. The likelihood of MnCO₃ acting as the solubility controlling solid for Mn(II) is consistent with the

elevated alkalinity (Fig. 4-5c) and observations by Lovley et al. (1988). As mentioned above, exhaustion of Mn(III/IV) in the solid phase is not observed in extractions and is not expected to contribute to Mn(II) decline near the upgradient boundary (Fig. 5-5d). The calibrated maximum effective rate constant (Table 5-8) for MnCO₃ precipitation, is consistent with the sluggish precipitation kinetics observed by Jensen et al. (2002) in laboratory studies designed to mirror typical groundwater conditions.

Conversely, although oversaturation with respect to siderite (FeCO₃) is predicted (Fig. 4-9b), numerical simulations indicated that all dissolved Fe(II) will be removed from solution at FeCO₃ precipitation rates greater than $1 \times 10^{-14} \text{ mol L}^{-1}(\text{bulk}) \text{ s}^{-1}$. In essence, suggesting that FeCO₃ precipitation and the presence of dissolved Fe(II) are mutually exclusive. For example, an area within the modeling domain exists where reductive dissolution of FeOOH persists, while FeCO₃ precipitation has ceased (Fig. 5-5c) and the absence of an accumulation of dissolved Fe(II) in this area of the domain, illustrates the negligible impact of the FeCO₃ precipitation on aqueous Fe(II) concentrations during simulations (Fig. 5-5a). As discussed with regards to MnCO₃ precipitation, it is possible that FeCO₃ precipitation is also limited by kinetics (Jensen et al., 2002). Additionally it may be possible that low concentrations of dissolved Fe(II) strongly limit FeCO₃ precipitation. For example, in other cases where FeCO₃ precipitation has been observed, dissolved Fe(II) concentrations are typically tens to hundreds of mg L⁻¹ (Tuccillo et al., 1999, Liu et al., 2001, Roh et al., 2003 and Zachara et al., 2003).

1D simulations based on Conceptual Model 2, provided a reasonable approximation of the redox zonation observed within the study area. Specifically, the peak of Mn(II) observed downgradient and the broad distribution of dissolved Fe(II) throughout much of the plume are well replicated. 2D simulations, discussed below, were used for a more detailed investigation of the redox geochemistry and other components present in the plume.

5.7.3 Results and Discussion - 2D Simulations

Redox Sensitive Components

The distributions and concentrations of dissolved Fe(II) and Mn(II) within the plume predicted using 2D simulations are similar to that predicted using 1D simulations (Fig. 5-6b,c). During 2D simulations mineral precipitation and dissolution rates similar to those used in 1D simulations were found to provide a reasonable fit to the field data. Due to the similarity of the reaction rates in both cases, an illustration of the distribution of the minerals phases within the 2D domain, to which the reaction rates apply is deemed more informative (Fig. 5-7d,e,f,g,h). Reductive dissolution reactions cause depletion of MnO₂ near the upgradient boundary of the modeling domain (Fig. 5-7d); however, MnO₂ volume fractions throughout the domain are maintained within the range defined by Na-Ascorbate extractions (See Fig 5-5d for range). The decrease in the FeOOH volume fraction near the upgradient boundary of the modeling domain is less significant due to its higher initial volume fraction (Fig. 5-7e).

The predicted appearance of MnCO₃ and FeCO₃ is constrained to the upgradient portion of the plume, where HCO₃⁻ remains elevated. Due to the maximum effective reaction rates assigned to each, increased precipitation of MnCO₃ is noted relative to FeCO₃, yet the predicted overall increase in the volume fraction of each is small (Fig. 5-7f,g). When the maximum changes in volume fractions observed in the modeling domain are expressed on a weight basis, FeCO₃ and MnCO₃ precipitation yield an increase of less than 0.1 mg g⁻¹ of Fe(II) and Mn(II) in the solid phase, respectively. Similarly dissolution of FeOOH and MnO₂ are predicted to yield a decrease of less than 0.1 mg g⁻¹ of Fe(III) and Mn(IV) respectively. Overall, changes of this magnitude are expected to be below the resolution of solid phase extractions. Again this is consistent with the relatively constant volume fractions of these phases predicted by the Na-Ascorbate extraction (Fig. 4-11 and Fig. 5-5d).

In 2D simulations, absolute reaction rates for SO₄ reduction and methanogenesis (Fig. 5-7b,c) remain similar to those observed in 1D simulations. In addition to

predicted elevated absolute aerobic degradation rates near the plume front, absolute aerobic reaction rates are predicted to be elevated upgradient, near the drainage ditch at the toe of the tailings dyke, where recharge is higher (Fig. 5-7a). When aerobic degradation was not considered, significant changes to the distribution of CH₂O concentrations in this area were not observed (results not shown). This is believed to result from low transverse vertical dispersivity, which limits vertical mixing at the top of the plume.

Overall the pH and alkalinity values generated by the model (Fig 5-6g,h) are consistent with the field measured values (Fig 4-5b,c). As discussed in Section 2.2, elevated alkalinity observed in the plume is a function of the extraction process and the aqueous geochemistry of connate water in the oil sand. Similarly, the alkaline pH observed near the upgradient boundary is also a function of NaOH used during the extraction process. During the simulations, the elevated initial alkalinity of the plume serves to buffer the comparatively smaller changes in alkalinity and pH related to reactions occurring within the domain.

Cl and Major Cations

Although some influence on plume geometry by heterogeneous porous medium properties is expected, generally the overall shape of the Cl plume in 2D simulations is suitably replicated using a single K value (Fig. 5-8a). However, to some degree, this interpretation is due to the coarse vertical and lateral distribution of the sampling points, which is envisioned to mask plume heterogeneity. K determined through calibrations using the 2D domain, $4.4 \times 10^{-5} \text{ m s}^{-1}$, is consistent with the arithmetic average defined through slug testing. It is possible that K values displayed in Figure 4-2d which deviate by more than an order of magnitude from the calibrated result are representative of smaller-scale, localized material properties or do not form continuous layers along the flowpath. Furthermore, when estimating K using steady state simulations, it is unknown what impact historical changes in the hydraulic gradient may have on flow velocities and thus the estimation of K.

Despite the relatively large scale of the domain, it is encouraging to note that using commonly accepted selectivity coefficients (Appelo and Postma 1999) and averaging CECs derived in the laboratory, a reasonable approximation of major cation distribution observed in the field is obtained (Fig. 5-8b,c,d). Again, it should be noted that this may reflect the coarse resolution of the field data.

Generally, the 2D simulations predict that mass action effects cause Na to displace Ca and Mg from the exchange sites, producing retardation of Na versus Cl, similar to that observed in the field (Fig. 4-2). Mass action effects are also predicted to yield areas of elevated aqueous concentrations of Ca and Mg near the leading edge of the plume (Fig. 5-8b,c), termed (hardness) halos by other authors (Dance et al., 1993). It is difficult to confirm the presence of these halos using field evidence, because monitoring well placement near the leading edge of the plume is sparse. However, some increases in dissolved Ca and Mg concentrations are noted in monitoring well nest 5 (Fig. 5-9a,b).

Lastly, the model predicts that liberation of Ca from the exchange sites, combined with elevated alkalinity will cause CaCO₃ oversaturation and subsequent precipitation near the upgradient boundary of the domain (Fig. 5-7h). In previous studies regarding zero valent iron permeable reactive barriers, precipitation of secondary minerals has been associated with noticeable lowering of effective porosity, thus altering the hydraulic properties of the porous medium (Blowes et al., 1992, Mayer et al., 2001). In this case, the decrease in porosity, predicted to occur via CaCO₃ dissolution is small, <1%. Furthermore, the impact of CaCO₃ precipitation on bulk aquifer mineralogy is considered insignificant when compared to much larger natural fluctuations observed in extraction data (Fig. 4-11). Additional effects, such as the potential for precipitation of CaCO₃ coatings on mineral surfaces, reducing mineral reactivity in areas near the tailings impoundment, was not assessed during this study.

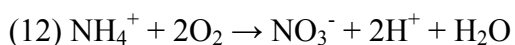
NH_4^+

Numerical simulations indicate that the retardation of NH_4^+ relative to Cl is approximately 3 (Fig. 5-6f and Fig. 5-8a). This is comparable to the range, 2.0 to 3.5,

noted by Ceazan et al. (1989) in an aquifer with a similar CEC (approximately 0.5 meq 100 g⁻¹). Ceazan et al. (1989) attributed the retardation primarily to cation exchange. Likewise, in the literature, cation exchange is often noted to impart the largest control on NH₄⁺ attenuation in the subsurface (Christensen et al., 2001, Buss et al., 2004, van Breukelen et al., 2004). Similarly, cation exchange is also predicted to be the major attenuation mechanism acting on NH₄⁺ present in the plume of process-affected water.

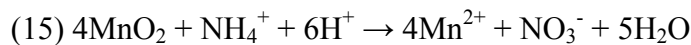
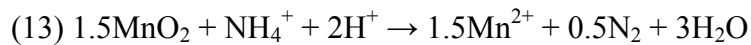
Commonly referenced sources (Appelo and Postma, 1998) and previous studies on landfill leachate plumes have indicated that NH₄⁺ typically has a higher affinity for exchange sites than Ca, Mg and Na (Thornton et al., 2000). This relationship may not apply to the current study, as decreasing NH₄⁺ selectivity below that of Ca and Mg was determined to best represent the NH₄⁺ migration distance during model calibrations. However it should be noted that other factors, such as variable input concentrations of exchangeable cations or a lag time prior to NH₄⁺ entering the domain could also yield an apparent lower selectivity for NH₄⁺.

Although numerical simulations are able to suitably represent the overall extent of the NH₄⁺ plume, a more thorough review indicates that in points near the water table, field concentrations are often lower than numerical results (Fig. 5-9c and Fig. 5-6f). Although, this may simply be related to source function variability, the location of these discrepancies suggests that lower than expected NH₄⁺ concentrations may be related to aerobic NH₄⁺ oxidation during mixing with meteoric recharge (12).



Although sporadic appearances of NO₃²⁻ in monitoring well 1A suggest aerobic NH₄⁺ oxidation may occur, the impact of this process is mainly at the plume fringe and not on the overall geochemistry of the plume. For this reason, it was not considered during numerical simulations.

Anaerobic oxidation of NH_4^+ using NO_3^{2-} as an electron acceptor is well established (Mulder et al., 1995, van de Graaf et al., 1995, Schmidt et al., 2002). However, because NO_3^{2-} is below detection limits throughout most groundwater samples collected from within the plume, anaerobic nitrification coupled with NO_3 reduction was not considered significant. Nitrification, using $\text{Fe}(\text{OH})_3$ -Fe(III) as an electron acceptor is not considered thermodynamically favourable at neutral pH (Luther III et al., 1997, Anschutz et al., 2000). Alternatively, in marine sediments, anaerobic nitrification via the reductive dissolution of Mn(III) or Mn(IV) bearing phases has been suggested by numerous authors (e.g. Luther III et al., 1997, Hulth et al., 1999, Anschutz et al., 2000) and is considered thermodynamically favourable in these settings at neutral pH (Luther III et al., 1997, Hulth et al., 1999). After Anschutz et al. (2000) nitrification via this mechanism is hypothesized to occur via the following reactions:



Based on the results of Thamdrup et al. (2000) and a review by Hulth et al. (2005), anaerobic nitrification via reductive dissolution of Mn-oxides has not been directly observed, only inferred based on pore water chemistry. Research directly evaluating anaerobic oxidation of NH_4^+ using MnO_2 -Mn(IV) or MnOOH -Mn(III) as electron acceptors in the subsurface is limited and evidence based on the field data at hand is not easily ascertained. Firstly, N_2 concentrations were not measured. Secondly, the absence of NO_3 in the plume cannot be used to refute anaerobic nitrification, because reduction of NO_3 to N_2 could be driven by other reduced components in the plume. Thirdly, although dissolved Mn(II) is observed in groundwater samples, it is not possible

to determine if its release is related to NH_4^+ oxidation, the oxidation of other reduced components or release from ion exchange sites.

As noted above, the attenuation of NH_4^+ in sandy soils by cation exchange has been well established in field and laboratory studies and may be used to reasonably account for the attenuation of NH_4^+ relative to Cl observed in the study area. Assuming the flux of NH_4^+ into the domain has remained constant, a higher selectivity coefficient for NH_4^+ would have been derived, if in addition to cation exchange, anaerobic oxidation of NH_4^+ is occurring. However further discussion is limited, because based on the field data, convincing evidence supporting or disproving anaerobic NH_4^+ oxidation by Mn(III/IV) oxidation is not available.

Identity of the Electron Donor(s)

Compared to the results from Conceptual Model 1, those of Conceptual Model 2 indicate that, although only present in a small quantity, an electron donor capable of producing Fe(II) and Mn(II) provides a better match to the distributions of dissolved Fe(II) and Mn(II) observed in the field. Because the identity of this electron donor(s) is unclear, numerical simulations presented above may be used to focus speculation regarding the nature of the electron donor(s). Firstly, as noted above, numerical simulations suggest that the concentration of the electron donor is small, less than 10 mg L^{-1} of C- CH_2O . Secondly, low calibrated FeOOH and MnO_2 reduction rates suggest that it is necessary for the electron donor to exhibit some persistence, in order to provide the elongated distribution of dissolved Fe(II) and Mn(II) noted throughout the plume. This is consistent with the absence of more readily degradable organic electron donors such as monoaromatics and non-volatile fatty acids.

As discussed above, although NH_4^+ oxidation may be related to Mn(III/IV) reduction, it is not believed to be related to Fe(III) reduction. It is possible that NH_4^+ oxidation may account for some of the dissolved Mn(II) observed in the study area. However, an electron donor capable of mediating reductive dissolution of Fe(III)-bearing

phases is also necessary based on Conceptual Model 2. For this same reason, $\text{CH}_{4(\text{aq})}$ is not believed to be a suitable candidate for the electron donor.

NAs form the most readily available source of organic carbon in the plume and as such remain the most obvious electron donors. Although evidence of NA degradation was not observed, degradation of the amounts suggested by Conceptual Model 2, could be masked by variability in field data. Based on the discussion of Holowenko et al. (2001), partial degradation of the NA molecule may occur via beta oxidation of the carboxylated side chain. In this scenario, the beta oxidation step may become rate limiting, while the reaction products, Acetate and H_2 would be quickly oxidized, limiting their appearance.

Alternatively, non-volatile fatty acids (NVFAs) have been identified to represent the largest fraction of dissolved organic carbon at the Bemidji Minnesota site (Thorn et al., 1998). In this case NVFAs are believed to arise from partial oxidation of crude oil (Thorn et al., 1998). If a parallel is drawn to the current setting, partial degradation of residual bitumen within the tailings dyke, may also yield the release of NVFAs. Analysis for NVFAs such as humic and fulvic acids was not performed, however the low reactivity of these compounds is consistent with the suggestions of Conceptual Model 2.

5.8 Model Sensitivity and Error

5.8.1 Model Sensitivity

Model sensitivity was evaluated using a 1D domain and altering CEC, initial solution composition and maximum effective reaction rates for FeOOH , MnO_2 , FeCO_3 and MnCO_3 . Particular attention was given to the second conceptual model involving CH_2O .

Naturally the distributions of dissolved Fe(II) and Mn(II) are sensitive to the amount of electron donor entering the system. However, when the concentration is decreased by half ($\text{C-CH}_2\text{O } 2.0 \text{ mg L}^{-1}$), the general distribution of Fe(II) and Mn(II) observed in field data could still be replicated (Fig. 5-10g). This suggests that the

concentration of the electron donor(s) may be quite small, but an electron donor is still required based on the results of Conceptual Model 1.

In conceptual model 2, CH_2O is oxidized using both FeOOH and MnO_2 as electron acceptors, such that the reaction rate of each represents a balance. Increasing the FeOOH reaction rate by an order of magnitude serves to significantly increase the amount of Fe(II) in solution (Fig. 5-10a). At the same time, this increase reduces the amount of CH_2O available for reductive dissolution of MnO_2 and accordingly reduces the amount of the Mn(II) released into solution (Fig. 5-10a). Much faster CH_2O consumption is incurred by increasing the MnO_2 reaction rate by an order of magnitude, resulting in more rapid exhaustion of CH_2O , such that Fe(II) and Mn(II) are absent in the downgradient half of the plume (Fig. 5-10b). Decreasing FeOOH reductive dissolution rates by an order of magnitude noticeably decreases dissolved Fe(II) within the plume but only slightly increases dissolved Mn(II) concentrations in the downgradient half of the plume (Fig. 5-10a). Conversely, decreasing the rate of MnO_2 dissolution by a similar magnitude, approximately doubles the concentrations of Fe(II) in the downgradient half of the plume, while significantly decreasing dissolved Mn(II) concentrations (Fig. 5-10b). Overall, because the rate of MnO_2 dissolution used in Conceptual Model 2 exceeds that of FeOOH dissolution by an order of magnitude, the concentrations of dissolved Fe(II) and Mn(II) are more sensitive to changes in the first.

Relative to that used for FeOOH dissolution, the rate of FeCO_3 precipitation used in Conceptual Model 2 is more than an order of magnitude larger. For this reason, the amount of dissolved Fe(II) in solution is less sensitive to further decreases in the rate of FeCO_3 (Fig. 5-10c). However, increasing the rate of FeCO_3 precipitation by an order of magnitude, causes almost complete removal of dissolved Fe(II) near the input boundary (Fig. 5-10c). The opposite is true for MnCO_3 , whereby decreasing the reaction rate by one order of magnitude causes a significant surplus of Mn(II) , relative to field data, in the upgradient portion of the domain. On the other hand, increasing the rate has no incremental effect.

Increasing the initial background concentrations of dissolved cations is predicted to increase concentrations of these components near the leading edge of the plume. This observation results from the release of cations from exchange sites due to mass action effects related to the advancing plume. For example, an increase in background Fe(II) and Mn(II) by 1 order of magnitude to 0.5 mg L^{-1} does not significantly affect results (Fig. 5-10e). However an increase of 2 orders of magnitude yields distinctly higher concentrations of Fe(II) near the leading edge of the plume. Although Mn(II) does not appear to have significantly increased in this case, it is worthwhile to mention that when an initial concentration of 5 mg L^{-1} is used, MnO_2 is not required to produce the peak of Mn(II) observed in the downgradient half of the plume. Although the limited background geochemical data does not support Mn(II) and Fe(II) background concentrations of 5 mg L^{-1} , it is worthwhile to note the effect of initial solution composition when interpreting aqueous geochemistry near the leading edge of the plume.

Varying CEC within the range determined by Marsh (2006) is observed to yield small shifts in the peaks in dissolved Fe(II) and Mn(II) (Fig. 5-10f). Generally, because such a narrow range of CECs is defined, the impact of using different values within this range is not significant.

A discussion and comparison of predicted to measured hydraulic head is provided in Appendix E. Furthermore calibration exercises for dispersivity and recharge are also shown in Appendix E.

5.8.2 *Mass Balance*

Based on the results of the numerical simulations, Tables 5-10 and 5-11 are provided to further highlight the impact of various processes on aqueous geochemistry. Specifically the importance of processes controlling the dissolved Fe(II), Mn(II) and CH_2O concentrations within each conceptual model are evaluated.

It is notable that the inflow of Fe(II) from the upgradient boundary accounts for a significant portion of Fe(II) in the plume in all simulations. Conversely, the relative

importance of Mn(II) originating from the upgradient boundary is minimal relative to that predicted to be produced within the plume by reductive dissolution of MnO₂.

With regards to the second conceptual model, the mass balance calculations help elucidate the relative impacts of carbonate precipitation and cation exchange on Mn(II) and Fe(II) removal from solution in the modeling domain. For example, relative to cation exchange reactions, MnCO₃ precipitation is predicted to impart a stronger control on dissolved Mn(II) concentrations. Whereas, the slower precipitation kinetics assigned to FeCO₃, reduce the effect of the latter on dissolved Fe(II) concentrations relative to cation exchange.

Shown in Table 5-12 is the relative importance of each TEAP for the degradation of CH₂O for Conceptual Model 2. The contribution of SO₄ and methanogenesis to the mass loss of CH₂O is insignificant, whereas O₂, FeOOH and MnO₂ represent much more significant TEAPs during simulations. Although confined to areas near the water table and plume front, the predicted impact of aerobic oxidation is similar to that of FeOOH reduction. This is a result of lower maximum effective reaction rates assigned for FeOOH reduction and a lower per mole oxidation capacity of FeOOH (1:4) relative to O_{2(aq)} (1:1) for CH₂O. The increased maximum effective reaction rate and oxidation capacity of 1 mole MnO₂ (1:2) coupled with anaerobic conditions throughout the plume interior, allows MnO₂ to impart the largest control on CH₂O oxidation during simulations.

During simulations of Conceptual Model 2, the perceived dominance of MnO₂ reduction with regards to CH₂O oxidation is a reflection of the conceptualization of the geochemical system. In order to simulate the observed distributions of dissolved Fe(II) and Mn(II), higher maximum effective reaction rates have been assigned to MnO₂ reduction as well as the inhibition of FeOOH reduction in the presence of MnO₂ (Tables 5.7 and 5.8). In reality, dissolved Mn(II) may arise through other mechanisms aside from CH₂O mediated reductive dissolution of Mn(III/IV) bearing minerals, such as Fe(II) mediated reductive dissolution of such phases. Thus it is important to acknowledge that

Fe(III) may account for a larger proportion of the oxidation of CH_2O , than that assumed based on numerical simulations.

5.9 Implications of Reactive Transport Modeling

Based on the field data, it appeared probable that the plume of process affected water was weakly reducing. The reactive transport modeling was used to evaluate this quantitatively and served to highlight that indeed this may be the case and specifically that oxidation of low concentrations of electron donors are able to give rise to the presently observed distribution of redox indicators. The reactive transport modeling served to highlight the difficulty in assigning dominant TEAPs based solely on aqueous geochemical data. Based on Fig 4-8f, Fe(III) reduction was considered the domain TEAP throughout a large portion of the plume, whereas, in Conceptual Model 2, Mn(IV) reduction is predicted to be the dominant TEAP throughout most of the plume, based on absolute reaction rates. Although based on simulations of sparse field data, this outcome can be used to emphasize the importance of secondary intra-aqueous and mineral precipitation-dissolution reactions when considering redox conditions. In addition to assessing redox conditions, simulations were helpful in considering the processes controlling the mobility of inorganic components: Cl, Na and NH_4^+ . Notably, simulations suggested that the mobility of Na and NH_4^+ are controlled by cation exchange processes.

Overall, the simulations were useful in identifying mechanisms giving rise to general trends and patterns presently observed in the geochemistry. It is not possible to use the simulations to evaluate small scale features within the study, because many of the input parameters for the simulations represent generalizations of the physical and geochemical properties of the study area. For example variations in hydraulic conductivity within the sand aquifer were not taken into account and many of the initial and input boundary geochemical conditions represent averages of analytical data. A major limitation when considering the results of the simulations, is that minimal field data is available regarding the history of the plume. Specifically, field data regarding the historical flux of process water into the domain and the chemical composition of these waters is not available. For this reason, steady-state conditions are assumed and flow

system dynamics and aqueous and solid phase geochemistry based on that presently observed are used when considering the evolution of the plume. If the flux of process affected water or the concentrations of dissolved components within the latter have varied dramatically in the past, the transport velocities, reaction rates and attenuative mechanisms described above, could in fact be quite different. If used for predictive purposes, the implications of steady-state conditions are significant. For example, if increasing or decreasing trends in component concentrations or hydraulic gradients are present, their effects will not be considered and the predicted solution may overestimate or underestimate the true outcome. For these reasons, the simulations should only be considered as a tool to supplement the interpretation of the field data.

6.0 Implications for Metal Release and Mobility

On the order of tens of $\mu\text{g L}^{-1}$ or less of heavy metals and oxyanions, collectively referred to as trace metals, are observed in the plume (Table 6-1). Generally concentrations in the upper range of those shown in Table 6-1 are observed in monitoring wells near the edge of the tailings dyke (distribution not shown). Concentrations of trace metals in tailings impoundment water and dyke construction water (MacKinnon, 1989) are comparable to those in process-water-impacted groundwater. This similarity suggests that leaching of additional trace metals from the aquifer solids during seepage from tailings dykes has not been significant. This is consistent with the weakly reducing nature of the plume, which suggests that the potential for trace metal mobilization via reductive dissolution reactions is low. However, despite the presently interpreted weakly reducing nature of the plume, an evaluation of trace metal content in the solid phase was considered appropriate in order to gauge the potential for future trace metal release if the character of the plume became more reducing. This possibility has been suggested (Gadd et al., 2000 and Lloyd et al., 2001) and demonstrated by various authors (e.g. Quantin et al., 2001, Quantin et al., 2002, Bennett et al., 2002 and Keimowitz et al., 2005) but for other situations. Notably, studies regarding As mobilization under reducing conditions are numerous in the literature (see review by Smedley et al., 2002).

Solid phase extraction supernatant was analyzed to estimate the quantity of trace metals present in reducible phases (Table 6-2 and 6-3). Generally trace metal concentrations are on the order of a few mg kg^{-1} (ppm) or less in both the 0.5M and 5.0M HCl extractions, while none were detected in supernatant from the Na-Ascorbate extraction. The latter may be related to interference from elevated sodium concentrations ($>25,000 \text{ mg L}^{-1}$), which increased the detection limit for trace metals to approximately 100 mg kg^{-1} .

Even if extractable, release of small quantities of Cd, Co, Cr, Cu, Ni, Pb and Zn are not expected to present an environmental risk at circumneutral pH, due to strong adsorption on negatively charged mineral surface sites (Smedley et al., 2002). For

example, in silty sediments, Lee et al. (1997) estimated that log sorption coefficients (pKd) for Cd, Pb and Zn were above 3.6 mL g⁻¹ at circumneutral pH. Similarly, Tessier et al. (1985) reviewed numerous sources and also calculated elevated retardation of heavy metals on (oxy)hydroxides in lake sediments based on in-situ pore water measurements.

Of the oxyanion forming elements, Se is not expected to be mobile, due to stronger adsorption of Se⁴⁺, the predominant form in reducing conditions (Plant et al., 2003 and Smedley et al., 2002). Additionally, the solubility of Se²⁻ and Se⁰ is expected to be low in reducing conditions (Plant et al., 2003 and Smedley et al., 2002). Conversely, As may remain mobile in reducing environments at circumneutral pH due to the formation of oxyanions in these settings (Smedley et al., 2002). However, low extractable concentrations of As in aquifer material (Table 6-2 and 6-3) are expected to limit release during reductive dissolution reactions. The maximum amounts of As removed, 3 and 4 mg kg⁻¹ using the 0.5M and 5.0M HCl extractions respectively, are similar to the average As crustal abundance of 1.5 mg kg⁻¹ (Plant et al., 2003). A comparison to cases where As release to groundwater has proven problematic, indicates that concentrations of total As in the solid phase are at least 1 order of magnitude larger (Keimowitz et al., 2005 and Bennett et al., 2002). It should be noted that the As solubilized by the 0.5M HCl and 5.0M HCl extractions don't represent the total As in the solid phase, rather only As present in reducible phases in addition to As associated with monosulfides, carbonate minerals and ion exchange sites (Table 3-3). Alternatively, concentrations of extractable As determined using the HCl based extractions are similar in magnitude to the minimum values specified for the range of As in oxide and carbonate minerals in Smedley et al. (2002). This comparison provides a more appropriate comparison when declaring a low potential for As release from the aquifer solids within the study area via reductive dissolution reactions.

7.0 Implications for Aquatic Toxicity

The potential contributors to acute aquatic toxicity from oil sands process water are NH_4^+ , NAs, BTEX compounds, PAHs and trace metals. Only NH_4^+ and NAs were found at significant concentrations in the plume at this site.

Figure 7-1 illustrates the relationships between NH_4^+ and NA concentrations and acute toxicity, where the latter is determined using the Microtox™ bioassay. Microtox results are reported as the effective concentration of original sample (% volume volume⁻¹), required to produce a 20 percent decline in photoluminescence emitted by the Microtox bacteria over a 15 minute period ($\text{EC}_{20}(15\text{min})$). For example a result of 25 % volume volume⁻¹ indicates that 1:4 dilution of the original sample will induce the appropriate toxic response. For this study, Microtox testing is useful as a screening method to determine which components are correlated most strongly with acute toxicity.

The results shown in Figure 7-1a are consistent with previous studies at Syncrude, which have indicated that acute toxicity in process water is strongly correlated to NA concentration (MacKinnon and Boerger, 1986, Verbeek et al., 1993 & Schramm, 2000). Although $\text{NH}_3/\text{NH}_4^+$ may contribute to acute aquatic toxicity, the correlation with Microtox toxicity is much weaker than with NAs (Fig. 7-1b). The poor correlation between $\text{NH}_3/\text{NH}_4^+$ and Microtox toxicity is a function of the elevated tolerance of the Microtox bacteria to NH_3 (Stronkhorst et al., 2003).

Because NA biodegradation is not suggested by the field data (Section 4.2.1), reduction in acute toxicity likely reflects decreases in NA concentrations (Fig. 7-1), via weak sorption and dispersive dilution.

8.0 Conclusions

Of the possible contributors to aquatic toxicity, PAHs, BTEX compounds, metals, NH_4^+ and NAs, only the latter two were found to be present in significant quantities in the plume. Furthermore, Microtox toxicity is most strongly related to NAs, which is consistent with the work of previous researchers.

NAs were found to be recalcitrant in the subsurface. Sorption in the sandy aquifer was deemed minimal, while a lack of evidence for biodegradation is consistent with the anaerobic microcosm results of previous researchers. Given the relatively conservative behaviour of NAs in the subsurface, the primary control on NA mobility will be the physical dynamics of the groundwater flow field.

Data obtained from groundwater sampling and solid phase extractions provided evidence for a weakly reducing plume. However, the processes giving rise to these conditions are largely unknown. The results of the reactive transport modeling support an origin for Fe(II) and Mn(II) within the transect, via oxidation of a yet-to-be identified electron donor. The use of Fe(III) and Mn(III/IV) as the primary electron acceptors is assumed based on the preferential use of the latter, rather than SO_4 and CO_2 and the anaerobic state of the plume as it enters the domain. Although the simulations suggested that Mn(IV) was the dominant TEA during CH_2O oxidation, in reality Mn(IV) reduction via Fe(II) oxidation may contribute to this observation.

The results of reactive transport modeling and the availability of more easily reduced electron acceptors Fe(III) and Mn(III/IV), indicates that $\text{CH}_{4(\text{aq})}$ observed in a localized portion of the input boundary most likely originates upgradient of the transect. Within the transect, anaerobic $\text{CH}_{4(\text{aq})}$ oxidation may occur, based on distinctly lower SO_4 concentrations in groundwater samples containing elevated $\text{CH}_{4(\text{aq})}$. However, the interpretation of $\text{CH}_{4(\text{aq})}$ attenuation, resulting from comparison to conservative tracers, may simply be a result of a large lag time prior to $\text{CH}_{4(\text{aq})}$ influx into the domain.

Groundwater samples analyzed for acetate, formate, PAH and BTEX compounds, indicated that concentrations of these compounds were not sufficient to give rise to the reducing conditions observed in the plume. It is hypothesized that both NVFAs and NAs could act as electron donors, capable of giving rise to the reducing conditions observed in the plume. However, further research is required to evaluate these possibilities. The presence of a weakly reducing plume implies that trace metal release via reductive dissolution reactions is limited relative to a strongly reducing case. Furthermore, a lack of significant amounts of extractable trace metals in the solid phase is also expected to ultimately limit trace metal release, should the plume become more strongly reducing in the future.

Numerical simulations were also employed to evaluate the processes governing the distribution of NH_4^+ and major ions, Cl, Ca, Mg and Na in the domain. Implementing a transient geochemical boundary condition and using the average of laboratory derived CECs, a reasonable match was observed between the distribution of major ions observed in the field and that predicted by numerical results. The predicted distribution of NH_4^+ closely mirrored that observed in the field, suggesting that cation exchange acts as the primary control on NH_4^+ mobility. Anaerobic oxidation of NH_4^+ via reductive dissolution of Mn(III/IV)-bearing solid phases was not directly evaluated using the code. Furthermore, field data did not provide strong evidence with respect to the occurrence or absence of this process.

TABLES

Table 3-1
Summary of Laboratory Analysis

Groundwater Sampling Event	UWOGL ^a	Analytical Laboratory		Syncrude ^d
		PSC ^b	ETL ^c	
September 2004	Quant-NA ^c , CH ₄ (aq)	Cations, Anions, NO ₃ , NO ₂ and NH ₃	-	Ca, K, Mg, Na, Cl, SO ₄ and Quant-NA
October 2004	BTEX ^g , PAH ^h , Qual- NA	-	-	-
June 2005	Quant-NA, CH ₄ (aq), BTEX, PAH, Acetate	-	Cations, Anions, NO ₃ , NO ₂ , NH ₃ and Microtox	-
November 2005	-	-	BOD ⁱ	-

^a UWOGL – University of Waterloo Organic Geochemistry Laboratory

^b PSC – PSC Analytical Services (Mississauga, Ontario)

^c ETL – Enviro-Test Labs (Edmonton, Alberta)

^d Syncrude – Syncrude Canada Ltd. Research Department (Edmonton, Alberta)

^e Quant-NA - Quantitative Naphthenic Acid Analysis

^f Qual-NA – Qualitative Naphthenic Acid Analysis

^g BTEX – Benzene, Toluene, Ethylbenzene and Xylene Compounds

^h PAH – Polycyclic Aromatic Hydrocarbons

ⁱ Biological oxygen demand

Table 3-2
Summary of Analytical Methods for Inorganic Parameters

Parameter	Analytical Laboratory		
	PSC ^a	ETL ^b	Syncrude ^c
Major Cations (Ca, K, Mg, Na)	ICP-MS ^d	ICP ^e	ICP ^e
Fe, Mn	ICP-MS ^d	ICP ^e	-
Cl	IC & CD ^f	CT ^g	IC & CD ^f
SO ₄	IC & CD ^f	ICP-OES ^h	IC & CD ^f
Trace Metals (Al, As, B, Ba, Be, Cd, Co, Cr, Cu, Mo, Ni, Pb, Sb, Se, Sn, Sr, Ti, V, Zn)	ICP-MS ^d	ICP-MS ^d	-
NH ₃ -N	CT ^g	CT ^g	-
NO ₂ , NO ₃	IC & CD ^f	CT ^g	-

^a PSC – PSC Analytical Services (Mississauga, Ontario)

^b ETL – Enviro-Test Labs (Edmonton, Alberta)

^c Syncrude – Syncrude Canada Ltd. Research Department (Edmonton, Alberta)

^d ICP-MS - Inductively Coupled Plasma – Mass Spectrometry

^e ICP – Inductively Coupled Plasma – Atomic Emission Spectroscopy

^f IC & CD – Separation by Ion Chromatography and detection with a conductivity detector.

^g CT – Automatic Colorimetric Techniques

^h ICP-OES - Inductively Coupled Plasma – Optical Emission Spectrometry

Table 3-3
 Overview of Solid Phase Extractions

Extraction	Target Phase	Reference
0.5M HCl	Ion Exchangeable metals, carbonates, amorphous (oxy)hydroxides, monosulphides	Heron et al. (1994)
5.0M HCl	Ion Exchangeable metals, carbonates, amorphous (oxy)hydroxides, monosulphides, silicates	Heron et al. (1994)
Na-Ascorbate	Ion Exchangeable metals, amorphous (oxy)hydroxides, monosulphides	Amirbahman et al. (1998)
Chittick	Carbonates	Dreamanis et al. (1962)
Acid Volatile Sulphides (AVS)	Monosulphides	Canfield (1986)

Table 4-1

Summary of Previous Sorption Studies of Naphthenic Acids

Kd ^a	Sorbent	pH	Source
<1	Quartz Sand	9.3	1
1	Kaolinite	8.5	1
2	Illite	7.0	1
2 – 3	Montmorillonite	7.0	1
<1	Tailings Sand	8.5	1
2 – 3	Extraction Fines	7.5	1
0.18 ^b	Sand from Syncrude Gravel Pit	7.0 – 8.0	2

¹ Schramm et al. 2000

² Gervais 2004

^a Soil – Water partition coefficient (mL g⁻¹)

^b Estimated for this study, based on linear regression of experimental data

Table 4-2

Criteria for Determining Dominant Redox Process (Based on Lyngkilde et al. 1992)

Parameter	Methanogenic	Sulfate Reducing	Iron Reducing	Manganese Reducing	Nitrate Reducing	Aerobic
CH _{4(aq)}	>1	<1	<1	<1	<1	<1
SO ₄	<40	-	-	-	-	-
Fe(aq)	-	-	>1.0	<1.0	<1.0	<1.0
Mn(aq)	-	-	-	>0.2	<0.2	<0.2
NH ₄ ⁺	-	-	-	-	-	<1
NO ₃	<0.2	<0.2	<0.2	<0.2	-	-
NO ₂	<0.1	<0.1	<0.1	<0.1	>0.1	<0.1
O _{2(aq)}	<1	<1	<1	<1	<1	>1

Concentrations are in mg L⁻¹

Table 4-3
 Dissolved Monoaromatic Concentrations¹ (June 2005)

Compound	Plume	Background
Benzene	<2 – 5 (<2) ²	<2
Toluene	All <2	<2
Ethylbenzene	All <1	<1
p+m-Xylene	All <2	<2
o-Xylene	All <1	<1

¹ Concentrations are in $\mu\text{g L}^{-1}$

² Values represent the minimum – maximum and arithmetic average of all measurements

Table 5-1
Physical Parameters Used during Reactive Transport Simulations

Parameter	Unit	1D Simulations	2D Simulations
Temperature	°C	10	10
Effective Porosity	%	see Figure 5-1	25
Hydraulic Conductivity	m s ⁻¹	6.3 x 10 ⁻⁵	4.4 x 10 ⁻⁵
Longitudinal Dispersivity	m	1	1
Transverse Vertical Dispersivity	m	-	0.005
Free Phase Aqueous Diffusion Coefficient	m s ⁻²	1.0 x 10 ⁻⁹	1.0 x 10 ⁻⁹
Hydraulic Gradient	m m ⁻¹	3.6 x 10 ⁻³	3.6 x 10 ⁻³
Length of Domain	m	900	900
Horizontal Discretization Interval	m	5	5
Height of Domain	m	1	7.5
Vertical Discretization Interval	m	-	0.1
Final Solution Time	year	27	27

Table 5-2

Inflow and Initial Aqueous Geochemistry (Concentrations in mg L⁻¹)

Parameter	Upper Inflow Boundary ^a	Lower Inflow Boundary	Initial Conditions and Meteoric Recharge ^b
Ca ^c	1.3 x 10 ¹	7.2 x 10 ¹	6.7 x 10 ¹
CH _{4(aq)}	8.1 x 10 ^{-2 e}	8.1 x 10 ⁻²	5.0 x 10 ⁻⁴
Cl ^c	1.7 x 10 ²	3.2 x 10 ^{2 d}	4.0 x 10 ⁰
CO ₃ ^f	1.2 x 10 ³	1.2 x 10 ³	2.9 x 10 ²
Fe(II) ^d	1.6 x 10 ⁰	3.0 x 10 ⁰	5.0 x 10 ⁻²
pH	7.94	7.64	7.53
HS ^g	3.3 x 10 ⁻⁶	3.3 x 10 ⁻⁶	3.3 x 10 ⁻⁶
K ^c	3.2 x 10 ⁰	2.4 x 10 ⁰	1.3 x 10 ⁰
Mg ^c	3.4 x 10 ⁰	1.2 x 10 ⁰	1.6 x 10 ¹
Mn(II) ^d	2.3 x 10 ⁻¹	7.6 x 10 ⁻²	4.4 x 10 ⁻²
Na ^c	5.3 x 10 ²	5.7 x 10 ²	2.5 x 10 ¹
NH ₄ ^{+ d,h}	4.2 x 10 ⁰	8.9 x 10 ⁻¹	1.4 x 10 ⁻¹
O _{2(aq)}	1.0 x 10 ^{-5 i}	1.0 x 10 ^{-5 i}	2.1 x 10 ^{0 j}
SO ₄ ^c	1.3 x 10 ^{2 k}	2.0 x 10 ²	3.5 x 10 ¹

^a Also inflow concentration for 1D simulations

^b Also initial condition for 1D simulations

^c Average of results from Syncrude Canada, PSC Analytical Services and Enviro-Test Labs

^d Average of results from Phillip Analytical Services and Enviro-Test Labs

^e In order to evaluate areas of elevated CH_{4(aq)}, 1.8 mg L⁻¹ was used during 1D simulations.

^f Based on field measurements of Alkalinity (June 2005)

^g Not measured, assumed low

^h Laboratory results reported as NH₃-N. Converted to NH₄⁺, assuming all N in NH₄⁺ form

ⁱ Despite trace quantities detected in field measurements, assumed low

^j This value decreased to 3.2 x 10⁻⁶ mg L⁻¹ for grey sand

^k Based only on values from monitoring well 1A

Table 5-3

Initial Mineral Volume Fractions (expressed as fraction of bulk porous medium)

Portion of Aquifer	Calcite (CaCO ₃)	Pyrolusite (MnO ₂)	Goethite (FeOOH)
Red Sand ^a	5.1 x 10 ⁻³	5.9 x 10 ⁻⁶	2.3 x 10 ⁻⁴
Grey Sand ^a	6.9 x 10 ⁻³	5.3 x 10 ⁻⁶	1.5 x 10 ⁻⁴

^a Refer to Figure 5-2 for illustration of location within domain

Table 5-4
Summary of Cation Exchange Parameters

Cation Exchange Reaction	Selectivity Coefficient ($K_{b/a}$) ^a
$\text{Na-X} + 0.5\text{Ca}^{2+} \rightarrow \text{Na}^+ + 0.5\text{Ca-X}_2$	3.33 ^b
$\text{Na-X} + 0.5\text{Fe}^{2+} \rightarrow \text{Na}^+ + 0.5\text{Fe-X}_2$	1.67 ^c
$\text{Na-X} + 0.5\text{Mg}^{2+} \rightarrow \text{Na}^+ + 0.5\text{Mg-X}_2$	2.50 ^b
$\text{Na-X} + 0.5\text{Mn}^{2+} \rightarrow \text{Na}^+ + 0.5\text{Mn-X}_2$	1.82 ^c
$\text{Na-X} + \text{K}^+ \rightarrow \text{Na}^+ + \text{K-X}$	1.43 ^e
$\text{Na-X} + \text{NH}_4^+ \rightarrow \text{Na}^+ + \text{NH}_4\text{-X}$	1.43 ^d
Cation Exchange Capacity	0.66 meq 100 g ⁻¹ ^f

^a $K_{b/a} = \frac{[a][b-X]}{[a-X][b]}$ Where: $a\text{-X} + b \rightarrow a + b\text{-X}$

^b Decreased from average value presented in Appelo and Postma (1998) based on calibration

^c Based on Appelo and Postma (1998)

^d Increased from average value presented in Appelo and Postma (1998) based on calibration

^e Increased for consistency with NH_4^+ exchange coefficient

^f Note CEC was modified for 1D simulations based on the discussion in Section 5.2

Table 5-5

Conceptual Model 1 – Intra-Aqueous and Mineral Dissolution/Precipitation Reactions

Reaction	Stoichiometry
1	$\text{Fe}^{2+} + 0.25\text{O}_2(\text{aq}) + \text{H}^+ \rightarrow \text{Fe}^{3+} + 0.5\text{H}_2\text{O}$
2	$2\text{Fe}^{2+} + \text{MnO}_2 + 4\text{H}^+ \rightarrow 2\text{Fe}^{3+} + \text{Mn}^{2+} + 2\text{H}_2\text{O}$
3	$\text{Fe}^{3+} + 2\text{H}_2\text{O} \rightarrow \text{FeOOH} + 3\text{H}^+$
4	$\text{Mn}^{2+} + 0.25\text{O}_2(\text{aq}) + \text{H}^+ \rightarrow \text{Mn}^{3+} + 0.5\text{H}_2\text{O}$
5	$\text{Mn}^{3+} + 2\text{H}_2\text{O} \rightarrow \text{MnOOH} + 3\text{H}^+$
6	$\text{Ca}^{2+} + \text{CO}_3^{2-} \rightarrow \text{CaCO}_3$

Table 5-6

Conceptual Model 2 – Rate and Half Saturation Constants for Reactions in Table 5.5

Reaction	$\text{pK}_{\text{eq}}^{\text{a}}$	k^{b} ($\text{mol L}^{-1} \text{s}^{-1}$)	Half Saturation Constants K_{s} (mol L^{-1})		Inhibition Constants K_{i} (mol L^{-1})	
			K_{s} (electron donor)	K_{s} (electron acceptor)	K_{i} (Oxygen)	K_{i} (Fe(II))
1	-	$1.0 \times 10^{-8 \text{ d, k}}$	$1.0 \times 10^{-5 \text{ d}}$	$3.1 \times 10^{-6 \text{ d}}$	-	-
2	-	$1.0 \times 10^{-10 \text{ e, l}}$	$1.0 \times 10^{-5 \text{ g}}$	-	$3.1 \times 10^{-6 \text{ e}}$	-
3	-	$1.0 \times 10^{-6 \text{ f, l}}$	$1.0 \times 10^{-8 \text{ i}}$	-	$3.1 \times 10^{-6 \text{ e}}$	-
4	-	$1.0 \times 10^{-8 \text{ g, k}}$	$1.0 \times 10^{-5 \text{ g}}$	$3.1 \times 10^{-6 \text{ g}}$	$3.1 \times 10^{-6 \text{ e}}$	$1.0 \times 10^{-7 \text{ e}}$
5	-	$1.0 \times 10^{-6 \text{ f, l}}$	$1.0 \times 10^{-8 \text{ j}}$	-	$3.1 \times 10^{-6 \text{ e}}$	-
6	8.18 ^c	$1.0 \times 10^{-7 \text{ h, l}}$	-	-	-	-

^a Equilibrium constant^b Rate constant^c From WATEQ4F database^d Mayer 2002^e Estimated value^f Assume nearly instantaneous at circumneutral pH^g Based on Fe(II) oxidation reaction in Mayer (2002)^h Assumed quasi-equilibriumⁱ Half saturation for Fe(III) limitation. Assumed small, since dissolved Fe(III) is not expected at circumneutral pH^j Half saturation for Mn(III) limitation. Assumed small, since dissolved Mn(III) is not expected at circumneutral pH^k Rate constant ($\text{mol} [\text{L H}_2\text{O}]^{-1} \text{s}^{-1}$)^l Rate constant ($\text{mol} [\text{L bulk porous medium}]^{-1} \text{s}^{-1}$)

Table 5-7

Conceptual Model 2 – Intra-Aqueous and Mineral Dissolution/Precipitation Reactions

Reaction	Stoichiometry
1	$\text{CH}_2\text{O} + \text{O}_2(\text{aq}) \rightarrow \text{CO}_3^{2-} + \text{H}^+$
2	$\text{CH}_2\text{O} + 0.5\text{SO}_4^{2-} \rightarrow \text{CO}_3^{2-} + 0.5\text{HS}^- + 1.5\text{H}^+$
3	$\text{CH}_2\text{O} + 0.5\text{H}_2\text{O} \rightarrow 0.5\text{CO}_3^{2-} + 0.5\text{CH}_4 + \text{H}^+$
4	$0.5\text{CH}_2\text{O} + \text{MnO}_2 + \text{H}^+ \rightarrow 0.5\text{CO}_3^{2-} + \text{Mn}^{2+} + \text{H}_2\text{O}$
5	$0.25\text{CH}_2\text{O} + \text{FeOOH} + 1.5\text{H}^+ \rightarrow 0.25\text{CO}_3^{2-} + \text{Fe}^{2+} + 1.5\text{H}_2\text{O}$
6	$\text{Fe}^{2+} + \text{CO}_3^{2-} \leftrightarrow \text{FeCO}_3$
7	$\text{Mn}^{2+} + \text{CO}_3^{2-} \leftrightarrow \text{MnCO}_3$
8	$\text{Ca}^{2+} + \text{CO}_3^{2-} \leftrightarrow \text{CaCO}_3$

Table 5-8

Conceptual Model 2 – Rate and Half Saturation Constants for Reactions in Table 5.7

Reaction	$\text{pK}_{\text{eq}}^{\text{a}}$	k^{b} ($\text{mol L}^{-1} \text{s}^{-1}$)	Half Saturation Constants K_{s} (mol L^{-1})		Inhibition Constants K_{i} (mol L^{-1})		
			K_{s} (electron donor)	K_{s} (electron acceptor)	K_{i} (Oxygen)	K_{i} (MnO ₂)	K_{i} (FeOOH)
1	-	$1.0 \times 10^{-10 \text{ e, k}}$	$1.0 \times 10^{-5 \text{ h}}$	$3.1 \times 10^{-6 \text{ h}}$	-	-	-
2	-	$1.0 \times 10^{-13 \text{ e, k}}$	$1.1 \times 10^{-4 \text{ i}}$	$1.6 \times 10^{-4 \text{ i}}$	$3.1 \times 10^{-6 \text{ i}}$	$1.0 \times 10^{-8 \text{ e}}$	$1.0 \times 10^{-8 \text{ e}}$
3	-	$1.0 \times 10^{-13 \text{ e, k}}$	$1.0 \times 10^{-4 \text{ h}}$	-	$3.1 \times 10^{-6 \text{ i}}$	$1.0 \times 10^{-8 \text{ e}}$	$1.0 \times 10^{-8 \text{ e}}$
4	-	$1.0 \times 10^{-12 \text{ f, l}}$	$5.0 \times 10^{-4 \text{ j}}$	-	$3.1 \times 10^{-6 \text{ i}}$	-	-
5	-	$4.0 \times 10^{-13 \text{ f, l}}$	$5.0 \times 10^{-4 \text{ h}}$	-	$3.1 \times 10^{-6 \text{ i}}$	-	-
6	10.45 ^d	$1.0 \times 10^{-14 \text{ f, l}}$	-	-	-	-	-
7	10.39 ^d	$1.0 \times 10^{-12 \text{ f, l}}$	-	-	-	-	-
8	8.48 ^d	$1.0 \times 10^{-8 \text{ g, l}}$	-	-	-	-	-

^a Equilibrium constant^b Rate constant^d From WATEQ4F database^e Estimated value^f Calibrated value^g Assumed quasi-equilibrium^h (Mayer et al. 2002)ⁱ (Mayer et al. 2001)^j (Watson et al. 2003)^k Rate constant ($\text{mol [L H}_2\text{O}]^{-1} \text{s}^{-1}$)^l Rate constant ($\text{mol [L bulk porous medium]}^{-1} \text{s}^{-1}$)

Table 5-9
 Analysis of Contributors to Biochemical Oxygen Demand (BOD)

Monitoring Well ^a	Total Laboratory Derived BOD	Calculated Inorganic Oxygen Demand ^b			Residual BOD ^c	Equivalent Concentration of CH ₂ O ^d
		CH ₄	Fe(II)	NH ₄ ⁺		
1B	18	7.5	0.4	18.1	0	0
2C	14	0.4	0.6	3.4	9.6	9.0

^a See Figure 4-1 for locations

^b Based on equations 7, 8 and 9

^c Residual BOD = Total Laboratory Derived BOD – Calculated Inorganic Oxygen Demand

^d Calculated from residual BOD based on equation 10

Table 5-10
Total Sources and Sinks for dissolved Fe(II) in Plume

	Mass ^a	1D ^b % of Sources or Sinks	Mass	1D ^c % of Sources or Sinks	Mass	2D ^d % of Sources or Sinks
Sources						
<i>FeOOH</i>	-	-	1125 g	81 %	3644 g	68 %
<i>Inflow</i>	257 g	100 %	257 g	19 %	1688 g	32 %
Sinks						
<i>Cation Exchange</i>	215 g	97 %	788 g	69 %	2945 g	65 %
<i>FeCO₃</i>	-	-	351 g	31 %	1545 g	34 %
<i>Outflow</i>	7 g	3 %	7 g	<1 %	47 g	1 %
Δ Storage in						
Aqueous Phase	35 g	-	236 g	-	795 g	-

^a Rounded to nearest g

^b Based on the results of Conceptual Model 1 when MnO₂ reduction was not considered

^c Based on the results of Conceptual Model 2, using a 1D domain

^d Based on the results of Conceptual Model 2, using a 2D domain

Table 5-11
Total Sources and Sinks for dissolved Mn(II) in Plume

	Mass ^a	1D ^b % of Sources or Sinks	Mass	1D ^c % of Sources or Sinks	Mass	2D ^d % of Sources or Sinks
Sources						
<i>MnO₂</i>	-	-	2336 g	98 %	7050 g	97 %
<i>Inflow</i>	37 g	100 %	37 g	2 %	196 g	3 %
Sinks						
<i>Cation Exchange</i>	28 g	82 %	342 g	15 %	1676 g	25 %
<i>MnCO₃</i>	-	-	1870 g	84 %	4979 g	74 %
<i>Outflow</i>	6 g	18 %	6 g	<1 %	38 g	<1 %
Δ Storage in						
Aqueous Phase	4 g	-	155 g	-	553 g	-

^a Rounded to nearest g

^b Based on the results of Conceptual Model 1 when MnO₂ reduction was not considered

^c Based on the results of Conceptual Model 2, using a 1D domain

^d Based on the results of Conceptual Model 2, using a 2D domain

Table 5-12
 Total Mass of CH₂O Oxidized via each TEAP

CH₂O Sinks	1D^b		2D^c	
	Mass ^a Degraded	% of Total Mass Degraded	Mass Degraded	% of Total Mass Degraded
<i>Aerobic Oxidation</i>	60 g	7 %	461 g	16 %
<i>Sulfate Reduction</i>	<1 g	<1 %	<1 g	<1 %
<i>Methanogenesis</i>	<1 g	<1 %	<1 g	<1 %
<i>FeOOH Reduction</i>	150 g	18 %	489 g	17 %
<i>MnO₂ Reduction</i>	630 g	75 %	1925 g	67 %

^a Rounded to nearest g

^b Based on the results of Conceptual Model 2, using a 1D domain

^c Based on the results of Conceptual Model 2, using a 2D domain

Table 6-1

Summary of Dissolved Trace Metal Concentrations in Plume (mg L⁻¹)

Component	Range (Average)	Alberta Environment Freshwater Aquatic Life Guideline
As	<0.0004 - 0.0074 (0.0021)	0.005
Cd	<0.0001	0.018 ^a
Co	<0.0001 - 0.0053 (0.0012)	-
Cr	<0.0005 - 0.0037 (0.0030)	0.0089 ^b
Ni	<0.0003 - 0.015 (0.004)	0.025 ^c
Pb	<0.0002 - 0.0014 (0.0004)	0.001 ^c
Se	<0.0005 - 0.0027 (0.0013)	0.001
V	<0.0001 - 0.0062 (0.0017)	-
Zn	<0.004 - 0.162 (0.16)	0.030

^a Based on hardness of 50 mg L⁻¹ (CaCO₃)

^b Cr³⁺ guideline

^c Based on hardness within range of 0-60 mg L⁻¹ (CaCO₃)

Table 6-2

Trace Metal Content in 0.5M HCl Extraction Supernatant (mg g⁻¹)

Element	Range (Average ^a)			Limit of Quantitation
As	<0.001	- 0.003	(0.002)	0.1
Cd	<0.0001	- 0.0001	(0.0001)	0.001
Co	0.001	- 0.002	(0.001)	0.001
Cr	0.001	- 0.002	(0.001)	0.001
Cu	<0.001	- 0.004	(0.001)	0.001
Ni	0.001	- 0.003	(0.001)	0.001
Pb	<0.0002	- 0.0020	(0.0010)	0.001
V	0.001	- 0.010	(0.002)	0.001
Zn	0.001	- 0.012	(0.004)	0.001

^aArithmitic Average

Table 6-3

Trace Metal Content in 5.0M HCl Extraction Supernatant (mg g⁻¹)

Element	Range (Average ^a)			Limit of Quantitation
As	0.002	- 0.004	(0.002)	0.1
Cd	<0.0001	- 0.0002	(0.0001)	0.001
Co	0.001	- 0.003	(0.002)	0.001
Cr	0.001	- 0.009	(0.003)	0.001
Cu	0.001	- 0.006	(0.002)	0.001
Ni	0.001	- 0.004	(0.002)	0.001
Pb	0.0002	- 0.0110	(0.0020)	0.001
V	0.003	- 0.019	(0.005)	0.001
Zn	0.003	- 0.024	(0.007)	0.001

^aArithmitic Average

FIGURES

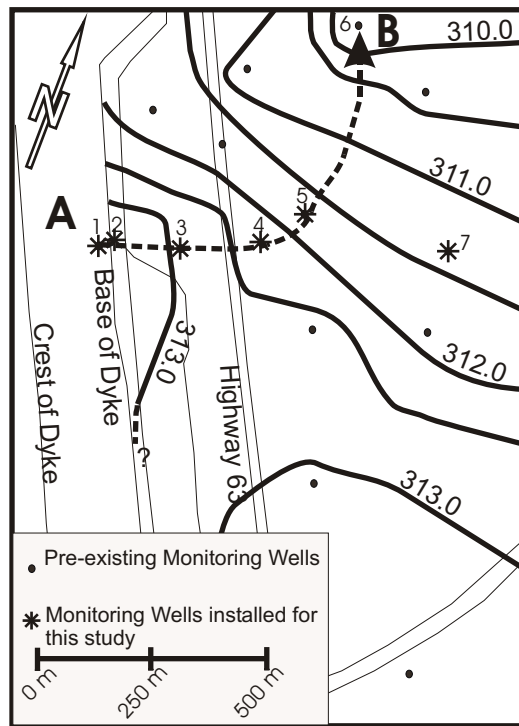
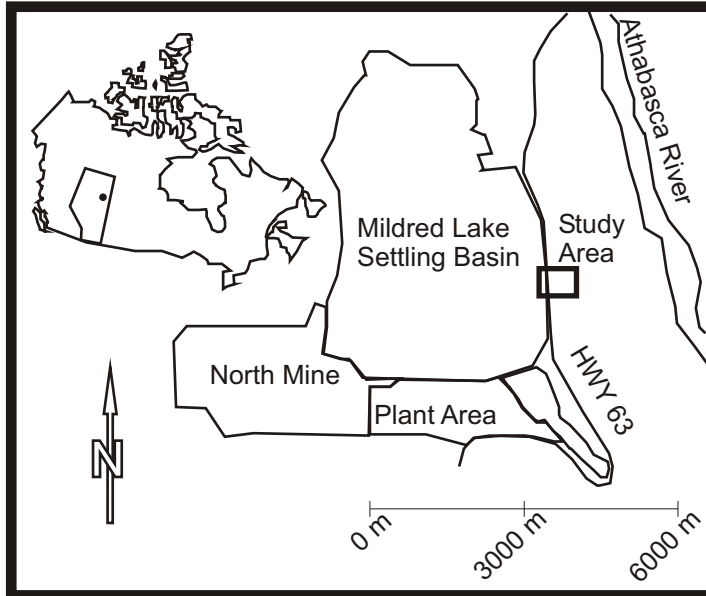


Figure 1-1 Location of study area (Top) and location of transect (Bottom).

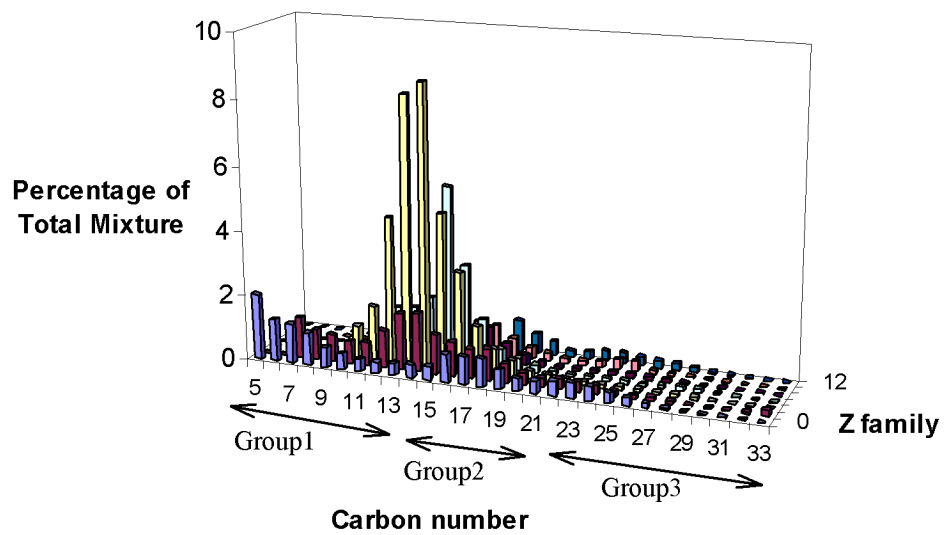


Figure 2-1 Illustration of GS-MS profile obtained using the characterization method for naphthenic acid mixtures of St. John et al. (1998), Holowenko et al. (2002) and Clemente (2003).

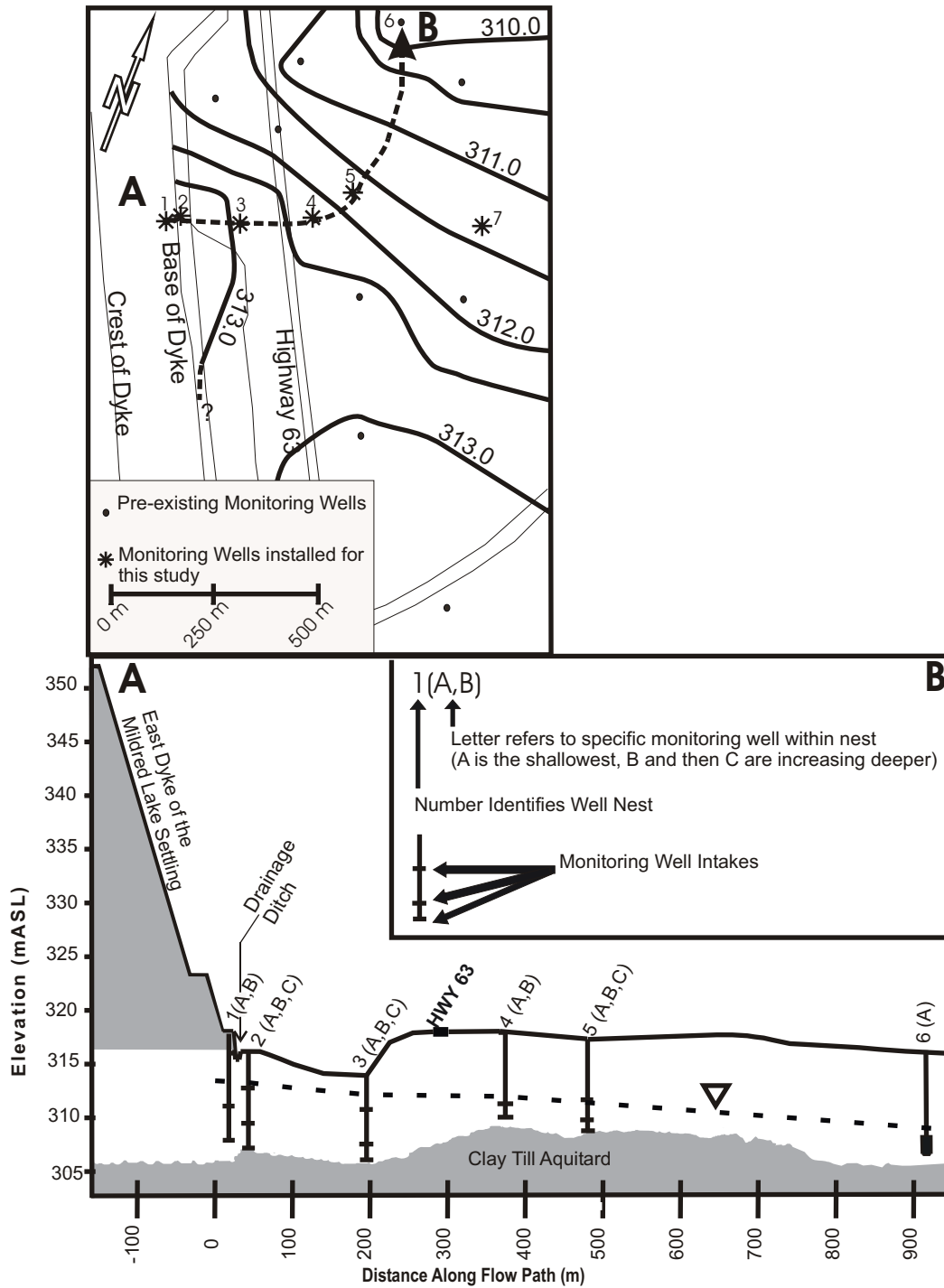


Figure 4-1 Water table surface as measured in November 2005 (Top) and illustration of monitoring well transect (Bottom). All elevations are meters above sea level (mASL). Flowpath represented by transect shown by arrow in top diagram.

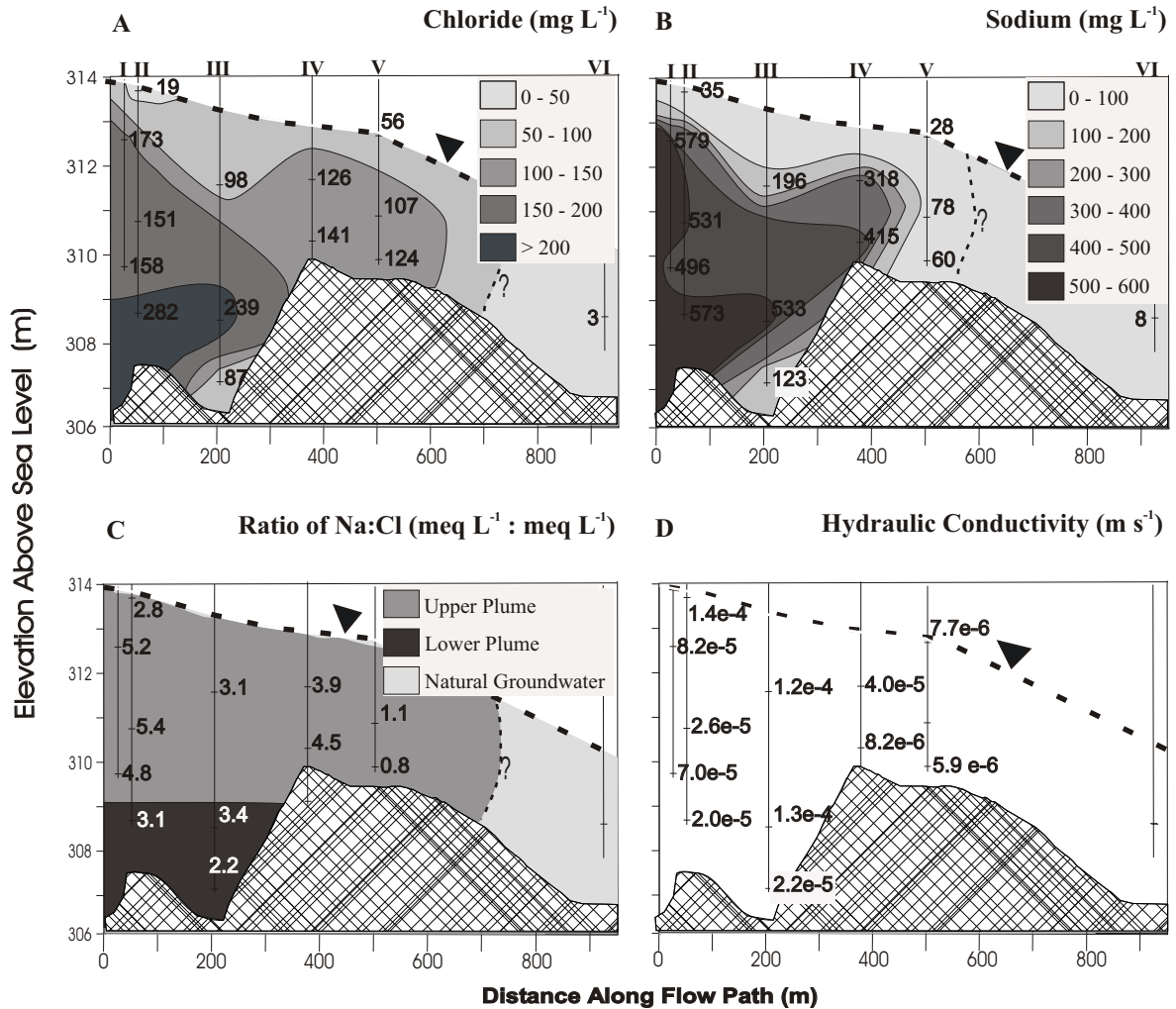


Figure 4-2 Transects showing Chloride (A) and Sodium (B) Distributions, Ratios of Sodium to Chloride in the Plume (C) and Hydraulic Conductivity measurements (D). All concentrations are in mg L^{-1} where the values represent the arithmetic average of all measured concentrations. The hydraulic conductivity measurements are in m s^{-1} and represent the arithmetic average of all slug tests performed at a given monitoring well. The ratio of Sodium:Chloride is determined in terms of meq L^{-1} . The location of the transect is shown in Figure 4-1. The roman numerals along the top of the top two figures represent the monitoring well nest number. The dotted line, with the inverted triangle represents the approximate location of the water table. The dotted line with the question mark represents the estimated front of the plume. The crosshatched area represents the aquitard.

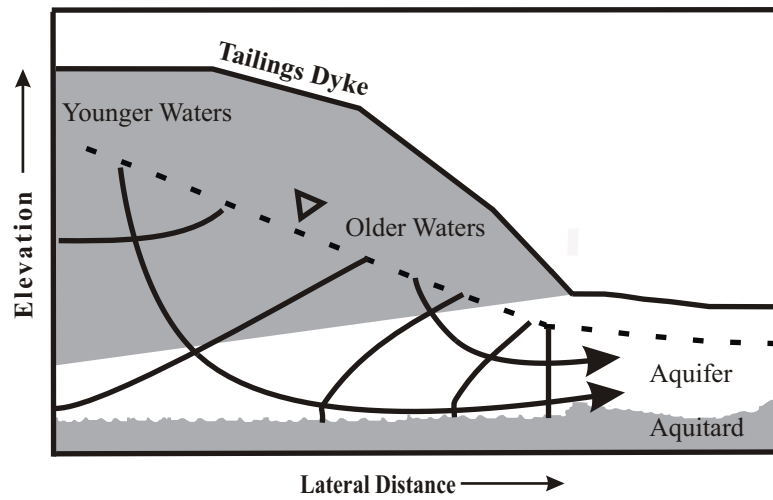


Figure 4-3 Non-quantitative flownet for dyke drainage. Shown are two hypothesized flowpaths and 5 hypothesized equipotential lines. The dashed line with the inverted triangle represents the hypothesized water table.

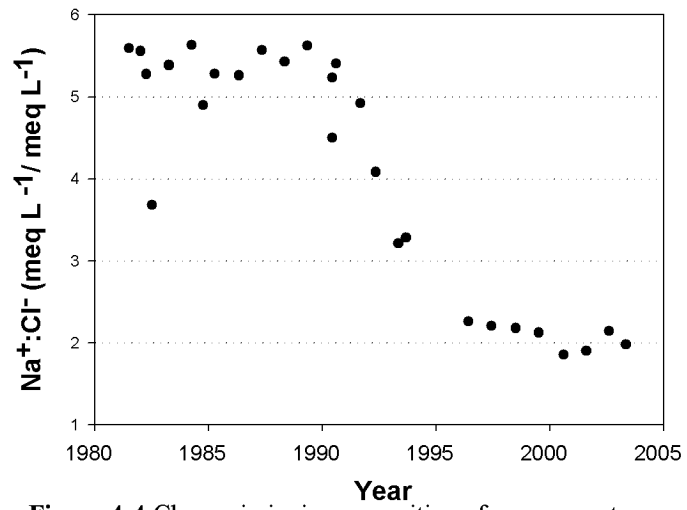


Figure 4-4 Change in ionic composition of process water contained in the MLSB (Syncrude 2003)

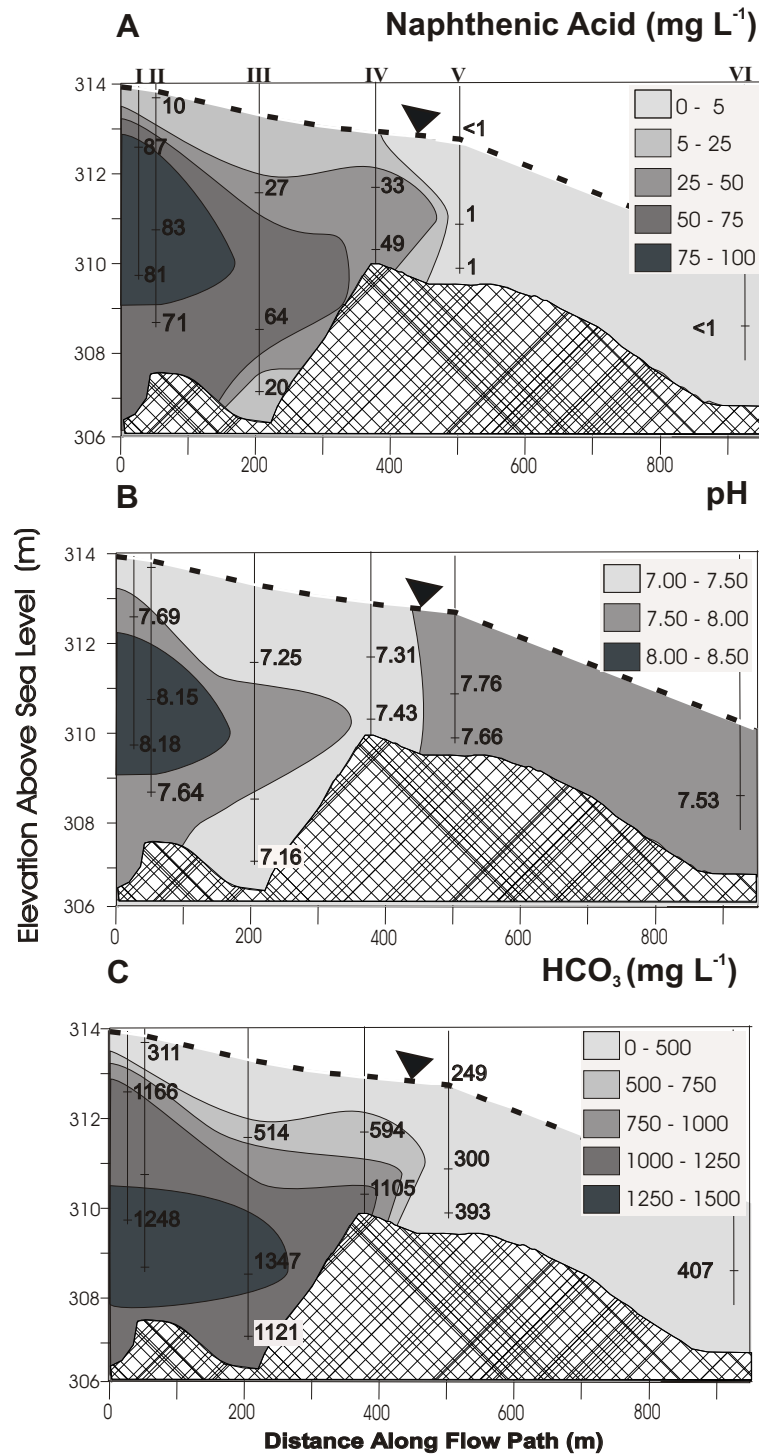


Figure 4-5 Transects showing naphthenic acid distribution (A), November 2005 field measured pH (B) and alkalinity (C). Naphthenic acid concentrations are in mg L^{-1} and represent the arithmetic average of all measured concentrations. Alkalinity is shown as HCO_3^- equivalent concentrations in mg L^{-1} based on measurements made during June 2005. The location of the transect is shown in Figure 4-1. The roman numerals at the top of the figure, refer to the well nest number. The dotted line, with the inverted triangle represents the approximate location of the water table. The crosshatched area represents the aquitard.

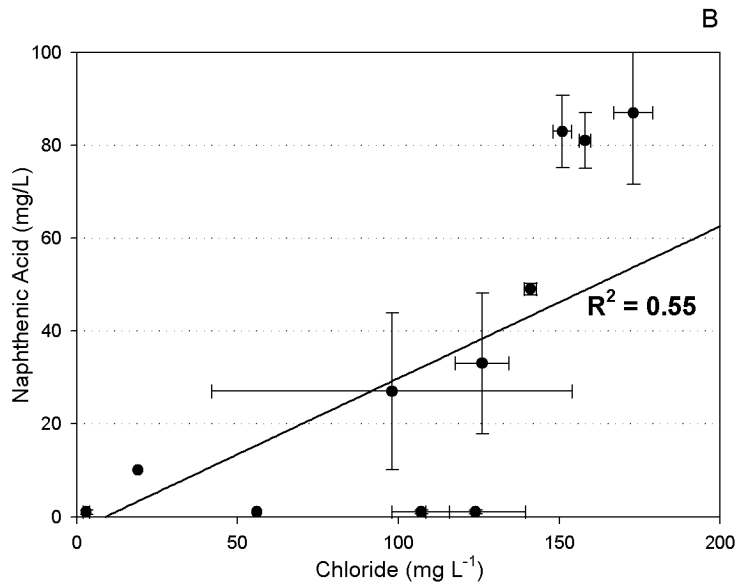
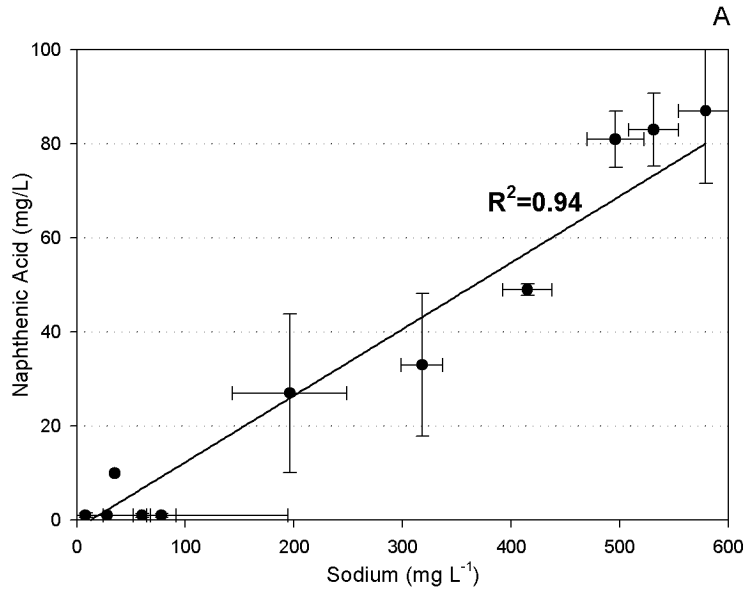


Figure 4-6 Comparison of aqueous naphthenic acid to sodium (A) and chloride (B) concentrations. All concentrations are based on arithmetically averaged values from September 2004 and June 2005 sampling events. Error bars represent one standard deviation.

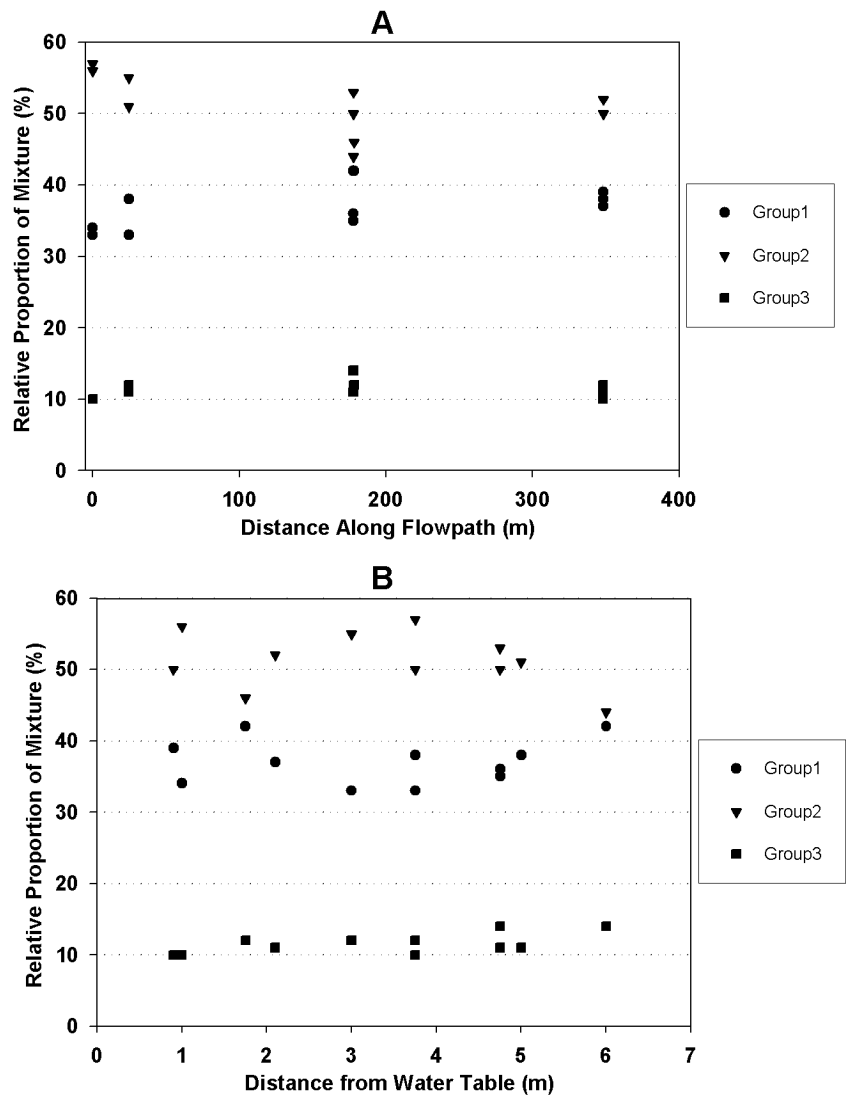


Figure 4-7 Naphthenic acid signatures versus distance from toe of tailings impoundment to plume front(A) and distance from water table (B) Group 1 (Circles), Group 2 (Triangles), Group 3 (Squares). Note, location of flowpath is shown in Figure 4-1

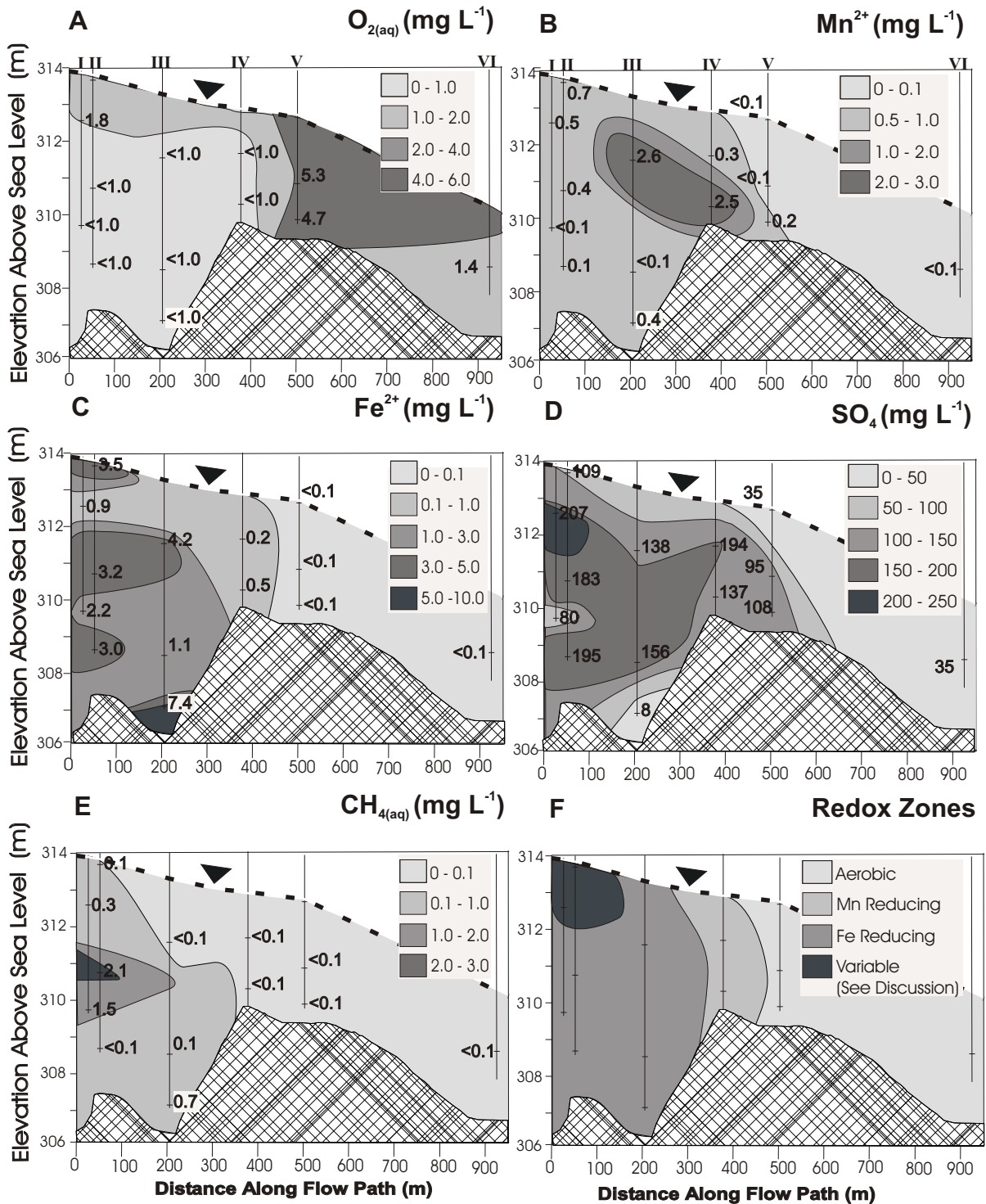


Figure 4-8 Transects showing dissolved oxygen (A), dissolved manganese (B), dissolved iron (C), dissolved sulfate (D), dissolved methane (E) distributions and interpreted redox zonation (F). Dissolved oxygen measurements were made on November 2005. Values shown for Manganese, Iron, Sulphate and Methane represent arithmetically averaged values based on samples collected during September 2004 and June 2005. All concentrations are shown in $mg L^{-1}$. Redox zones shown in (F) were assigned based on the criteria in Table 4-2. The location of the transect is shown in Figure 4-1. The roman numerals along the top figures refer to the monitoring well nests. The dotted line, with the inverted triangle represents the approximate location of the water table. The crosshatched area represents the aquitard.

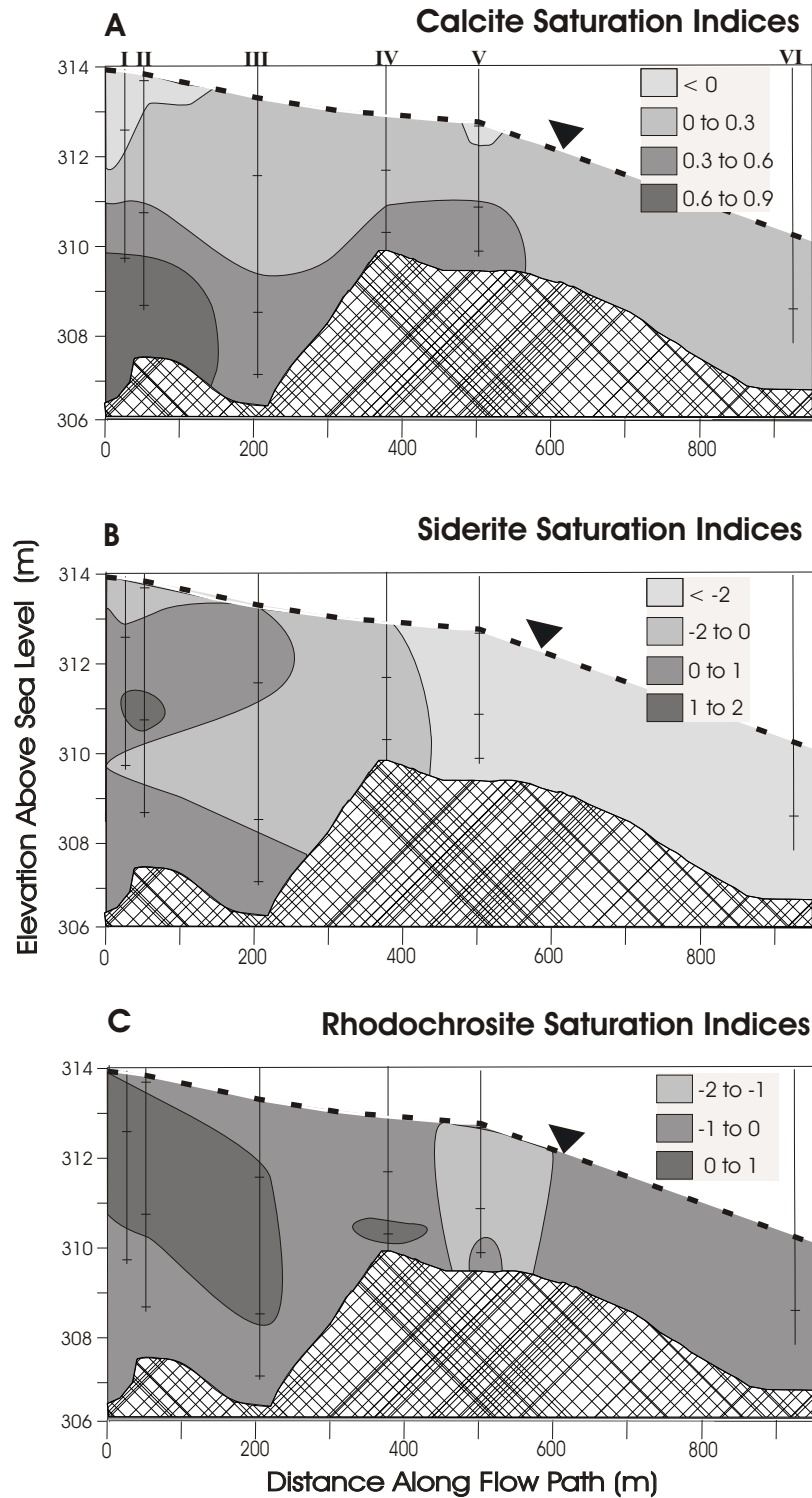


Figure 4-9 Carbonate Saturation Indices, Calcite (A), Siderite (B) and Rhodochrosite (C) Calcium, iron and manganese concentrations used during saturation index calculations are averaged values from the September 2004 and June 2005 sampling events. Alkalinity used during saturation index calculations is based on field measured values obtained June 2005. The location of the transect is shown in Figure 4-1. The roman numerals along the top of the uppermost figure refer to the well nest number. The dotted line, with the inverted triangle represents the approximate location of the water table. The crosshatched area represents the aquitard.

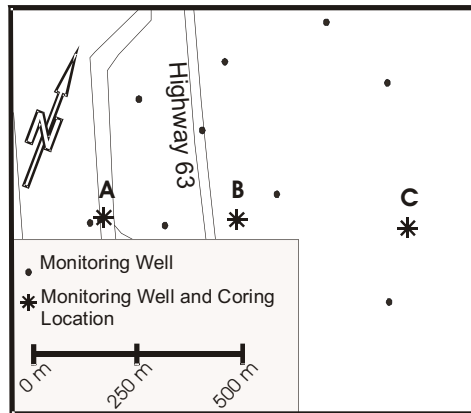


Figure 4-10 Soil coring locations. The area shown above is the same as that shown in Figure 4-1.

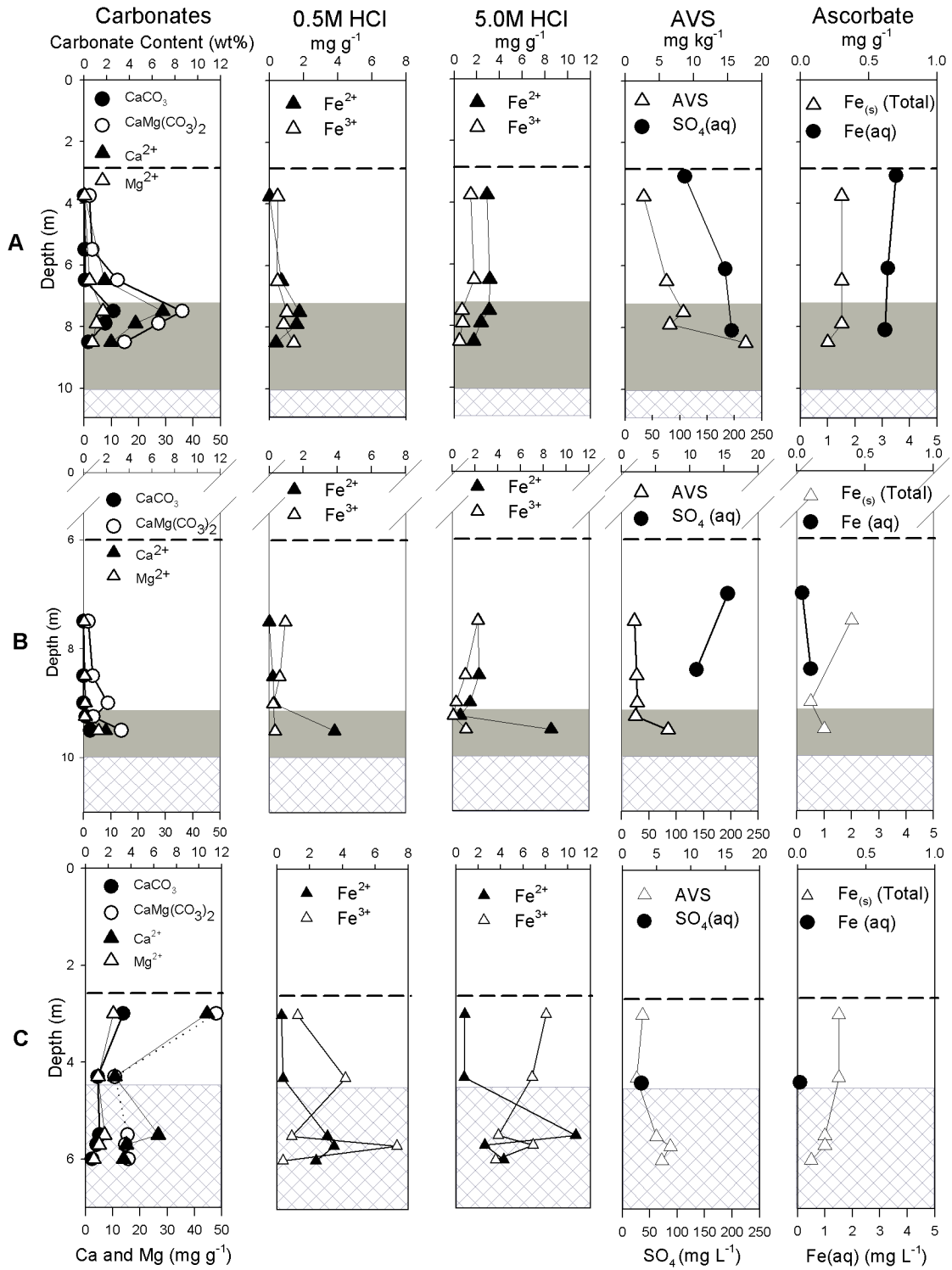


Figure 4-11 Solid phase extraction data. Components shown in each case are listed in each plot. Abbreviations for the specific extraction method used are listed in the text. Shaded areas represent grey colored sand whereas white areas represent red colored sand. The cross-hatched area represents the aquitard. The dotted line represents the water table. Refer to Figure 4-9 for the location where each soil core (A,B,C) was obtained.

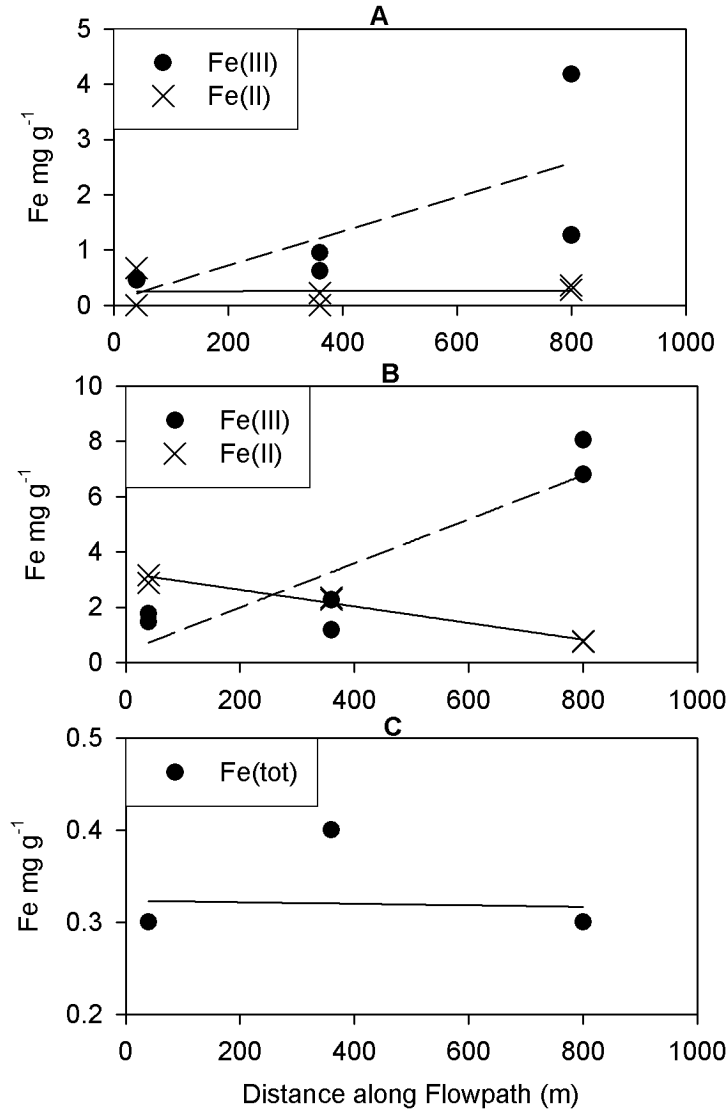


Figure 4-12 Distribution of extractable Fe along flowpath
 Extractions shown above are: 0.5 M HCl (A), 5.0 M HCl (B) and Na-Ascorbate (C). Data points shown above represent only sampling locations from the red coloured sand. Note that two sampling points are shown in (A) and (B) for both Fe(II) and Fe(III) at each position on the flowpath, however in many cases they are very similar and plot on top of one another. Note also that there are 5 data points in (C) however the two data points on both the left and right side are identical. Refer to Figure 4-10 for soil coring locations.

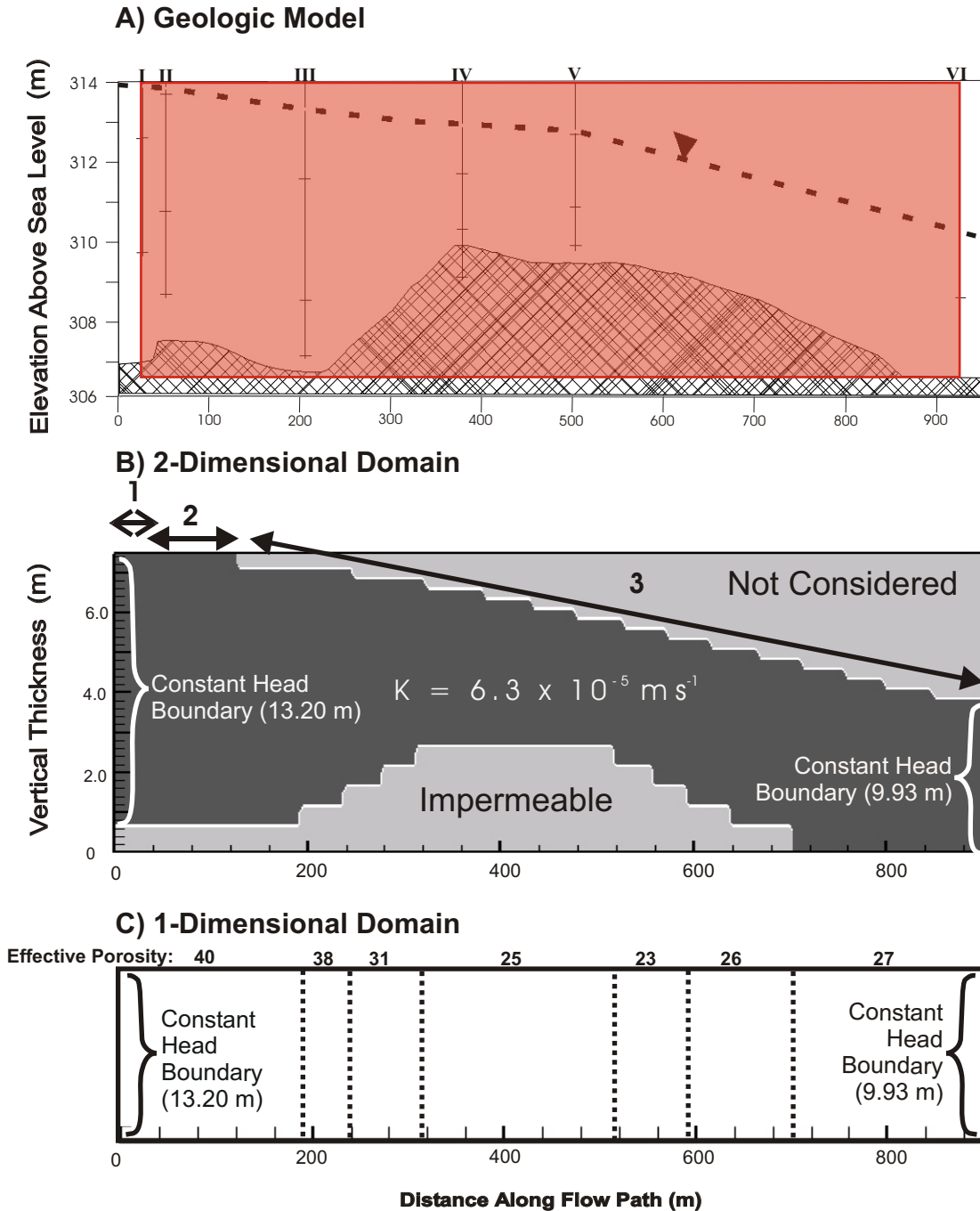


Figure 5-1 Illustration of Geologic Model (A), Domains and Boundary Conditions used for 2-Dimensional (B) and 1-Dimensional Simulations (C). The shaded portion the geologic model (A) represents the area considered during the simulations. The roman numerals in the top diagram (A), refer to the well nest number. Arrows in middle diagram (B) refer to different recharge boundary fluxes, 250 mm year⁻¹ (1), 63 mm year⁻¹ (2), 40 mm year⁻¹ (3). Divisions in the bottom (C) diagram represent zones of constant effective porosity in the 1-Dimensional domain.

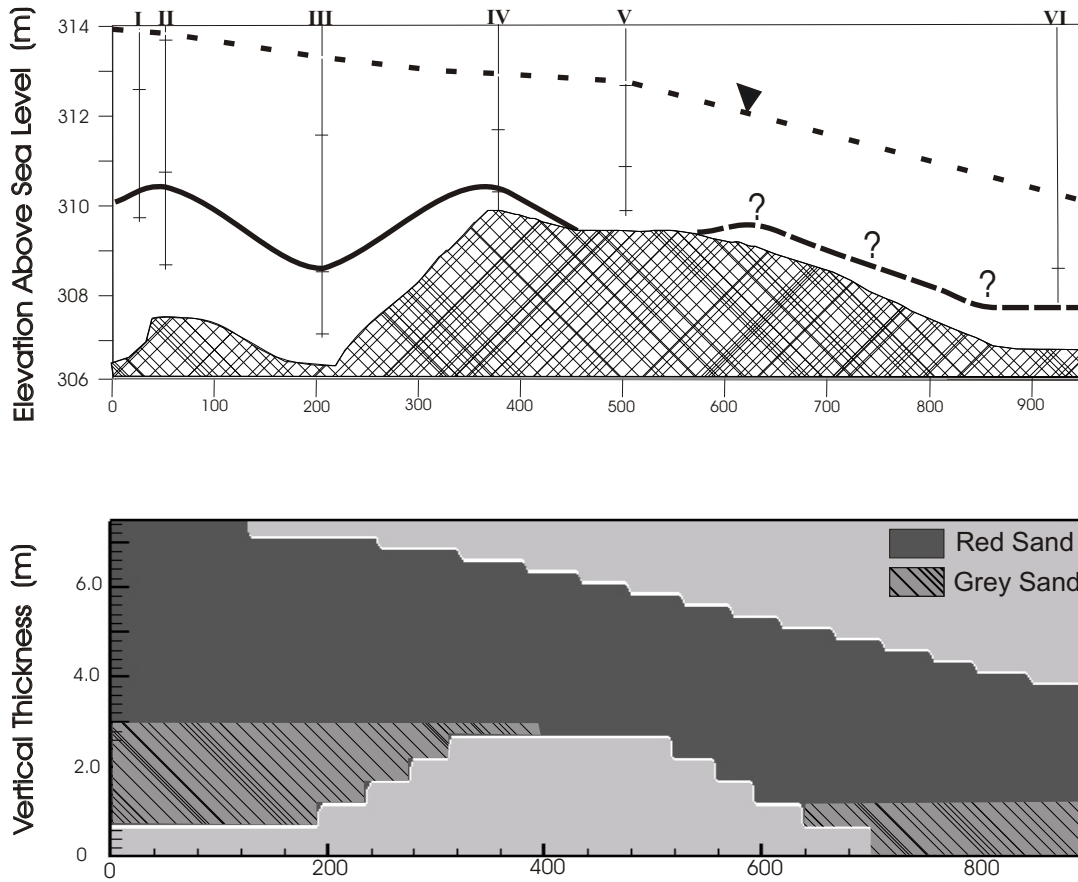


Figure 5-2 Illustration of the distribution of red and grey sand at the field site (top). Conceptualization of the distribution of red and grey sand in the 2D Domain (bottom). In the top illustration, the solid line represents the interface between the red and grey sand defined based on borehole data. The dotted line with question marks, indicates the predicted location of this interface. Roman numerals in the uppermost figure refer to the well nest number. Furthermore in the uppermost figure, the dashed line with the inverted triangle represents the approximate location of the water table and the crosshatched area represents the aquitard.

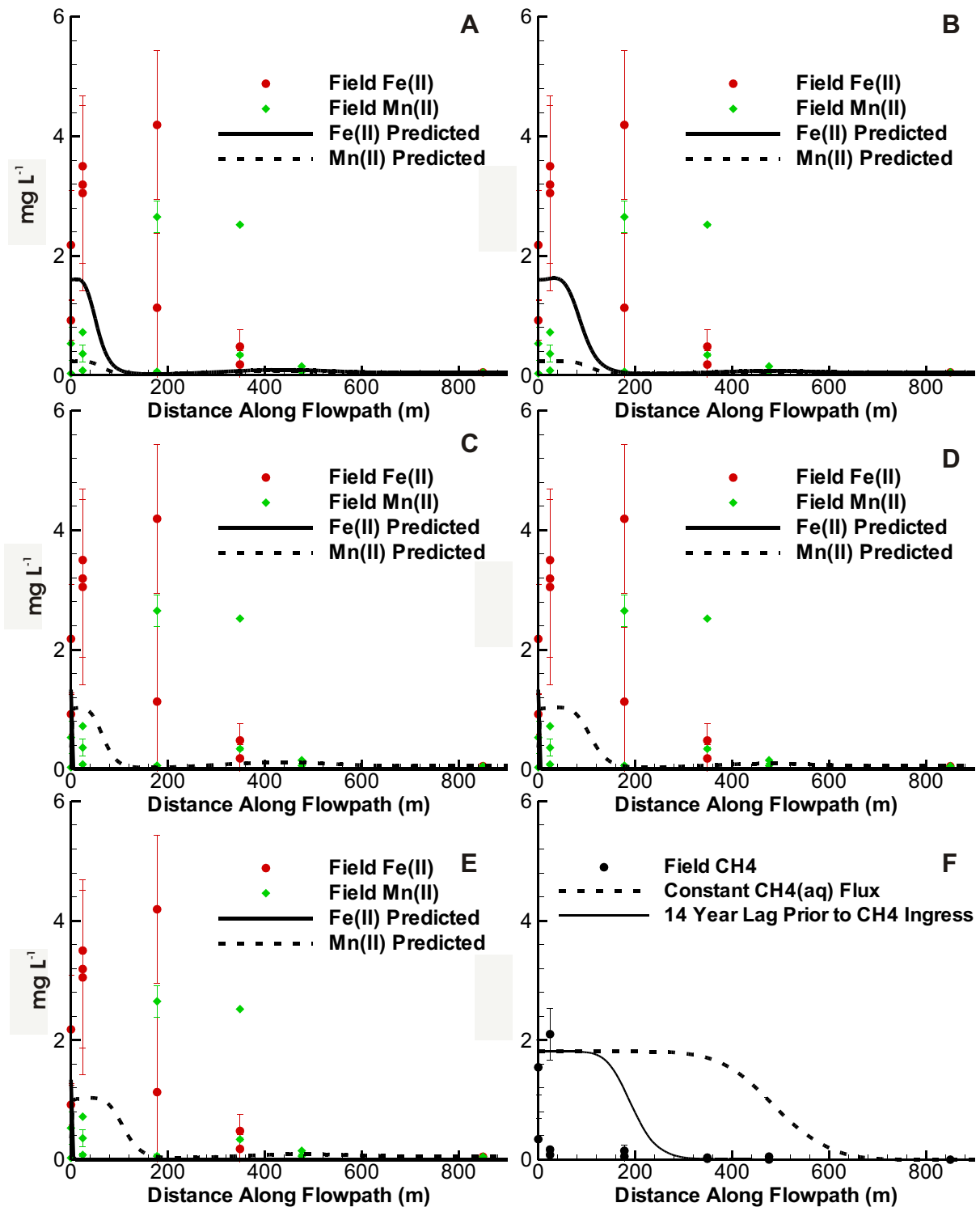


Figure 5-3 Comparison of field to predicted results based on conceptual model 1 after 27 years. All plots consider aerobic oxidation of Fe(II) and Mn(II) in addition to: CEC (high estimate) (A), CEC (low estimate) (B), CEC (high estimate) and oxidation of MnO₂ (high rate) (C), CEC (low estimate) and oxidation of MnO₂ (high rate) (D), CEC (low estimate) and oxidation of MnO₂ (low rate) (E) and a comparison of field to predicted CH₄(aq) if a constant flux or a 14 year lag is observed prior to CH₄(aq) ingress into the domain (F). Refer to the text for specific CEC and rate constants used in each case. Field data is based on the arithmetic average of September 2004 and June 2005 Sampling Events.

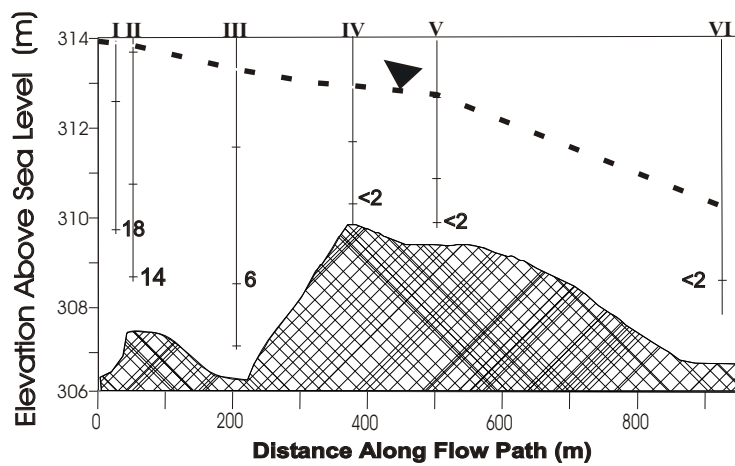


Figure 5-4 Transect showing biological oxygen demand measurements. Biological oxygen demand measurements are expressed as mg L^{-1} . Each measurement represents the laboratory derived biological oxygen demand measurement. No correction has been performed for the effect of reduced inorganic or organic constituents. The roman numerals refer to the well nest number. The dotted line with the inverted triangle represents the water table and the cross-hatched area represents the underlying aquitard.

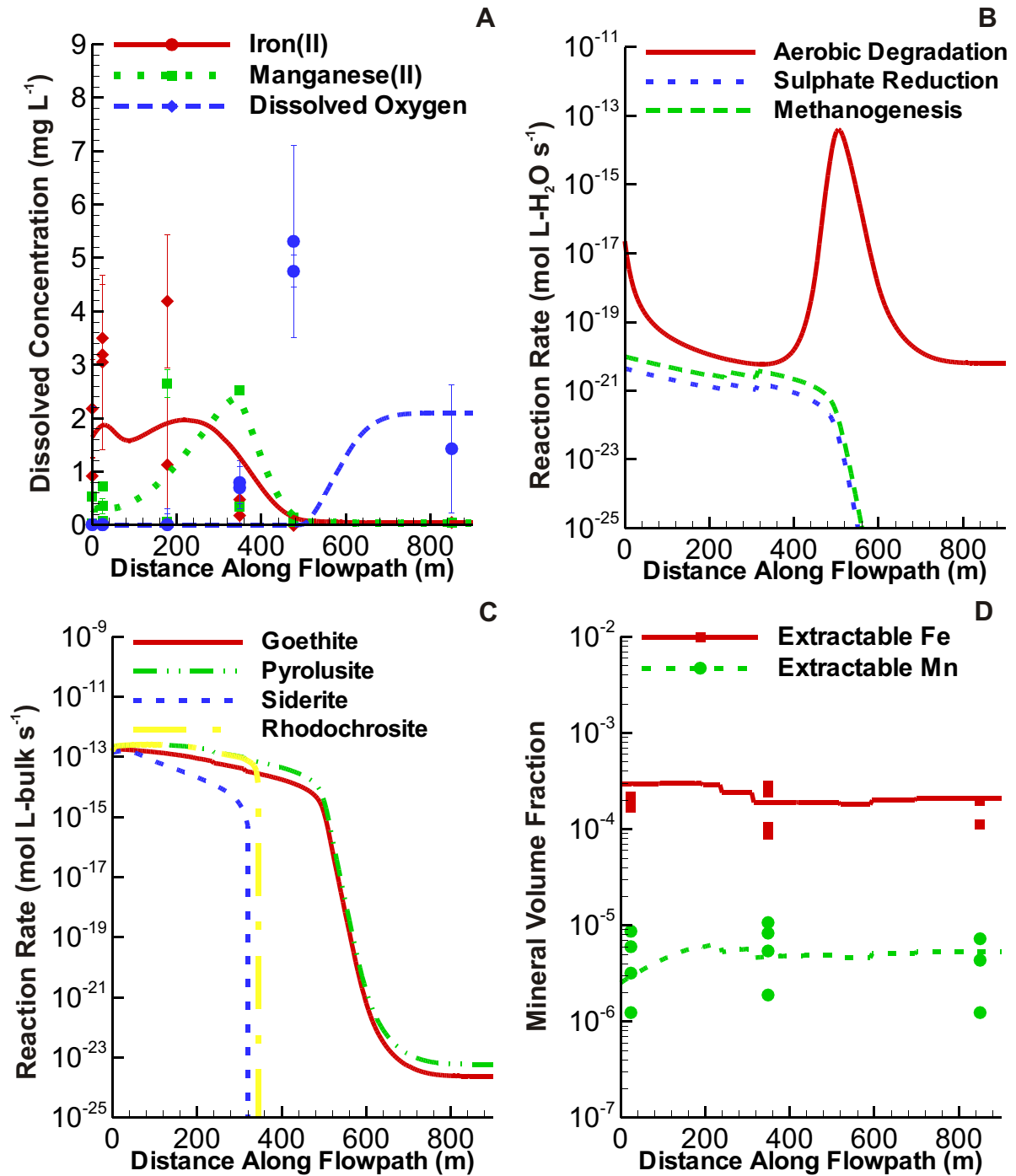


Figure 5-5 Results from conceptual model 2 using 1D simulations after 27 years. Plots represent the following: Total dissolved Fe(II), Mn(II) and $\text{O}_{2(\text{aq})}$ (A), Intra-Aqueous Reaction Rates (B), Mineral Dissolution-Precipitation Reaction Rates (C) and Mineral Volume Fractions (D). Dots represent field measured or experimentally derived values. Lines represent values determined using MIN3P. Concentrations of Fe(II) and Mn(II) are based on the arithmetic average of September 2004 and June 2005 Sampling Events. Dissolved oxygen concentrations are based on the arithmetic average of September 2004 and November 2005 measurements. Extractable Fe and Mn data is based on values determined using the Na-Ascorbate extraction.

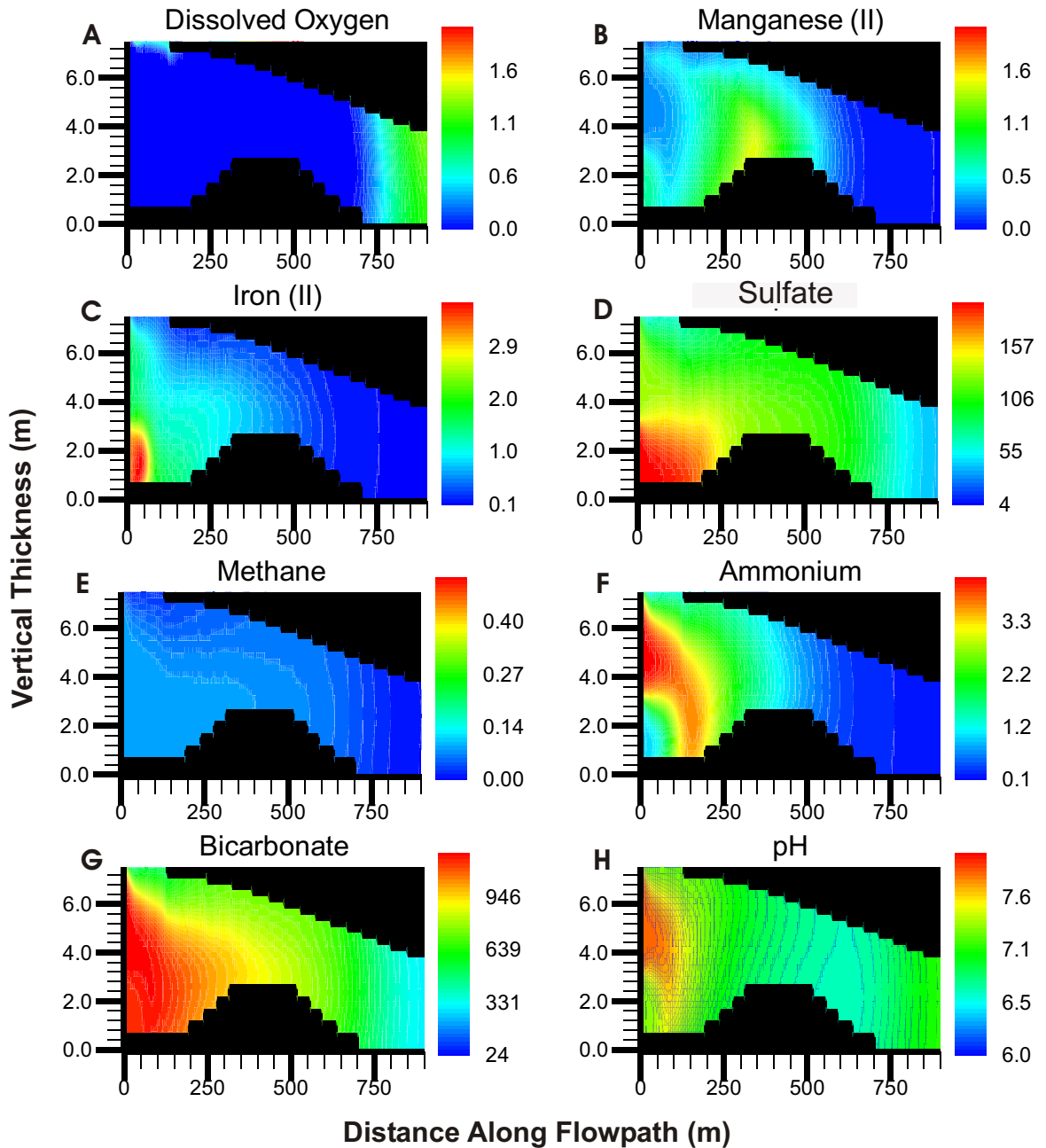


Figure 5-6 Distributions of redox sensitive components, HCO_3^- and pH based on Conceptual Model 2 using 2D Simulations after 27 years. Concentrations are in mg L^{-1} , with the exception of pH, which is in pH units. Plots shown are: $\text{O}_{2(\text{aq})}$ (A), Mn(II) (B), Fe(II) (C), SO_4 (D), $\text{CH}_{4(\text{aq})}$ (E), NH_4^+ (F), HCO_3^- (G) and pH (H). Blacked-out area represents the unsaturated zone and the underlying aquitard, which were not considered during simulations.

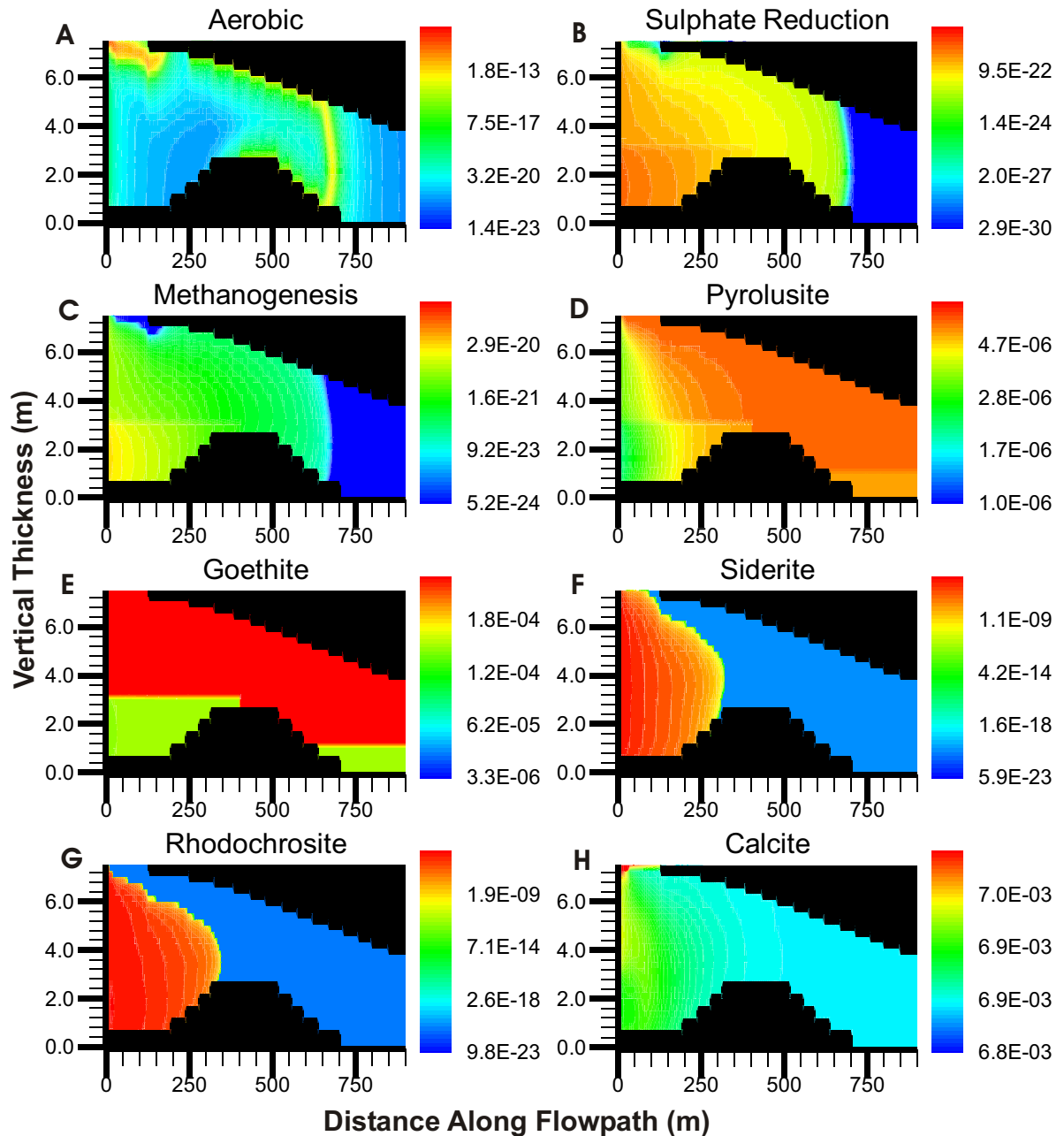


Figure 5-7 Intra-aqueous reaction rates and mineral volume fractions based on conceptual model 2 using 2D simulations after 27 years. Intra-aqueous reaction rates are expressed as $\text{mol L}^{-1}(\text{H}_2\text{O}) \text{ s}^{-1}$. Plots shown are: Aerobic Degradation Rates (A), Sulphate Reduction Rates (B), Methanogenesis Rates (C), Pyrolusite Volume Fraction (D), Goethite Volume Fraction (E), Siderite Volume Fraction (F), Rhodochrosite Volume Fraction (G) and Calcite Volume Fraction (H). Blacked-out area represents the unsaturated zone and the underlying aquitard, which were not considered during simulations.

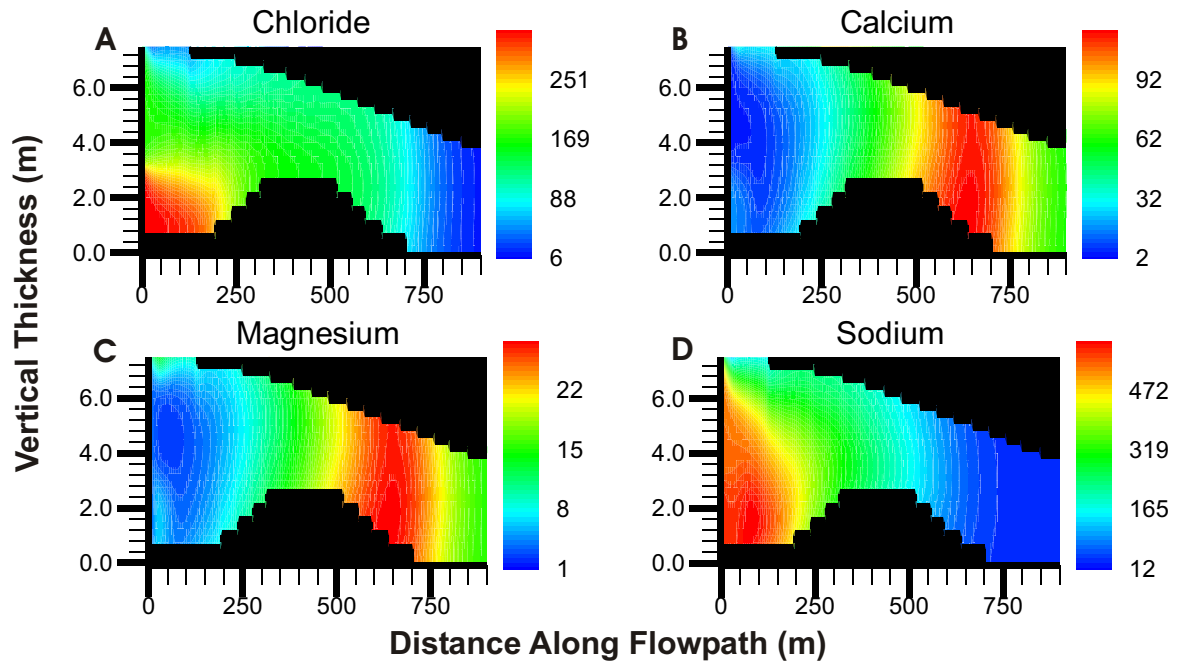


Figure 5-8 Distributions of chloride and major cations based on conceptual model 2 using 2D simulations after 27 years. Plots shown are: Chloride (A), Calcium (B), Magnesium (C) and Sodium (D). Concentrations are in (mg L^{-1}). Blacked-out area represents the unsaturated zone and the underlying aquitard, which were not considered during simulations.

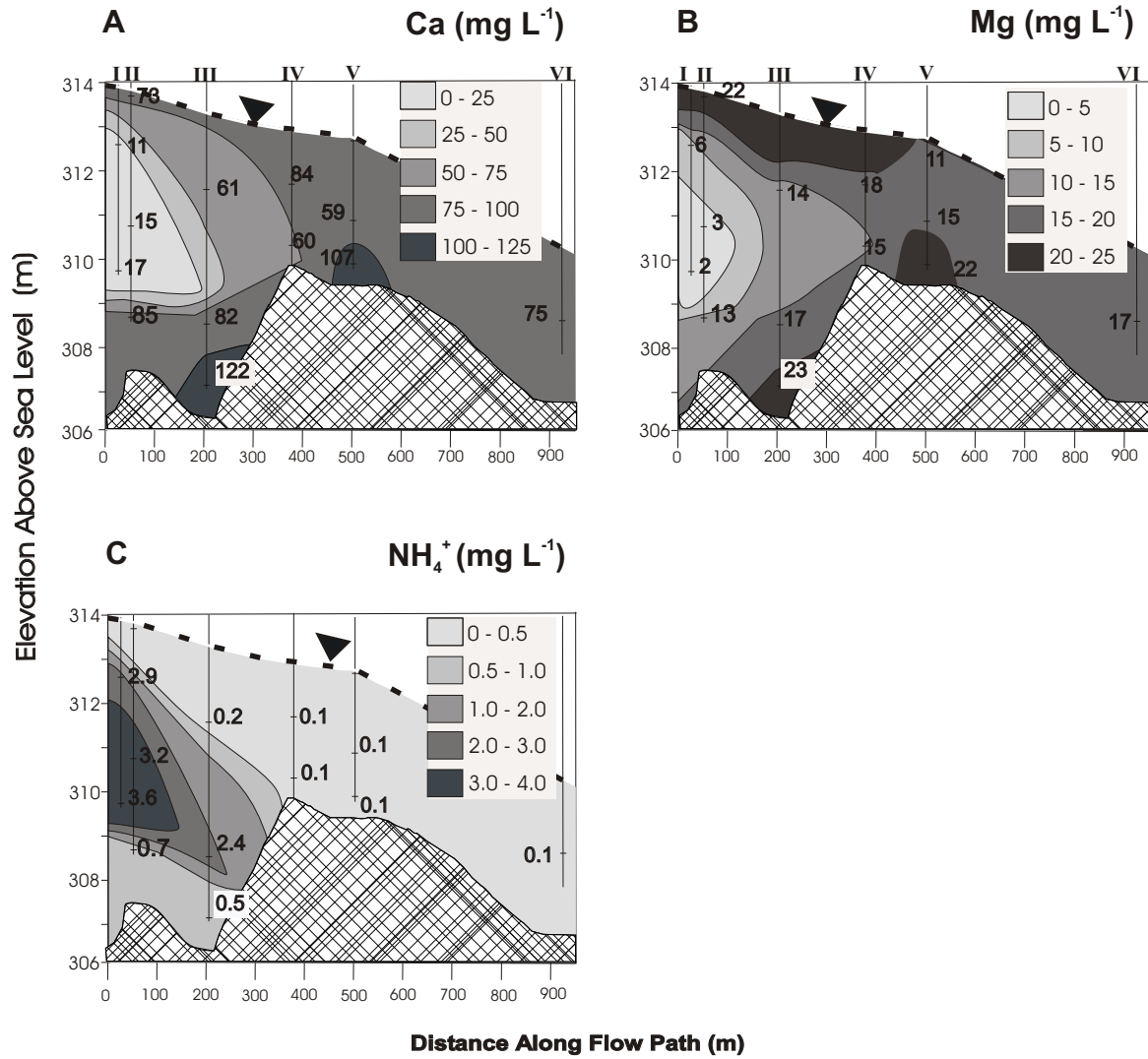


Figure 5-9 Transects showing field measured values of Calcium (A), Magnesium (B) and Ammonium (C). The value shown in each case is the arithmetic average of analysis performed on groundwater samples collected during September 2004 and June 2005. The location of the transect is shown in Figure 4-1. The roman numerals along the top of the uppermost diagrams, refer to the well nest number. The dotted line, with the inverted triangle represents the approximate location of the water table. The crosshatched area represents the aquitard.

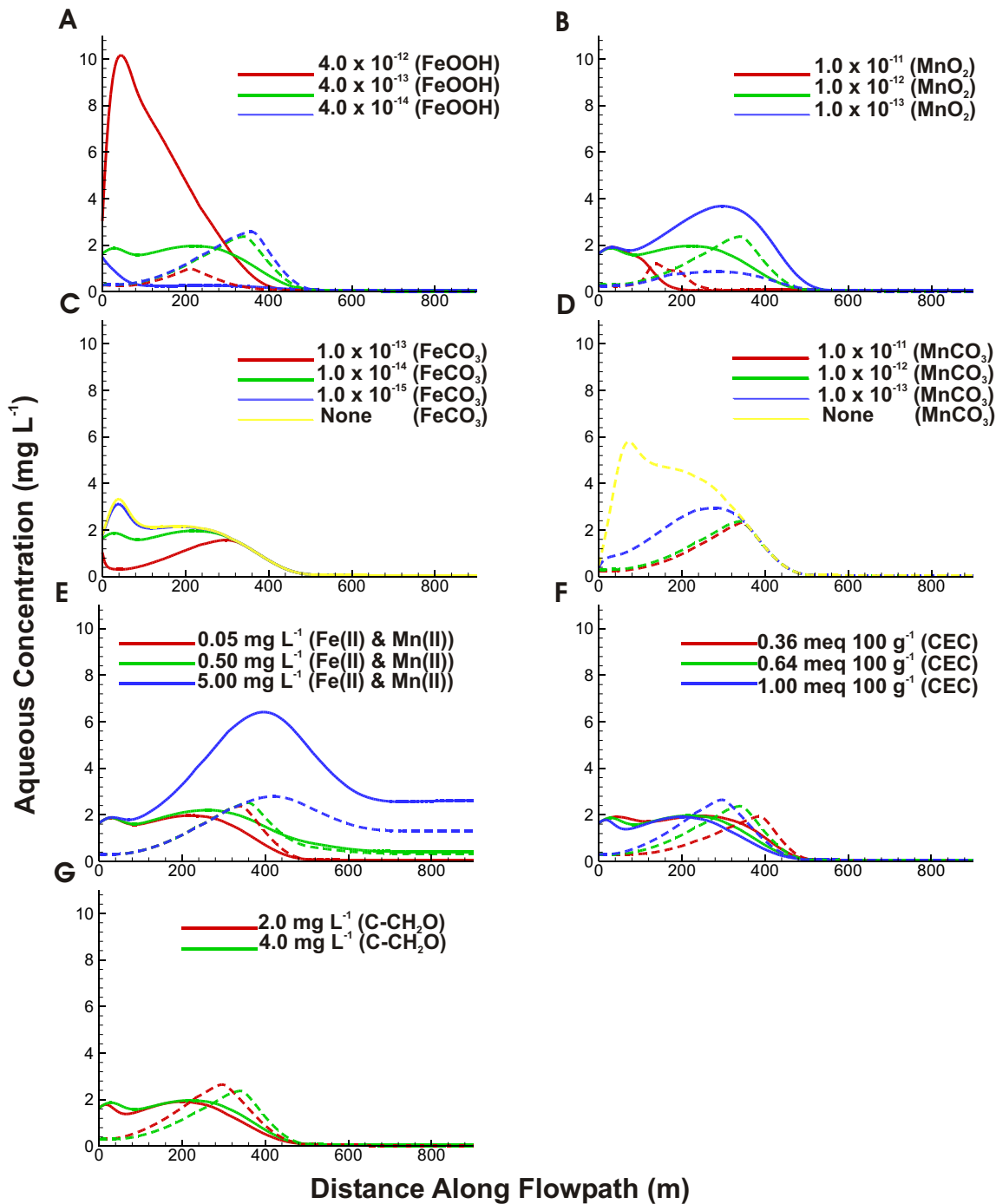


Figure 5-10 Sensitivity analysis of various geochemical parameters. Solid lines represent dissolved Fe(II), while dashed lines represent dissolved Mn(II). Plots are as follows: Sensitivity to FeOOH dissolution rates (A), Sensitivity to MnO₂ dissolution rates (B), Sensitivity to FeCO₃ dissolution/precipitation rates (C), Sensitivity to MnCO₃ dissolution/precipitation rates (D), Sensitivity to an increase in background dissolved Fe(II) and Mn(II) (E), Sensitivity to cation exchange capacity (F) and Sensitivity to a decrease in CH₂O, in the plume (G).

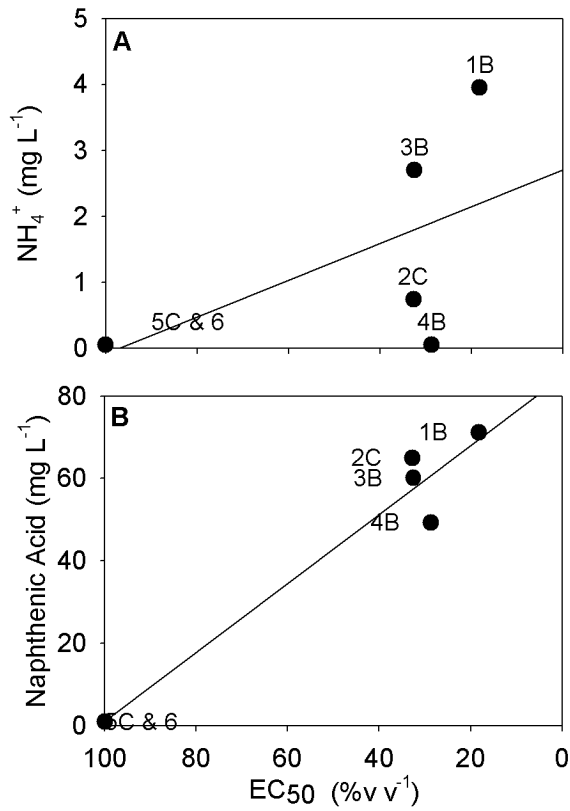


Figure 7-1 Correlation of toxic response to Ammonium (A) and Naphthenic Acid concentrations. Note all concentrations are in mg L⁻¹. Naphthenic acid and ammonium concentrations were determined based on samples collected in June 2005. Labels adjacent to each point refer to the monitoring well at which each sample was collected (see Figure 4-1 for locations).

REFERENCES

- Alberta Environment. (1999). Surface Water Quality Guidelines for Use in Alberta: 1999. Environmental Science Division and Water Management Division, Alberta Environment, Edmonton, Alberta, Canada.
- Allison, J.D., Brown, D.S. and Novo-Gradac, K.J. (1990). MINTEQA2/PRODEFA2, A Geochemical Assessment Model for Environmental Systems: User's Manual. Environmental Research Laboratory, Office of Research and Development, US EPA, Athens, Georgia, U.S.A.
- Amirbahman, A., Schonenberger, R., Johnson, C.A. and Sigg, L. (1998). Aqueous- and solid-phase biogeochemistry of a calcareous aquifer system downgradient from a municipal solid waste landfill (Winterthur, Switzerland). *Environ. Sci. Technol.*, 32: 1933-1940.
- Anschutz, P., Sundby, B., Lefrancois, L., Luther III, G.W. and Mucci, A. (2000). Interactions between metal oxides and species of nitrogen and iodine in bioturbated marine sediments. *Geochim. et Cosmochim.* 64(16): 2751-2763.
- Appelo, C.A.J. (1994). Cation and proton exchange, pH variations, and carbonate reactions in a freshening aquifer. *Water Resources Research*, 30(10): 2793-2805.
- Appelo, C.A.J. and Postma, D. (1999). *Geochemistry, Groundwater and Pollution*. A.A. Balkema, Brookfield, Vermont, U.S.A.
- Baedecker, M.J., Cozzarelli, I.M., Eganhouse, R.P., Siegel, D.I. and Bennett, P.C. (1993). Crude Oil in a Shallow Sand and Gravel Aquifer – III. biogeochemical reactions and mass balance modeling in anoxic groundwater. *App. Geochem.*, 8: 569-586.
- Baker, K.M. (1999). Identification of Process Water in a Surficial Aquifer at Syncrude's Mildred Lake Site. B.Sc. Thesis, University of Waterloo, Waterloo, Ontario, Canada.
- Ball, J.W. and Nordstrom, D.K. (1991). User's Manual for WATEQ4F, with Revised Thermodynamic Database and Test Cases for Calculating Speciation of Major, Trace and Redox Elements in Natural Water. US Geological Survey, Open-File Report 91-183.
- Bennett, B. and Dudas, M.J. (2002). Release of arsenic and molybdenum by reductive dissolution of iron oxides in a soil with enriched levels of native arsenic. *J Environ. Eng. Sci.*, 2: 265-272.
- Bjerg, P.L., Ruge, K., Pedersen, J.K. and Christensen, T.H. (1995). Distribution of redox-sensitive groundwater parameters downgradient of a landfill (Grindsted, Denmark). *Environ. Sci. Technol.*, 29: 1387-1394.
- Blowes, D. W., Gillham, R.W., Ptacek, C.J., Puls, R.W., Bennett, T.A., Bain, J.G., Hanton-Fong C.J., and Paul C.J. (1999). An In-Situ Permeable Reactive Barrier for the

Treatment of Hexavalent Chromium and Trichloroethylene in Groundwater, Vol. 2, Performance Monitoring, Tech. Rep. EPA/600/R-99/0956, U.S. Environmental Protection Agency, Washington, D. C., U.S.A.

Buss, S.R., Herbert, A.W., Morgan, P., Thornton, S.F. and Smith, J.W.N. (2004). A review of ammonium attenuation in soil and groundwater. *Quart. J. of Eng. Geol. and Hydrogeol.*, 37: 347-359.

Canfield, D.E., Raiswell, R., Westrich, J.T., Reaves, C.M., Berner, R.A. (1986). The use of chromium reduction in the analysis of reduced inorganic sulfur in sediments and shales. *Chem. Geol.*, 54: 149-155.

Carlyle, H.F., Tellam, J.H. and Parker, K.E. (2004). The use of laboratory-determined ion exchange parameters in the predictive modelling of field-scale major cation migration in groundwater over a 40-year period. *J. of Cont. Hydrol.*, 68: 55-81.

Ceazan, M.L., Thurman, E.M. and Smith, R.L. (1989). Retardation of ammonium and potassium transport through a contaminated sand and gravel aquifer: the role of cation exchange. *Environ. Sci. Technol.*, 23: 1402-1408.

CEATAG (CONRAD Environmental Aquatics Technical Advisory Group). (1998). Naphthenic Acids Background Information Discussion Report. Alberta Department of Energy, Edmonton, AB.

Chapelle, F.H. (2001). *Ground-Water Microbiology and Geochemistry* (2nd Edition). John Wiley and Sons, Inc. New York, New York, U.S.A.

Christensen, T.H., Kjeldsen, P., Bjerg, P.L., Jensen, D.L., Christensen, J.B., Baun, A., Albrechtsen, H.-J. and Heron, G. (2001). Biogeochemistry of landfill leachate plumes. *App. Geochem.*, 16: 659-718.

Churcher, P.L. and Dickhout, R.D. (1987). Analysis of ancient sediments for total organic carbon - some new ideas. *J. Geochem. Exploration* 29: 235-246.

Clemente, J.S., Prasad, N.G.N., MacKinnon, M.D. and Fedorak, P.M. (2003). A statistical comparison of naphthenic acids characterized by gas chromatography-mass spectrometry. *Chemosphere*, 50: 1265-1274.

Clemente, J.S., MacKinnon, M.D. and Fedorak, P.M. (2004). Aerobic biodegradation of two commercial naphthenic acids preparations. *Environ. Sci. Technol.* 38: 1009-1016.

Clemente, J.S. and Fedorak, P.M. (2005). A review of the occurrence, analyses, toxicity, and biodegradation of naphthenic acids. *Chemosphere*, 60: 585-600.

Dai, Q., Chung, K.H. and Czarnecki, J. (1992). Formation of calcium carbonate in the bitumen/aqueous sodium hydroxide system. *AOSTRA J. of Res.*, 8: 95-101.

- Dance, J.T. and Reardon, E.J. (1983). Migration of contaminants in groundwater at a landfill: a case study – 5. cation migration in the dispersion test. *J. of Hydrol.*, 63: 109-130.
- Delle Site, A. (2001). Factors affecting sorption of organic compounds in natural sorbent/water systems and sorption coefficients for selected pollutants. A Review. *J. Phys. Chem. Ref. Data*, 30(1): 187-439.
- Dreimanis, A. (1962). Quantitative gasometric determination of calcite and dolomite by using chittick apparatus. *J. of Sed. Petrol.*, 32(3): 520-529.
- Environment Canada. (2005). Online daily data reports.
http://www.climate.weatheroffice.ec.gc.ca/climateData/dailydata_e.html?timeframe=2&Prov=XX&StationID=2519&Year=1997&Month=12&Day=1.
- Fedorak, P.M., Coy, D.L., Salloum, M.J. and Dudas, M.J. (2002). Methanogenic potential of tailings samples from oil sands extraction plants. *Can. J. Microbiol.*, 48: 21-33.
- Fetter, C.W. (2001). *Applied Hydrogeology* (3rd Edition). Prentice Hall, Upper Saddle River, New Jersey, U.S.A.
- Fisher, T.G. and Smith, D.G. (1993). Exploration for pleistocene aggregate resources using process-depositional models in the Fort McMurray region, NE Alberta, Canada. *Quat. Internat.*, 20: 71-80.
- Gadd, G.M. (2000). Bioremedial potential of microbial mechanisms of metal mobilization and immobilization. *Curr. Opinion in Biotech.*, 11: 271-279.
- Gal'chenko, V.F. (2004). On the problem of anaerobic methane oxidation. *Microbiology*, 73(5): 599-608.
- Garabedian, S.P. and Leblanc, D.R. (1991). Large-scale natural gradient tracer test in sand and gravel, Cape Cod, Massachusetts – 2. analysis of spatial moments for a nonreactive tracer. *Water Res. Research*, 27(5): 911-924.
- Gervais, F.J.M. (2004). Fate and Transport of Naphthenic Acids in a Glacial Aquifer. MSc Thesis, University of Waterloo, Waterloo, Ontario, Canada.
- Gibbs, M.M. (1979). A simple method for the rapid determination of iron in natural waters. *Water Res. Research*, 13: 295-297.
- Hanson, R.S. and Hanson, T.E. (1996). Methanotrophic bacteria. *Microbiological Rev.*, 60(2): 439-471.

Havre, T. E., Sjoblom, J. and Vindstad, J.E. (2003). Oil/water-partitioning and interfacial behavior of naphthenic acids. *J. of Dispersion Sci. and Tech.*, 24(6): 789-801.

Headley, J.V. and McMartin, D.W. (2004). A review of the occurrence and fate of naphthenic acids in aquatic environments. *J. of Environ. Sci. and Health (Part A – Toxic/Hazardous Substances & Environmental Engineering)*, A39(8): 1989-2010.

Headley, J.V., Tanapat, S., Putz, G. and Peru, K.M. (2002). Biodegradation kinetics of geometric isomers of model naphthenic acids in Athabasca river water. *Water Res. J. of Canada*, 27(1): 25-42.

Henderson, J.E., G.R. Peyton and Glaze, W.H. (1976). A Convenient Liquid-Liquid Extraction Method for the Determination of Halomethanes in Water at the Parts-Per-Billion Level. In: Keith, L.H. (Ed.), *Identification and Analysis of Organic Pollutants in Water*. Ann Arbor Science Publishers Inc., Ann Arbor, Michigan, U.S.A.

Herman, D.C., Fedorak, P.M. and Costerton, J.W. (1993). Biodegradation of cycloalkane carboxylic acids in oil sand tailings. *Can. J. Microbiol.*, 39: 576-580.

Herman, D.C., Fedorak, P.M., MacKinnon, M.D. and Costerton, J.W. (1994). Biodegradation of naphthenic acids by microbial populations indigenous to oil sands tailings. *Can. J. Microbiol.*, 40: 467-477.

Heron, G., Crouzet, C., Bourg, A.C. and Christensen, T.H. (1994). Speciation of Fe(II) and Fe(III) in contaminated aquifer sediments using chemical extraction techniques. *Environ. Sci. Technol.*, 28: 1698-1705.

Heron, G. and Christensen, T.H. (1995). Impact of sediment-bound iron on redox buffering in a landfill leachate polluted aquifer (Vejen, Denmark). *Environ. Sci. Technol.*, 29: 187-192.

Holowenko, F.M., MacKinnon, M.D. and Fedorak, P.M. (2000). Methanogens and sulfate-reducing bacteria in oil sands fine tailings waste. *Can. J. Microbiol.*, 46: 927-937.

Holowenko, F.M., MacKinnon, M.D. and Fedorak, P.M. (2001). Naphthenic acids and surrogate naphthenic acids in methanogenic microcosms. *Wat. Res.*, 35(11): 2595-2606.

Holowenko, F.M., MacKinnon, M.D. and Fedorak, P.M. (2002). Characterization of naphthenic acids in oil sands wastewaters by gas chromatography-mass spectrometry. *Water Res.*, 36: 2843-2855.

Hostettler, F.D. and Kvenvolden, K.A. (2002). Alkylcyclohexanes in environmental geochemistry. *Environ. Forensics*, 3(3): 293-301.

Hulth, S., Aller, R.C. and Gilbert, F. (1999). Coupled anoxic nitrification/manganese reduction in marine sediments. *Geochim. et Cosmochim.* 63(1): 49-66.

Hulth, S., Aller, R.C., Canfield, D.E., Dalsgaard, T., Engstrom, P., Gilbert, F., Sundback, K. and Thamdrup, B. (2005). Nitrogen removal in marine environments: recent findings and future research challenges. *Marine Chem.* 94:125-145.

Hunter, G.P. (2001). Investigation of Groundwater Flow Within an Oil Sand Tailings Impoundment and Environmental Implications. MSc Thesis, University of Waterloo, Waterloo, Ontario, Canada.

Hunter, K.S., Wang, Y. and Van Cappellen, P. (1998). Kinetic modeling of microbially-driven redox chemistry of subsurface environments: coupling transport, microbial metabolism and geochemistry. *J. of Hydrol.*, 209: 53-80.

Hvorslev, M.J. (1951). Time Lag and Soil Permeability in Ground-Water Observations. U.S. Army Corps of Engineers, Bulletin 36, Waterways Experiment Station, Vicksburg, Mississippi.

Jensen, D.L. Boddum, J.K., Tjell, J.C. and Christensen, T.H. (2002). The solubility of rhodochrosite ($MnCO_3$) and siderite ($FeCO_3$) in anaerobic aquatic environments. *Appl. Geochem.*, 17: 503-511.

Jivraj, M.N. MacKinnon and M.D., Fung, B. (1995). Naphthenic Acids Extraction and Quantitative Analyses with FT-IR Spectroscopy. *Syncrude Analytical Methods Manual*. 4th ed. Syncrude Canada Ltd. Research Department, Edmonton, Alberta, Canada.

Kampbell, D.H., and Vandergrift, S.A. (1998). Analysis of dissolved methane, ethane and ethylene in ground water by a standard gas chromatographic technique. *J. of Chromatographic Sci.*, 36: 253-256.

Kasperski, K.L. (1992). A review of properties and treatment of oil sands tailings. *AOSTRA J. of Res.*, 8: 11-53.

Keimowitz, A.R., Simpson, H.J., Stute, M., Datta, S., Chillrud, S.N., Ross, J. and Tsang, M. (2005). Naturally occurring arsenic: mobilization at a landfill in maine and implications for remediation. *Appl. Geochem.*, 20: 1985-2002.

Kostka, J.E. Luther, G.W. III. (1994). Partitioning and speciation of solid phase iron in saltmarsh sediments. *Geochim. et Cosmochim. Acta*, 58(7): 1701-1710.

Lai, J.W.S., Pinto, L.J., Kiehlmann, E., Bendell-Young, L.I. and Moore, M.M. (1996). Factors that affect the degradation of naphthenic acids in oil sands wastewater by indigenous microbial communities. *Environ. Tox. and Chem.*, 15(9): 1482-1491.

Lake, W. and Rogers, W. (1979). Volume 1: Acute Lethality of Mine Depressurization Water to Trout-Perch (*Percopsis Omiscomaycus*) and Rainbow Trout (*Salmo Gairdneri*).

Prepared for the Alberta Oil Sands Environmental Research Program by Alberta Environment, Water Quality Control Branch. AOSERP Report 23.

Lindberg, R.D. and Runnels, D.D. (1994). Ground water redox reactions: an analysis of equilibrium state applied to Eh measurements and geochemical modeling. *Science*, 225: 925-927.

Liu, C., Kota, S., Zachara, J.M., Fredrickson, J.K. and Brinkman, C.K. (2001). Kinetic analysis of the bacterial reduction of goethite. *Environ. Sci. Technol.*, 35: 2482-2490.

Lloyd, J.R. and Lovley, D.R. (2001). Microbial detoxification of metals and radionuclides. *Cur. Opinion in Biotech.*, 12: 248-253.

Lovley, D.R. and Klug, M.J. (1986). Model for the distribution of sulfate reduction and methanogenesis in freshwater sediments. *Geochim. et Cosmochim. Acta*, 50: 11-18.

Lovley, D.R. and Phillips, E.J.P. (1986). Organic matter mineralization with reduction of ferric iron in anaerobic sediments. *Appl. and Environ. Microbiol.*, 51(4): 683-689.

Lovley, D.R. and Phillips, E.J.P. (1987). Competitive mechanisms for inhibition of sulfate reduction and methane production in the zone of ferric iron reduction in Sediments. *Appl. and Environ. Microbiol.*, 53(11): 2636-2641.

Lovley, D.R. and Phillips, E.J.P. (1988). Novel mode of microbial energy metabolism: organic carbon oxidation coupled to dissimilatory reduction of iron or manganese. *Appl. and Environ. Microbiol.*, 54(6): 1472-1480.

Lovley, D.R. (1991). Dissimilatory Fe(III) and Mn(IV) reduction. *Microbiol. Rev.*, 55(2): 259-287.

Ludvigsen, L., Albrechtsen, H.J., Heron, G., Bjerg, P.L. and Christensen, T.H. (1998). Anaerobic microbial redox processes in a landfill leachate contaminated aquifer (Grindsted, Denmark). *J. of Cont. Hydrol.*, 33: 273-291.

Luther III, G.W., Sundby, B., Lewis, B.L., Brendel, P.J. and Silverberg, N. (1997). Interactions of manganese with nitrogen cycle: alternative pathways to dinitrogen. *Geochim. et Cosmochim.* 61(19): 4043-4052.

Lyngkilde, J. and Christensen, T.H. (1992). Fate of organic contaminants in the redox zones of a landfill leachate pollution plume (Vejen, Denmark). *J. of Cont. Hydrol.*, 10(4): 291-307.

MacKinnon, M.D. and Boerger, H. (1986). Description of two treatment methods for detoxifying oil sands tailings pond water. *Water Poll. Res. J. Canada*, 21(4): 496-512.

MacKinnon, M.D. (1989). Development of the Tailings Pond at Syncrude's Oil Sands Plant: 1978-1987. *AOSTRA Journal of Research*, 5: 109-133.

MacKinnon, M., Kampala, G., Marsh, B., Fedorak, P. and Guigard, S. (2004). Indicators for assessing transport of oil sands process-affected waters. In: Thomson, N.R. (Ed), *Bringing Groundwater Quality Research to the Watershed Scale, Proceedings of GQ2004, the 4th International Groundwater Quality Conference*, Waterloo, Ontario, Canada.

Marsh, W. (2006). MSc Thesis in Progress. University of Alberta, Alberta, Canada.

Mayer, K.U., Benner, S.G., Frind, E.O., Thorton, S.F. and Lerner, D.N. (2001). Reactive transport modeling of processes controlling the distribution and natural attenuation of phenolic compounds in a deep sandstone aquifer. *J. of Cont. Hydrol.*, 53: 341-368.

Mayer, K.U., Frind, E.O. and Blowes, D.W. (2002). Multicomponent reactive transport modeling in variably saturated porous media using a generalized formulation for kinetically controlled reactions. *Water Res. Research*, 38(9): 1174.

Mulder, A., van de Graaf, A.A., Robertson, L.A. and Kuenen, J.G. (1995). Anaerobic ammonium oxidation discovered in a denitrifying fluidized bed reactor. *FEMS Microbiol. Ecol.* 16: 177-184.

Peng, J., Headley, J.V. and Barbour, S.L. (2002). Adsorption of single-ring model naphthenic acids on soils. *Can. Geotech. J.*, 39: 1419-1426.

Pitkin, S.E., Cherry, J.A., Ingelton, R.A. and Broholm, M. (1999). Field demonstrations using the waterloo ground water profiler. *Ground Water Monit. Remediat.* 19(2): 122-131.

Plant, J.A., Kinniburgh, D.G., Smedley, P.L., Fordyce, F.M. and Klinck, B.A. (2003). Arsenic and Selenium. *Treatise on Geochemistry*. 9: 17-66.

Postma, D. and Boesen, C. (1991). Nitrate reduction in an unconfined sandy aquifer: water chemistry, reduction processes, and geochemical modeling. *Water Res. Research*, 27(8): 2027-2045.

Postma, D., Appelo, C.A.J. (2000). Reduction of Mn-oxides by ferrous iron in a flow system: column experiments and reactive transport modeling. *Geochim. et Cosmochim. Acta*, 64(7): 1237-1247.

Quantin, C., Becquer, T., Rouiller, J.H. and Berthelin, J. (2001). Oxide weathering and trace metal release by bacterial reduction in a New Caledonia ferralsol. *Biogeochem.*, 53: 323-340.

- Quantin, C., Becquer, T., Rouiller, J.H. and Berthelin, J. (2002). Redistribution of metals in a New Caledonia ferralsol after microbial weathering. *Soil Sci. Soc. Am. J.*, 66: 1797-1804.
- Rickard, D. (1995). Kinetics of FeS Precipitation: Part 1. Competing reaction mechanisms. *Geochim. et Cosmochim. Acta*, 59(21): 4567-4379.
- Robertson, W.D., Cherry, J.A. and Sudicky, E.A. (1991). Groundwater contamination from two small septic systems on sand squifers. *Ground Water*, 29(1): 82-92.
- Robertson, W.D., Russell, B.M. and Cherry, J.A. (1996). Attenuation of nitrate in aquitard sediments of southern Ontario. *J. of Hydrol.*, 180: 267-281.
- Roh, Y., Zhang, C-L., Vali, H., Lauf, R.J., Zhou, J. and Phelps, T.J. (2003). biogeochemical and environmental factors in Fe biomineralization: magnetite and siderite formation. *Clays and Clay Min.*, 51(1): 83-95.
- RSKSOP_175 (EPA _ R. S. KERR LABORATORY, ADA, OKLAHOMA (not promulgated))
- Schmidt, I., Sliemers, O., Schmid, M., Cirpus, I., Strous, M., Bock, E., Kuenen, J.G. and Jetten, M.S.M. (2002). Mini Review: Aerobic and anaerobic ammonia oxidizing bacteria – competitors or natural partners. *FEMS Microbiol. Ecol.* 39:175-181.
- Schramm, L.L., Stasiuk, E.N. and MacKinnon, M. (2000). Surfactants in Athabasca Oil Sands Slurry Conditioning, Flotation Recovery, and Tailings Processes. In: *Surfactants: Fundamentals and Applications in the Petroleum Industry* (ed. by L.L. Schramm). Cambridge University Press, Cambridge, United Kingdom.
- Schwarzenbach, R.P. Gschwend, P.M., Imboden, D.M. (2003). *Environmental Organic Chemistry* (2nd Edition). Wiley-Interscience, New Jersey, U.S.A.
- Scott, J.D., Dusseault, M.B. and Carrier, W.D. III. (1985). Behavior of the clay/bitumen/water sludge system from oil sands extraction plants. *Appl. Clay Sci.*, 1: 207-218.
- Scott, A.C., MacKinnon, M.D. and Fedorak, P.M. (2005). Naphthenic acids in Athabasca oil sands tailings waters are less biodegradable than commercial naphthenic acids. *Environ. Sci. & Technol.*, 39(21): 8388-8394.
- Smedley, P.L. and Kinniburgh, D.G. (2002). A review of the source, behavior and distribution of arsenic in natural waters. *Appl. Geochem.*, 17: 517-568.
- Smith, D.G. and Fisher, T.G. (1993). Glacial Lake Agassiz: The northwestern outlet and paleoflood. *Geol.*, 21: 9-12.

- Smith, R.G. and Schramm, L.L. (1992). The influence of mineral components on the generation of natural surfactants from Athabasca oil sands in the alkaline hot water process. *Fuel Proc. Tech.* 30: 1-14.
- St. John, W.P., Rughani, J., Green, S.A. and McGinnis, G.D. (1998) Analysis and characterization of naphthenic acids by gas chromatography-electron impact mass spectrometry of tert-butyltrimethylsilyl derivatives. *J. Chromatogr. A.*, 807: 241-251.
- Starr, R.C. and Ingleton, R.A. (1992). A new method for collecting core samples without a drill rig. *Groundwater Mon. Rev.*, 41: 91-95.
- Strong, W., and Leggat, K.R. 1992. Ecoregions of Alberta. *Resour. Inf. Branch Publ. No. T:245*. Land Information Services Division, Alberta Forestry, Lands, and Wildlife, Edmonton, Alberta, Canada.
- Stronkhorst, J., Schipper, C., Brils, J., Dubbeldam, M., Postma, J. and van de Hoeven, N. (2003). Using marine bioassays to classify the toxicity of dutch harbour sediments. *Environ. Tox. and Chem.* 22(7): 1535-1547.
- Sudicky, E.A. (1986). A natural gradient experiment on solute transport in a sand aquifer: spatial variability of hydraulic conductivity and its role in the dispersion process. *Water Res. Research*, 22(13): 2069-2082.
- Syncrude Canada Ltd. (2003). 2002 Groundwater Monitoring Report – Syncrude Canada Ltd. Mildred Lake Site (Leases 17 and 22). Syncrude Canada Ltd.
- Syncrude Canada Ltd. (2003). Syncrude Factbook (4th Edition). Syncrude Canada Ltd Government and Public Affairs Department. Fort McMurray, Alberta, Canada.
- Tessier, A., Rapin, F. and Carignan, R. (1985). Trace metals in oxic lake sediments: possible adsorption onto iron oxyhydroxides. *Geochim. et Cosmochim. Acta*, 49: 183-194.
- Thamdrup, B. and Dalsgaard, T. (2000). The fate of ammonium in anoxic manganese oxide-rich marine sediment. *Geochim. et Cosmochim.* 64(24): 4157-4164.
- Thorn, K.A. and Aiken, G.R. (1998). Biodegradation of crude oil into nonvolatile organic acids in a contaminated aquifer near Bemidji, Minnesota, *Org. Geochem.*, 29(4): 909-931.
- Thornton, S.F., Tellam, J.H. and Lerner, D.N. (2000). Attenuation of landfill leachate by UK Triassic sandstone aquifer materials – 1. fate of inorganic pollutants in laboratory columns. *J. of Cont. Hydrol.*, 43: 327-354.
- Tuccillo, M.E., Cozzarelli, I.M. and Herman, J.S. (1999). Iron reduction in the sediments of a hydrocarbon-contaminated aquifer. *Appl. Geochem.*, 14: 655-667.

- Valava, V.M., Kretzschmar, R. Barmettler, K, Voegelin, A., Grolimund, D. and Borkovec, M. (2002). Cation competition in a natural subsurface material: prediction of transport behavior. *Water Res. Research*, 38(5)
- Valentine, D.L. and Reeburgh, W.S. (2000). New perspectives on anaerobic methane oxidation. *Environ. Microbiol.*, 2(5): 477-484.
- Valocchi, A.J., Street, R.L. and Roberts, P.V. (1981). Transport of ion-exchanging solutes in groundwater: chromatographic theory and field simulation. *Water Res. Research*, 17(5): 1517-1527.
- van Breukelen, B.M., Appelo, C.A.J., Olsthoorn, T.N. (1998). Hydrogeochemical transport modeling of 24 years of Rhine water infiltration in the dunes of the Amsterdam water supply. *J. of Hydrol.*, 209: 281-296.
- van Breukelen B.M., Roling, W.F.M., Groen, J., Griffioen, J. and van Verseveld, H.W. (2003). Biogeochemistry and isotope geochemistry of a landfill leachate plume. *J. of Contaminant Hydrol.*, 65: 245-268.
- van Breukelen, B.M. and Griffioen, J. (2004). Biogeochemical processes at the fringe of a landfill leachate pollution plume: potential for dissolved organic carbon, Fe(II), Mn(II), NH₄ and CH₄ oxidation. *J. of Contaminant Hydrol.*, 73: 181-205.
- van Breukelen, B.M., Griffioen, J., Roling, W.F.M. and van Verseveld, H.W. (2004). Reactive transport modelling of biogeochemical processes and carbon isotope geochemistry inside a landfill leachate plume. *J. of Contaminant Hydrol.*, 70: 249-269.
- van de Graaf, A., Mulder, A., de Bruijn, P., Jetten, M.S.M., Robertson, L.A. and Kuenen, J.G. (1995). Anaerobic oxidation of ammonium is a biologically mediated process. *Appl. and Environ. Microbiol.* 61(4): 1246-1251.
- Verbeek, A., Mackay, W. and MacKinnon, M. (1993). Isolation and Characterization of the Acutely Toxic Compounds in Oil Sands Process Water from Syncrude and Suncor. In: Liu, J.K. (Ed.), *Oil Sands – Our Petroleum Future Conference. Fine Tailings Fundamentals Consortium*. Edmonton, Alberta, Canada.
- Whalen, S.C., Reeburgh, W.S. and Sandbeck, K.A. (1990). Rapid methane oxidation in a landfill cover soil. *Appl. and Environ. Microbiol.*, 56(11): 3405-3411.
- Wilde, F.D. and Radtke, D.B., Eds. (August 2005). *General Information and Guidelines (Version 1.2): U.S. Geological Survey Techniques of Water-Resources Investigations*, book 9, chap. A6 Field Measurements, section 6.0, accessed from <http://pubs.water.usgs.gov/twri9A6/>.
- Wright, B. (1991). *Overburden Facies Chart*. Syncrude Canada Ltd.

Zachara, J.M., Fredrickson, J.K., Smith, S.C. and Gassman, P.L. (2001). Solubilization of Fe(III) oxide-bound trace metals by a dissimilatory Fe(III) reducing bacterium. *Geochim. et Cosmochim. Acta*, 65(1): 75-93.

Zou, L., Han, B., Yan, H., Kasperski, K.L., Xu, Y. and Hepler, L.G. (1997). Enthalpy of adsorption and isotherms for adsorption of naphthenic acid onto clays. *J. of Colloid and Interface Sci.*, 190: 472-475.

Appendix A
Oil Sand Mass Balance and Dyke Construction and Seepage

Construction of and Seepage from Oil Sands Tailings Impoundments

The MLSB was created using hydraulic construction techniques. Whereby, the tailings stream is redirected into construction cells oriented parallel to the dyke center-line and compacted in order to create the dykes forming the perimeter of the tailings impoundment (Fair et al. 1986). When not used for dyke construction, tailings are discharged into the tailings pond near the dyke crest, where the coarser fraction settles out quickly forming beaches, while finer fractions accumulates nearer to the center of the tailings impoundment (Mackinnon 1989). Consequently bitumen, not recovered during the extraction process will also settle out, forming localized mats throughout the tailings pond (Kasperski, 1992 and Hunter, 2001).

It is unclear the degree to which free water and saturated tailings stored within the tailings pond are hydraulically connected with the dyke structures and the natural foundation materials. If the connection to the surrounding porous media is poor, this suggests that seepage from the tailings pond may be minimal. An investigation by Hunter (2001), indicated that seepage of process water contained within a nearby tailings pond constructed in a similar manner, was inhibited by layers of fine grained sediments and residual bitumen, such that unsaturated conditions were noted beneath the tailings pond. Subsequently, numerical modeling performed by Hunter (2001), indicated that much of the seepage from the tailings pond was related drainage of the dyke structures. The hypothesis of Hunter (2001) is supported at the current site based on the observation of process water chemistry indicative of post 1990 waters (See Section 4.1). Basically the arrival of Post-1990 process waters in the domain would not be expected if seepage was primarily occurring through fine grained sediments in the base of the pond.

Regardless of the source, in order to prevent groundwater contamination by seepage, drainage ditches are constructed around the perimeter of tailings ponds. However, as is the case in the current study, the ditches become ineffective at this role when the vertical extent of permeable surficial sediments exceeds that of the ditch. For this reason, the

spatial distribution of seepage plumes becomes highly dependant on the geometry of local aquifer systems.

Appendix B
Statistical Analysis of Naphthenic Acids

Notes:

- Statistical analysis is performed using the method of Clemente (2003). Regarding sample ID's, the last three characters refer to the sampling points shown in Figure 4.1, with the following exception:
 1. UW-OW04-07: This monitoring well is not discussed in the text and was installed north of the transect in the East Toe Berm area. Mine coordinates are 55122.93/53820.78 (Northing/Easting).
- Generally, with reference to the thesis, a different labelling system is used in the appendix for monitoring wells:

Appendix Label	Label used in Thesis
UWOW04-01a,b	1a,b
UWOW04-02a,b,c	2a,b,c
UWOW04-03a,b,c	3a,b,c
UWOW04-04a,b,c	4a,b,c
UWOW04-05a,b,c	5a,b,c
UWOW04-06a,b	7 (note this refers to UWOW0406b, the shallower well UWOW04-06a was never sampled)
UWOW04-07	Not discussed in text, note coordinates on borehole log for location.

Summary Table		UW-OW04-01A	UW-OW04-01B	UW-OW04-02B	UW-OW04-02C	UW-OW04-03A	UW-OW04-03B	UW-OW04-03B (duplicate)	UW-OW04-03C	UW-OW04-04A	UW-OW04-04B	UW-OW04-04C
UW-OW04-01B	Group1	0.959										
	Group2	0.934										
	Group3	0.635										
UW-OW04-02B	Group1	0.952	0.994									
	Group2	0.947	0.880									
	Group3	0.314	0.057									
UW-OW04-02C	Group1	0.738	0.701	0.688								
	Group2	0.747	0.690	0.787								
	Group3	0.709	0.409	0.541								
UW-OW04-03A	Group1	0.546	0.515	0.501	0.782							
	Group2	0.468	0.426	0.490	0.711							
	Group3	0.372	0.177	0.904	0.620							
UW-OW04-03B	Group1	0.903	0.861	0.851	0.825	0.618						
	Group2	0.709	0.653	0.748	0.966	0.737						
	Group3	0.033	0.011	0.235	0.081	0.191						
UW-OW04-03B(dup)	Group1	0.829	0.790	0.779	0.904	0.692	0.921					
	Group2	0.853	0.794	0.898	0.900	0.624	0.866					
	Group3	0.873	0.548	0.425	0.843	0.493	0.058					
UW-OW04-03C	Group1	0.534	0.501	0.486	0.788	0.982	0.611	0.691				
	Group2	0.380	0.345	0.395	0.594	0.844	0.614	0.521				
	Group3	0.043	0.016	0.259	0.097	0.214	0.990	0.070				
UW-OW04-04A	Group1	0.694	0.661	0.649	0.936	0.855	0.772	0.846	0.865			
	Group2	0.726	0.672	0.765	0.968	0.758	1.000	0.874	0.643			
	Group3	0.982	0.630	0.337	0.733	0.397	0.039	0.893	0.049			
UW-OW04-04B	Group1	0.813	0.776	0.766	0.936	0.731	0.898	0.973	0.733	0.878		
	Group2	0.781	0.723	0.823	0.965	0.677	0.930	0.934	0.564	0.935		
	Group3	0.509	0.269	0.747	0.778	0.837	0.141	0.637	0.161	0.534		
UW-OW04-04C	Group1	0.750	0.714	0.702	0.997	0.785	0.834	0.910	0.791	0.934	0.941	
	Group2	0.715	0.659	0.753	0.967	0.743	1.000	0.868	0.623	0.999	0.932	
	Group3	0.449	0.232	0.830	0.703	0.922	0.173	0.570	0.194	0.473	0.918	
East Toe Berm Well (UW-OW04-07)	Group1	0.908	0.951	0.955	0.649	0.468	0.807	0.737	0.450	0.613	0.727	0.664
	Group2	0.969	0.963	0.914	0.711	0.427	0.671	0.820	0.342	0.692	0.746	0.678
	Group3	0.666	0.383	0.593	0.949	0.674	0.097	0.797	0.114	0.690	0.832	0.756

	1	2
Compound	Alkane mixture in diesel and crude oil	n-Alkylated cyclohexane mixture in diesel and crude oil
Breif Summary of Results	Degradation results in decrease of higher molecular weight homologues and increase in lower molecular weight homologues	Degradation results in decrease of higher molecular weight homologues and increase in lower molecular weight homologues
Experimental Conditions	Field study, anearobic groundwater plume from hydrocarbon spill	Field study, anearobic groundwater plume from hydrocarbon spill
Microorganisms associated with Biodegradation	Indigeneous microorganisms in contaminated aquifer	Indigeneous microorganisms in contaminated aquifer
Medium	Unconfined sand aquifer	Unconfined sand aquifer
Extent of Degradation	Assumption of degradation is based on dissapearance of components/peaks in chemical signature and enrichment of ^{13}C rather than specific changes in concentrations	Assumption of degradation is based on dissapearance of components/peaks in chemical signature and enrichment of ^{13}C rather than specific changes in concentrations
Change in Chemical Signature	Relative and absolute increase in (lighter) C15-C16 fractions and relative and absolute decrease in (heavier) C25-C26 fraction	Relative and absolute increase in (lighter) C13-C14 fraction and relative and absolute increase in (heavier) C18-C19 fraction
Analytical Method	GCMS	GCMS
Comments	Authors suggest that in anearobic conditions the high molecular weight alkanes will be degraded preferentially and split into lower molecular weight alkanes. Therefore the decrease in the former and the increase in the latter is both relative and absolute. The authors also noted that in a mixture of alkanes of similar structure, degradation rates will be compound specific and thus some alkanes will remain resistant to degradation over long periods of time.	Authors suggest that in anearobic conditions the high molecular weight n-alkylcyclohexanes will be degraded preferentially and split into lower molecular weight n-alkylcyclohexanes. Therefore the decrease in the former and the increase in the latter is both relative and absolute. The authors also noted that in a mixture of n-alylcyclohexanes of similar structure, degradation rates will be compound specific and thus some n-alkylcyclohexanes will remain resistant to degradation over long periods of time.
Reference	Hostettler et al 2002	Hostettler et al 2002

	3	4
Compound	Hexadecanoic Acid (¹⁴ C labeled)	Hexadecanoic Acid (¹⁴ C labeled)
Breif Summary of Results	Some degradation in process affected waters in aerobic conditions	Some degradation in process affected waters in aerobic conditions however lesser amount due to temperature decrease
Experimental Conditions	Laboratory study conducted at 15 degrees celcius and at aerobic conditions	Laboratory study conducted at 5 degrees celcius and at aerobic conditions
Microorganisms associated with Biodegradation	Indigeneous microorganisms in tailings water	Indigeneous microorganisms in tailings water
Medium	One of: Suncor tailings water, Syncrude tailings water or Syncrude reclaimed water containing kodak naphthenic acids	One of: Suncor tailings water, Syncrude tailings water or Syncrude reclaimed water containing kodak naphthenic acids
Extent of Degradation	10-13% reduction in concentration in tailings water and 2% reduction in the concentration in reclaimed water containing commercial naphthenic acids over 4 week duration of study	4% reduction in concentration in tailings water and 1-2% reduction in concentration in reclaimed water containing commercial naphthenic acids over 4 week duration of study
Change in Chemical Signature	not reported	not reported
Analytical Method	Liquid Scintillation Counting	Liquid Scintillation Counting
Comments	Generally temperature was found to inpart a larger influence on degradation rates than oxygen supply, however it should be noted that in many cases the oxygen supply was quickly consumed leaving the microcosm in an aneorobic or near aneorobic state by the next sampling event. Thus a large difference between degradation rates in aerobic and anaerobic microcosms may not be apparent due to the fact that the former may only be truly aerobic for a short time.	Generally temperature was found to inpart a larger influence on degradation rates than oxygen supply, however it should be noted that in many cases the oxygen supply was quickly consumed leaving the microcosm in an aneorobic or near aneorobic state by the next sampling event. Thus a large difference between degradation rates in aerobic and anaerobic microcosms may not be apparent due to the fact that the former may only be truly aerobic for a short time.
Reference	lai et al 1994	lai et al 1994

	5	6
Compound	Hexadecanoic Acid (¹⁴ C labeled)	Hexadecanoic Acid (¹⁴ C labeled)
Breif Summary of Results	Some degradation in process affected waters in anaerobic conditions	Some increase degradation in process affected waters in aerobic conditions when nutrients added
Experimental Conditions	Laboratory study conducted at 15 degrees celcius and at anearobic or near anearobic conditions	Laboratory study conducted at 15 degress celcius, aerobic conditions and phophorus added
Microorganisms associated with Biodegradation	Indigeneous microorganisms in tailings water	Indigeneous microorganisms in tailings water
Medium	One of: Suncor tailings water, Syncrude tailings water or Syncrude reclaimed water containing kodak naphthenic acids	One of: Suncor tailings water, Syncrude tailings water or Syncrude reclaimed water containing kodak naphthenic acids
Extent of Degradation	8-9% reduction in concentration in tailings water and 2% reduction in concentration in reclaimed water containing commercial naphthenic acids over four week duration of study	13-20% reduction in concentration in tailings water and 8% reduction in concentration in reclaimed water containing commercial naphthenic acids over four week duration of study
Change in Chemical Signature	not reported	not reported
Analytical Method	Liquid Scintillation Counting	Liquid Scintillation Counting
Comments	Generally temperature was found to inpart a larger influence on degradation rates than oxygen supply, however it should be noted that in many cases the oxygen supply was quickly consumed leaving the microcosm in an anearobic or near aneorobic state by the next sampling event. Thus a large difference between degradation rates in aerobic and anaerobic microcosms may not be apparent due to the fact that the former may only be truly aerobic for a short time.	Degradation rates were noted to increase when phosphorus and nitrogen were added
Reference	lai et al 1994	lai et al 1994

	7
Compound	Cyclohexane carboxylic acid
Breif Summary of Results	In aerobic tailings water no degradation observed in the absence of nutrients and complete degradation in the presence of nutrients
Experimental Conditions	Laboratory study conducted at ambient temperatures in aerobic conditions
Microorganisms associated with Biodegradation	Indigenous microorganisms in tailings pore water
Medium	Tailings pore water
Extent of Degradation	An initial solution concentration of approximately 1000 mg/L was completely degraded by the day 16 sampling event in the presence of nitrogen and phosphorus. However no degradation was observed in the absence of these nutrients.
Change in Chemical Signature	not reported
Analytical Method	GC/FID
Comments	Initially, during the study additional phosphorus and nitrogen were not added to the microcosms. When this was the case no degradation was noted and it was only when nutrients were added that degradation begun.
Reference	Herman et. al. 1993

	8
Compound	Cyclohexane carboxylic acid
Breif Summary of Results	Degradation observed in aerobic conditions, in the presence of supplemental amounts of nitrogen and phosphorus
Experimental Conditions	Laboratory study conducted at ambient temperatures in aerobic conditions
Microorganisms associated with Biodegradation	Cultured indigeneous microorganisms of either: tailings pond derived, oil sands naphthenic acid degraders (<i>Acinebacter Calcoacetius</i> , <i>Pseudomonas Fluorescens</i> , <i>Kurthia sp.</i>) or tailings pond derived commercial (kodak) naphthenic acid degraders (<i>Pseudomonas stutzeri</i> & <i>Alcaligenes Denitrificans</i>) or uncultered mixture of microorganisms added via raw tailings water
Medium	Modified Bushnell-Haas medium and tailings water
Extent of Degradation	41-57% reduction of a 1 mM solution by the day 24 sampling event based on the amount of CO ₂ produced.
Change in Chemical Signature	not reported
Analytical Method	GC
Comments	Degradation may not occur in the absence of nitrogen and phosphorus.
Reference	Herman et. al. 1994

	9	10
Compound	1-methyl-1-Cyclohexane carboxylic acid	1-methyl-1-Cyclohexane carboxylic acid
Breif Summary of Results	In aerobic tailings water supplemented with nitrogen and phosphorus no degradation occurred.	In aerobic saturated fine tailings degradation only occurred when supplemental nitrogen and phosphorus were added
Experimental Conditions	Laboratory study conducted at ambient temperatures in aerobic conditions	Laboratory study conducted at ambient temperatures in aerobic conditions
Microorganisms associated with Biodegradation	Indigenous microorganisms in tailings pore water	Indigenous microorganisms in tailings
Medium	Tailings pore water	Saturated fine tailings
Extent of Degradation	An initial solution concentration of approximately 1000 mg/L showed no degradation over 40 day duration of the study both in the presence and absence of nitrogen and phosphorus	An initial concentration of approximately 1000 mg/L was completely degraded by the week 9 sampling event. However no degradation was noted before week six, at which point nitrogen and phosphorus were added.
Change in Chemical Signature	not reported	not reported
Analytical Method	GC/FID	GC/FID
Comments	Degradation not observed despite the presence of nutrients. However the same study showed that degradation did occur in saturated tailings in the presence of nutrients.	Initially, during the study additional phosphorus and nitrogen were not added to the microcosms. When this was the case no degradation was noted and it was only when nutrients were added that degradation began.
Reference	Herman et. al. 1993	Herman et. al. 1993

	11
Compound	2-methyl-1-Cyclohexane carboxylic acid
Breif Summary of Results	In aerobic tailings water degradation only occurred when supplemental nitrogen and phosphorus were added
Experimental Conditions	Laboratory study conducted at ambient temperatures in aerobic conditions
Microorganisms associated with Biodegradation	Indigenous microorganisms in tailings porewater
Medium	Tailings pore water
Extent of Degradation	An initial concentration of 1000 mg/L was completely degraded by the day 40 sampling event in the presence of nitrogen however no degradation was observed over the same period in the absence of these nutrients
Change in Chemical Signature	not reported
Analytical Method	GC/FID
Comments	Initially, during the study additional phosphorus and nitrogen were not added to the microcosms. When this was the case no degradation was noted and it was only when nutrients were added that degradation begun.
Reference	Herman et. al. 1993

	12
Compound	2-methyl-1-Cyclohexane carboxylic acid
Breif Summary of Results	Degradation observed in aerobic conditions, in the presence of supplemental amounts of nitrogen and phosphorus
Experimental Conditions	Laboratory study conducted at ambient temperatures in aerobic conditions
Microorganisms associated with Biodegradation	Cultured indigeneous microorganisms of either: tailings pond derived, oil sands naphthenic acid degraders (<i>Acinebacter Calcoacetius</i> , <i>Pseudomonas Fluorescens</i> , <i>Kurthia sp.</i>) or tailings pond derived commercial (Kodak) naphthenic acid degraders (<i>Pseudomonas stutzeri</i> & <i>Alcaligenes Denitrificans</i>) or uncultered mixture of microorganisms added via raw tailings water
Medium	Modified Bushnell-Haas medium and tailings water
Extent of Degradation	Over 24 day study a 7% reduction in the microcoms containing cultured oil sands naphthenic acid degraders was observed and a 47-67% reduction in microcosms containing cultured commercial (Kodak) naphthenic acid degraders was observed
Change in Chemical Signature	not reported
Analytical Method	GC
Comments	Greater amounts of degradation were observed in the presence of microorganicism cultured for commercial naphthenic acid degradation as opposed to those cultured for oil sands naphthenic acid degradation
Reference	Herman et. al. 1994

	13	14
Compound	cis-3-methyl-Cyclohexane carboxylic acid	cis-4-methyl-Cyclohexane carboxylic acid
Breif Summary of Results	Degradation observed in aerobic conditions, however trans isomer degrades more quickly than cis isomer.	Degradation observed in aerobic conditions, with trans isomer degradation more quickly than cis isomer. Temperature had a distict effect on degradation rates while pH did not.
Experimental Conditions	Laboratory studies conducted in aerobic conditions, in dark at 30°C	Laboratory studies conducted in aerobic conditions, in dark, with varying temperatures and pH
Microorganisms associated with Biodegradation	Indigenous microorganisms from Athabasca River water	Indigenous microorganisms from Athabasca River water
Medium	Athabasca River Water	Athabasca River Water
Extent of Degradation	Based on an initial concentration of 12 mg/L a half life of approximately 18 days was observed	Based on an initial concentration of 9 mg/L half lives were approximately 48 days in non-amended river water, 48 days at a pH of 6, 24 days at 30°C and 58 days at 10°C
Change in Chemical Signature	not reported	not reported
Analytical Method	GC/FID	GC/FID
Comments	The author indicates that the trans isomer degrades faster than the cis isomer because it has a more open structure which prevents the formation of intramolecular hydrogen bonds. The author reports that degradation proceeds via first order kinetics.	The author indicates that the trans isomer degrades faster than the cis isomer because it has a more open structure which prevents the formation of intramolecular hydrogen bonds. pH did not significantly affect degradation rates, while increased degradation rates were associated with higher temperatures. Author reports that degradation proceeds via first order kinetics
Reference	Headly et. al. 2001	Headly et. al. 2001

	15	16
Compound	trans-3-methyl-Cyclohexane carboxylic acid	trans-4-methyl-Cyclohexane carboxylic acid
Breif Summary of Results	Degradation observed in aerobic conditions, however trans isomer degrades more quickly than cis isomer.	Degradation observed in aerobic conditions, with trans isomer degradation more quickly than cis isomer. Temperature had a distict effect on degradation rates while pH did not.
Experimental Conditions	Laboratory studies conducted in aerobic conditions, in dark at 30°C	Laboratory studies conducted in aerobic conditions, in dark with varying temperatures and pH
Microorganisms associated with Biodegradation	Indigenous microorganisms from Athabasca River water	Indigenous microorganisms from Athabasca River water
Medium	Athabasca River Water	Athabasca River Water
Extent of Degradation	Based on an initial concentration of 12 mg/L a half life of approximately 14 days was observed	Based on an initial concentration of 9 mg/L half lives were approximately 10 days in non-amended river water, 21 days at a pH of 6, 5 days at 30°C and 41 days at 10°C
Change in Chemical Signature	not reported	not reported
Analytical Method	GC/FID	GC/FID
Comments	The author indicates that the trans isomer degrades faster than the cis isomer because it has a more open structure which prevents the formation of intramolecular hydrogen bonds. The author reports that degradation proceeds via first order kinetics.	The author indicates that the trans isomer degrades faster than the cis isomer because it has a more open structure which prevents the formation of intramolecular hydrogen bonds. pH did not significantly affect degradation rates, while increased degradation rates were associated with higher temperatures. Author reports that degradation proceeds via first order kinetics
Reference	Headly et. al. 2001	Headly et. al. 2001

17	
Compound	trans-4-pentyl-Cyclohexane carboxylic acid
Breif Summary of Results	Degradation observed in aerobic conditions, in the presence of supplemental amounts of nitrogen and phosphorus
Experimental Conditions	Laboratory study conducted in aerobic conditions at ambient temperatures
Microorganisms associated with Biodegradation	Cultured indigeneous microorganisms of either: tailings pond derived, oil sands naphthenic acid degraders (<i>Acinebacter Calcoacetius</i> , <i>Pseudomonas Fluorescens</i> , <i>Kurthia sp.</i>) or tailings pond derived commercial (kodak) naphthenic acid degraders (<i>Pseudomonas stutzeri</i> & <i>Alcaligenes Denitrificans</i>) or uncultured mixture of microorganisms added via raw tailings water
Medium	Modified Bushnell-Haas medium and tailings water
Extent of Degradation	From a 1 mM initial solution a 24% reduction by the day 24 sampling event in the microcoms containing either tailings water or cultured oil sands naphthenic acid degraders and 6% reduction in microcosms containing cultured commercial (Kodak) naphthenic acid degraders
Change in Chemical Signature	not reported
Analytical Method	GC
Comments	Degradation observed to proceed the most slowly in the presence of microorganisms cultured for commercial naphthenic acid degradation
Reference	Herman et. al. 1994

	18	19
Compound	trans-1-4-pentyl-Cyclohexane carboxylic acid	Cyclopentane carboxylic acid
Breif Summary of Results	Degradation observed in aerobic conditions, in the presence of supplemental amounts of nitrogen and phosphorus	In aerobic tailings water degradation only occurred when supplemental nitrogen and phosphorus were added
Experimental Conditions	Laboratory study conducted at neutral pH, in aerobic conditions at ambient temperatures	Laboratory study conducted in aerobic conditions, ambient temperatures with nitrogen and phosphorus added
Microorganisms associated with Biodegradation	Mixed cultures of oil sands, Kodak and Merichem naphthenic acid degraders	Indigenous microorganisms in tailings pore water
Medium	Modified Bushnell-Haas medium and tailings water	Tailings pore water
Extent of Degradation	From an initial concentration of 100 mg/L, approximately 90% is degraded over 30 days relative to concentrations in sterile controls	An initial concentration of approximately 1000 mg/L was completely degraded by the day 10 sampling event in the presence of nitrogen and phosphorus however no degradation was observed in the absence of these nutrients
Change in Chemical Signature	not reported	not reported
Analytical Method	HPLC	GC/FID
Comments	A lag or period of reduced degradation is noted for the first 8 days of the study. Furthermore, concentration decrease over the course of the study, in active relative to sterile microcosms was found to be statistically significant.	Initially, during the study additional phosphorus and nitrogen were not added to the microcosms. When this was the case no degradation was noted and it was only when nutrients were added that degradation began.
Reference	Clemente et al. 2003	Herman et. al. 1993

	20
Compound	Cyclopentane carboxylic acid
Breif Summary of Results	In aerobic saturated tailings degradation occurred in the absence of nitrogen and phosphorus.
Experimental Conditions	Laboratory studies conducted in aerobic conditions and at ambient temperatures
Microorganisms associated with Biodegradation	Indigenous microorganisms in tailings water
Medium	Saturated fine tailings
Extent of Degradation	An initial concentration of 1000 mg/L was completely degraded by week 2 sampling event in the absence of nitrogen and phosphorus
Change in Chemical Signature	not reported
Analytical Method	GC/FID
Comments	The same study showed the same compound was not degraded in the absence of nitrogen and phosphorus in the tailings water
Reference	Herman et. al. 1993

	21
Compound	Cyclohexane pentanoic acid
Breif Summary of Results	Degradation observed in aerobic conditions, in the presence of supplental amounts of nitrogen and phosphorus
Experimental Conditions	Laboratory study conducted in aerobic conditions and at ambient temperatures
Microorganisms associated with Biodegradation	Cultured indigeneous microorganisms of either: tailings pond derived, oil sands naphthenic acid degraders (<i>Acinebacter Calcoacetius</i> , <i>Pseudomonas Fluorescens</i> , <i>Kurthia sp.</i>) or tailings pond derived commercial (kodak) naphthenic acid degraders (<i>Pseudomonas stutzeri</i> & <i>Alcaligenes Denitrificans</i>) or uncultured mixture of microorganisms added via raw tailings water
Medium	Modified Bushnell-Haas medium and tailings water
Extent of Degradation	From a 1mM initial solution a 45-58% reduction was observed by the day 24 sampling event in the microcosms containing either cultured oil sands naphthenic acid degraders, cultured commercial naphthenic acid degraders or solely tailings water
Change in Chemical Signature	not reported
Analytical Method	GC
Comments	The amount of degradation is relatively similar for the different types of microorganisms
Reference	Herman et. al. 1994

	22	23
Compound	Cyclohexane pentanoic acid	4-Cyclohexyl butanoic acid
Breif Summary of Results	Degradation observed in aerobic tailings water and degradation rates increased in the presence of nitrogen and phosphate	Some degradation in anaerobic fine tailings, however no degradation observed in anaerobic sewage sludge
Experimental Conditions	Laboratory study conducted in aerobic conditions, at ambient temperatures with nitrogen and phosphorus added	Laboratory study conducted in the dark, in anaerobic conditions, at ambient temperatures and at pH 7.2-7.4
Microorganisms associated with Biodegradation	Indigenous microorganisms in tailings water	Indigenous microorganisms from sewage sludge or tailings water
Medium	Tailings water	Sewage sludge and saturated fine tailings
Extent of Degradation	Substrate was added until 60 mg/L dissolved organic carbon content was attained. Degradation is assumed to have occurred based on CO ₂ production and O ₂ utilization over the course of the 35 day study. Increased O ₂ consumption and CO ₂ production was observed when nitrogen and phosphorus were added.	Using initial concentrations of 200-800 mg/L, by the day 223 sampling event no degradation observed in sewage sludge based on lack of methane production and some degradation in fine tailings medium after 175 days based on methane production
Change in Chemical Signature	not reported	not reported
Analytical Method	GC	FT-IR/GC-EIMS
Comments	The extent of biodegradation is based on CO ₂ production and O ₂ consumption. When nitrogen and phosphorus are added, degradation rates are observed to increase.	When substrate is present in elevated concentrations, initially inhibition of methanogenesis may occur in fine tailings. Also methanogenesis was only observed in some fine tailings samples.
Reference	Herman et. al. 1994	Holowenko et. al. 2001

	24	25
Compound	5-Cyclohexyl pentanoic acid	3-Cyclohexyl propanoic acid
Breif Summary of Results	Some degradation in anaerobic sewage sludge, however no degradation observed in anearobic fine tailings	Some degradation in either anaerobic sewage sludge or fine tails
Experimental Conditions	Laboratory study conducted in the dark, in anearobic conditions, at ambient temperatures and at pH 7.2-7.4	Laboratory study conducted in the dark, in anearobic conditions, at ambient temperatures and at pH 7.2-7.4
Microorganisms associated with Biodegradation	Indigenous microorganisms from sewage sludge or tailings water	Indigenous microorganisms from sewage sludge or tailings water
Medium	Sewage sludge and saturated fine tailings	Sewage sludge and saturated fine tailings
Extent of Degradation	Using initial concentrations of 200-800 mg/L, by the day 223 sampling event, some degradation had occurred in sewage sludge based on methane production and after 175 days no degradation had occurred in the fine tailings.	Using initial concentrations of 200-800 mg/L, by the day 223 sampling event, some degradation had occurred in sewage sludge based on methane production and after 175 days some degradation had occurred in the fine tailings based on methane production.
Change in Chemical Signature	not reported	not reported
Analytical Method	FT-IR/GC-EIMS	FT-IR/GC-EIMS
Comments	When substrate is present in elevated concentrations, initially inhibition of methanogenesis in fine tailings may occur.	When substrate is present in elevated concentrations, initially inhibition of methanogenesis may occur in fine tailings samples. Also methanogenesis was only observed in some fine tailings samples.
Reference	Holowenko et. al. 2001	Holowenko et. al. 2001

	26	27
Compound	cis-4-methyl-Cyclohexane acetic acid	trans-4-methyl-Cyclohexane acetic acid
Breif Summary of Results	Degradation found to occur in aerobic river water. Temperature and chemical structure distinctly affected degradation rates and pH and organic carbon content did not	Degradation found to occur in aerobic river water. Temperature and chemical structure distinctly affected degradation rates and pH and organic carbon content did not
Experimental Conditions	Laboratory study conducted in the dark at varying temperatures, in aerobic conditions and with varying pH and amounts of dissoved organic carbon	Laboratory study conducted in the dark at varying temperatures, in aerobic conditions and with varying pH and amounts of dissoved organic carbon
Microorganisms associated with Biodegradation	Indigenous microorganisms from Athabasca River water	Indigenous microorganisms from Athabasca River water
Medium	Athabasca River Water	Athabasca River Water
Extent of Degradation	Based on initial concentrations of 9 mg/L half lives were approximately 41 days in non-amended river water, 58 days in river water containing 5 mg/L humic acid, 72 days at pH 7 and 36 days in river water at unknown pH with 7.5 mg/L humic acid. Using an initial concentration of 7.5 mg/L half lives were 16 days at 30°C and 140 days at 10°C.	Based on initial concentrations of 9 mg/L half lives were approximately 12 days in non-amended river water, 11 days in river water containing 5 mg/L humic acid, 12 days at pH 7 and 10 days in river water at unknown pH with 7.5 mg/L humic acid. Using an initial concentration of 7.5 mg/L, half lives were 4 days at 30°C and 48 days at 10°C.
Change in Chemical Signature	not reported	not reported
Analytical Method	GC/FID	GC/FID
Comments	The author indicates that the trans isomer degrades faster than the cis isomer because it has a more open structure which prevents the formation of intramolecular hydrogen bonds. pH and dissolved organic carbon did not significantly affect degradation rates, while increased degradation rates were associated with higher temperatures. Author reports that degradation proceeds via first order kinetics	The author indicates that the trans isomer degrades faster than the cis isomer because it has a more open structure which prevents the formation of intramolecular hydrogen bonds. pH and dissolved organic carbon did not significantly affect degradation rates, while increased degradation rates were associated with higher temperatures. Author reports that degradation proceeds via first order kinetics
Reference	Headly et. al. 2001	Headly et. al. 2001

	28	29
Compound	6-Phenyl hexanoic acid	Decahydro-2-naphthoic acid-8 (¹⁴ C)
Breif Summary of Results	Some degradation in anaerobic sewage sludge.	No degradation in anaerobic saturated fine tailings
Experimental Conditions	Laboratory study conducted in the dark, in anaerobic conditions, at ambient temperatures and at pH 7.2-7.4	Laboratory study conducted in the dark, in anaerobic conditions, at ambient temperatures and at pH 7.2-7.4
Microorganisms associated with Biodegradation	Indigenous microorganisms from sewage sludge	Indigenous microorganisms from tailings water
Medium	Sewage Sludge	Saturated fine tailings
Extent of Degradation	Using initial concentrations of 200-800mg/L, by the day 223 sampling event, some degradation had occurred in sewage sludge based on methane production	Initially a 0.5 uC activity solution was added and no degradation was observed over the 405 day study, based on measurements of radiolabeled methane and carbon dioxide
Change in Chemical Signature	not reported	not reported
Analytical Method	FT-IR/GC-EIMS	FT-IR/GC-EIMS
Comments	When substrate is present in elevated concentrations, initially inhibition of methanogenesis in fine tailings may occur.	Despite the duration of the study no degradation was observed, however aerobic degradation has been observed in other studies.
Reference	Holowenko et. al. 2001	Holowenko et. al. 2001

	30
Compound	Commercial (Kodak) Naphthenic Acid Sodium Salts Mixture
Breif Summary of Results	Degradation observed in aerobic conditions, in the presence of supplental amounts of nitrogen and phosphorus
Experimental Conditions	Laboratory study conducted in the dark, in aerobic conditions at ambient temperatures.
Microorganisms associated with Biodegradation	Kodak naphthenic acid cultured microorganisms in tailings water
Medium	Modified Bushnell-Haas medium and tailings water
Extent of Degradation	From an initial concentration of 100 mg/L, approximately a 30% decrease in naphthenic acid concentration was noted based on inorganic carbon measurements and relative to sterile controls
Change in Chemical Signature	not reported
Analytical Method	HPLC for naphthenic acid concentrations and GC for inorganic carbon measurement
Comments	Notably, only half of the carbon removed from naphthenic acids was released as inorganic carbon. Presumably, the other half is used in microorganism growth
Reference	Clemente et al. 2003

	31
Compound	Commercial (Kodak) Naphthenic Acid Sodium Salts Mixture
Breif Summary of Results	Degradation observed in aerobic conditions, in the presence of supplantal amounts of nitrogen and phosphorus
Experimental Conditions	Laboratory study conducted in aerobic conditions and at ambient temperatures
Microorganisms associated with Biodegradation	Cultured indogeneous microorganisms from tailings pond derived commercial (kodak) naphthenic acid degraders (Pseudomonas stutzeri & Alcaligenes Denitrificans)
Medium	Modified Bushnell-Haas medium and tailings water
Extent of Degradation	From a 1mM initial solution a 49-62% reduction was observed by the day 24 sampling event in the microcosms containing either cultured oil sands naphthenic acid degraders, cultured commercial naphthenic acid degraders or solely tailings water
Change in Chemical Signature	Visual inspection of GC profiles show a marked decrease in the size of the "hump" associated with the naphthenic acid mixture in the active microcosms compared to the control microcosm. Furthermore specific comparisons of the size of specific peaks to standards indicates that a statistically significant change has occurred in the signature due to degradation.
Analytical Method	GC/FID for GC profiles. GC for CO ₂ and O ₂ content and Total Organic Carbon Analyzer for TOC
Comments	The extent of biodegradation is based on comparison of CO ₂ production to initial total organic carbon content. This may underestimate the total amount of degradation since some DOC would be expected to be used for microorganism growth. The initial acute toxicity was approximately EC ₅₀ = 39% and subsequently no acute toxicity was noted by the sampling event on day 9.
Reference	Herman et. al. 1994

	32
Compound	Commercial (Kodak) Naphthenic Acid Sodium Salts Mixture
Breif Summary of Results	Degradation observed in aerobic tailings water and degradation rates increased in the presence of nitrogen and phosphate
Experimental Conditions	Laboratory study conducted in aerobic conditions, at ambient temperatures and nitrogen and phosphorus added
Microorganisms associated with Biodegradation	Indigenous microorganisms from tailings water
Medium	Tailings water
Extent of Degradation	Substrate was added until 60 mg/L dissolved organic carbon was attained. Degradation has occurred based on CO ₂ production and O ₂ utilization over the course of the 70 day study. Increased O ₂ consumption and CO ₂ production was observed in the presence of nitrogen and phosphorus.
Change in Chemical Signature	not reported
Analytical Method	GC/FID for GC profiles. GC for CO ₂ and O ₂ content and Total Organic Carbon Analyzer for TOC
Comments	The extent of biodegradation is based on a comparison CO ₂ production and O ₂ consumption to initial total organic carbon content. This may underestimate the total amount of degradation since some DOC would be expected to be used for microorganism growth. When nitrogen and phosphorus are added, degradation rates are observed to increase.
Reference	Herman et. al. 1994

	33
Compound	Commercial (Kodak) Naphthenic Acid Sodium Salts Mixture
Breif Summary of Results	Degradation observed in aerobic conditions in the presence of cultured oil sands microorganisms and supplemental nitrogen and phosphorus
Experimental Conditions	Laboratory study conducted in aerobic conditions in the dark and at ambient temperatures
Microorganisms associated with Biodegradation	Indigenous microorganisms from Syncrude Mildred Lake Settling Basin
Medium	Modified Bushnell-Haas medium
Extent of Degradation	By the day 12 sampling event a 90% reduction was observed from approximately 90 mg/L to less than 10 mg/L
Change in Chemical Signature	Absolute and relative decrease in C5-C13 fraction and relative increase in C14-C21 fraction, however not drastic because naphthenic acid mixture was originally comprised of mostly of C14-C21 fraction (>70%) and to a lesser extent the C5-C21 fraction (<30%)
Analytical Method	GCMS/HPLC
Comments	The initial acute toxicity was approximately IC50 = 16% and subsequently no acute toxicity was noted by day 43 sampling event. A lag time of 3 days was noted before biodegradation begun. Palmitic and steric acids are observed to be formed over duration of the study and are assumed to represent the growth of bacterial biomass
Reference	Clemente et. al. 2004

	34	35
Compound	Commercial (Kodak) Naphthenic Acid Sodium Salts Mixture	Commercial (Kodak) Naphthenic Acid Sodium Salts Mixture
Breif Summary of Results	Degradation observed in aerobic conditions in the presence of cultured oil sands microorganisms and supplemental nitrogen and phosphorus	No degradation in anearobic sewage sludge.
Experimental Conditions	Laboratory study conducted in aerobic conditions in the dark and at ambient temperatures	Laboratory study conducted in the dark, in anearobic conditions, at ambient temperatures and at pH 7.2-7.4
Microorganisms associated with Biodegradation	Indigenous microorganisms from Syncrude tailings water	Indigenous microorganisms from sewage sludge
Medium	Modified Bushnell-Haas medium and water	Sewage Sludge
Extent of Degradation	Almost complete degradation (>90%) of a 100 mg/L solution over the 40 day study	Using initial concentrations of 50 to 2000 mg/L, no degradation was observed after 450days, based on methane production
Change in Chemical Signature	not reported	not reported
Analytical Method	HPLC	FT-IR/GC-EIMS
Comments	Although degradation occurred over the entire duration of the study, the bulk of the degradation, a decrease from 100 mg/L to approximately 50 mg/L, occurred between days 4 and 7. Furthermore, using Suncor tailings water, instead of Syncrude tailings water yielded similar results.	The addition of naphthenic acids are observed to temporarily decrease amount of methanogenesis. The authors believe the production of methane observed in oil sands tailings impoundments is unrelated to naphthenic acid degradation.
Reference	Scott et al. 2005	Holowenko et. al. 2001

	36	37
Compound	Comercial (Merichem) Naphthenic Acid Mixture	Comercial (Merichem) Naphthenic Acid Mixture
Breif Summary of Results	Degradation observed in aerobic laboratory conditions	No degradation in anearobic bioreactor with supplemental nitrogen, phosphorus, glucose, acetate and toluene
Experimental Conditions	Laboratory study conducted in the dark, in aerobic conditions at ambient temperatures and approximately neutral pH.	Laboratory study conducted in anearobic conditions, in bioreactor, at neutral pH and ambient temperatures
Microorganisms associated with Biodegradation	Mixed cultures of oil sands, Kodak and Merichem naphthenic acid degraders	Indigenous bacteria from a munipal wastewater plant (methanosarcina sicilae & methanosarcina)
Medium	Modified Bushnell-Haas medium and tailings water	Simulated sea water with added glucose, toluene, acetate, ammonia, phosphorus and glass beads
Extent of Degradation	From an initial concentration of 100 mg/L, approximately 30% is degraded over 40 days relative to concentrations in sterile controls	Fluids added to bioreactor had a concentration of 500 mg/L and no degradation was observed after 1-2 day residence time in bioreactor based on naphthenic acid concentrations in the outflow.
Change in Chemical Signature	not reported	not reported
Analytical Method	HPLC	GC/FID
Comments	Change of naphthenic acid concentration ratio in active relative to control microcosms was found to be statistically significant.	Glucose, acetate, phosphorus and nitrogen were added to the bioreactor to simulate anearobic degradation however the residence time in the bioreactor was only 1 day.
Reference	Clemente et al. 2003	Gallagher 2001

	38	39
Compound	Comercial (Merichem) Naphthenic Acid Mixture	Comercial (Merichem) Naphthenic Acid Mixture
Breif Summary of Results	No degradation in anearobic bioreactor with supplemental nitrogen, phosphorus, glucose, acetate and toluene	Some degradation of non cyclic naphthenic acids in aerobic batch test in the presence of nitrogen and phosphorus
Experimental Conditions	Laboratory study conducted in anearobic conditions, in bioreactor, at neutral pH, ambient temperatures and supplemented with glucose	Laboratory batch test study conducted in aerobic conditions at 35°C
Microorganisms associated with Biodegradation	Indigenous microorganisms from a municipal wastewater plant and microorganisms from a produced water holding pond at an oil well site	Indienous microorganisms from brackish wetland
Medium	Simulated sea water with added toluene, acetate, ammonia, phosphorus, glass beads and modified methanogenic medium	Brackish aerobic wetland sediment with modified methanogenic medium
Extent of Degradation	Fluids added to bioreactor had a concentration of 500 mg/L and no degradation was observed after 1-2 day residence time in bioreactor based on naphthenic acid concentrations in the outflow.	Over the course of the 35 day study, degradation of naphthenic acids was observed based on a decrease in concentration from approximately 105 to 92 mg/L
Change in Chemical Signature	not reported	A decrease in what was thought to be straight chain fatty acids was noted
Analytical Method	GC/FID	GC/FID
Comments	The residence time in the bioreactor was only 1 day. In addition to the addition of glucose, acetate, phosphorus and nitrogen a 50/50 seawater medium/methanogenic medium mix was added to the bioreactor. Over the course of the study the mix became entirely methanogenic medium in order to simulate degradation.	The decrease in naphthenic acid concentration was interpreted by the author to reflect degradation of fatty acid type naphthenic acids. This is based on GC analysis
Reference	Gallagher 2001	Gallagher 2001

	40	41
Compound	Comercial (Merichem) Naphthenic Acid Mixture	Comercial (Merichem) Naphthenic Acid Mixture
Breif Summary of Results	No degradation in anaerobic batch test in the presence of supplemental nitrogen and phosphorus	No degradation in anaerobic batch test in the presence of supplemental nitrogen and phosphorus
Experimental Conditions	Laboratory batch test study conducted in anaerobic conditions at 35°C	Laboratory batch test study conducted in anaerobic conditions at 35°C
Microorganisms associated with Biodegradation	Indienous microorganims from brackish wetland	Microorganisms present on beads from bioreactor used earlier in study
Medium	Brackish anearobic wetland sediment with modified methanogenic medium	Modified methanogenic medium and anearobic biomass taken from bioreactor beads used earlier in study
Extent of Degradation	Using an initial concentration of 2000 mg/L, no degradation over course of 35 day study	Using an initial concentration of 2000 mg/L, no degradation over course of 35 day study
Change in Chemical Signature	not reported	not reported
Analytical Method	GC/FID	GC/FID
Comments	No degradation was observed over the course of the study despite the elevated temperatures and addition of nutrients.	No degradation was observed over the course of the study despite the elevated temperatures and addition of nutrients.
Reference	Gallagher 2001	Gallagher 2001

	42
Compound	Comercial (Merichem) Naphthenic Acid Mixture
Breif Summary of Results	Degradation in aerobic conditions with the addition of supplemental nitrogen and phosphorus
Experimental Conditions	Laboratory study conducted in aerobic conditions, in the dark and at ambient temperatures
Microorganisms associated with Biodegradation	Indigenous microorganims from Syncrude Mildred Lake Settling Basin.
Medium	Modified Bushnell-Haas medium
Extent of Degradation	By the day 10 sampling event, the concentration was observed to have been reduced from 109 mg/L to 8 mg/L.
Change in Chemical Signature	Significant relative and absolute decrease in C5-C13 fraction and relative increase in C14-C21 fraction. The significant change is related to the large initial relative proportion C5-C13 fractions (approximately 80%) versus that of the C14-C21 fraction (approximately 20%)
Analytical Method	GCMS/HPLC
Comments	Palmitic and salicylic acids were shown to increase over the duration of the study. The authors associate palmitic with biomass growth and salicylic acid was thought to represent and intermediate product during naphthenic acid degradation. The initial acute toxicity was approximately IC50 = 10% and subsequently no acute toxicity was noted by day 17.
Reference	Clemente et. al. 2004

	43
Compound	Naphthenic Acid Mixture derived from Oil Sands Tailings Impoundment and Kodak Naphthenic Acid Sodium Salts Mixture
Breif Summary of Results	Degradation of Kodak naphthenic acids is evident, while little degradation of oil sands derived naphthenic acids is apparent
Experimental Conditions	Laboratory study conducted in aerobic conditions, in the dark and at ambient temperatures
Microorganisms associated with Biodegradation	Indigenous microorganims from Syncrude Mildred Lake Settling Basin.
Medium	Modified Bushnell-Haas medium and tailings water
Extent of Degradation	Within approximately 7 days, the naphthenic acid concentration had decreased from 94 mg/L to 64 mg/L. While from 7 to 40 days, the concentration decreased to approximately 48 mg/L.
Change in Chemical Signature	The GC profile indicates that the hump associated with Kodak naphthenic acids is removed over the course of the study. With the exception of some removal of lower molecular weight components, the hump associated with oil sand naphthenic acids remains unchanged.
Analytical Method	GCMS/HPLC
Comments	The relatively larger amount of initial (up to day 7) degradation reflects the removal of commercial naphthenic acids, while lower amount of degradation after day 7 reflects removal of oil sands naphthenic acids. Compared to other microcoms in the study, a greater amount of oil sands naphthenic acid was noted when microcosms were mixed with Kodak naphthenic acids.
Reference	Scott et al. 2005

	44
Compound	Naphthenic Acid Mixture derived from Oil Sands Tailings Impoundments
Breif Summary of Results	Degradation in aerobic conditions with the addition of supplemental nitrogen and phosphorus
Experimental Conditions	Laboratory study conducted in the dark, in aerobic conditions at ambient temperatures and approximately neutral pH.
Microorganisms associated with Biodegradation	Mixed cultures of oil sands, Kodak and Merichem naphthenic acid degraders
Medium	Modified Bushnell-Haas medium and tailings water
Extent of Degradation	From an initial concentration of 100 mg/L, approximately 40% degradation is noted relative to sterile cultures after 40 days.
Change in Chemical Signature	not reported
Analytical Method	HPLC
Comments	Change of naphthenic acid concentrations in active relative to control microcosms was found to be statistically significant.
Reference	Clemente et al. 2003

	45
Compound	Naphthenic Acid Mixture derived from Oil Sands Tailings Impoundments
Breif Summary of Results	Degradation in aerobic conditions with the addition of supplemental nitrogen and phosphorus
Experimental Conditions	Laboratory study conducted in aerobic conditions at ambient temperatures
Microorganisms associated with Biodegradation	Cultured indogeneous microorganisms from tailings pond derived commercial (kodak) naphthenic acid degraders (Pseudomonas stutzeri & Alcaligenes Denitrificans)
Medium	Modified Bushnell-Haas medium
Extent of Degradation	By the day 20 sampling event, degradation has occurred and is expressed as the conversion of approximately 20-50% of substrate organic carbon into CO ₂ . The variation in degradation is due to the amount of dilution of the naphthenic acid solution. Dilutions of 1:20 and 1:50 were used.
Change in Chemical Signature	A visual inspection of GC profiles shows only a slight decrease in the size of the "hump" associated with the naphthenic acid mixture in the active microcoms compared to the control microcosm. Furthermore specific comparisons of the size of specific peaks to standards was problematic due to variability of the naphthenic acid signatures in active microcosms.
Analytical Method	GC/FID for GC profiles. GC for CO ₂ and O ₂ content and Total Organic Carbon Analyzer for TOC
Comments	The extent of degradation is based on a comparison of CO ₂ production to initial total organic carbon. This technique may underestimate degradation since some DOC is expected to be used for microorganism growth. In the dilute sample, the acute toxicity was reduced from approximately EC50 = 53% to EC50 = 90% over the duration of the 20 day study. In the concentrated sample, acute toxicity was reduced from approximately EC50 = 28% to EC50 = 50% over the 20 day study.
Reference	Herman et. al. 1994

	46
Compound	Naphthenic Acid Mixture derived from Oil Sands Tailings Impoundments
Breif Summary of Results	Degradation in aerobic conditions with the addition of supplemental nitrogen and phosphorus
Experimental Conditions	Laboratory study conducted in aerobic conditions at ambient temperatures
Microorganisms associated with Biodegradation	Cultured indigenous microorganisms from tailings pond derived oil sands naphthenic acid degraders (<i>Acinebacter Calcoacetius</i> , <i>Pseudomonas Fluorescens</i> , <i>Kurthia</i> sp.)
Medium	Modified Bushnell-Haas medium
Extent of Degradation	By the day 30 sampling event, in a 1:50 dilution, degradation was observed and is expressed as the conversion of approximately 70% of substrate organic carbon into CO ₂ .
Change in Chemical Signature	not reported
Analytical Method	GC/FID for GC profiles. GC for CO ₂ and O ₂ content and Total Organic Carbon Analyzer for TOC
Comments	The extent of degradation is based on a comparison of CO ₂ production to initial total organic carbon content. This technique may underestimate degradation since some DOC is expected to be used for microorganism growth. Acute toxicity was shown to decrease from EC ₅₀ = 24% to EC ₅₀ = 41% over the course of the 30 day study.
Reference	Herman et. al. 1994

	47	48
Compound	Naphthenic Acid Mixture derived from Oil Sands Tailings Impoundments	Naphthenic Acid Mixture derived from Oil Sands Tailings Impoundments
Breif Summary of Results	Degradation observed in aerobic tailings water and degradation rates increased in the presence of nitrogen and phosphate	Degradation observed in aerobic groundwater with supplemental amounts of nitrogen and phosphorus
Experimental Conditions	Laboratory study conducted in aerobic conditions, at ambient temperatures	Laboratory study conducted in the dark, at aerobic conditions and ambient temperatures
Microorganisms associated with Biodegradation	Indigenous microorganims from tailings water	Indigenous microorganisms from process water impacted aquifer at Suncor site
Medium	Tailings water	Sand and groundwater taken from impacted aquifer at suncor site and modified bushnell haas medium
Extent of Degradation	In a 1:50 dilution, by the day 70 sampling event, some degradation has occurred based on CO ₂ production and O ₂ utilization. Increased O ₂ consumption and CO ₂ production was observed in the presence of nitrogen and phosphorus.	Based on an initial concentration of 30 mg/L, a 60% decrease was observed over the 140 day study. The decrease represents the ratio of naphthenic acid concentrations in control microcosms versus active microcosms
Change in Chemical Signature	not reported	Relative and absolute decrease in C5-C14 fraction and relative increase in C22-C33 fraction
Analytical Method	GC/FID for GC profiles. GC for CO ₂ and O ₂ content and Total Organic Carbon Analyzer for TOC	FTIR/GCMS
Comments	The extent of biodegradation is based on a comparison of CO ₂ production and O ₂ consumption to initial total organic carbon content. This technique may underestimate degradation since some DOC is expected to be used for microorganism growth. When nitrogen and phosphorus are added, degradation rates are observed to increase.	A lag time of 14 to 42 days was noted before degradation was observed.
Reference	Herman et. al. 1994	Gervais, 2004

	49	50
Compound	Naphthenic Acid Mixture derived from Oil Sands Tailings Impoundments	Naphthenic Acid Mixture derived from Oil Sands Tailings Impoundments
Breif Summary of Results	Degradation observed in aerobic groundwater with supplemental amounts of nitrogen and phosphorus	No degradation observed in anaerobic groundwater with supplemental amounts of nitrogen and phosphorus
Experimental Conditions	Laboratory study conducted in the dark, at aerobic conditions and ambient temperatures	Laboratory study conducted in the dark, at anaerobic conditions and ambient temperatures
Microorganisms associated with Biodegradation	Indigenous microorganisms from tailings water	Indigenous microorganisms from process water impacted aquifer at Suncor site
Medium	Modified Bushnell-Haas medium and tailings water	Sand and groundwater taken from impacted aquifer at suncor site and modified bushnell haas medium
Extent of Degradation	A decrease from 60 mg/L to approximately 50 mg/L was noted over the 40 day study	No measurable change over 6 month study based a comparison of naphthenic acid concentrations in control microcosms versus active microcosms. Initial concentrations were approximately 30 mg/L.
Change in Chemical Signature	Not reported, however based on other microcoms associated with the study, it is likely that the lower molecular weight naphthenic acids were preferentially removed	No statistically significant change in signature
Analytical Method	HPLC	FTIR/GCMS
Comments	Using Suncor tailings water in place of Syncrude tailings water produced similar results.	A slight increase in naphthenic acid concentration was noted over time, which the author believed may be related to a change in the analytical method or an increase in pH.
Reference	Scott et al. 2005	Gervais, 2004

	51
Compound	Naphthenic Acid Mixture derived from Oil Sands Tailings Impoundments
Breif Summary of Results	No degradation observed in anaerobic tailings water
Experimental Conditions	Laboratory study conducted in the dark, in anearobic conditions, at ambient temperatures and at pH 7.2-7.4
Microorganisms associated with Biodegradation	Indigenous microorganims from tailings water
Medium	Saturated fine tailings
Extent of Degradation	Using initial concentrations of 50 to 500 mg/L above initial concentrations, no degradation was observed over 240 day study based on methane production
Change in Chemical Signature	not reported
Analytical Method	FT-IR/GC-EIMS
Comments	The addition of naphthenic acids are observed to temporarily decrease amount of methanogenesis. The authors believe the production of methane in the tailings impoundments is unrelated to naphthenic acid degradation.
Reference	Holowenko et. al. 2001

Appendix C
Solid Phase Analysis

Notes:

The sample ID's refer to the coring locations shown in Figure 4.10 as follows:

1. UWOW04-02: Coring Location A
2. UWOW04-04: Coring Location B
3. UWOW04-06: Coring Location C

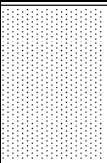

The number in brackets beside the sample ID refers to the depth of sample, in terms of meters below ground level.

- Generally, with reference to the thesis, a different labelling system is used in the appendix for monitoring wells:

Appendix Label	Label used in Thesis
UWOW04-01a,b	1a,b
UWOW04-02a,b,c	2a,b,c
UWOW04-03a,b,c	3a,b,c
UWOW04-04a,b,c	4a,b,c
UWOW04-05a,b,c	5a,b,c
UWOW04-06a,b	7 (note this refers to UWOW0406b, the shallower well UWOW04-06a was never sampled)
UWOW04-07	Not discussed in text, note coordinates on borehole log for location.

- The monitoring well referred to in the text as 6A is listed here using the label originally assigned by Syncrude Canada Ltd. (OW01-04B)

Borehole Log		Project M Sc Thesis	Sheet Number 1 of 1	Hole Number UW OW04-01	Date 12 September, 2004				
Site Location MLSB (Cell 25)		Logged By Alex Oiffer	Checked By AO	Northing 53166.26	Easting 53816.00				
Driller Mobile Augers	Drill Equipment Solid Stem Auger	Boring Diameter (m) 0.15	Total Depth (m) 11.9 m	Pipe Top Elevation (mASL) 318.86	Stickup (m) 0.80				
Monitoring Well Installed See Below		Screened Interval (mBGL) See Below		Weather Conditions Overcast and rainy	Sample Type				
Piezometer & Well Diagram(s)	Main Component Summary	Depth (m)	Graphic Log	U.S.C.S.	Snyderite Classification	Description and Classification Colour, Size Range, Main Component, Minor Components, Moisture Content, Structure, Angularity, Odor	Lab Sample		
							Field ID	Depth Range (m)	
	Sandy Silt	1				Sandy Silt, Tailings Sand, light reddish brown, moist (0 - 2.4 m)			
			2			Sandy Clay, black, low plasticity, moist (1.5 - 1.8 m)			
	Sandy Silt	3				Sandy Silt, light reddish brown, damp, clay stringers throughout (2.4 - 3.5 m)			
	Medium Fine Sand	4				Medium to Fine Sand, light reddish brown/grey, damp, saturated at 4.0 m, rare black clay stringers throughout (3.3 - 5.2 m)			
			5						
	Oil Sand	6				Medium to Fine Oilsand, black, saturated (5.2 - 5.6 m)			
	Medium Fine Sand	7				Medium to Fine Sand, dark brown-red, saturated, rare black clay stringers and organics throughout (5.6 - 8.5 m)			
			8				Medium to Fine Oilsand, black, saturated (8.4 - 8.5 m)		
	Medium Fine Sand	9				Medium to Fine Sand, medium grey, saturated (8.5 - 9.4 m)			
	Sandy Silt	10				Sandy Silt, medium grey, saturated			
Notes: Two monitoring wells were installed at this location using a direct push M5T Drilling Rig. An expendable stainless steel point is located below each piezometer. The riser pipe is constructed with schedule 40 PVC casing, with 21 mm ID and 27 mm OD. The screen has an ID of 21 mm and an OD of 36 mm. The screen is comprised of three layers: an innermost layer of schedule 40, 10 slot PVC screen, a layer of 20x40 silica sand and an outermost layer of 65 mesh stainless steel. The length of the screen is 0.15 m. Each well is capped with a slip on PVC well cap. A standard red, protective well casing is installed over each piezometer. Bentonite chips and 10-20 silica sand was used to fill the annular space above the water table and in the protective casing.									

Borehole Log		Project M Sc Thesis		Sheet Number 1 of 1		Hole Number UW OW04-01		Date 12 September, 2004	
Site Location MLSB (Cell 25)		Logged By Alex Oiffer		Checked By AO		Northing 53166.26		Easting 53816.00	
Driller Mobile Augers		Drill Equipment Solid Stem Auger		Boring Diameter (m) 0.15		Total Depth (m) 11.9 m		Pipe Top Elevation (mASL) 318.86	
Monitoring Well Installed See Below				Screened Interval (mBGL) See Below		Weather Conditions Overcast and rainy		Sample Type	
Piezometer & Well Diagram(s)	Main Component Summary	Depth (m)	Graphic Log	U.S.C.S.	Synecude Classification	Description and Classification Colour, Size Range, Main Component, Minor Components, Moisture Content, Structure, Angularity, Odor	Lab Sample		
							Field ID	Depth Range (m)	
	Medium Fine Sand	11				Medium to Fine Sand, medium grey, saturated (8.5 - 11.6 m)			
		12							
	13	END OF HOLE 11.9 m							
Notes: Two monitoring wells were installed at this location using a direct push M5T Drilling Rig. An expendable stainless steel point is located below each piezometer. The riser pipe is constructed with schedule 40 PVC casing, with 21 mm ID and 27 mm OD. The screen has an ID of 21 mm and an OD of 36 mm. The screen is comprised of three layers: an innermost layer of schedule 40, 10 slot PVC screen, a layer of 20x40 silica sand and an outermost layer of 65 mesh stainless steel. The length of the screen is 0.15 m. Each well is capped with a slip on PVC well cap. A standard red, protective well casing is installed over each piezometer. Bentonite chips and 10-20 silica									

Borehole Log		Project M Sc Thesis		Sheet Number 1 of 1		Hole Number UW OW04-02		Date 12 September, 2004	
Site Location MLSB (Cell 25)			Logged By Alex Oiffer		Checked By AO		Northing 53172.416		Easting 53840.782
Driller Mobile Augers		Drill Equipment Solid Stem Auger		Boring Diameter (m) 0.15		Total Depth (m) 10.1 m		Pipe Top Elevation (mASL) 316.78	
Monitoring Well Installed See Below				Screened Interval (mBGL) See Below			Weather Conditions Overcast and rainy		Sample Type Core
Piezometer & Well Diagram(s)	Main Component Summary	Depth (m)	Graphic Log	U.S.C.S.	Symbende Classification	Description and Classification Colour, Size Range, Main Component, Minor Components, Moisture Content, Structure, Angularity, Odor	Lab Sample		
							Field ID	Depth Range (m)	
	Medium Fine Sand	1	[Dotted pattern]			Medium to Fine Sand, dark brown-red, very coarse gravel throughout, moist (0 - 2.4 m)	Core Obtained for 3 - 10 mBGL		
		2							
	Medium Fine Sand	3	[Dotted pattern]			Medium to Fine Sand, light brown-red, saturated (2.4 - 6.2 m)			
		4							
		5							
	Medium Fine Sand	6	[Dotted pattern]			Medium to Fine Sand, medium grey, saturated (6.2 - 8.8 m)			
		7							
		8	[Dotted pattern]			Sandy Silt, medium grey, saturated (8.8 - 10.1 m)			
		9							
	Sandy Silt	10				Rounded very coarse gravel starts at 9.9 m			
		11				END OF HOLE 10.1 M			

Notes:

Two monitoring wells were installed at this location using a direct push M5T Drilling Rig. An expendable stainless steel point is located below each piezometer. The riser pipe is constructed with schedule 40 PVC casing, with 21 mm ID and 27 mm OD. The screen has an ID of 21 mm and an OD of 36 mm. The screen is comprised of three layers: an innermost layer of schedule 40, 10 slot PVC screen, a layer of 20x40 silica sand and an outermost layer of 65 mesh stainless steel. The length of the screen is 0.15 m. Each well is capped with a slip on PVC well cap. A standard red, protective well casing is installed over each piezometer. Bentonite chips and 10-20 silica sand was used to fill the annular space above the water table and in the protective casing.

Borehole Log		Project M Sc Thesis		Sheet Number 1 of 1	Hole Number UW OW04-03	Date 11 September, 2004			
Site Location MLSB (Cell 25)			Logged By Alex Oiffer	Checked By AO	Northing 53159.33	Easting 53994.02			
Driller Mobile Augers		Drill Equipment Solid Stem Auger	Boring Diameter (m) 0.15	Total Depth (m) 10.1 m	Pipe Top Elevation (mASL) 314.91		Stickup (m) 0.80		
Monitoring Well Installed See Below				Screened Interval (mBGL) See Below	Weather Conditions Overcast and rainy		Sample Type		
Piezometer & Well Diagram(s)		Main Component Summary	Depth (m)	Graphic Log	U.S.C.S.	Snyder Classification	Description and Classification Colour, Size Range, Main Component, Minor Components, Moisture Content, Structure, Angularity, Odor	Lab Sample	
								Field ID	Depth Range (m)
		Medium Fine Sand	1				Medium to Fine Sand (Topsoil), dark brown-red, organics throughout, moist (0 - 0.6 m)		
			2		Medium to Fine Sand, light red-brown, saturated near 1 m (0.6 - 5.2 m)				
		Medium Fine Sand	3		Medium to coarse gravel and dark clay stringers 0.6 - 0.9 m				
			4						
			5						
		Medium Coarse Sand	6		Medium to Coarse Sand, light red-brown grading into grey, saturated (5.2 - 5.9 m)				
		Medium Fine Sand	7		Medium to Fine Sand, medium grey, saturated (5.9 - 7.9 m)				
			8						
		Clay Silt	9		Clayey Silt, medium grey, saturated, oil sand odor (7.9 - 9.6 m)				
		Clay Silt	10		Clayey Silt, medium grey, very coarse angular - rounded gravel throughout, saturated, oil sand odor (9.6 - 10.1 m)				
			11		END OF HOLE 10.1 m				

Notes:

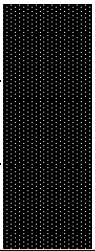
Two monitoring wells were installed at this location using a direct push M5T Drilling Rig. An expendable stainless steel point is located below each piezometer. The riser pipe is constructed with schedule 40 PVC casing, with 21 mm ID and 27 mm OD. The screen has an ID of 21 mm and an OD of 36 mm. The screen is comprised of three layers: an innermost layer of schedule 40, 10 slot PVC screen, a layer of 20x40 silica sand and an outermost layer of 65 mesh stainless steel. The length of the screen is 0.15 m. Each well is capped with a slip on PVC well cap. A standard red, protective well casing is installed over each piezometer. Bentonite chips and 10-20 silica sand was used to fill the annular space above the

Borehole Log		Project	Sheet Number	Hole Number	Date			
Site Location		M Sc Thesis	1 of 1	UW OW04-04	11 September, 2004			
MLSB (Cell 25)		Logged By	Checked By	Northing	Easting			
Driller		Alex Oiffer	AO	53172.24	54164.34			
Mobile Augers		Drill Equipment	Boring Diameter (m)	Total Depth (m)	Pipe Top Elevation (mASL)			
Monitoring Well Installed		Solid Stem Auger	0.15	10.1 m	319.08			
See Below		Screened Interval (mBGL)		Weather Conditions	Sample Type			
		See Below		Overcast and rainy	Core			
Piezometer & Well Diagram(s)	Main Component Summary	Depth (m)	Graphic Log	U.S.C.S.	Synchronode Classification	Description and Classification Colour, Size Range, Main Component, Minor Components, Moisture Content, Structure, Angularity, Odor	Lab Sample	
							Field ID	Depth Range (m)
	Medium Sand	1				Medium Sand, dark brown-red, organics, coarse gravel and black clay stringers near ground surface, moist (0 - 1.5 m)	Core Obtained for 5 - 9.7 mBGL	
	Medium Sand	2		Medium Sand, light brown-red, moist (1.5 - 8.2 m)				
		3		Clay stringers (2.4 - 2.7 m)				
		4						
		5						
		6						
		7						
		8		Sand becomes saturated at 5.5 m				
		8.2						
	Medium Fine Sand	9		Medium Fine Sand, medium grey, saturated (8.2 - 8.5 m)				
	Clay Silt	9.4		Clayey Silt, medium grey, oxidized staining (8.5 - 9.8 m)				
9.8								
		10	REFUSAL AT 9.8 m					
		11						

Notes:
Two monitoring wells were installed at this location using a direct push M5T Drilling Rig. An expendable stainless steel point is located below each piezometer. The riser pipe is constructed with schedule 40 PVC casing, with 21 mm ID and 27 mm OD. The screen has an ID of 21 mm and an OD of 36 mm. The screen is comprised of three layers: an innermost layer of schedule 40, 10 slot PVC screen, a layer of 20x40 silica sand and an outermost layer of 65 mesh stainless steel. The length of the screen is 0.15 m. Each well is capped with a slip on PVC well cap. A standard red, protective well casing is installed over each piezometer. Bentonite chips and 10-20 silica sand was used to fill the annular space above the water table

Borehole Log		Project M Sc Thesis		Sheet Number 1 of 2		Hole Number UW OW04-05		Date 10 September, 2004						
Site Location MLSB (Cell 25)			Logged By Alex Oiffer		Checked By AO		Northing 53230.67		Easting 54257.86					
Driller Mobile Augers		Drill Equipment Solid Stem Auger		Boring Diameter (m) 0.15		Total Depth (m) 10.1 m		Pipe Top Elevation (mASL) 317.71		Stickup (m) 0.80				
Monitoring Well Installed See Below				Screened Interval (mBGL) See Below			Weather Conditions Overcast and rainy		Sample Type					
Piezometer & Well Diagram(s)			Main Component Summary	Depth (m)	Graphic Log	U.S.C.S.	Syracuse Classification	Description and Classification Colour, Size Range, Main Component Minor Components, Moisture Content Structure, Angularity, Odor		Lab Sample				
										Field ID	Depth Range (m)			
			Medium Sand	1	[Dotted pattern]			Medium Sand, light brown-red, organics and fine gravel near ground surface, moist (0 - 3.0 m)						
				2										
				3										
						Sandy Clay	4	[Cross-hatched pattern]			Sandy Clay, black, fine gravel, moist (3.0 - 4.0 m)			
						Medium Sand	5				Medium Sand, light brown, moist, oxidized stains throughout (4.0 - 8.8 m)			
							6			Saturated at 5.2 m				
							7			Clay lenses and organics from 7.0 - 8.8 m				
							8			Gravel at 7.9 m				
						Sandy Clay	9	[Cross-hatched pattern]			Sandy Clay, grey, rounded to angular, fine to very coarse gravel, medium to high plasticity, saturated (8.8 - 11.6 m)			
							10							
							11							
						Sandy Clay	12	[Cross-hatched pattern]			Sandy Clay, grey, rounded to angular, fine to very coarse gravel, low plasticity, saturated (11.6 - 13.9 m)			
							13							
							14							

Notes:
Two monitoring wells were installed at this location using a direct push M5T Drilling Rig. An expendable stainless steel point is located below each piezometer. The riser pipe is constructed with schedule 40 PVC casing, with 21 mm ID and 27 mm OD. The screen has an ID of 21 mm and an OD of 36 mm. The screen is comprised of three layers: an innermost layer of schedule 40, 10 slot PVC screen, a layer of 20x40 silica sand and an outermost layer of 65 mesh stainless steel. The length of the screen is 0.15 m. Each well is capped with a slip on PVC well cap. A standard red, protective well casing is installed over each piezometer. Bentonite chips and 10-20 silica sand was used to fill the annular space

Borehole Log		Project M Sc Thesis		Sheet Number 1 of 2		Hole Number UW OW04-05		Date 10 September, 2004	
Site Location MLSB (Cell 25)			Logged By Alex Oiffer		Checked By AO		Northing 53230.67		Easting 54257.86
Driller Mobile Augers		Drill Equipment Solid Stem Auger	Boring Diameter (m) 0.15		Total Depth (m) 10.1 m	Pipe Top Elevation (mASL) 317.71		Stickup (m) 0.80	
Monitoring Well Installed See Below			Screened Interval (mBGL) See Below			Weather Conditions Overcast and rainy		Sample Type	
Piezometer & Well Diagram(s)	Main Component Summary	Depth (m)	Graphic Log	U.S.C.S.	Sieve Classification	Description and Classification Colour, Size Range, Main Component Minor Components, Moisture Content Structure, Angularity, Odor	Lab Sample		
							Field ID	Depth Range (m)	
	Clayey Sand	15				Clayey Sand (Oil sand), medium to fine sand, gravel throughout, saturated, oil sand odor (13.9 - 17.0 m)			
		16							
		17							
		18				END OF HOLE 17.0 M			
Notes: Two monitoring wells were installed at this location using a direct push M5T Drilling Rig. An expendable stainless steel point is located below each piezometer. The riser pipe is constructed with schedule 40 PVC casing, with 21 mm ID and 27 mm OD. The screen has an ID of 21 mm and an OD of 36 mm. The screen is comprised of three layers: an innermost layer of schedule 40, 10 slot PVC screen, a layer of 20x40 silica sand and an outermost layer of 65 mesh stainless steel. The length of the screen is 0.15 m. Each well is capped with a slip on PVC well cap. A standard red, protective well casing is installed over each piezometer. Bentonite chips and 10-20 silica sand was used to fill the annular space									

Borehole Log		Project	Sheet Number	Hole Number	Date			
MLS (Cell 25)		M Sc Thesis	1 of 1	UW OW04-06	09 September, 2004			
Site Location		Logged By	Checked By	Northing	Easting			
MLSB (Cell 25)		Alex Oiffer	AO	53154.02	54571.45			
Driller		Drill Equipment	Boring Diameter (m)	Total Depth (m)	Pipe Top Elevation (mASL)			
Mobile Augers		MST Direct Push Rig	0.05	8.0 m	314.66			
Monitoring Well Installed			Screened Interval (mBGL)	Weather Conditions	Sample Type			
See Below			See Below	Partly Sunny	Core			
Piezometer & Well Diagram(s)	Main Component Summary	Depth (m)	Graphic Log	U.S.C.S.	Snyder Classification	Description and Classification Colour, Size Range, Main Component, Minor Components, Moisture Content, Structure, Angularity, Odor	Core Sample	
							Field ID	Depth Range (m)
	NOT SAMPLED	1	[Solid black bar]			NOT SAMPLED (0 - 3.0 m)	Core Obtained for 3 - 8 mBGL	[X]
		2						
		3						
		4	[Medium coarse sand pattern]			Medium Coarse Sand, light red-brown, clay lenses moist (3.0 - 3.5 m)		
		5	[Silty medium-fine sand pattern]			Silty Medium-Fine Sand, light red-brown, saturated (3.5 - 4.6 m)		
		6	[Clay pattern]			Clay, black, fine gravel throughout, coarse to medium grained sand lenses throughout, saturated, oil sands smell (4.6 - 8.0 m)		
		7						
		8						
		9				END OF HOLE 8.0 m		
		10						

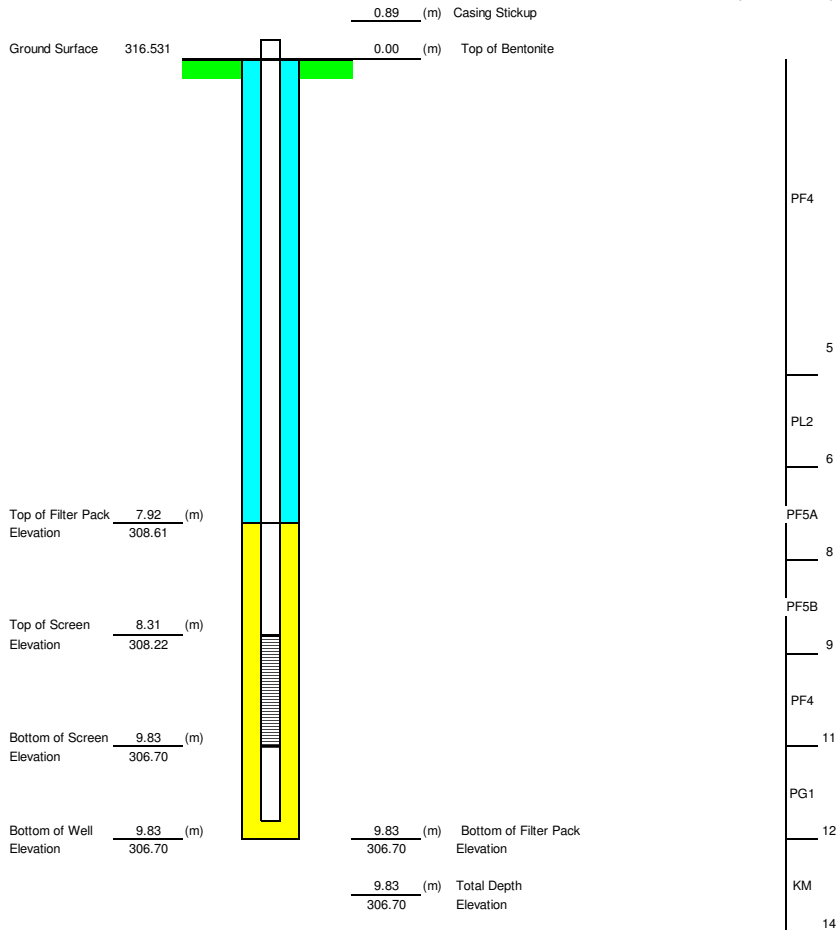
Notes:
Two monitoring wells were installed at this location using a direct push MST Drilling Rig. An expendable stainless steel point is located below each piezometer. The riser pipe is constructed with schedule 40 PVC casing, with 21 mm ID and 27 mm OD. The screen has an ID of 21 mm and an OD of 36 mm. The screen is comprised of three layers: an innermost layer of schedule 40, 10 slot PVC screen, a layer of 20x40 silica sand and an outermost layer of 65 mesh stainless steel. The length of the screen is 0.15 m. Each well is capped with a slip on PVC well cap. A standard red, protective well casing is installed over each piezometer. Bentonite chips and 10-20 silica sand was used to fill the annular space above the water

Borehole Log		Project	Sheet Number	Hole Number	Date				
		M Sc Thesis	1 of 1	UW OW04-07	12 September, 2004				
Site Location		Logged By	Checked By	Northing	Easting				
MLSB-ETB (Cell 23)		Alex Oiffer	AO	55122.93	53820.78				
Driller	Drill Equipment	Boring Diameter (m)	Total Depth (m)	Pipe Top Elevation (mASL)	Stickup (m)				
Mobile Augers	Solid Stem Auger	0.15	8.5 m	309.44	0.80				
Monitoring Well Installed		Screened Interval (mBGL)		Weather Conditions	Sample Type				
See Below		See Below		Overcast and rainy					
Piezometer & Well Diagram(s)	Main Component Summary	Depth (m)	Graphic Log	U.S.C.S.	Synchronide Classification	Description and Classification Colour, Size Range, Main Component, Minor Components, Moisture Content, Structure, Angularity, Odor	Lab Sample		
							Field ID	Depth Range (m)	
	Medium Sand	1 2 3	[Dotted pattern]			Medium Sand, medium dark red, very coarse gravel throughout, oxidized staining, clay stringers, moist (0 - 3.0 m)			
	Sandy Silt	4 5 6	[Dotted pattern]			Sandy Silt, light brown, moist (3.0 - 6.1 m) Saturated at 4.3 m			
	Medium Fine Sand	7	[Dotted pattern]			Medium to Fine Sand, medium grey, clay stringers, saturated (4.3 - 7.3 m)			
	Silty, Sandy Clay	8 9 10	[Dotted pattern]			Silty, Sandy Clay (Till), medium grey, angular fine to medium gravel throughout, saturated (7.3 - 8.5 m)			
			11				END OF HOLE 8.5 M		
	Notes: Two monitoring wells were installed at this location using a direct push M5T Drilling Rig. An expendable stainless steel point is located below each piezometer. The riser pipe is constructed with schedule 40 PVC casing, with 21 mm ID and 27 mm OD. The screen has an ID of 21 mm and an OD of 36 mm. The screen is comprised of three layers: an innermost layer of schedule 40, 10 slot PVC screen, a layer of 20x40 silica sand and an outermost layer of 65 mesh stainless steel. The length of the screen is 0.15 m. Each well is capped with a slip on PVC well cap. A standard red, protective well casing is installed over each piezometer. Bentonite chips and 10-20 silica sand was used to fill the								

Observation Well Installation Record

Material Information	Site Information	Hole Information	
Monument: Lockable Steel Casing		Hole ID: OW01-04B	
Casing: 2" sch 80 PVC	Northing: 53642.299 Easting: 54377.739	Old Hole ID: None	
Screen: 2" sch 80 PVC	Ground Elevation: 316.531 m Stickup Elevation: 317.421 m	Drilling Contractor: LAYNE Driller: Lenard Loney	Installation Date: 02-Jan-02 Total Depth: 9.83 (m)
Screen Slot Size: 0.02 slot (0.508 mm)	Stickup: 0.89 m	Rig Type:	Water Table Elev.:
Filter Pack: 10-20 Colorado Silica Sand	Location Description: Within Forestry Camp Area	Rig: GP1900C	Water Table Date:
Bentonite: Pure Gold bentonite chips (medium)		Hole Diameter: 8" hollow Stem	Monitors: A. Duffy Office Geologist: Barry Esford
		Comments:	

**Stratigraphic Column
(not to scale)**



Solid Phase Extraction Summary

Components concentrations are shown relative to the quantification limit.

Note: All units are in mg/g, with the exception of Blank Samples, which are measured in mg/L

Sample	Depth (m)	DI Water												
		Al	As	B	Ba	Be	Cd	Co	Cr	Cu				
OW 04-02	3.75	<0.1	<0.1	0.01	<0.01	<0.001	<0.001	<0.001	<0.001	<0.001	<0.001	<0.001	<0.001	<0.001
	6.50	<0.1	<0.1	0.01	<0.01	<0.001	<0.001	<0.001	<0.001	<0.001	<0.001	<0.001	<0.001	<0.001
	7.50	<0.1	<0.1	0.01	<0.01	<0.001	<0.001	<0.001	<0.001	<0.001	<0.001	<0.001	<0.001	<0.001
	7.90	<0.1	<0.1	0.01	<0.01	<0.001	<0.001	<0.001	<0.001	<0.001	<0.001	<0.001	<0.001	<0.001
	8.50	<0.1	<0.1	0.01	<0.01	<0.001	<0.001	<0.001	<0.001	<0.001	<0.001	<0.001	<0.001	<0.001
OW 04-04	7.50	<0.1	<0.1	0.01	<0.01	<0.001	<0.001	<0.001	<0.001	<0.001	<0.001	<0.001	<0.001	<0.001
	8.50	<0.1	<0.1	0.01	<0.01	<0.001	<0.001	<0.001	<0.001	<0.001	<0.001	<0.001	<0.001	<0.001
	9.00	<0.1	<0.1	0.01	<0.01	<0.001	<0.001	<0.001	<0.001	<0.001	<0.001	<0.001	<0.001	<0.001
	9.25	<0.1	<0.1	0.01	<0.01	<0.001	<0.001	<0.001	<0.001	<0.001	<0.001	<0.001	<0.001	<0.001
	9.50	<0.1	<0.1	0.01	<0.01	<0.001	<0.001	<0.001	<0.001	<0.001	<0.001	<0.001	<0.001	<0.001
OW 04-06	3.00	<0.1	<0.1	<0.01	<0.01	<0.001	<0.001	<0.001	<0.001	<0.001	<0.001	<0.001	<0.001	<0.001
	4.30	<0.1	<0.1	0.01	<0.01	<0.001	<0.001	<0.001	<0.001	<0.001	<0.001	<0.001	<0.001	<0.001
	5.50	<0.1	<0.1	<0.01	<0.01	<0.001	<0.001	<0.001	<0.001	<0.001	<0.001	<0.001	<0.001	<0.001
	5.70	<0.1	<0.1	0.01	<0.01	<0.001	<0.001	<0.001	<0.001	<0.001	<0.001	<0.001	<0.001	<0.001
	6.00	<0.1	<0.1	<0.01	<0.01	<0.001	<0.001	<0.001	<0.001	<0.001	<0.001	<0.001	<0.001	<0.001
OW04-02	6.50	<0.1	<0.1	<0.01	<0.01	<0.001	<0.001	<0.001	<0.001	<0.001	<0.001	<0.001	<0.001	<0.001
	7.50	<0.1	<0.1	0.01	<0.01	<0.001	<0.001	<0.001	<0.001	<0.001	<0.001	<0.001	<0.001	<0.001
	5.70	<0.1	<0.1	<0.01	<0.01	<0.001	<0.001	<0.001	<0.001	<0.001	<0.001	<0.001	<0.001	<0.001
Blank		<0.1	<0.1	<0.01	<0.01	<0.001	<0.001	<0.001	<0.001	<0.001	<0.001	<0.001	<0.001	<0.001
Sample	Depth (m)	Na Ascorbate/Citrate/Bicarbonate												
		Al	As	Ba	Be	B	Cd	Cr	Co	Cu				
OW 04-02	3.75	<0.1	<0.1	0.01	<0.01	<0.1	<0.01	<0.01	<0.01	<0.1	<0.01	<0.01	<0.01	<0.1
	6.50	<0.1	<0.1	<0.01	<0.01	<0.1	<0.01	<0.01	<0.01	<0.1	<0.01	<0.01	<0.01	<0.1
	7.50	<0.1	<0.1	<0.01	<0.01	<0.1	<0.01	<0.01	<0.01	<0.1	<0.01	<0.01	<0.01	<0.1
	8.50	<0.1	<0.1	<0.01	<0.01	<0.1	<0.01	<0.01	<0.01	<0.1	<0.01	<0.01	<0.01	<0.1
	7.50	<0.1	<0.1	<0.01	<0.01	<0.1	<0.01	<0.01	<0.01	<0.1	<0.01	<0.01	<0.01	<0.1
OW 04-04	7.50	<0.1	<0.1	<0.01	<0.01	<0.1	<0.01	<0.01	<0.01	<0.1	<0.01	<0.01	<0.01	<0.1
	8.50	<0.1	<0.1	0.01	<0.01	<0.1	<0.01	<0.01	<0.01	<0.1	<0.01	<0.01	<0.01	<0.1
	9.00	<0.1	<0.1	0.01	<0.01	<0.1	<0.01	<0.01	<0.01	<0.1	<0.01	<0.01	<0.01	<0.1
	9.25	<0.1	<0.1	0.01	<0.01	<0.1	<0.01	<0.01	<0.01	<0.1	<0.01	<0.01	<0.01	<0.1
	9.50	<0.1	<0.1	0.02	<0.01	<0.1	<0.01	<0.01	<0.01	<0.1	<0.01	<0.01	<0.01	<0.1
OW 04-06	3.00	<0.1	<0.1	<0.01	<0.01	<0.1	<0.01	<0.01	<0.01	<0.1	<0.01	<0.01	<0.01	<0.1
	4.30	<0.1	<0.1	0.01	<0.01	<0.1	<0.01	<0.01	<0.01	<0.1	<0.01	<0.01	<0.01	<0.1
	5.50	0.1	<0.1	0.06	<0.01	<0.1	<0.01	<0.01	<0.01	<0.1	<0.01	<0.01	<0.01	<0.1
	5.70	0.1	<0.1	0.06	<0.01	<0.1	<0.01	<0.01	<0.01	<0.1	<0.01	<0.01	<0.01	<0.1
	6.00	<0.1	<0.1	0.01	<0.01	<0.1	<0.01	<0.01	<0.01	<0.1	<0.01	<0.01	<0.01	<0.1
OW04-02	6.50	<0.1	<0.1	<0.01	<0.01	<0.1	<0.01	<0.01	<0.01	<0.1	<0.01	<0.01	<0.01	<0.1
	7.50	<0.1	<0.1	<0.01	<0.01	<0.1	<0.01	<0.01	<0.01	<0.1	<0.01	<0.01	<0.01	<0.1
	5.70	<0.1	<0.1	0.06	<0.01	<0.1	<0.01	<0.01	<0.01	<0.1	<0.01	<0.01	<0.01	<0.1

Solid Phase Extraction Summary

Components concentrations are shown relative to the quantification limit.

Note: All units are in mg/g, with the exception of Blank Samples, which are measured in mg/L

Sample	Depth (m)	0.5 M HCl												
		Al	As	B	Ba	Be	Cd	Co	Cr	Cu				
OW 04-02	3.75	0.2	<0.1	0.01	0.01	<0.001	<0.001	<0.001	<0.001	<0.001	<0.001	<0.001	<0.001	0.001
	6.50	0.1	<0.1	0.01	0.01	<0.001	<0.001	<0.001	<0.001	<0.001	<0.001	<0.001	<0.001	0.001
	7.50	0.1	<0.1	0.02	0.01	<0.001	<0.001	<0.001	<0.001	<0.001	<0.001	<0.001	<0.001	<0.001
	7.90	0.1	<0.1	0.02	0.01	<0.001	<0.001	<0.001	<0.001	<0.001	<0.001	<0.001	<0.001	<0.001
	8.50	0.1	<0.1	0.02	0.01	<0.001	<0.001	<0.001	<0.001	<0.001	<0.001	<0.001	<0.001	<0.001
OW 04-04	7.50	0.1	<0.1	0.02	<0.01	<0.001	<0.001	<0.001	<0.001	<0.001	<0.001	<0.001	<0.001	0.001
	8.50	0.2	<0.1	0.02	0.01	<0.001	<0.001	<0.001	<0.001	<0.001	<0.001	<0.001	<0.001	0.001
	9.00	0.2	<0.1	0.01	0.01	<0.001	<0.001	<0.001	<0.001	<0.001	<0.001	<0.001	<0.001	0.001
	9.25													
	9.50	1.0	<0.1	0.03	0.02	<0.001	<0.001	<0.001	<0.001	<0.001	<0.001	<0.001	<0.001	<0.001
OW 04-06	3.00	0.1	<0.1	0.02	0.01	<0.001	<0.001	<0.001	<0.001	<0.001	<0.001	<0.001	<0.001	0.002
	4.30	1.0	<0.1	0.03	0.02	<0.001	<0.001	<0.001	<0.001	<0.001	<0.001	<0.001	<0.001	0.002
	5.50	2.2	<0.1	0.03	0.08	<0.001	<0.001	<0.001	<0.001	<0.001	<0.001	<0.001	<0.001	0.003
	5.70	5.5	<0.1	0.05	0.10	<0.001	<0.001	<0.001	<0.001	<0.001	<0.001	<0.001	<0.001	0.003
	6.00	0.5	<0.1	0.02	0.02	<0.001	<0.001	<0.001	<0.001	<0.001	<0.001	<0.001	<0.001	<0.001
OW04-02	6.50	0.1	<0.1	0.01	0.01	<0.001	<0.001	<0.001	<0.001	<0.001	<0.001	<0.001	<0.001	0.001
	7.50	0.1	<0.1	<0.01	<0.01	<0.001	<0.001	<0.001	<0.001	<0.001	<0.001	<0.001	<0.001	0.001
Blank		0.1	<0.1	<0.01	0.01	<0.001	<0.001	<0.001	<0.001	<0.001	<0.001	<0.001	<0.001	<0.001
Sample	Depth (m)	5.0 M HCl												
		Al	As	B	Ba	Be	Cd	Co	Cr	Cu				
OW 04-02	3.75	0.6	<0.1	0.03	0.01	<0.001	<0.001	0.001	0.001	0.001				
	6.50	0.7	<0.1	0.03	0.01	<0.001	<0.001	0.002	0.002	0.001				
	7.50	0.7	<0.1	0.03	0.01	<0.001	<0.001	0.001	0.003	0.001				
	7.90	0.6	<0.1	0.03	0.01	<0.001	<0.001	0.001	0.003	0.001				
	8.50	0.5	<0.1	0.02	0.01	<0.001	<0.001	0.001	0.002	0.001				
OW 04-04	7.50	0.6	<0.1	0.03	0.01	<0.001	<0.001	0.002	0.001	0.002				
	8.50	0.7	<0.1	0.03	0.01	<0.001	<0.001	0.002	0.001	0.002				
	9.00	0.8	<0.1	0.17	0.01	<0.001	<0.001	0.001	0.001	0.001				
	9.25	0.5	<0.1	0.02	0.01	<0.001	<0.001	0.001	0.001	0.001				
	9.50	4.2	<0.1	0.05	0.03	<0.001	<0.001	0.003	0.009	0.006				
OW 04-06	3.00	0.7	<0.1	0.04	0.01	<0.001	<0.001	0.002	0.003	0.003				
	4.30	2.2	<0.1	0.04	0.03	<0.001	<0.001	0.003	0.005	0.004				
	5.50	10.7	<0.1	0.06	0.11	<0.001	<0.001	0.001	0.015	0.004				
	5.70	5.8	<0.1	0.04	0.10	<0.001	<0.001	0.003	0.008	0.006				
	6.00	2.9	<0.1	0.04	0.03	<0.001	<0.001	0.001	0.005	0.001				
OW04-02	6.50													
	7.50													
	5.70	0.6	<0.1	<0.01	<0.01	<0.001	<0.001	<0.001	0.005	<0.001				
Blank														

Solid Phase Extraction Summary
Components concentrations are shown relative to the quantification limit.
Note: All units are in mg/g, with the exception of Blank Samples, which are measured in mg/L

DI Water														
Fe (ICP)	Metals						Majors							
	Li	Mn	Mo	Ni	Pb	Zn	Ca	Mg	Na	Na	K	Mg	Na	
0.004	<0.001	<0.01	<0.001	<0.001	<0.001	<0.001	0.2	<0.1	0.1	<100	<0.1	699		
0.005	<0.001	<0.001	<0.001	0.001	<0.001	<0.001	0.2	<0.1	0.1	<100	<0.1	574		
0.002	<0.001	<0.01	<0.001	<0.001	<0.001	<0.001	0.2	<0.1	<0.1	<100	<0.1	534		
0.001	<0.001	<0.01	<0.001	<0.001	<0.001	<0.001	0.2	<0.1	0.1	<100	<0.1	542		
0.003	<0.001	<0.01	<0.001	<0.001	<0.001	<0.001	0.2	<0.1	0.1	<100	<0.1	551		
0.002	<0.001	<0.01	<0.001	<0.001	<0.001	<0.001	<0.1	<0.1	<0.1	<100	0.1	572		
0.006	<0.001	<0.01	<0.001	0.001	<0.001	<0.001	<0.1	<0.1	<0.1	<100	<0.1	484		
0.003	<0.001	<0.01	<0.001	<0.001	<0.001	<0.001	<0.1	<0.1	<0.1	<100	<0.1	468		
0.008	<0.001	<0.01	<0.001	<0.001	<0.001	<0.001	0.1	<0.1	0.2	<100	0.3	503		
0.011	<0.001	<0.01	<0.001	<0.001	0.002	<0.001	0.1	<0.1	0.2	<100	0.1	573		
0.001	<0.001	<0.01	<0.001	0.001	<0.001	<0.001	0.2	<0.1	<0.1	<100	<0.1	399		
0.001	<0.001	<0.01	<0.001	<0.001	0.001	<0.001	0.2	<0.1	<0.1	<100	<0.1	453		
0.001	<0.001	<0.01	<0.001	<0.001	<0.001	<0.001	0.3	<0.1	<0.1	<100	<0.1	466		
<0.001	<0.001	<0.01	<0.001	<0.001	<0.001	<0.001	0.3	<0.1	<0.1	<100	<0.1	466		
<0.001	<0.001	0.01	0.012	0.017	0.028	<0.001	<0.1	<0.1	<0.1	<100	<0.1	26500		
Na Ascorbate/Citrate/Bicarbonate														
Fe (ICP)	Metals						Majors							
	Pb	Li	Mn	Mo	Ni	Se	Si	Sr	V	Zn	Ca	K	Mg	Na
0.3	<0.1	<0.1	<0.01	<0.1	<0.01	<0.1	<0.1	0.01	<0.1	<0.01	0.2	<100	<0.1	699
0.3	<0.1	<0.1	0.01	<0.1	<0.01	<0.1	<0.1	0.01	<0.1	<0.01	0.9	<100	<0.1	574
0.2	<0.1	<0.1	0.01	<0.1	<0.01	<0.1	<0.1	0.01	<0.1	<0.01	1.9	<100	<0.1	534
0.4	<0.1	<0.1	0.02	<0.1	<0.01	<0.1	<0.1	0.01	<0.1	<0.01	0.2	<100	<0.1	542
0.1	<0.1	<0.1	0.01	<0.1	<0.01	<0.1	<0.1	0.01	<0.1	<0.01	0.4	<100	<0.1	551
0.2	<0.1	<0.1	<0.01	<0.1	<0.01	<0.1	<0.1	0.01	<0.1	<0.01	0.8	<100	0.1	572
0.3	<0.1	<0.1	0.01	<0.1	<0.01	<0.1	0.1	0.01	<0.1	<0.01	0.5	<100	<0.1	484
0.3	<0.1	<0.1	0.01	<0.1	<0.01	<0.1	<0.1	0.01	<0.1	<0.01	0.6	<100	<0.1	468
0.2	<0.1	<0.1	<0.01	<0.1	<0.01	<0.1	0.2	0.01	<0.1	<0.01	1.5	<100	0.3	492
0.2	<0.1	<0.1	<0.01	<0.1	<0.01	<0.1	0.1	0.01	<0.1	<0.01	1.7	<100	0.3	503
0.1	<0.1	<0.1	0.01	<0.1	<0.01	<0.1	<0.1	0.01	<0.1	<0.01	1.0	<100	0.1	573
0.3	<0.1	<0.1	0.01	<0.1	<0.01	<0.1	<0.1	0.01	<0.1	<0.01	0.3	<100	<0.1	399
0.4	<0.1	<0.1	0.01	<0.1	<0.01	<0.1	<0.1	0.01	<0.1	<0.01	0.2	<100	<0.1	453
0.2	<0.1	<0.1	<0.01	<0.1	<0.01	<0.1	<0.1	0.01	<0.1	<0.01	1.7	<100	0.3	466
<0.1	<0.1	<0.1	<0.01	<0.1	<0.01	<0.1	<0.1	<0.01	<0.1	<0.01	<0.1	<100	<0.1	26500

Solid Phase Extraction Summary

Components concentrations are shown relative to the quantification limit.

Note: All units are in mg/g, with the exception of Blank Samples, which are measured in mg/L

0.5 M HCl															
Fe (ICP)	Metals							Major							
	Fe (FZ)	Fe ²⁺ (FZ)	Fe ³⁺ (FZ)	Li	Mn	Mo	Ni	Pb	Sr	V	Zn	Ca	K	Mg	Na
0.4	0.5	<0.1	0.5	<0.001	<0.01	<0.001	<0.001	<0.001	0.004	<0.001	0.001	0.2	<0.1	0.1	<0.1
1	1.1	0.7	0.5	<0.001	0.04	<0.001	0.001	<0.001	0.004	0.001	0.002	8.7	<0.1	1.8	0.2
2	2.8	1.8	1.0	<0.001	0.07	0.001	0.001	<0.001	0.015	0.001	0.002	30.0	0.1	5.9	0.1
2	2.4	1.6	0.8	<0.001	0.04	0.001	0.001	<0.001	0.001	0.001	0.002	18.3	0.1	3.8	0.1
1	1.8	0.4	1.4	<0.001	0.04	<0.001	0.001	<0.001	0.007	0.001	0.002	10.5	<0.1	2.3	0.1
0.9	1.0	<0.1	1.0	<0.001	0.03	<0.001	0.001	<0.001	0.001	<0.001	0.001	0.2	<0.1	0.1	0.2
0.7	0.8	0.2	0.6	<0.001	0.04	<0.001	<0.001	<0.001	0.001	0.001	0.002	0.5	<0.1	0.2	0.2
0.5	0.6	0.3	0.2	<0.001	0.01	<0.001	0.001	<0.001	0.001	0.001	0.003	0.8	0.1	0.3	<0.1
3	4.2	3.8	0.3	0.002	0.05	<0.001	0.003	0.002	0.007	0.005	0.012	7.4	0.2	3.5	0.2
1	1.6	0.3	1.3	0.001	0.05	0.001	0.001	<0.001	0.016	0.001	0.002	42.0	<0.1	8.6	<0.1
3	4.5	0.4	4.2	0.002	0.03	<0.001	0.003	0.002	0.007	0.005	0.012	10.8	0.2	4.5	<0.1
3	4.0	3.1	0.9	0.003	0.07	<0.001	0.002	0.006	0.014	0.006	0.009	19.6	0.4	4.5	0.1
8	10.8	3.5	7.3	0.008	0.08	<0.001	0.005	0.014	0.019	0.013	0.016	16.0	1.0	5.4	0.1
2	2.7	2.4	0.4	0.001	0.07	0.001	0.001	<0.001	0.013	0.003	0.005	15.7	0.1	4.7	<0.1
1.0				<0.001	0.04	<0.001	0.001	<0.001	0.003	0.001	0.002	6.9	<0.1	1.6	0.1
1				<0.001	0.03	<0.001	0.001	<0.001	0.001	0.001	0.001	0.2	<0.1	0.1	0.1
<1				<0.001	<0.01	<0.001	<0.001	0.040	<0.001	<0.001	<0.001	<0.1	<0.1	<0.1	<0.1

5.0 M HCl														
Fe (ICP)	Metals							Major						
	Fe _T (FZ)	Fe ²⁺ (FZ)	Fe ³⁺ (FZ)	Mn	Mo	Ni	Pb	Sr	V	Zn	Ca	K	Mg	Na
4	4.3	2.9	1.5	0.03	<0.001	0.002	<0.001	0.003	0.003	0.003	0.2	0.1	0.2	0.1
4	4.9	3.1	1.8	0.05	<0.001	0.002	<0.001	0.006	0.003	0.005	7.4	0.1	1.9	0.2
3	3.8	3.1	0.7	0.07	0.001	0.001	<0.001	0.016	0.003	0.004	28.7	0.2	7.0	0.1
2	3.1	2.4	0.7	0.05	0.001	0.001	<0.001	0.012	0.003	0.004	18.8	0.2	4.4	0.1
2	2.2	1.7	0.5	0.04	0.001	0.001	<0.001	0.008	0.003	0.003	9.9	0.1	3.0	0.1
3	4.6	2.3	2.3	0.04	<0.001	0.002	<0.001	0.003	0.004	0.005	0.3	0.1	0.3	0.2
3	3.5	2.4	1.2	0.05	<0.001	0.002	<0.001	0.004	0.004	0.005	0.6	0.2	0.5	0.1
2	1.9	1.6	0.4	0.02	<0.001	0.002	0.001	0.004	0.004	0.005	0.9	0.2	0.6	0.2
1	0.8	0.7	0.1	0.01	<0.001	0.001	<0.001	0.003	0.002	0.004	0.9	0.1	0.4	0.1
7	9.9	8.7	1.2	0.07	<0.001	0.006	0.011	0.012	0.015	0.025	8.2	0.7	5.5	0.3
5	8.8	8.1	0.8	0.06	0.001	0.003	<0.001	0.019	0.004	0.006	44.5	0.2	10.2	<0.1
5	7.5	6.8	0.7	0.03	<0.001	0.004	0.006	0.012	0.008	0.014	10.8	0.4	4.6	<0.1
9	14.5	3.8	10.7	0.10	<0.001	0.005	0.023	0.043	0.020	0.017	26.7	1.6	7.0	0.2
6	9.5	6.9	2.6	0.08	<0.001	0.006	0.014	0.021	0.012	0.016	14.9	1.0	5.1	0.2
5	7.8	3.5	4.3	0.12	<0.001	0.002	0.008	0.022	0.011	0.024	13.9	0.7	3.1	0.1
1				0.01	0.006	0.011	0.046	0.002	0.007	0.014	<0.1	<0.1	<0.1	<0.1

Fractional Organic Carbon (FOC)

Alex Oiffer
 Department of Earth Science
 University of Waterloo

Report Date: March 22, 2005
 Submitted: February, 2004
 Lab Number: 050205
 Analyst: Shirley Chatten

Sample I.D.	% FOC	Sample I.D.	% FOC	Sample I.D.	% FOC
OW 04-02 (3.75)	0.029	OW 04-04 (7.50)	0.031	OW 04-06 (3.00)	0.113
	0.030		0.030		0.121
Average	0.030	Average	0.031	Average	0.117
STD	0.001	STD	0.001	STD	0.006
%S	2.9	%S	2.0	%S	5.1
OW 04-02 (5.50)	0.044	OW 04-04 (8.50)	0.040	OW 04-06 (4.30)	0.287
	0.046		0.047		0.294
Average	0.045	Average	0.043	Average	0.291
STD	0.002	STD	0.004	STD	0.005
%S	4.1	%S	10.1	%S	1.7
OW 04-02 (6.5)	0.224	OW 04-04 (9.00)	0.048	OW 04-06 (5.50)	1.003
	0.220		0.049		1.195
Average	0.222	Average	0.048	Average	1.099
STD	0.003	STD	0.001	STD	0.136
%S	1.3	%S	2.3	%S	12.4
OW 04-02 (7.50)	0.091	OW 04-04 (9.25)	0.040	OW 04-06 (5.70)	1.470
	0.093		0.035		1.530
Average	0.092	Average	0.037	Average	1.500
STD	0.001	STD	0.004	STD	0.042
%S	1.6	%S	9.5	%S	2.8
OW 04-02 (7.80)	0.081	OW 04-04 (9.50)	0.554	OW 04-06 (6.00)	2.080
	0.071		0.568		1.860
Average	0.076	Average	0.561	Average	1.970
STD	0.007	STD	0.010	STD	0.156
%S	9.8	%S	1.8	%S	7.9
OW 04-02 (8.50)	0.047				
	0.047				
Average	0.047				
STD	0.000				
%S	0.5				

QUALITY ASSURANCE DATA

ACCURACY AND PRECISION OF STANDARDS AND METHOD DETECTION LIMIT

LOW STD	%FOC	MID STD	%FOC	MID STD	%FOC
TRUE CONC	0.041	TRUE CONC	0.202	TRUE CONC	###
MEASURED C AVG	0.041	MEASURED C AVG	0.202	MEASURED C AVG	###
STD	0.003	STD	0.017	STD	###
N	4	N	4	N	2
%S	7.2	%S	8.5	%S	0.5
%E	-1.4	%E	0.1	%E	###
MDL	0.006				
LOQ	0.012				

LEGEND

%FOC - percent fractional organic carbon by weight (w/w)
 MDL - Method Detection Limit
 LOQ - Limit of Quantification (2*MDL)
 STD - standard deviation of replicate determinations
 %S - relative percent standard deviation
 %E - percent error of determination from true (spiked) value

Scanning Electron Microscope and Quantitative Rietveld Analysis

Specific cored intervals were selected for quantitative mineralogical analysis by the Rietveld method. The Rietveld analysis is an X-Ray Diffraction (XRD) based quantitative method, which from a finely powdered sample produces a series of peaks. Based on the position and intensity of the peaks, minerals may be identified through comparison with the International Centre for Diffraction Database PDF-4. The relative quantities of each mineral are determined and normalized to 100%. With regards to sample preparation, the samples were first ground on a ring grinder so that the grain size was <200 mesh. Further sample preparation and handling was performed by personnel at the University of British Columbia Electron-microbeam/X-ray diffraction Facility. When interpreting the results, it should be noted that clays cannot be identified using the Rietveld technique, since they exhibit a preferred orientation. Results of the Rietveld analysis are shown in the following laboratory report.

QUANTITATIVE PHASE ANALYSIS OF FIVE SAMPLES USING THE RIETVELD METHOD AND X-RAY POWDER DIFFRACTION DATA.

**Alex Oiffer
Earth & Ocean Sciences Department
The University of British Columbia
Vancouver, B.C. V6T 1Z4**

**Mati Raudsepp, Ph.D.
Elisabetta Pani, Ph.D.
Dept. of Earth & Ocean Sciences
6339 Stores Road
The University of British Columbia
Vancouver, BC V6T 1Z4**

May 24, 2005

EXPERIMENTAL METHOD

The samples **OW04-02-3.75**, **OW04-02-7.80**, **OW04-04-7.50**, **OW04-04-9.00** and **OW04-06-4.30** were ground into fine powder to the optimum grain-size range for X-ray analysis (<10 μ m) by grinding under ethanol in a vibratory McCrone Micronising Mill for 7 minutes. Fine grain-size is an important factor in reducing micro-absorption contrast between phases. Samples were pressed from the bottom of an aluminum sample holder against a ground glass slide; the cavity in the holder measures 43 \times 24 \times 1.5 mm. The textured surface of the glass minimizes preferred orientation of anisotropic grains in the part of the powder that is pressed against the glass. The surface was also serrated with a razor blade to break up residual preferred orientation. Step-scan X-ray powder-diffraction data were collected over a range 3-70 $^{\circ}$ 2 θ with CuK α radiation on a standard Siemens (Bruker) D5000 Bragg-Brentano diffractometer equipped with a diffracted-beam graphite monochromator crystal, 2 mm (1 $^{\circ}$) divergence and antiscatter slits, 0.6 mm receiving slit and incident-beam Soller slit. The long fine-focus Cu X-ray tube was operated at 40 kV and 40 mA, using a take-off angle of 6 $^{\circ}$.

RESULTS AND DISCUSSION

The X-ray diffractograms were analyzed using the International Centre for Diffraction Database PDF-4 using Search-Match software by Siemens (Bruker). X-ray powder-diffraction data were refined with the Rietveld program Topas 2.1 (Bruker AXS). The results of quantitative phase analysis by Rietveld refinement are given in Table 1. These amounts represent the relative amounts of crystalline phases normalized to 100%. The Rietveld refinement plots for the samples are shown in Figures 1-5.

Table 1. Results of quantitative phase analysis (wt.%)

	Ideal Formula	OW04-02- 3.75	OW04-02- 7.80	OW04-04- 7.50	OW04-04- 9.00	OW04-06- 4.30
Quartz	SiO ₂	94.8	87.5	94.4	94.0	79.4
Muscovite	KAl ₂ AlSi ₃ O ₁₀ (OH,F) ₂					4.7
Plagioclase	NaAlSi ₃ O ₈ – CaAl ₂ Si ₂ O ₈	2.0	3.4	2.0	2.6	5.1
K-feldspar	KAlSi ₃ O ₈	3.2	2.9	3.0	3.4	5.1
Clinocllore	(Mg,Fe ²⁺) ₅ Al(Si ₃ Al)O ₁₀ (OH) ₈					1.9
Tremolite	Ca ₂ Mg ₅ Si ₈ O ₂₂ (OH) ₂					0.4
Calcite	CaCO ₃		2.0			0.6
Dolomite	CaMg(CO ₃) ₂		3.9			2.8
Pyrite	FeS ₂		0.3	0.6		
Total		100.0	100.0	100.0	100.0	100.0

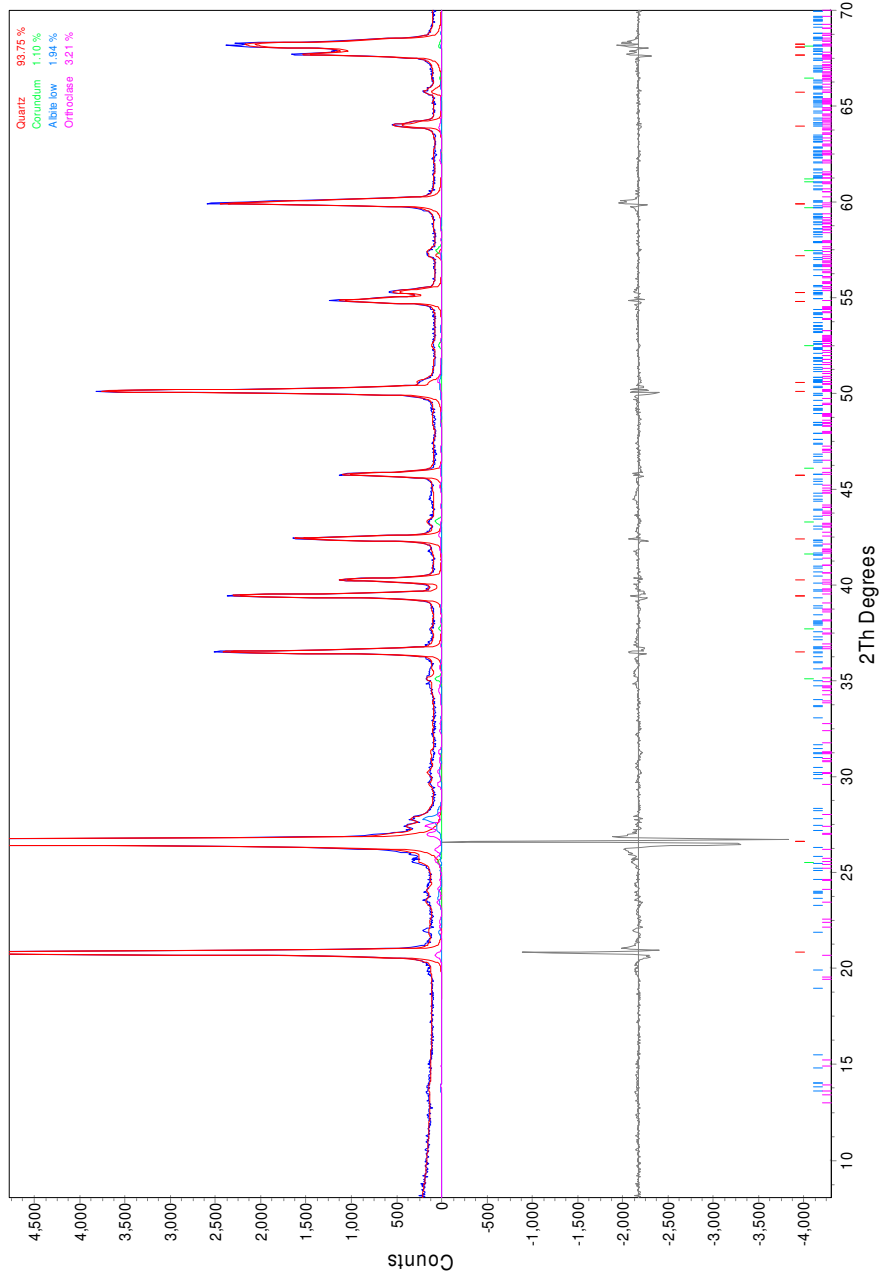


Figure 1. Rietveld refinement plot for sample **OW04-02-3.75** (blue line - observed intensity at each step; red line - calculated pattern; solid grey line below - difference between observed and calculated intensities; vertical bars, positions of all Bragg reflections). Coloured lines are individual diffraction patterns of all phases.

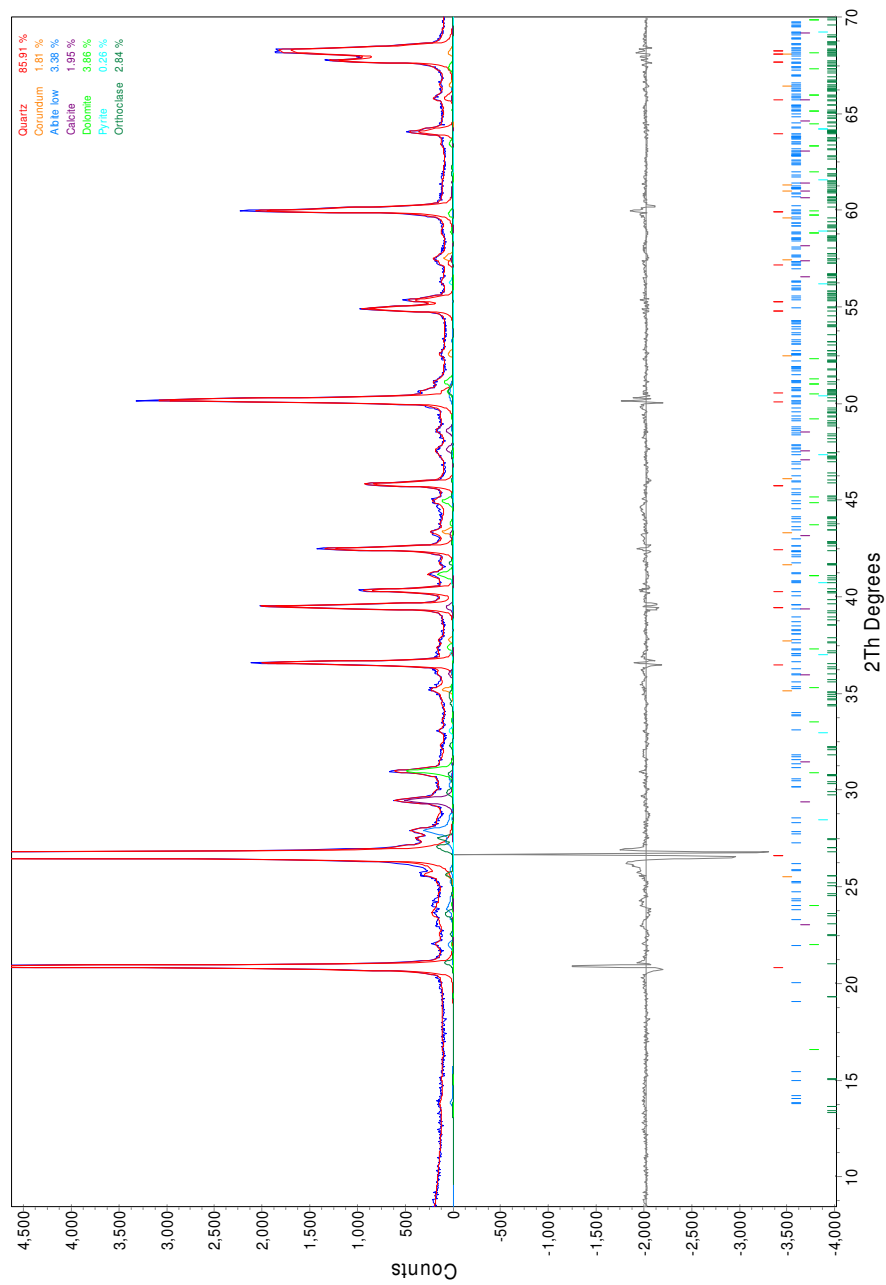


Figure 2. Rietveld refinement plot for sample **OW04-02-7.80** (blue line - observed intensity at each step; red line - calculated pattern; solid grey line below - difference between observed and calculated intensities; vertical bars, positions of all Bragg reflections). Coloured lines are individual diffraction patterns of all phases.

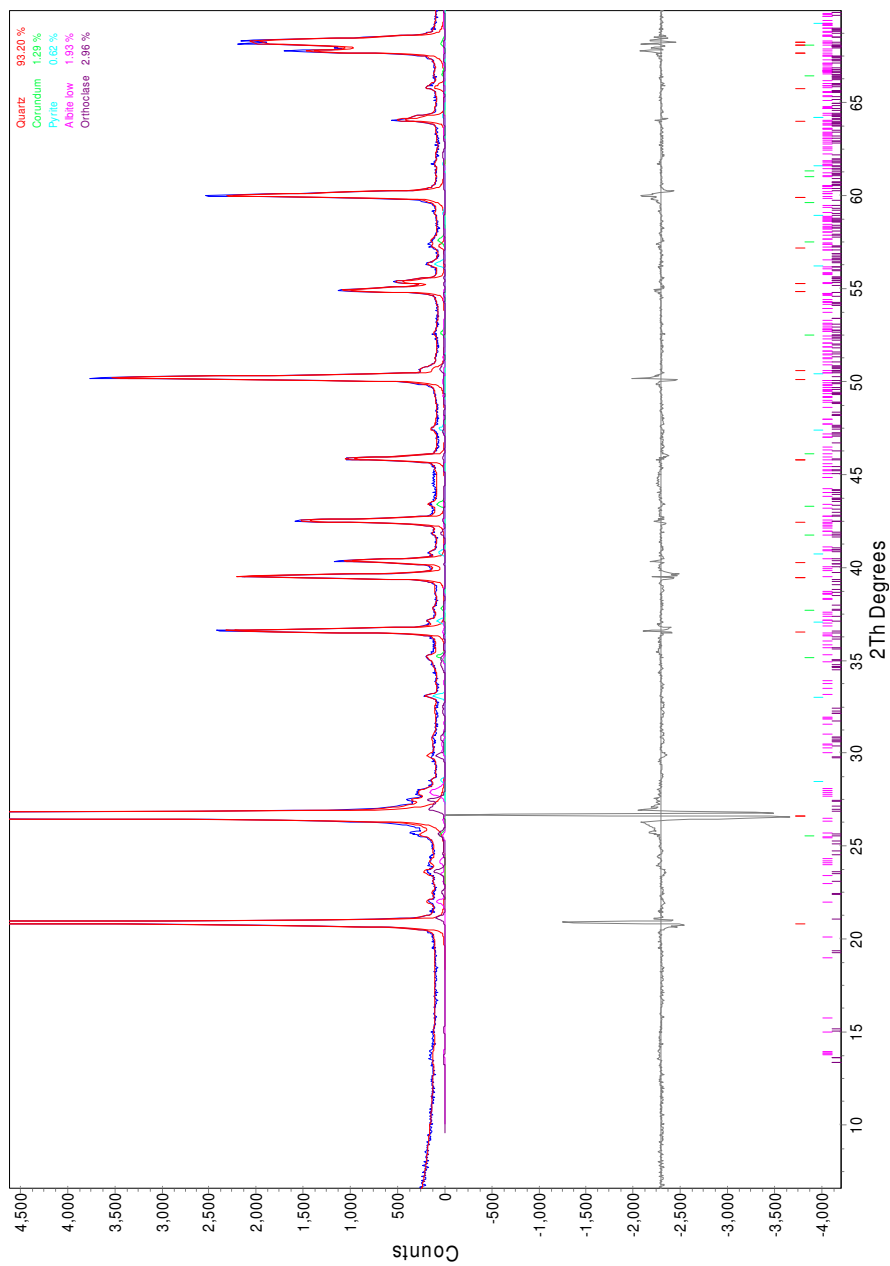


Figure 3. Rietveld refinement plot for sample **OW04-04-7.50** (blue line - observed intensity at each step; red line - calculated pattern; solid grey line below - difference between observed and calculated intensities; vertical bars, positions of all Bragg reflections). Coloured lines are individual diffraction patterns of all phases.

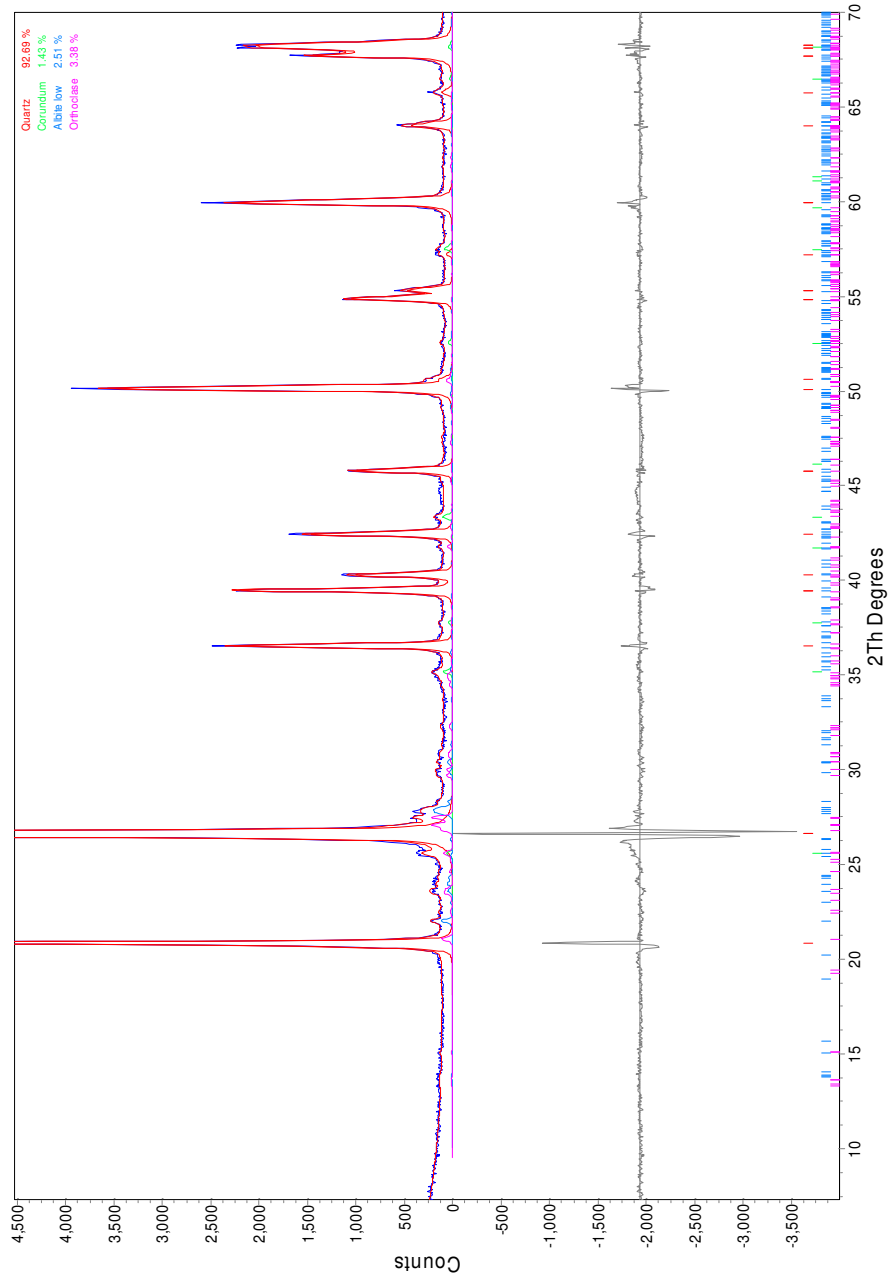


Figure 4. Rietveld refinement plot for sample **OW04-04-9.00** (blue line - observed intensity at each step; red line - calculated pattern; solid grey line below - difference between observed and calculated intensities; vertical bars, positions of all Bragg reflections). Coloured lines are individual diffraction patterns of all phases.

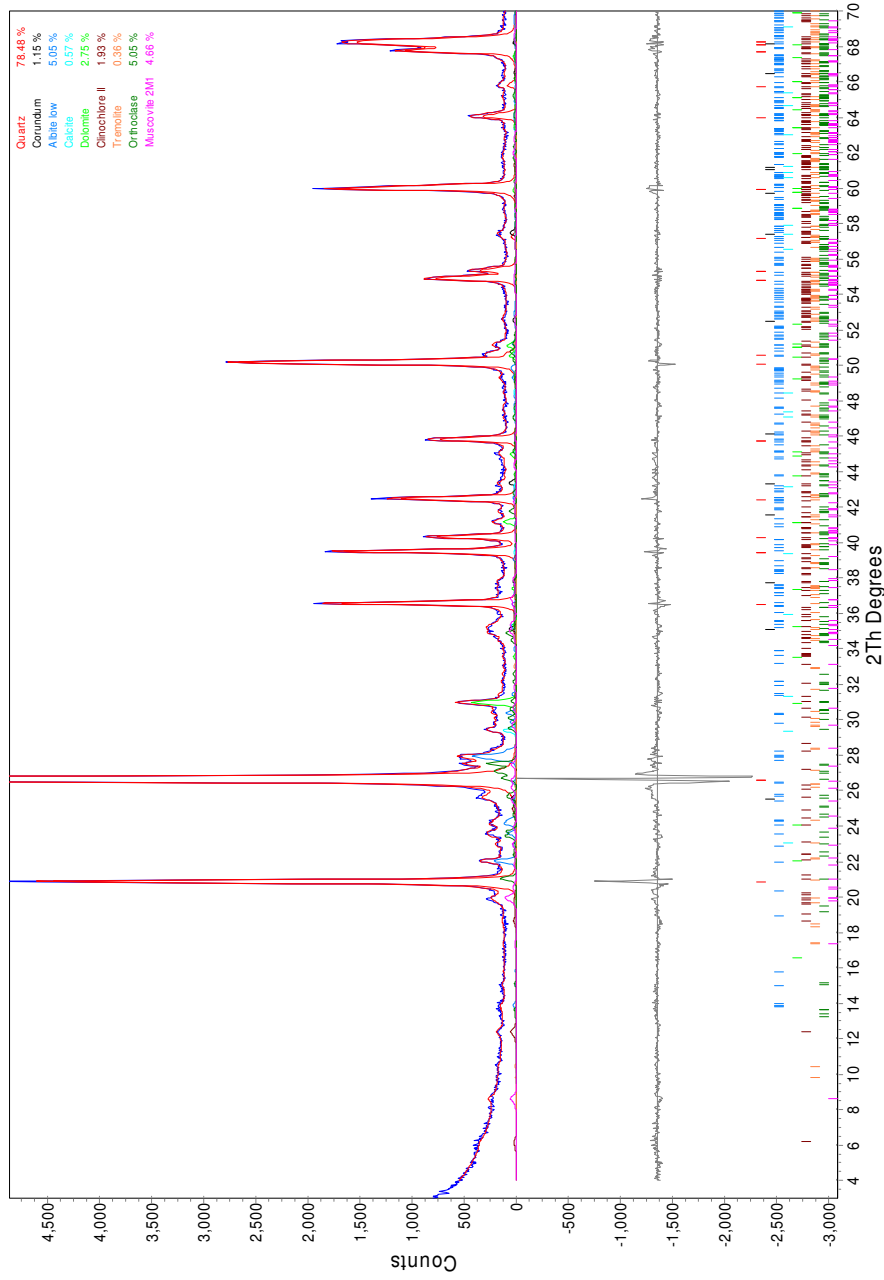


Figure 5. Rietveld refinement plot for sample **OW04-06-4.30** (blue line - observed intensity at each step; red line - calculated pattern; solid grey line below - difference between observed and calculated intensities; vertical bars below - positions of all Bragg reflections). Coloured lines are individual diffraction patterns of all phases.



Borehole Elevations of the Base of the Surficial Sand Aquifer.

All elevations are in meters above sea level. Map coordinates are in Syncrude mine metric. Borehole records from the current study and those supplied by Syncrude Canada Ltd. were used when determining the elevations shown above.

Appendix D
Aqueous Phase Geochemistry

- Generally, with reference to the thesis, a different labelling system is used in the appendix for monitoring wells:

Appendix Label	Label used in Thesis
UWOW04-01a,b	1a,b
UWOW04-02a,b,c	2a,b,c
UWOW04-03a,b,c	3a,b,c
UWOW04-04a,b,c	4a,b,c
UWOW04-05a,b,c	5a,b,c
UWOW04-06a,b	7 (note this refers to UWOW0406b, the shallower well UWOW04-06a was never sampled)
UWOW04-07	Not discussed in text, note coordinates on borehole log for location.

- The monitoring well referred to in the text as 6A is listed here using the label originally assigned by Syncrude Canada Ltd. (OW01-04B)

Sample ID	Unit	Ditch-01			
		PSC	SCL*	ETL & UW	ETL & UW
Lab					
Date		17-Sep-04	17-Sep-04	23-Jun-05	23-Jun-05
Northing	m				
Easting	m				
Charge Balance	RPD	4.6	2.8	4.1	5.6
Conductivity (Lab)	mg/L	2591	2100	1920	1930
Hardness	mg/L	181.8		139	162
pH (Lab)	pH units	8.37	7.97	8.4	8.4
Total Dissolved Solids (Lab)	mg/L	1380		1140	1170
Total Ammonia-Nitrogen	mg/L	0.55	0.83	0.53	0.50
Bicarbonate (Lab)	mg/L	954	970	768	764
Bromide	mg/L	<0.5			
Carbonate (Lab)	mg/L	1	0	7	9
Chloride	mg/L	254	260	186	190
Fluoride	mg/L	1.4	BDL		
Hydioxide	mg/L			<5	<5
Nitrate-Nitrogen	mg/L	<0.2	BDL	0.2	0.2
Nitrite-Nitrogen	mg/L	<0.2	BDL	<0.05	<0.05
Ortho Phosphate	mg/L	<1	BDL		
Phosphorous	mg/L	<0.05	BDL		
Total Sulphur	mg/L		41.4		
Sulphate	mg/L	137	143	118	125
Aluminum	mg/L	0.019	BDL	0.01	<0.01
Antimony	mg/L	<0.0005	BDL	<0.0004	0.0006
Arsenic	mg/L	<0.002		0.0007	0.0006
Barium	mg/L	0.107	0.025	0.121	0.113
Beryllium	mg/L	<0.001		<0.0005	<0.0005
Bismuth	mg/L	<0.001		<0.00005	<0.00005
Boron	mg/L	1.21	1.26	1.13	1.06
Cadmium	mg/L	<0.0001	BDL	<0.0001	<0.0001
Calcium	mg/L	49	50	48.9	49.3
Chromium	mg/L	<0.005	BDL	0.0006	0.0008
Cobalt	mg/L	0.0012	BDL	0.0008	0.0007
Copper	mg/L	<0.0005	BDL	<0.0006	<0.0006
Iron	mg/L	0.03	BDL	0.378	0.263
Lead	mg/L	<0.0005	BDL	<0.0001	<0.0001
Lithium	mg/L		BDL		
Magnesium	mg/L	14.4	15.5	14.3	14.2
Manganese	mg/L	0.774	0.772	0.42	0.41
Molybdenum	mg/L	0.009	BDL	0.0078	0.0075
Nickle	mg/L	0.006	BDL	0.0038	0.0036
Potassium	mg/L	3.5	0.1	3.8	2.6
Selenium	mg/L	<0.002	BDL	<0.0004	<0.0004
Silicon	mg/L	4.68	5.13		
Silver	mg/L	<0.0001		<0.0002	<0.0002
Sodium	mg/L	452	481	343	335
Strontium	mg/L	0.144	0.181	0.145	0.14
Tin	mg/L	<0.001	ENA	<0.0002	<0.0002
Titanium	mg/L	<0.005	BDL	0.0008	0.0007
Thallium	mg/L			<0.00005	<0.00005
Uranium	mg/L			0.0017	0.0016
Vanadium	mg/L	<0.0005	BDL	0.0008	0.0005
Zinc	mg/L	0.042	0.031	0.002	0.002
Zirconium	mg/L		BDL		

PSC - Phillip Analytical Services

SCL - Syncrude Canada Ltd. Research Laboratory

UW - University of Waterloo Organic Geochemistry Lab

ETL - Envirotest Labs

*SCL - Note samples for nutrients and metals analyzed by SCL were not preserved

Sample ID	Unit	Ditch-01			
		PSC	SCL*	ETL & UW	ETL & UW
Lab		17-Sep-04	17-Sep-04	23-Jun-05	23-Jun-05
Date					
Northing	m				
Easting	m				
Total Well Depth	mBTOC	NA			
Casing Elevation	mASL				
Dissolved Organic Carbon	mg/L	25.7			
Methane	ug/L	0.4		9.0	9.0
Total Naphthenic Acids	mg/L	54.6	61.5	38.6	37.7
benzene	ug/L				ND
toluene	ug/L				ND
ethylbenzene	ug/L				ND
p+m-xylene	ug/L				ND
o-xylene	ug/L				ND
1,3,5-trimethylbenzene	ug/L				ND
1,2,4-trimethylbenzene	ug/L				ND
1,2,3-trimethylbenzene	ug/L				ND
naphthalene	ug/L				ND
indole+2-methyl naphthalene	ug/L				ND
1-methyl naphthalene	ug/L				ND
biphenyl	ug/L				ND
acenaphthylene	ug/L				ND
acenaphthene	ug/L				ND
dibenzofuran	ug/L				ND
fluorene	ug/L				ND
phenanthrene	ug/L				ND
anthracene	ug/L				ND
carbazole	ug/L				ND
fluoranthene	ug/L				ND
pyrene	ug/L				ND
B(A)anthracene	ug/L				ND
chrysene	ug/L				ND
B(b+k)fluoranthene	ug/L				ND
B(a)pyrene	ug/L				ND
indeno(1,2,3,c,d)pyrene+dibenzo(a,h)anthracene	ug/L				ND
benzo(g,h,i)perylene	ug/L				ND

PSC - Phillip Analytical Services

SCL - Syncrude Canada Ltd. Research Laboratory

UW - University of Waterloo Organic Geochemistry Lab

ETL - Envirotest Labs

*SCL - Note samples for nutrients and metals analyzed by SCL were not preserved

Sample ID	Unit	UW OW04-01A			
		PSC & UW	SCL*	UW	ETL & UW
Lab					
Date		17-Sep-04	17-Sep-04	23-Oct-04	22-Jun-04
Northing	m	53170.31	53170.31	53170.31	
Easting	m	53816.27	53816.27	53816.27	
Charge Balance	RPD	-0.5	2.6		-5.1
Conductivity (Lab)	mg/L	2634	2210		2340
Hardness	mg/L	27.9			51
pH (Lab)	pH units	8.63	8.02		8.5
Total Dissolved Solids (Lab)	mg/L	1437			1490
Total Ammonia-Nitrogen	mg/L	2.17	1.24		3.34
Bicarbonate (Lab)	mg/L	935	1050		1030
Bromide	mg/L	<0.5			
Carbonate (Lab)	mg/L	7	0		24
Chloride	mg/L	170	180		169
Fluoride	mg/L	3.2	1.9		
Hydioxide	mg/L				<5
Nitrate-Nitrogen	mg/L	2.4	BDL		<0.1
Nitrite-Nitrogen	mg/L	<0.2	BDL		<0.05
Ortho Phosphate	mg/L	2	BDL		
Phosphorous	mg/L	1.38	1.13		
Total Sulphur	mg/L		69.1		
Sulphate	mg/L	219	236		166
Aluminum	mg/L	0.136	0.546		0.20
Antimony	mg/L	0.0013	BDL		0.0009
Arsenic	mg/L	0.007			0.0046
Barium	mg/L	0.021	BDL		0.0336
Beryllium	mg/L	<0.001			<0.0005
Bismuth	mg/L	<0.001			<0.00005
Boron	mg/L	2	1.85		1.82
Cadmium	mg/L	<0.0001	BDL		<0.0001
Calcium	mg/L	6.1	6.2		10.6
Chromium	mg/L	<0.005	BDL		0.0007
Cobalt	mg/L	0.0005	BDL		0.0007
Copper	mg/L	<0.0005	BDL		0.0007
Iron	mg/L	0.68	0.692		1.15
Lead	mg/L	<0.0005	BDL		0.0003
Lithium	mg/L		BDL		
Magnesium	mg/L	3.06	3.4		6.0
Manganese	mg/L	0.339	0.296		0.726
Molybdenum	mg/L	0.082	0.082		0.0066
Nickle	mg/L	0.003	BDL		0.0025
Potassium	mg/L	6.1	6.05		5.2
Selenium	mg/L	<0.002	BDL		0.0009
Silicon	mg/L	3.44	4.4		
Silver	mg/L	<0.0001			<0.0002
Sodium	mg/L	557	575		606
Strontium	mg/L	0.096	0.12		0.170
Tin	mg/L	<0.001	ENA		<0.0002
Titanium	mg/L	0.007	0.009		0.0117
Thallium	mg/L				<0.00005
Uranium	mg/L				0.0003
Vanadium	mg/L	0.0030	BDL		0.0060
Zinc	mg/L	<0.005	0.033		0.022
Zirconium	mg/L		BDL		

PSC - Phillip Analytical Services

SCL - Syncrude Canada Ltd. Research Laboratory

UW - University of Waterloo Organic Geochemistry Lab

ETL - Envirotest Labs

*SCL - Note samples for nutrients and metals analyzed by SCL were not preserved

Sample ID	Unit	UW OW04-01A			
		PSC & UW	SCL*	UW	ETL & UW
Lab					
Date		17-Sep-04	17-Sep-04	23-Oct-04	22-Jun-04
Northing	m	53170.31	53170.31	53170.31	
Easting	m	53816.27	53816.27	53816.27	
Total Well Depth	mBTC	6.88	6.88	6.88	
Casing Elevation	mASL				
Dissolved Organic Carbon	mg/L	52.3			
Methane	ug/L	667.0			18.1
Total Naphthenic Acids	mg/L	80.2	105		76.8
benzene	ug/L			0.29	2.83
toluene	ug/L			0.11	ND
ethylbenzene	ug/L			ND	ND
p+m-xylene	ug/L			1.61	ND
o-xylene	ug/L			ND	ND
1,3,5-trimethylbenzene	ug/L			ND	ND
1,2,4-trimethylbenzene	ug/L			ND	ND
1,2,3-trimethylbenzene	ug/L			ND	ND
naphthalene	ug/L			ND	1.93
indole+2-methyl naphthalene	ug/L			ND	ND
1-methyl naphthalene	ug/L			1.62	2.36
biphenyl	ug/L			ND	1.89
acenaphthylene	ug/L			ND	0.91
acenaphthene	ug/L			ND	ND
dibenzofuran	ug/L			ND	ND
fluorene	ug/L			ND	ND
phenanthrene	ug/L			ND	ND
anthracene	ug/L			ND	ND
carbazole	ug/L			ND	ND
fluoranthene	ug/L			ND	ND
pyrene	ug/L			ND	ND
B(A)anthracene	ug/L			ND	ND
chrysene	ug/L			ND	ND
B(b+k)fluoranthene	ug/L			ND	ND
B(a)pyrene	ug/L			ND	ND
indeno(1,2,3,c,d)pyrene+dibenzo(a,h)anthracene	ug/L			ND	ND
benzo(g,h,i)perylene	ug/L			ND	ND

PSC - Phillip Analytical Services

SCL - Syncrude Canada Ltd. Research Laboratory

UW - University of Waterloo Organic Geochemistry Lab

ETL - Envirotest Labs

*SCL - Note samples for nutrients and metals analyzed by SCL were not preserved

Sample ID	Unit	UW OW04-01B			
Lab		PSC & UW	PSC & UW	SCL*	SCL*
Date		17-Sep-04	17-Sep-04	17-Sep-04	17-Sep-04
Northing	m	53170.31	53170.31	53170.31	53170.31
Easting	m	53816.27	53816.27	53816.27	53816.27
Charge Balance	RPD	1.3	1.1	2.0	-1.4
Conductivity (Lab)	mg/L	2281	2248	1940	1950
Hardness	mg/L	57.6	56.5		
pH (Lab)	pH units	8.04	8.07	7.66	7.63
Total Dissolved Solids (Lab)	mg/L	1242	1222		
Total Ammonia-Nitrogen	mg/L	3.36	3.36	3.94	3.90
Bicarbonate (Lab)	mg/L	1030	1000	1100	988
Bromide	mg/L	<0.5	<0.5		
Carbonate (Lab)	mg/L	1	1	0	0
Chloride	mg/L	157	159	160	160
Fluoride	mg/L	2.6	2.7	1.6	1.6
Hydioxide	mg/L				
Nitrate-Nitrogen	mg/L	0.3	0.3	BDL	BDL
Nitrite-Nitrogen	mg/L	<0.2	<0.2	BDL	BDL
Ortho Phosphate	mg/L	<1	<1	BDL	BDL
Phosphorous	mg/L	<0.05	<0.05	BDL	BDL
Total Sulphur	mg/L			24.0	24.3
Sulphate	mg/L	70	70	73	72
Aluminum	mg/L	0.142	0.052	0.122	0.106
Antimony	mg/L	<0.0005	<0.0005	BDL	BDL
Arsenic	mg/L	0.005	0.004		
Barium	mg/L	0.07	0.068	BDL	BDL
Beryllium	mg/L	<0.001	<0.001		
Bismuth	mg/L	<0.001	<0.001		
Boron	mg/L	1.52	1.46	1.42	1.44
Cadmium	mg/L	<0.0001	<0.0001	BDL	BDL
Calcium	mg/L	17.8	17.4	19.7	18.1
Chromium	mg/L	<0.005	<0.005	BDL	BDL
Cobalt	mg/L	0.0008	0.0006	BDL	BDL
Copper	mg/L	0.0025	0.0021	BDL	BDL
Iron	mg/L	2.51	1.13	4.47	3.85
Lead	mg/L	0.0014	0.0013	BDL	BDL
Lithium	mg/L			BDL	BDL
Magnesium	mg/L	3.22	3.14	3.4	3.06
Manganese	mg/L	0.040	0.038	0.035	0.034
Molybdenum	mg/L	0.015	0.008	BDL	BDL
Nickle	mg/L	0.006	0.005	BDL	BDL
Potassium	mg/L	2.8	2.7	0.1	0.1
Selenium	mg/L	<0.002	<0.002	BDL	BDL
Silicon	mg/L	7.38	7.14	7.89	7.91
Silver	mg/L	<0.0001	<0.0001		
Sodium	mg/L	478	473	495	492
Strontium	mg/L	0.034	0.032	0.061	0.060
Tin	mg/L	<0.001	<0.001	ENA	ENA
Titanium	mg/L	0.008	0.032	BDL	BDL
Thallium	mg/L				
Uranium	mg/L				
Vanadium	mg/L	0.0031	0.0023	BDL	BDL
Zinc	mg/L	0.009	0.014	0.035	0.034
Zirconium	mg/L			BDL	BDL

PSC - Phillip Analytical Services

SCL - Syncrude Canada Ltd. Research Laboratory

UW - University of Waterloo Organic Geochemistry Lab

ETL - Envirotest Labs

*SCL - Note samples for nutrients and metals analyzed by SCL were not preserved

Sample ID	Unit	UW OW04-01B			
		PSC & UW	PSC & UW	SCL*	SCL*
Lab					
Date		17-Sep-04	17-Sep-04	17-Sep-04	17-Sep-04
Northing	m	53170.31	53170.31	53170.31	53170.31
Easting	m	53816.27	53816.27	53816.27	53816.27
Total Well Depth	mBTOC	9.73	9.73	6.88	6.88
Casing Elevation	mASL				
Dissolved Organic Carbon	mg/L	60.0	61.7		
Methane	ug/L	1571.6	1884.5		
Total Naphthenic Acids	mg/L	80.6	79.9	86.2	85.5
benzene	ug/L				
toluene	ug/L				
ethylbenzene	ug/L				
p+m-xylene	ug/L				
o-xylene	ug/L				
1,3,5-trimethylbenzene	ug/L				
1,2,4-trimethylbenzene	ug/L				
1,2,3-trimethylbenzene	ug/L				
naphthalene	ug/L				
indole+2-methyl naphthalene	ug/L				
1-methyl naphthalene	ug/L				
biphenyl	ug/L				
acenaphthylene	ug/L				
acenaphthene	ug/L				
dibenzofuran	ug/L				
fluorene	ug/L				
phenanthrene	ug/L				
anthracene	ug/L				
carbazole	ug/L				
fluoranthene	ug/L				
pyrene	ug/L				
B(A)anthracene	ug/L				
chrysene	ug/L				
B(b+k)fluoranthene	ug/L				
B(a)pyrene	ug/L				
indeno(1,2,3,c,d)pyrene+dibenzo(a,h)anthracene	ug/L				
benzo(g,h,i)perylene	ug/L				

PSC - Phillip Analytical Services

SCL - Syncrude Canada Ltd. Research Laboratory

UW - University of Waterloo Organic Geochemistry Lab

ETL - Envirotest Labs

*SCL - Note samples for nutrients and metals analyzed by SCL were not preserved

Sample ID	Unit	UW OW04-01B		
		UW	UW	ETL & UW
Lab				
Date		23-Oct-04	23-Oct-04	21-Jun-05
Northing	m	53170.31	53170.31	53170.31
Easting	m	53816.27	53816.27	53816.27
Charge Balance	RPD			-1.8
Conductivity (Lab)	mg/L			2180
Hardness	mg/L			51
pH (Lab)	pH units			8.2
Total Dissolved Solids (Lab)	mg/L			1350
Total Ammonia-Nitrogen	mg/L			3.95
Bicarbonate (Lab)	mg/L			1050
Bromide	mg/L			
Carbonate (Lab)	mg/L			<5
Chloride	mg/L			156
Fluoride	mg/L			
Hydroxide	mg/L			<5
Nitrate-Nitrogen	mg/L			<0.1
Nitrite-Nitrogen	mg/L			<0.05
Ortho Phosphate	mg/L			
Phosphorous	mg/L			
Total Sulphur	mg/L			
Sulphate	mg/L			117
Aluminum	mg/L			0.05
Antimony	mg/L			0.0007
Arsenic	mg/L			0.0074
Barium	mg/L			0.0881
Beryllium	mg/L			<0.0005
Bismuth	mg/L			<0.00005
Boron	mg/L			1.48
Cadmium	mg/L			<0.0001
Calcium	mg/L			16.6
Chromium	mg/L			0.0008
Cobalt	mg/L			0.0003
Copper	mg/L			<0.0006
Iron	mg/L			2.85
Lead	mg/L			0.0006
Lithium	mg/L			
Magnesium	mg/L			2.3
Manganese	mg/L			0.011
Molybdenum	mg/L			0.0154
Nickle	mg/L			0.0018
Potassium	mg/L			2.6
Selenium	mg/L			0.0027
Silicon	mg/L			
Silver	mg/L			<0.0002
Sodium	mg/L			540
Strontium	mg/L			0.0201
Tin	mg/L			<0.0002
Titanium	mg/L			0.0035
Thallium	mg/L			<0.00005
Uranium	mg/L			0.0001
Vanadium	mg/L			0.0038
Zinc	mg/L			0.013
Zirconium	mg/L			

PSC - Phillip Analytical Services

SCL - Syncrude Canada Ltd. Research Laboratory

UW - University of Waterloo Organic Geochemistry Lab

ETL - Envirotec Labs

*SCL - Note samples for nutrients and metals analyzed by SCL were not preserved

Sample ID	Unit	UW OW04-01B		
		UW	UW	ETL & UW
Lab				
Date		23-Oct-04	23-Oct-04	21-Jun-05
Northing	m	53170.31	53170.31	53170.31
Easting	m	53816.27	53816.27	53816.27
Total Well Depth	mBTOC	9.73	9.73	9.73
Casing Elevation	mASL			
Dissolved Organic Carbon	mg/L			
Methane	ug/L			1183.9
Total Naphthenic Acids	mg/L			71.2
benzene	ug/L	9.84	9.57	4.92
toluene	ug/L	ND	ND	ND
ethylbenzene	ug/L	ND	ND	ND
p+m-xylene	ug/L	ND	ND	ND
o-xylene	ug/L	ND	ND	ND
1,3,5-trimethylbenzene	ug/L	ND	ND	ND
1,2,4-trimethylbenzene	ug/L	ND	ND	ND
1,2,3-trimethylbenzene	ug/L	ND	ND	ND
naphthalene	ug/L	ND	ND	ND
indole+2-methyl naphthalene	ug/L	ND	ND	ND
1-methyl naphthalene	ug/L	1.78	1.86	2.02
biphenyl	ug/L	0.11	ND	ND
acenaphthylene	ug/L	ND	ND	1.13
acenaphthene	ug/L	ND	ND	ND
dibenzofuran	ug/L	ND	ND	ND
fluorene	ug/L	ND	ND	ND
phenanthrene	ug/L	ND	ND	ND
anthracene	ug/L	ND	ND	ND
carbazole	ug/L	ND	ND	ND
fluoranthene	ug/L	ND	ND	ND
pyrene	ug/L	ND	ND	ND
B(A)anthracene	ug/L	ND	ND	ND
chrysene	ug/L	ND	ND	ND
B(b+k)fluoranthene	ug/L	ND	ND	ND
B(a)pyrene	ug/L	ND	ND	ND
indeno(1,2,3,c,d)pyrene+dibenzo(a,h)anthracene	ug/L	ND	ND	ND
benzo(g,h,i)perylene	ug/L	ND	ND	ND

PSC - Phillip Analytical Services

SCL - Syncrude Canada Ltd. Research Laboratory

UW - University of Waterloo Organic Geochemistry Lab

ETL - Envirotest Labs

*SCL - Note samples for nutrients and metals analyzed by SCL were not preserved

Sample ID	Unit	UW OW04-02A		
Lab				ETL & UW
Date		17-Sep-04	23-Oct-04	21-Jun-05
Northing	m	53172.39	53172.39	
Easting	m	53840.49	53840.49	
Charge Balance	RPD			-1.7
Conductivity (Lab)	mg/L			645
Hardness	mg/L			272
pH (Lab)	pH units			7.6
Total Dissolved Solids (Lab)	mg/L			387
Total Ammonia-Nitrogen	mg/L			0.18
Bicarbonate (Lab)	mg/L			254
Bromide	mg/L			
Carbonate (Lab)	mg/L			<5
Chloride	mg/L			19
Fluoride	mg/L			
Hydioxide	mg/L			<5
Nitrate-Nitrogen	mg/L			0.1
Nitrite-Nitrogen	mg/L			<0.05
Ortho Phosphate	mg/L			
Phosphorous	mg/L			
Total Sulphur	mg/L			
Sulphate	mg/L			109
Aluminum	mg/L			<0.01
Antimony	mg/L			0.0006
Arsenic	mg/L			0.0005
Barium	mg/L			0.0982
Beryllium	mg/L			<0.0005
Bismuth	mg/L			<0.00005
Boron	mg/L			0.285
Cadmium	mg/L			<0.0001
Calcium	mg/L			73.2
Chromium	mg/L			0.0037
Cobalt	mg/L			0.0015
Copper	mg/L			<0.0006
Iron	mg/L			3.5
Lead	mg/L			<0.0001
Lithium	mg/L			
Magnesium	mg/L			21.7
Manganese	mg/L			0.716
Molybdenum	mg/L			0.0020
Nickle	mg/L			0.0015
Potassium	mg/L			3.5
Selenium	mg/L			<0.0004
Silicon	mg/L			
Silver	mg/L			<0.0002
Sodium	mg/L			35
Strontium	mg/L			0.421
Tin	mg/L			<0.0002
Titanium	mg/L			0.0004
Thallium	mg/L			0.00005
Uranium	mg/L			0.0006
Vanadium	mg/L			<0.0001
Zinc	mg/L			0.004
Zirconium	mg/L			

PSC - Phillip Analytical Services

SCL - Syncrude Canada Ltd. Research Laboratory

UW - University of Waterloo Organic Geochemistry Lab

ETL - Envirotec Labs

*SCL - Note samples for nutrients and metals analyzed by SCL were not preserved

Sample ID	Unit	UW OW04-02A		
Lab				ETL & UW
Date		17-Sep-04	23-Oct-04	21-Jun-05
Northing	m	53172.39	53172.39	
Easting	m	53840.49	53840.49	
Total Well Depth	mBTOC	3.92	3.92	
Casing Elevation	mASL			
Dissolved Organic Carbon	mg/L			
Methane	ug/L			169.1
Total Naphthenic Acids	mg/L			10.4
benzene	ug/L			ND
toluene	ug/L			ND
ethylbenzene	ug/L			ND
p+m-xylene	ug/L			ND
o-xylene	ug/L			ND
1,3,5-trimethylbenzene	ug/L			ND
1,2,4-trimethylbenzene	ug/L			ND
1,2,3-trimethylbenzene	ug/L			ND
naphthalene	ug/L			ND
indole+2-methyl naphthalene	ug/L			ND
1-methyl naphthalene	ug/L			ND
biphenyl	ug/L			ND
acenaphthylene	ug/L			ND
acenaphthene	ug/L			ND
dibenzofuran	ug/L			ND
fluorene	ug/L			ND
phenanthrene	ug/L			ND
anthracene	ug/L			ND
carbazole	ug/L			ND
fluoranthene	ug/L			ND
pyrene	ug/L			ND
B(A)anthracene	ug/L			ND
chrysene	ug/L			ND
B(b+k)fluoranthene	ug/L			ND
B(a)pyrene	ug/L			ND
indeno(1,2,3,c,d)pyrene+dibenzo(a,h)anthracene	ug/L			ND
benzo(g,h,i)perylene	ug/L			ND

PSC - Phillip Analytical Services

SCL - Syncrude Canada Ltd. Research Laboratory

UW - University of Waterloo Organic Geochemistry Lab

ETL - Envirotest Labs

*SCL - Note samples for nutrients and metals analyzed by SCL were not preserved

Sample ID	Unit	UW OW04-02B	
		PSC & UW	SCL*
Lab			
Date		16-Sep-04	16-Sep-04
Northing	m	53172.39	53172.39
Easting	m	53840.49	53840.49
Charge Balance	RPD	-2.1	1.3
Conductivity (Lab)	mg/L	2438	2030
Hardness	mg/L	49.6	
pH (Lab)	pH units	8.16	7.68
Total Dissolved Solids (Lab)	mg/L	1327	
Total Ammonia-Nitrogen	mg/L	2.84	3.27
Bicarbonate (Lab)	mg/L	912	975
Bromide	mg/L	<0.5	
Carbonate (Lab)	mg/L	1	0
Chloride	mg/L	155	150
Fluoride	mg/L	3.2	1.9
Hydroxide	mg/L		
Nitrate-Nitrogen	mg/L	0.4	BDL
Nitrite-Nitrogen	mg/L	<0.2	BDL
Ortho Phosphate	mg/L	<1	BDL
Phosphorous	mg/L	<0.05	BDL
Total Sulphur	mg/L		59.1
Sulphate	mg/L	177	173
Aluminum	mg/L	0.166	BDL
Antimony	mg/L	<0.0005	BDL
Arsenic	mg/L	0.003	
Barium	mg/L	0.086	BDL
Beryllium	mg/L	<0.001	
Bismuth	mg/L	<0.001	
Boron	mg/L	1.91	1.83
Cadmium	mg/L	<0.0001	BDL
Calcium	mg/L	14.2	13.4
Chromium	mg/L	<0.005	BDL
Cobalt	mg/L	0.001	BDL
Copper	mg/L	0.001	BDL
Iron	mg/L	4.11	0.591
Lead	mg/L	0.001	BDL
Lithium	mg/L		BDL
Magnesium	mg/L	3.41	3.18
Manganese	mg/L	0.462	0.308
Molybdenum	mg/L	0.045	0.064
Nickle	mg/L	0.004	BDL
Potassium	mg/L	3.9	0.1
Selenium	mg/L	<0.002	BDL
Silicon	mg/L	5.54	4.93
Silver	mg/L	<0.0001	
Sodium	mg/L	523	509
Strontium	mg/L	0.051	0.071
Tin	mg/L	<0.001	ENA
Titanium	mg/L	0.051	BDL
Thallium	mg/L		
Uranium	mg/L		
Vanadium	mg/L	0.0017	BDL
Zinc	mg/L	0.006	0.03
Zirconium	mg/L		BDL

PSC - Phillip Analytical Services

SCL - Syncrude Canada Ltd. Research Laboratory

UW - University of Waterloo Organic Geochemistry Lab

ETL - Envirotest Labs

*SCL - Note samples for nutrients and metals analyzed by SCL were not preserved

Sample ID	Unit	UW OW04-02B	
		PSC & UW	SCL*
Lab			
Date		16-Sep-04	16-Sep-04
Northing	m	53172.39	53172.39
Easting	m	53840.49	53840.49
Total Well Depth	mBTOC	6.88	6.88
Casing Elevation	mASL		
Dissolved Organic Carbon	mg/L	58	
Methane	ug/L	1669.1	
Total Naphthenic Acids	mg/L	82.9	94.1
benzene	ug/L		
toluene	ug/L		
ethylbenzene	ug/L		
p+m-xylene	ug/L		
o-xylene	ug/L		
1,3,5-trimethylbenzene	ug/L		
1,2,4-trimethylbenzene	ug/L		
1,2,3-trimethylbenzene	ug/L		
naphthalene	ug/L		
indole+2-methyl naphthalene	ug/L		
1-methyl naphthalene	ug/L		
biphenyl	ug/L		
acenaphthylene	ug/L		
acenaphthene	ug/L		
dibenzofuran	ug/L		
fluorene	ug/L		
phenanthrene	ug/L		
anthracene	ug/L		
carbazole	ug/L		
fluoranthene	ug/L		
pyrene	ug/L		
B(A)anthracene	ug/L		
chrysene	ug/L		
B(b+k)fluoranthene	ug/L		
B(a)pyrene	ug/L		
indeno(1,2,3,c,d)pyrene+dibenzo(a,h)anthracene	ug/L		
benzo(g,h,i)perylene	ug/L		

PSC - Phillip Analytical Services

SCL - Syncrude Canada Ltd. Research Laboratory

UW - University of Waterloo Organic Geochemistry Lab

ETL - Envirotest Labs

*SCL - Note samples for nutrients and metals analyzed by SCL were not preserved

Sample ID	Unit	UW OW04-02B		
		UW	ETL & UW	ETL & UW
Lab				
Date		23-Oct-04	21-Jun-05	21-Jun-05
Northing	m	53172.39		
Easting	m	53840.49		
Charge Balance	RPD		-3.2	0.8
Conductivity (Lab)	mg/L		2220	2240
Hardness	mg/L		51	50
pH (Lab)	pH units		8.2	8.2
Total Dissolved Solids (Lab)	mg/L		1410	1390
Total Ammonia-Nitrogen	mg/L		3.41	3.29
Bicarbonate (Lab)	mg/L		997	999
Bromide	mg/L			
Carbonate (Lab)	mg/L		<5	<5
Chloride	mg/L		148	151
Fluoride	mg/L			
Hydroxide	mg/L		<5	<5
Nitrate-Nitrogen	mg/L		<0.1	<0.1
Nitrite-Nitrogen	mg/L		<0.05	<0.05
Ortho Phosphate	mg/L			
Phosphorous	mg/L			
Total Sulphur	mg/L			
Sulphate	mg/L		186	194
Aluminum	mg/L		<0.01	<0.01
Antimony	mg/L		0.0008	0.0006
Arsenic	mg/L		0.0022	0.0022
Barium	mg/L		0.0719	0.0706
Beryllium	mg/L		<0.0005	<0.0005
Bismuth	mg/L		<0.00005	<0.00005
Boron	mg/L		1.50	1.70
Cadmium	mg/L		0.0001	<0.0001
Calcium	mg/L		15	14.6
Chromium	mg/L		<0.0004	0.0009
Cobalt	mg/L		0.0007	0.0007
Copper	mg/L		<0.0006	<0.0006
Iron	mg/L		3.79	1.68
Lead	mg/L		0.0003	0.0002
Lithium	mg/L			
Magnesium	mg/L		3.3	3.2
Manganese	mg/L		0.420	0.199
Molybdenum	mg/L		0.0513	0.0511
Nickle	mg/L		0.0030	0.0027
Potassium	mg/L		4.1	3.8
Selenium	mg/L		0.0007	0.0006
Silicon	mg/L			
Silver	mg/L		<0.0002	<0.0002
Sodium	mg/L		564	527
Strontium	mg/L		0.0349	0.0327
Tin	mg/L		<0.0002	<0.0002
Titanium	mg/L		0.0013	0.0016
Thallium	mg/L		<0.00005	<0.00005
Uranium	mg/L		0.0005	0.0006
Vanadium	mg/L		0.0012	0.0012
Zinc	mg/L		0.014	0.016
Zirconium	mg/L			

PSC - Phillip Analytical Services

SCL - Syncrude Canada Ltd. Research Laboratory

UW - University of Waterloo Organic Geochemistry Lab

ETL - Envirotest Labs

*SCL - Note samples for nutrients and metals analyzed by SCL were not preserved

Sample ID	Unit	UW OW04-02B		
		UW	ETL & UW	ETL & UW
Lab				
Date		23-Oct-04	21-Jun-05	21-Jun-05
Northing	m	53172.39		
Easting	m	53840.49		
Total Well Depth	mBTOC	6.88		
Casing Elevation	mASL			
Dissolved Organic Carbon	mg/L			
Methane	ug/L		2097.4	2536.1
Total Naphthenic Acids	mg/L		78.8	76.5
benzene	ug/L	ND	1.56	1.69
toluene	ug/L	ND	ND	ND
ethylbenzene	ug/L	ND	ND	ND
p+m-xylene	ug/L	1.73	ND	ND
o-xylene	ug/L	ND	ND	ND
1,3,5-trimethylbenzene	ug/L	ND	ND	ND
1,2,4-trimethylbenzene	ug/L	ND	ND	ND
1,2,3-trimethylbenzene	ug/L	ND	ND	ND
naphthalene	ug/L	ND	ND	ND
indole+2-methyl naphthalene	ug/L	ND	ND	ND
1-methyl naphthalene	ug/L	2.00	2.24	2.52
biphenyl	ug/L	ND	ND	ND
acenaphthylene	ug/L	ND	ND	1.65
acenaphthene	ug/L	ND	ND	ND
dibenzofuran	ug/L	ND	ND	ND
fluorene	ug/L	ND	ND	ND
phenanthrene	ug/L	ND	ND	ND
anthracene	ug/L	ND	ND	ND
carbazole	ug/L	ND	ND	ND
fluoranthene	ug/L	ND	ND	ND
pyrene	ug/L	ND	ND	ND
B(A)anthracene	ug/L	ND	ND	ND
chrysene	ug/L	ND	ND	ND
B(b+k)fluoranthene	ug/L	ND	ND	ND
B(a)pyrene	ug/L	ND	ND	ND
indeno(1,2,3,c,d)pyrene+dibenzo(a,h)anthracene	ug/L	ND	ND	ND
benzo(g,h,i)perylene	ug/L	ND	ND	ND

PSC - Phillip Analytical Services

SCL - Syncrude Canada Ltd. Research Laboratory

UW - University of Waterloo Organic Geochemistry Lab

ETL - Envirotest Labs

*SCL - Note samples for nutrients and metals analyzed by SCL were not preserved

Sample ID	Unit	UW OW04-02C			
		PSC & UW	SCL*	UW	ETL & UW
Lab					
Date		16-Sep-04	16-Sep-04	23-Oct-04	21-Jun-05
Northing	m	53172.39	53172.39	53172.39	
Easting	m	53840.49	53840.49	53840.49	
Charge Balance	RPD	1.1	3.2		-2.0
Conductivity (Lab)	mg/L	3166	2580		2840
Hardness	mg/L	213.6			263
pH (Lab)	pH units	7.93	7.47		8.0
Total Dissolved Solids (Lab)	mg/L	1679			1820
Total Ammonia-Nitrogen	mg/L	0.64	0.31		0.74
Bicarbonate (Lab)	mg/L	1020	1130		1140
Bromide	mg/L	<0.5			
Carbonate (Lab)	mg/L	1	0		<5
Chloride	mg/L	314	210		322
Fluoride	mg/L	2	0.67		
Hydioxide	mg/L				<5
Nitrate-Nitrogen	mg/L	<0.2	BDL		<0.1
Nitrite-Nitrogen	mg/L	<0.2	BDL		<0.05
Ortho Phosphate	mg/L	<1	BDL		
Phosphorous	mg/L	0.16	BDL		
Total Sulphur	mg/L		55.7		
Sulphate	mg/L	207	179		198
Aluminum	mg/L	0.015	BDL		0.01
Antimony	mg/L	<0.0005	BDL		0.0006
Arsenic	mg/L	<0.002			0.0005
Barium	mg/L	0.225	0.1		0.326
Beryllium	mg/L	<0.001			<0.0005
Bismuth	mg/L	<0.001			<0.00005
Boron	mg/L	1.62	1.38		1.58
Cadmium	mg/L	<0.0001	BDL		<0.0001
Calcium	mg/L	66.7	63		84.9
Chromium	mg/L	<0.005	BDL		0.0008
Cobalt	mg/L	0.0003	BDL		0.0002
Copper	mg/L	<0.0005	BDL		<0.0006
Iron	mg/L	4.20	0.84		1.89
Lead	mg/L	<0.0005	BDL		<0.0001
Lithium	mg/L		BDL		
Magnesium	mg/L	11.4	11.7		12.5
Manganese	mg/L	0.092	0.08		0.060
Molybdenum	mg/L	0.007	BDL		0.0003
Nickle	mg/L	0.002	BDL		0.0013
Potassium	mg/L	4	0.1		3.0
Selenium	mg/L	<0.002	BDL		0.0005
Silicon	mg/L	5.01	4.47		
Silver	mg/L	<0.0001			<0.0002
Sodium	mg/L	569	512		637
Strontium	mg/L	0.21	0.197		0.153
Tin	mg/L	<0.001	ENA		<0.0002
Titanium	mg/L	0.21	BDL		0.004
Thallium	mg/L				<0.00005
Uranium	mg/L				0.0002
Vanadium	mg/L	0.0048	BDL		0.0062
Zinc	mg/L	0.007	0.03		0.015
Zirconium	mg/L		BDL		

PSC - Phillip Analytical Services

SCL - Syncrude Canada Ltd. Research Laboratory

UW - University of Waterloo Organic Geochemistry Lab

ETL - Envirotest Labs

*SCL - Note samples for nutrients and metals analyzed by SCL were not preserved

Sample ID	Unit	UW OW04-02C			
		PSC & UW	SCL*	UW	ETL & UW
Lab					
Date		16-Sep-04	16-Sep-04	23-Oct-04	21-Jun-05
Northing	m	53172.39	53172.39	53172.39	
Easting	m	53840.49	53840.49	53840.49	
Total Well Depth	mBTC	8.93	8.93	8.93	
Casing Elevation	mASL				
Dissolved Organic Carbon	mg/L	54.4			
Methane	ug/L				98.2
Total Naphthenic Acids	mg/L	70.0	77.1		65
benzene	ug/L			ND	ND
toluene	ug/L			ND	ND
ethylbenzene	ug/L			ND	ND
p+m-xylene	ug/L			1.31	ND
o-xylene	ug/L			ND	ND
1,3,5-trimethylbenzene	ug/L			ND	ND
1,2,4-trimethylbenzene	ug/L			ND	ND
1,2,3-trimethylbenzene	ug/L			ND	ND
naphthalene	ug/L			ND	ND
indole+2-methyl naphthalene	ug/L			ND	ND
1-methyl naphthalene	ug/L			ND	1.68
biphenyl	ug/L			ND	ND
acenaphthylene	ug/L			ND	1.40
acenaphthene	ug/L			ND	ND
dibenzofuran	ug/L			ND	ND
fluorene	ug/L			ND	ND
phenanthrene	ug/L			ND	ND
anthracene	ug/L			ND	ND
carbazole	ug/L			ND	ND
fluoranthene	ug/L			ND	ND
pyrene	ug/L			ND	ND
B(A)anthracene	ug/L			ND	ND
chrysene	ug/L			ND	ND
B(b+k)fluoranthene	ug/L			ND	ND
B(a)pyrene	ug/L			ND	ND
indeno(1,2,3,c,d)pyrene+dibenzo(a,h)anthracene	ug/L			ND	ND
benzo(g,h,i)perylene	ug/L			ND	ND

PSC - Phillip Analytical Services

SCL - Syncrude Canada Ltd. Research Laboratory

UW - University of Waterloo Organic Geochemistry Lab

ETL - Envirotest Labs

*SCL - Note samples for nutrients and metals analyzed by SCL were not preserved

Sample ID	Unit	UW OW04-03A			
		PSC & UW	SCL*	UW	ETL & UW
Lab					
Date		16-Sep-04	16-Sep-04	23-Oct-04	21-Jun-05
Northing	m	53158.4	53158.4	53158.4	
Easting	m	53993.87	53993.87	53993.87	
Charge Balance	RPD	2.7	1.6		-1.8
Conductivity (Lab)	mg/L	1859	1500		912
Hardness	mg/L	334.4			212
pH (Lab)	pH units	7.46	6.98		7.7
Total Dissolved Solids (Lab)	mg/L	984			559
Total Ammonia-Nitrogen	mg/L	0.15	0.32		0.17
Bicarbonate (Lab)	mg/L	685	565		429
Bromide	mg/L	<0.5			
Carbonate (Lab)	mg/L	1	0		<5
Chloride	mg/L	130	130		33
Fluoride	mg/L	0.2	BDL		
Hydioxide	mg/L				<5
Nitrate-Nitrogen	mg/L	<0.2	BDL		<0.1
Nitrite-Nitrogen	mg/L	<0.2	BDL		<0.05
Ortho Phosphate	mg/L	<1	BDL		
Phosphorous	mg/L	<0.05	BDL		
Total Sulphur	mg/L		46		
Sulphate	mg/L	159	155		101
Aluminum	mg/L	<0.005	BDL		<0.01
Antimony	mg/L	<0.0005	BDL		0.0007
Arsenic	mg/L	<0.002			0.0006
Barium	mg/L	0.124	0.016		0.0696
Beryllium	mg/L	<0.001			<0.0005
Bismuth	mg/L	<0.001			<0.00005
Boron	mg/L	0.696	0.664		0.368
Cadmium	mg/L	<0.0001	BDL		<0.0001
Calcium	mg/L	95.1	87		61.4
Chromium	mg/L	<0.005	BDL		0.0010
Cobalt	mg/L	0.0053	BDL		0.0044
Copper	mg/L	<0.0005	BDL		<0.0006
Iron	mg/L	5.07	BDL		3.31
Lead	mg/L	<0.0005	BDL		<0.0001
Lithium	mg/L		BDL		
Magnesium	mg/L	23.5	21.7		14.3
Manganese	mg/L	2.83	2.71		2.46
Molybdenum	mg/L	0.001	BDL		0.0010
Nickle	mg/L	0.009	BDL		0.0051
Potassium	mg/L	2.1	0.1		2.0
Selenium	mg/L	<0.002	BDL		<0.0004
Silicon	mg/L	6.03	5.7		
Silver	mg/L	<0.0001			<0.0002
Sodium	mg/L	235	216		136
Strontium	mg/L	0.279	0.28		0.165
Tin	mg/L	<0.001	ENA		<0.0002
Titanium	mg/L	0.279	BDL		0.0011
Thallium	mg/L				<0.00005
Uranium	mg/L				0.0009
Vanadium	mg/L	<0.0005	BDL		<0.0001
Zinc	mg/L	<0.005	0.028		0.01
Zirconium	mg/L		BDL		

PSC - Phillip Analytical Services

SCL - Syncrude Canada Ltd. Research Laboratory

UW - University of Waterloo Organic Geochemistry Lab

ETL - Envirotest Labs

*SCL - Note samples for nutrients and metals analyzed by SCL were not preserved

Sample ID	Unit	UW OW04-03A			
		PSC & UW	SCL*	UW	ETL & UW
Lab					
Date		16-Sep-04	16-Sep-04	23-Oct-04	21-Jun-05
Northing	m	53158.4	53158.4	53158.4	
Easting	m	53993.87	53993.87	53993.87	
Total Well Depth	mBTC	3.83	3.83	3.83	
Casing Elevation	mASL				
Dissolved Organic Carbon	mg/L	38.9			
Methane	ug/L	49.0			59.8
Total Naphthenic Acids	mg/L	33.9	38.7		7.3
benzene	ug/L			ND	ND
toluene	ug/L			ND	ND
ethylbenzene	ug/L			ND	ND
p+m-xylene	ug/L			ND	ND
o-xylene	ug/L			ND	ND
1,3,5-trimethylbenzene	ug/L			ND	ND
1,2,4-trimethylbenzene	ug/L			ND	ND
1,2,3-trimethylbenzene	ug/L			ND	ND
naphthalene	ug/L			ND	ND
indole+2-methyl naphthalene	ug/L			ND	ND
1-methyl naphthalene	ug/L			2.49	ND
biphenyl	ug/L			ND	ND
acenaphthylene	ug/L			ND	ND
acenaphthene	ug/L			ND	ND
dibenzofuran	ug/L			ND	ND
fluorene	ug/L			ND	ND
phenanthrene	ug/L			ND	ND
anthracene	ug/L			ND	ND
carbazole	ug/L			ND	ND
fluoranthene	ug/L			ND	ND
pyrene	ug/L			ND	ND
B(A)anthracene	ug/L			ND	ND
chrysene	ug/L			ND	ND
B(b+k)fluoranthene	ug/L			ND	ND
B(a)pyrene	ug/L			ND	ND
indeno(1,2,3,c,d)pyrene+dibenzo(a,h)anthracene	ug/L			ND	ND
benzo(g,h,i)perylene	ug/L			ND	ND

PSC - Phillip Analytical Services

SCL - Syncrude Canada Ltd. Research Laboratory

UW - University of Waterloo Organic Geochemistry Lab

ETL - Envirotest Labs

*SCL - Note samples for nutrients and metals analyzed by SCL were not preserved

Sample ID	Unit	UW OW04-03B	
Lab		PSC & UW	SCL*
Date		16-Sep-04	16-Sep-04
Northing	m	53158.4	53158.4
Easting	m	53993.87	53993.87
Charge Balance	RPD	0.1	-1.3
Conductivity (Lab)	mg/L	2889	2310
Hardness	mg/L	195.9	
pH (Lab)	pH units	7.8	7.36
Total Dissolved Solids (Lab)	mg/L	1542	
Total Ammonia-Nitrogen	mg/L	2.03	1.98
Bicarbonate (Lab)	mg/L	1090	955
Bromide	mg/L	<0.5	
Carbonate (Lab)	mg/L	1	0
Chloride	mg/L	244	240
Fluoride	mg/L	1.3	BDL
Hydroxide	mg/L		
Nitrate-Nitrogen	mg/L	<0.2	BDL
Nitrite-Nitrogen	mg/L	<0.2	BDL
Ortho Phosphate	mg/L	<1	BDL
Phosphorous	mg/L	0.2	BDL
Total Sulphur	mg/L		42.4
Sulphate	mg/L	141	138
Aluminum	mg/L	0.014	BDL
Antimony	mg/L	<0.0005	BDL
Arsenic	mg/L	<0.002	
Barium	mg/L	0.276	0.153
Beryllium	mg/L	<0.001	
Bismuth	mg/L	<0.001	
Boron	mg/L	1.33	1.26
Cadmium	mg/L	<0.0001	BDL
Calcium	mg/L	60.8	57.3
Chromium	mg/L	<0.005	BDL
Cobalt	mg/L	0.0002	BDL
Copper	mg/L	<0.0005	BDL
Iron	mg/L	2.01	0.459
Lead	mg/L	<0.0005	BDL
Lithium	mg/L		BDL
Magnesium	mg/L	10.7	10.4
Manganese	mg/L	0.082	0.083
Molybdenum	mg/L	0.003	BDL
Nickle	mg/L	0.001	BDL
Potassium	mg/L	3.6	0.1
Selenium	mg/L	<0.002	BDL
Silicon	mg/L	5.74	5.87
Silver	mg/L	<0.0001	
Sodium	mg/L	540	508
Strontium	mg/L	0.126	0.147
Tin	mg/L	<0.001	ENA
Titanium	mg/L	0.126	BDL
Thallium	mg/L		
Uranium	mg/L		
Vanadium	mg/L	0.0030	BDL
Zinc	mg/L	0.031	0.031
Zirconium	mg/L		BDL

PSC - Phillip Analytical Services

SCL - Syncrude Canada Ltd. Research Laboratory

UW - University of Waterloo Organic Geochemistry Lab

ETL - Envirotest Labs

*SCL - Note samples for nutrients and metals analyzed by SCL were not preserved

Sample ID	Unit	UW OW04-03B	
		PSC & UW	SCL*
Lab			
Date		16-Sep-04	16-Sep-04
Northing	m	53158.4	53158.4
Easting	m	53993.87	53993.87
Total Well Depth	mBTOC	6.88	6.88
Casing Elevation	mASL		
Dissolved Organic Carbon	mg/L	54.6	
Methane	ug/L	15.4	
Total Naphthenic Acids	mg/L	62.4	70.2
benzene	ug/L		
toluene	ug/L		
ethylbenzene	ug/L		
p+m-xylene	ug/L		
o-xylene	ug/L		
1,3,5-trimethylbenzene	ug/L		
1,2,4-trimethylbenzene	ug/L		
1,2,3-trimethylbenzene	ug/L		
naphthalene	ug/L		
indole+2-methyl naphthalene	ug/L		
1-methyl naphthalene	ug/L		
biphenyl	ug/L		
acenaphthylene	ug/L		
acenaphthene	ug/L		
dibenzofuran	ug/L		
fluorene	ug/L		
phenanthrene	ug/L		
anthracene	ug/L		
carbazole	ug/L		
fluoranthene	ug/L		
pyrene	ug/L		
B(A)anthracene	ug/L		
chrysene	ug/L		
B(b+k)fluoranthene	ug/L		
B(a)pyrene	ug/L		
indeno(1,2,3,c,d)pyrene+dibenzo(a,h)anthracene	ug/L		
benzo(g,h,i)perylene	ug/L		

PSC - Phillip Analytical Services

SCL - Syncrude Canada Ltd. Research Laboratory

UW - University of Waterloo Organic Geochemistry Lab

ETL - Envirotest Labs

*SCL - Note samples for nutrients and metals analyzed by SCL were not preserved

Sample ID	Unit	UW OW04-03B		
		UW	UW	ETL & UW
Lab				
Date		23-Oct-04	23-Oct-04	21-Oct-05
Northing	m	53158.4	53158.4	
Easting	m	53993.87	53993.87	
Charge Balance	RPD			-2.4
Conductivity (Lab)	mg/L			2520
Hardness	mg/L			273
pH (Lab)	pH units			7.9
Total Dissolved Solids (Lab)	mg/L			1610
Total Ammonia-Nitrogen	mg/L			2.70
Bicarbonate (Lab)	mg/L			1090
Bromide	mg/L			
Carbonate (Lab)	mg/L			<5
Chloride	mg/L			233
Fluoride	mg/L			
Hydioxide	mg/L			<5
Nitrate-Nitrogen	mg/L			<0.1
Nitrite-Nitrogen	mg/L			<0.05
Ortho Phosphate	mg/L			
Phosphorous	mg/L			
Total Sulphur	mg/L			
Sulphate	mg/L			188
Aluminum	mg/L			0.01
Antimony	mg/L			0.0007
Arsenic	mg/L			<0.0004
Barium	mg/L			0.346
Beryllium	mg/L			0.0005
Bismuth	mg/L			<0.00005
Boron	mg/L			1.54
Cadmium	mg/L			<0.0001
Calcium	mg/L			82.1
Chromium	mg/L			0.0010
Cobalt	mg/L			0.0002
Copper	mg/L			<0.0006
Iron	mg/L			0.241
Lead	mg/L			<0.0001
Lithium	mg/L			
Magnesium	mg/L			16.5
Manganese	mg/L			0.039
Molybdenum	mg/L			0.0022
Nickle	mg/L			0.0013
Potassium	mg/L			4.2
Selenium	mg/L			0.0006
Silicon	mg/L			
Silver	mg/L			<0.0002
Sodium	mg/L			552
Strontium	mg/L			0.141
Tin	mg/L			<0.0002
Titanium	mg/L			0.0026
Thallium	mg/L			<0.00005
Uranium	mg/L			0.0002
Vanadium	mg/L			0.0039
Zinc	mg/L			0.011
Zirconium	mg/L			

PSC - Phillip Analytical Services

SCL - Syncrude Canada Ltd. Research Laboratory

UW - University of Waterloo Organic Geochemistry Lab

ETL - Envirotest Labs

*SCL - Note samples for nutrients and metals analyzed by SCL were not preserved

Sample ID	Unit	UW OW04-03B		
		UW	UW	ETL & UW
Lab				
Date		23-Oct-04	23-Oct-04	21-Oct-05
Northing	m	53158.4	53158.4	
Easting	m	53993.87	53993.87	
Total Well Depth	mBTOC	6.88	6.88	
Casing Elevation	mASL			
Dissolved Organic Carbon	mg/L			
Methane	ug/L			282.1
Total Naphthenic Acids	mg/L			60.1
benzene	ug/L	ND	ND	ND
toluene	ug/L	ND	ND	ND
ethylbenzene	ug/L	ND	ND	ND
p+m-xylene	ug/L	ND	ND	ND
o-xylene	ug/L	ND	ND	ND
1,3,5-trimethylbenzene	ug/L	ND	ND	ND
1,2,4-trimethylbenzene	ug/L	ND	ND	ND
1,2,3-trimethylbenzene	ug/L	ND	ND	ND
naphthalene	ug/L	ND	ND	ND
indole+2-methyl naphthalene	ug/L	ND	ND	ND
1-methyl naphthalene	ug/L	ND	ND	ND
biphenyl	ug/L	ND	ND	1.06
acenaphthylene	ug/L	ND	ND	ND
acenaphthene	ug/L	ND	ND	ND
dibenzofuran	ug/L	ND	ND	ND
fluorene	ug/L	ND	ND	ND
phenanthrene	ug/L	ND	1.90	ND
anthracene	ug/L	ND	ND	ND
carbazole	ug/L	ND	ND	ND
fluoranthene	ug/L	ND	ND	ND
pyrene	ug/L	ND	ND	ND
B(A)anthracene	ug/L	ND	ND	ND
chrysene	ug/L	ND	ND	ND
B(b+k)fluoranthene	ug/L	ND	ND	ND
B(a)pyrene	ug/L	ND	ND	ND
indeno(1,2,3,c,d)pyrene+dibenzo(a,h)anthracene	ug/L	ND	ND	ND
benzo(g,h,i)perylene	ug/L	ND	ND	ND

PSC - Phillip Analytical Services

SCL - Syncrude Canada Ltd. Research Laboratory

UW - University of Waterloo Organic Geochemistry Lab

ETL - Envirotest Labs

*SCL - Note samples for nutrients and metals analyzed by SCL were not preserved

Sample ID	Unit	UW OW04-03C			
		PSC & UW	SCL*	UW	ETL & UW
Lab					
Date		16-Sep-04	16-Sep-04	23-Oct-04	21-Jun-05
Northing	m	53158.4	53158.4	53158.4	
Easting	m	53993.87	53993.87	53993.87	
Charge Balance	RPD	0.9	1.9		0.6
Conductivity (Lab)	mg/L	1070	898		1770
Hardness	mg/L	405.3			398
pH (Lab)	pH units	7.71	7.02		7.8
Total Dissolved Solids (Lab)	mg/L	544			1050
Total Ammonia-Nitrogen	mg/L	0.42	0.15		0.53
Bicarbonate (Lab)	mg/L	550	565		979
Bromide	mg/L	<0.5			
Carbonate (Lab)	mg/L	1	0		<5
Chloride	mg/L	67	59		134
Fluoride	mg/L	0.1	BDL		
Hydioxide	mg/L				<5
Nitrate-Nitrogen	mg/L	<0.2	BDL		<0.1
Nitrite-Nitrogen	mg/L	<0.2	BDL		<0.05
Ortho Phosphate	mg/L	<1	BDL		
Phosphorous	mg/L	0.06	BDL		
Total Sulphur	mg/L		1.15		
Sulphate	mg/L	3	4		15.9
Aluminum	mg/L	0.006	BDL		<0.01
Antimony	mg/L	<0.0005	BDL		0.0007
Arsenic	mg/L	<0.002			<0.0004
Barium	mg/L	0.405	0.236		0.469
Beryllium	mg/L	<0.001			<0.0005
Bismuth	mg/L	<0.001			<0.00005
Boron	mg/L	0.061	0.076		0.239
Cadmium	mg/L	<0.0001	BDL		<0.0001
Calcium	mg/L	127	128		122
Chromium	mg/L	<0.005	BDL		<0.0004
Cobalt	mg/L	0.0001	BDL		0.0002
Copper	mg/L	<0.0005	BDL		<0.0006
Iron	mg/L	9.55	BDL		5.31
Lead	mg/L	<0.0005	BDL		<0.0001
Lithium	mg/L		BDL		
Magnesium	mg/L	21.2	24.8		22.6
Manganese	mg/L	0.387	0.357		0.376
Molybdenum	mg/L	0.002	BDL		0.0002
Nickle	mg/L	<0.001	BDL		0.0003
Potassium	mg/L	3.4	0.1		3.3
Selenium	mg/L	<0.002	BDL		0.0007
Silicon	mg/L	5.26	4.87		
Silver	mg/L	<0.0001			<0.0002
Sodium	mg/L	51	49		268
Strontium	mg/L	0.327	0.318		0.320
Tin	mg/L	<0.001	ENA		<0.0002
Titanium	mg/L	0.327	BDL		0.0016
Thallium	mg/L				<0.00005
Uranium	mg/L				<0.0001
Vanadium	mg/L	<0.0005	BDL		0.0010
Zinc	mg/L	0.162	0.028		0.012
Zirconium	mg/L		BDL		

PSC - Phillip Analytical Services

SCL - Syncrude Canada Ltd. Research Laboratory

UW - University of Waterloo Organic Geochemistry Lab

ETL - Envirotest Labs

*SCL - Note samples for nutrients and metals analyzed by SCL were not preserved

Sample ID	Unit	UW OW04-03C			
		PSC & UW	SCL*	UW	ETL & UW
Lab					
Date		16-Sep-04	16-Sep-04	23-Oct-04	21-Jun-05
Northing	m	53158.4	53158.4	53158.4	
Easting	m	53993.87	53993.87	53993.87	
Total Well Depth	mBTC	8.27	8.27	8.27	
Casing Elevation	mASL				
Dissolved Organic Carbon	mg/L	20.6			
Methane	ug/L				1127.0
Total Naphthenic Acids	mg/L	12.3	10.6		36.3
benzene	ug/L			ND	ND
toluene	ug/L			ND	ND
ethylbenzene	ug/L			ND	ND
p+m-xylene	ug/L			ND	ND
o-xylene	ug/L			ND	ND
1,3,5-trimethylbenzene	ug/L			ND	ND
1,2,4-trimethylbenzene	ug/L			ND	ND
1,2,3-trimethylbenzene	ug/L			ND	ND
naphthalene	ug/L			ND	ND
indole+2-methyl naphthalene	ug/L			ND	ND
1-methyl naphthalene	ug/L			ND	2.02
biphenyl	ug/L			1.02	0.92
acenaphthylene	ug/L			ND	ND
acenaphthene	ug/L			ND	ND
dibenzofuran	ug/L			ND	ND
fluorene	ug/L			ND	ND
phenanthrene	ug/L			ND	ND
anthracene	ug/L			ND	ND
carbazole	ug/L			ND	ND
fluoranthene	ug/L			ND	ND
pyrene	ug/L			ND	ND
B(A)anthracene	ug/L			ND	ND
chrysene	ug/L			ND	ND
B(b+k)fluoranthene	ug/L			ND	ND
B(a)pyrene	ug/L			ND	ND
indeno(1,2,3,c,d)pyrene+dibenzo(a,h)anthracene	ug/L			ND	ND
benzo(g,h,i)perylene	ug/L			ND	ND

PSC - Phillip Analytical Services

SCL - Syncrude Canada Ltd. Research Laboratory

UW - University of Waterloo Organic Geochemistry Lab

ETL - Envirotest Labs

*SCL - Note samples for nutrients and metals analyzed by SCL were not preserved

Sample ID	Unit	UW OW04-04A			
		PSC & UW	SCL*	UW	ETL & UW
Lab					
Date		16-Sep-04	16-Sep-04	23-Oct-04	22-Jun-05
Northing	m	53172.26	53172.26	53172.26	
Easting	m	54164.9	54164.9	54164.9	
Charge Balance	RPD	0.8	0.7		-2.1
Conductivity (Lab)	mg/L	2229	1769		1630
Hardness	mg/L	334.8			284
pH (Lab)	pH units	7.87	7.24		8.0
Total Dissolved Solids (Lab)	mg/L	1193			1050
Total Ammonia-Nitrogen	mg/L	0.05	0.33		0.07
Bicarbonate (Lab)	mg/L	878	857		579
Bromide	mg/L	<0.5			
Carbonate (Lab)	mg/L	1	0		<5
Chloride	mg/L	131	130		116
Fluoride	mg/L	0.1	BDL		
Hydroxide	mg/L				<5
Nitrate-Nitrogen	mg/L	<0.2	BDL		0.2
Nitrite-Nitrogen	mg/L	<0.2	BDL		<0.05
Ortho Phosphate	mg/L	<1	BDL		
Phosphorous	mg/L	<0.05	BDL		
Total Sulphur	mg/L		53.1		
Sulphate	mg/L	171	164		247
Aluminum	mg/L	0.005	BDL		<0.01
Antimony	mg/L	<0.0005	BDL		0.0008
Arsenic	mg/L	<0.002			<0.0004
Barium	mg/L	0.084	BDL		0.0689
Beryllium	mg/L	<0.001			<0.0005
Bismuth	mg/L	<0.001			<0.00005
Boron	mg/L	0.905	0.89		0.925
Cadmium	mg/L	<0.0001	BDL		<0.0001
Calcium	mg/L	102	102		83.9
Chromium	mg/L	<0.005	BDL		0.0005
Cobalt	mg/L	0.0022	BDL		0.0016
Copper	mg/L	0.0009	BDL		0.0011
Iron	mg/L	0.35	0.021		0.019
Lead	mg/L	<0.0005	BDL		<0.0001
Lithium	mg/L		BDL		
Magnesium	mg/L	19.4	19.5		18.0
Manganese	mg/L	0.356	0.363		0.315
Molybdenum	mg/L	0.002	BDL		0.0004
Nickle	mg/L	0.006	BDL		0.0055
Potassium	mg/L	2.2	0.1		2.3
Selenium	mg/L	<0.002	BDL		0.0005
Silicon	mg/L	4.16	4.71		
Silver	mg/L	<0.0001			<0.0002
Sodium	mg/L	334	324		297
Strontium	mg/L	0.139	0.162		0.109
Tin	mg/L	<0.001	ENA		<0.0002
Titanium	mg/L	0.139	BDL		0.0009
Thallium	mg/L				<0.00005
Uranium	mg/L				0.0014
Vanadium	mg/L	<0.0005	BDL		0.0008
Zinc	mg/L	<0.005	0.027		0.011
Zirconium	mg/L		BDL		

PSC - Phillip Analytical Services

SCL - Syncrude Canada Ltd. Research Laboratory

UW - University of Waterloo Organic Geochemistry Lab

ETL - Envirotest Labs

*SCL - Note samples for nutrients and metals analyzed by SCL were not preserved

Sample ID	Unit	UW OW04-04A			
		PSC & UW	SCL*	UW	ETL & UW
Lab		16-Sep-04	16-Sep-04	23-Oct-04	22-Jun-05
Date		53172.26	53172.26	53172.26	
Northing	m	54164.9	54164.9	54164.9	
Easting	m	7.82	7.82	7.82	
Total Well Depth	mBTOC				
Casing Elevation	mASL				
Dissolved Organic Carbon	mg/L	39.4			
Methane	ug/L	10.8			20.3
Total Naphthenic Acids	mg/L	39.1	43.7		15.3
benzene	ug/L			ND	ND
toluene	ug/L			ND	ND
ethylbenzene	ug/L			ND	ND
p+m-xylene	ug/L			ND	ND
o-xylene	ug/L			ND	ND
1,3,5-trimethylbenzene	ug/L			ND	ND
1,2,4-trimethylbenzene	ug/L			ND	ND
1,2,3-trimethylbenzene	ug/L			ND	ND
naphthalene	ug/L			ND	ND
indole+2-methyl naphthalene	ug/L			ND	2.94
1-methyl naphthalene	ug/L			2.53	ND
biphenyl	ug/L			ND	1.60
acenaphthylene	ug/L			4.09	ND
acenaphthene	ug/L			ND	ND
dibenzofuran	ug/L			ND	ND
fluorene	ug/L			ND	ND
phenanthrene	ug/L			ND	ND
anthracene	ug/L			ND	ND
carbazole	ug/L			ND	ND
fluoranthene	ug/L			ND	ND
pyrene	ug/L			ND	ND
B(A)anthracene	ug/L			ND	ND
chrysene	ug/L			ND	ND
B(b+k)fluoranthene	ug/L			ND	ND
B(a)pyrene	ug/L			ND	ND
indeno(1,2,3,c,d)pyrene+dibenzo(a,h)anthracene	ug/L			ND	ND
benzo(g,h,i)perylene	ug/L			ND	ND

PSC - Phillip Analytical Services

SCL - Syncrude Canada Ltd. Research Laboratory

UW - University of Waterloo Organic Geochemistry Lab

ETL - Envirotest Labs

*SCL - Note samples for nutrients and metals analyzed by SCL were not preserved

Sample ID	Unit	UW OW04-04B		
		PSC & UW	PSC & UW	SCL*
Lab				
Date		16-Sep-04	16-Sep-04	16-Sep-04
Northing	m	53172.26	53172.26	53172.26
Easting	m	54164.9	54164.9	54164.9
Charge Balance	RPD	1.6	1.4	1.4
Conductivity (Lab)	mg/L	2349	2338	1884
Hardness	mg/L	214.1	212.3	
pH (Lab)	pH units	8.03	8.04	7.29
Total Dissolved Solids (Lab)	mg/L	1274	1267	
Total Ammonia-Nitrogen	mg/L	0.07	0.07	0.21
Bicarbonate (Lab)	mg/L	1000	995	954
Bromide	mg/L	<0.5	<0.5	
Carbonate (Lab)	mg/L	1	1	0
Chloride	mg/L	144	143	140
Fluoride	mg/L	0.1	0.1	BDL
Hydioxide	mg/L			
Nitrate-Nitrogen	mg/L	<0.2	<0.2	BDL
Nitrite-Nitrogen	mg/L	<0.2	<0.2	BDL
Ortho Phosphate	mg/L	<1	<1	BDL
Phosphorous	mg/L	<0.05	<0.05	BDL
Total Sulphur	mg/L			42.7
Sulphate	mg/L	137	137	132
Aluminum	mg/L	0.014	0.012	BDL
Antimony	mg/L	<0.0005	<0.0005	BDL
Arsenic	mg/L	<0.002	<0.002	
Barium	mg/L	0.23	0.228	0.133
Beryllium	mg/L	<0.001	<0.001	
Bismuth	mg/L	<0.001	<0.001	
Boron	mg/L	1	0.984	0.957
Cadmium	mg/L	<0.0001	<0.0001	BDL
Calcium	mg/L	65.4	64.9	63.3
Chromium	mg/L	<0.005	<0.005	BDL
Cobalt	mg/L	0.003	0.003	BDL
Copper	mg/L	<0.0005	<0.0005	BDL
Iron	mg/L	0.65	0.62	BDL
Lead	mg/L	<0.0005	<0.0005	BDL
Lithium	mg/L			BDL
Magnesium	mg/L	12.3	12.2	12.3
Manganese	mg/L	2.54	2.51	2.56
Molybdenum	mg/L	0.002	0.002	BDL
Nickle	mg/L	0.015	0.015	BDL
Potassium	mg/L	2	2	0.1
Selenium	mg/L	<0.002	<0.002	BDL
Silicon	mg/L	6.34	6.31	6.72
Silver	mg/L	<0.0001	<0.0001	
Sodium	mg/L	416	417	401
Strontium	mg/L	0.111	0.111	0.132
Tin	mg/L	<0.001	<0.001	ENA
Titanium	mg/L	0.111	0.111	BDL
Thallium	mg/L			
Uranium	mg/L			
Vanadium	mg/L	<0.0005	<0.0005	BDL
Zinc	mg/L	<0.005	<0.005	0.028
Zirconium	mg/L			BDL

PSC - Phillip Analytical Services

SCL - Syncrude Canada Ltd. Research Laboratory

UW - University of Waterloo Organic Geochemistry Lab

ETL - Envirotest Labs

*SCL - Note samples for nutrients and metals analyzed by SCL were not preserved

Sample ID	Unit	UW OW04-04B		
		PSC & UW	PSC & UW	SCL*
Lab				
Date		16-Sep-04	16-Sep-04	16-Sep-04
Northing	m	53172.26	53172.26	53172.26
Easting	m	54164.9	54164.9	54164.9
Total Well Depth	mBTOC	9.18	9.18	9.18
Casing Elevation	mASL			
Dissolved Organic Carbon	mg/L	40.8	44.6	
Methane	ug/L	39.0	50.1	
Total Naphthenic Acids	mg/L	47.8	47.7	50.4
benzene	ug/L			
toluene	ug/L			
ethylbenzene	ug/L			
p+m-xylene	ug/L			
o-xylene	ug/L			
1,3,5-trimethylbenzene	ug/L			
1,2,4-trimethylbenzene	ug/L			
1,2,3-trimethylbenzene	ug/L			
naphthalene	ug/L			
indole+2-methyl naphthalene	ug/L			
1-methyl naphthalene	ug/L			
biphenyl	ug/L			
acenaphthylene	ug/L			
acenaphthene	ug/L			
dibenzofuran	ug/L			
fluorene	ug/L			
phenanthrene	ug/L			
anthracene	ug/L			
carbazole	ug/L			
fluoranthene	ug/L			
pyrene	ug/L			
B(A)anthracene	ug/L			
chrysene	ug/L			
B(b+k)fluoranthene	ug/L			
B(a)pyrene	ug/L			
indeno(1,2,3,c,d)pyrene+dibenzo(a,h)anthracene	ug/L			
benzo(g,h,i)perylene	ug/L			

PSC - Phillip Analytical Services

SCL - Syncrude Canada Ltd. Research Laboratory

UW - University of Waterloo Organic Geochemistry Lab

ETL - Envirotest Labs

*SCL - Note samples for nutrients and metals analyzed by SCL

were not preserved

Sample ID	Unit	UW OW04-04B		
		SCL*	UW	ETL & UW
Lab				
Date		16-Sep-04	23-Oct-04	22-Jun-05
Northing	m	53172.26	53172.26	
Easting	m	54164.9	54164.9	
Charge Balance	RPD	2.9		-1.0
Conductivity (Lab)	mg/L	1912		2080
Hardness	mg/L			209
pH (Lab)	pH units	7.32		8.0
Total Dissolved Solids (Lab)	mg/L			1310
Total Ammonia-Nitrogen	mg/L	0.21		<0.05
Bicarbonate (Lab)	mg/L	958		1010
Bromide	mg/L			
Carbonate (Lab)	mg/L	0		<5
Chloride	mg/L	140		140
Fluoride	mg/L	BDL		
Hydioxide	mg/L			<5
Nitrate-Nitrogen	mg/L	BDL		<0.1
Nitrite-Nitrogen	mg/L	BDL		<0.05
Ortho Phosphate	mg/L	BDL		
Phosphorous	mg/L	BDL		
Total Sulphur	mg/L	41.4		
Sulphate	mg/L	134		144
Aluminum	mg/L	BDL		<0.01
Antimony	mg/L	BDL		0.0009
Arsenic	mg/L			0.0004
Barium	mg/L	0.129		0.269
Beryllium	mg/L			<0.0005
Bismuth	mg/L			<0.00005
Boron	mg/L	0.929		1.13
Cadmium	mg/L	BDL		<0.0001
Calcium	mg/L	61.2		59.5
Chromium	mg/L	BDL		0.0006
Cobalt	mg/L	BDL		0.0027
Copper	mg/L	BDL		0.0007
Iron	mg/L	0.018		0.155
Lead	mg/L	BDL		<0.0001
Lithium	mg/L	BDL		
Magnesium	mg/L	11.9		14.7
Manganese	mg/L	2.5		2.51
Molybdenum	mg/L	BDL		0.0005
Nickle	mg/L	BDL		0.0145
Potassium	mg/L	0.1		2.6
Selenium	mg/L	BDL		0.0005
Silicon	mg/L	6.4		
Silver	mg/L			<0.0002
Sodium	mg/L	391		451
Strontium	mg/L	0.130		0.0942
Tin	mg/L	ENA		<0.0002
Titanium	mg/L	BDL		0.0012
Thallium	mg/L			0.00006
Uranium	mg/L			0.0015
Vanadium	mg/L	BDL		0.0010
Zinc	mg/L	0.029		0.015
Zirconium	mg/L	BDL		

PSC - Phillip Analytical Services

SCL - Syncrude Canada Ltd. Research Laboratory

UW - University of Waterloo Organic Geochemistry Lab

ETL - Envirotest Labs

*SCL - Note samples for nutrients and metals analyzed by SCL were not preserved

Sample ID	Unit	UW OW04-04B		
		SCL*	UW	ETL & UW
Lab				
Date		16-Sep-04	23-Oct-04	22-Jun-05
Northing	m	53172.26	53172.26	
Easting	m	54164.9	54164.9	
Total Well Depth	mBTOC	9.18	9.18	
Casing Elevation	mASL			
Dissolved Organic Carbon	mg/L			
Methane	ug/L			15.9
Total Naphthenic Acids	mg/L	49.7		49.3
benzene	ug/L		ND	ND
toluene	ug/L		0.40	ND
ethylbenzene	ug/L		ND	ND
p+m-xylene	ug/L		ND	ND
o-xylene	ug/L		ND	ND
1,3,5-trimethylbenzene	ug/L		ND	ND
1,2,4-trimethylbenzene	ug/L		ND	ND
1,2,3-trimethylbenzene	ug/L		ND	ND
naphthalene	ug/L		ND	5.07
indole+2-methyl naphthalene	ug/L		ND	8.04
1-methyl naphthalene	ug/L		6.15	6.04
biphenyl	ug/L		ND	ND
acenaphthylene	ug/L		5.90	ND
acenaphthene	ug/L		ND	ND
dibenzofuran	ug/L		ND	ND
fluorene	ug/L		ND	ND
phenanthrene	ug/L		ND	ND
anthracene	ug/L		ND	ND
carbazole	ug/L		ND	ND
fluoranthene	ug/L		ND	ND
pyrene	ug/L		ND	ND
B(A)anthracene	ug/L		ND	ND
chrysene	ug/L		ND	ND
B(b+k)fluoranthene	ug/L		ND	ND
B(a)pyrene	ug/L		ND	ND
indeno(1,2,3,c,d)pyrene+dibenzo(a,h)anthracene	ug/L		ND	ND
benzo(g,h,i)perylene	ug/L		ND	ND

PSC - Phillip Analytical Services

SCL - Syncrude Canada Ltd. Research Laboratory

UW - University of Waterloo Organic Geochemistry Lab

ETL - Envirotest Labs

*SCL - Note samples for nutrients and metals analyzed by SCL were not preserved

Sample ID	Unit	UW OW04-04C		
		PSC & UW	SCL*	UW
Lab				
Date		16-Sep-04	16-Sep-04	23-Oct-04
Northing	m	53172.26	53172.26	53172.26
Easting	m	54164.9	54164.9	54164.9
Charge Balance	RPD	-5.6	2.1	
Conductivity (Lab)	mg/L	1860	1470	
Hardness	mg/L	254.4		
pH (Lab)	pH units	8.34	8.07	
Total Dissolved Solids (Lab)	mg/L	985		
Total Ammonia-Nitrogen	mg/L	0.19	0.15	
Bicarbonate (Lab)	mg/L	811	735	
Bromide	mg/L	<0.5		
Carbonate (Lab)	mg/L	1	0	
Chloride	mg/L	108	120	
Fluoride	mg/L	0.1	BDL	
Hydioxide	mg/L			
Nitrate-Nitrogen	mg/L	<0.2	BDL	
Nitrite-Nitrogen	mg/L	<0.2	BDL	
Ortho Phosphate	mg/L	<1	BDL	
Phosphorous	mg/L	<0.05	BDL	
Total Sulphur	mg/L		18.5	
Sulphate	mg/L	53	58	
Aluminum	mg/L	<0.005	BDL	
Antimony	mg/L	<0.0005	BDL	
Arsenic	mg/L	<0.002		
Barium	mg/L	0.256	0.045	
Beryllium	mg/L	<0.001		
Bismuth	mg/L	<0.001		
Boron	mg/L	0.475	0.439	
Cadmium	mg/L	<0.0001	BDL	
Calcium	mg/L	74.7	30.5	
Chromium	mg/L	<0.005	BDL	
Cobalt	mg/L	0.0005	BDL	
Copper	mg/L	<0.0005	BDL	
Iron	mg/L	1.06	BDL	
Lead	mg/L	<0.0005	BDL	
Lithium	mg/L		BDL	
Magnesium	mg/L	16.4	15.2	
Manganese	mg/L	0.201	0.007	
Molybdenum	mg/L	0.007	BDL	
Nickle	mg/L	0.004	BDL	
Potassium	mg/L	3	0.1	
Selenium	mg/L	<0.002	BDL	
Silicon	mg/L	5.58	6.03	
Silver	mg/L	<0.0001		
Sodium	mg/L	329	303	
Strontium	mg/L	0.176	0.153	
Tin	mg/L	0.002	ENA	
Titanium	mg/L	0.176	BDL	
Thallium	mg/L			
Uranium	mg/L			
Vanadium	mg/L	0.0007	BDL	
Zinc	mg/L	0.011	0.027	
Zirconium	mg/L		BDL	

PSC - Phillip Analytical Services

SCL - Syncrude Canada Ltd. Research Laboratory

UW - University of Waterloo Organic Geochemistry Lab

ETL - Envirotest Labs

*SCL - Note samples for nutrients and metals analyzed by SCL were not preserved

Sample ID	Unit	UW OW04-04C		
		PSC & UW	SCL*	UW
Lab				
Date		16-Sep-04	16-Sep-04	23-Oct-04
Northing	m	53172.26	53172.26	53172.26
Easting	m	54164.9	54164.9	54164.9
Total Well Depth	mBTOC	10.40	10.40	10.40
Casing Elevation	mASL			
Dissolved Organic Carbon	mg/L	37.5		
Methane	ug/L	43.6		
Total Naphthenic Acids	mg/L	33.8	39.9	
benzene	ug/L			ND
toluene	ug/L			0.40
ethylbenzene	ug/L			ND
p+m-xylene	ug/L			ND
o-xylene	ug/L			ND
1,3,5-trimethylbenzene	ug/L			ND
1,2,4-trimethylbenzene	ug/L			ND
1,2,3-trimethylbenzene	ug/L			ND
naphthalene	ug/L			ND
indole+2-methyl naphthalene	ug/L			3.02
1-methyl naphthalene	ug/L			ND
biphenyl	ug/L			ND
acenaphthylene	ug/L			ND
acenaphthene	ug/L			ND
dibenzofuran	ug/L			ND
fluorene	ug/L			ND
phenanthrene	ug/L			ND
anthracene	ug/L			ND
carbazole	ug/L			1.35
fluoranthene	ug/L			ND
pyrene	ug/L			ND
B(A)anthracene	ug/L			ND
chrysene	ug/L			ND
B(b+k)fluoranthene	ug/L			ND
B(a)pyrene	ug/L			ND
indeno(1,2,3,c,d)pyrene+dibenzo(a,h)anthracene	ug/L			ND
benzo(g,h,i)perylene	ug/L			ND

PSC - Phillip Analytical Services

SCL - Syncrude Canada Ltd. Research Laboratory

UW - University of Waterloo Organic Geochemistry Lab

ETL - Envirotest Labs

*SCL - Note samples for nutrients and metals analyzed by SCL were not preserved

Sample ID	Unit	UW OW04-05A		
Lab				ETL & UW
Date		15-Sep-04	22-Oct-04	28-Jun-05
Northing	m	53230.42	53230.42	53230.42
Easting	m	54256.87	54256.87	54256.87
Charge Balance	RPD			3.6
Conductivity (Lab)	mg/L			530
Hardness	mg/L			199
pH (Lab)	pH units			8.1
Total Dissolved Solids (Lab)	mg/L			297
Total Ammonia-Nitrogen	mg/L			<0.05
Bicarbonate (Lab)	mg/L			189
Bromide	mg/L			
Carbonate (Lab)	mg/L			<5
Chloride	mg/L			56
Fluoride	mg/L			
Hydioxide	mg/L			<5
Nitrate-Nitrogen	mg/L			1.1
Nitrite-Nitrogen	mg/L			<0.05
Ortho Phosphate	mg/L			
Phosphorous	mg/L			
Total Sulphur	mg/L			
Sulphate	mg/L			35.1
Aluminum	mg/L			<0.01
Antimony	mg/L			0.0006
Arsenic	mg/L			<0.0004
Barium	mg/L			0.0631
Beryllium	mg/L			<0.0005
Bismuth	mg/L			<0.00005
Boron	mg/L			0.008
Cadmium	mg/L			<0.0001
Calcium	mg/L			59.2
Chromium	mg/L			0.0005
Cobalt	mg/L			<0.0001
Copper	mg/L			<0.0006
Iron	mg/L			<0.005
Lead	mg/L			<0.0001
Lithium	mg/L			
Magnesium	mg/L			10.5
Manganese	mg/L			0.011
Molybdenum	mg/L			0.0006
Nickle	mg/L			<0.0001
Potassium	mg/L			0.7
Selenium	mg/L			<0.0004
Silicon	mg/L			
Silver	mg/L			<0.0002
Sodium	mg/L			27.8
Strontium	mg/L			0.0548
Tin	mg/L			0.0004
Titanium	mg/L			<0.0003
Thallium	mg/L			<0.00005
Uranium	mg/L			0.0002
Vanadium	mg/L			<0.0001
Zinc	mg/L			0.013
Zirconium	mg/L			

PSC - Phillip Analytical Services

SCL - Syncrude Canada Ltd. Research Laboratory

UW - University of Waterloo Organic Geochemistry Lab

ETL - Envirotest Labs

*SCL - Note samples for nutrients and metals analyzed by SCL were not preserved

Sample ID	Unit	UW OW04-05A		
Lab				ETL & UW
Date		15-Sep-04	22-Oct-04	28-Jun-05
Northing	m	53230.42	53230.42	53230.42
Easting	m	54256.87	54256.87	54256.87
Total Well Depth	mBTOC	6.28	6.28	
Casing Elevation	mASL			
Dissolved Organic Carbon	mg/L			
Methane	ug/L			0.4
Total Naphthenic Acids	mg/L			<1.0
benzene	ug/L			ND
toluene	ug/L			ND
ethylbenzene	ug/L			ND
p+m-xylene	ug/L			ND
o-xylene	ug/L			ND
1,3,5-trimethylbenzene	ug/L			ND
1,2,4-trimethylbenzene	ug/L			ND
1,2,3-trimethylbenzene	ug/L			ND
naphthalene	ug/L			ND
indole+2-methyl naphthalene	ug/L			ND
1-methyl naphthalene	ug/L			ND
biphenyl	ug/L			ND
acenaphthylene	ug/L			ND
acenaphthene	ug/L			ND
dibenzofuran	ug/L			ND
fluorene	ug/L			ND
phenanthrene	ug/L			ND
anthracene	ug/L			ND
carbazole	ug/L			ND
fluoranthene	ug/L			ND
pyrene	ug/L			ND
B(A)anthracene	ug/L			ND
chrysene	ug/L			ND
B(b+k)fluoranthene	ug/L			ND
B(a)pyrene	ug/L			ND
indeno(1,2,3,c,d)pyrene+dibenzo(a,h)anthracene	ug/L			ND
benzo(g,h,i)perylene	ug/L			ND

PSC - Phillip Analytical Services

SCL - Syncrude Canada Ltd. Research Laboratory

UW - University of Waterloo Organic Geochemistry Lab

ETL - Envirotest Labs

*SCL - Note samples for nutrients and metals analyzed by SCL were not preserved

Sample ID	Unit	UW OW04-05B			
		PSC & UW	SCL*	UW	ETL & UW
Lab					
Date		15-Sep-04	15-Sep-04	22-Oct-04	28-Jun-05
Northing	m	53230.42	53230.42	53230.42	
Easting	m	54256.87	54256.87	54256.87	
Charge Balance	RPD	1.2	3.4		3.1
Conductivity (Lab)	mg/L	1234	968		833
Hardness	mg/L	370.6			241
pH (Lab)	pH units	8.2	7.54		8.1
Total Dissolved Solids (Lab)	mg/L	622			458
Total Ammonia-Nitrogen	mg/L	0.08	BDL		<0.05
Bicarbonate (Lab)	mg/L	359	365		251
Bromide	mg/L	<0.5			
Carbonate (Lab)	mg/L	1	0		<5
Chloride	mg/L	114	110		97
Fluoride	mg/L	0.1	BDL		
Hydioxide	mg/L				<5
Nitrate-Nitrogen	mg/L	1	4.6		1.7
Nitrite-Nitrogen	mg/L	<0.2	BDL		<0.05
Ortho Phosphate	mg/L	<1	BDL		
Phosphorous	mg/L	<0.05	BDL		
Total Sulphur	mg/L		31.8		
Sulphate	mg/L	109	107		70.3
Aluminum	mg/L	<0.005	BDL		<0.01
Antimony	mg/L	<0.0005	BDL		0.0007
Arsenic	mg/L	<0.002			<0.0004
Barium	mg/L	0.124	0.028		0.0897
Beryllium	mg/L	<0.001			<0.0005
Bismuth	mg/L	<0.001			<0.00005
Boron	mg/L	0.011	0.01		0.008
Cadmium	mg/L	<0.0001	BDL		<0.0001
Calcium	mg/L	112	103		77.5
Chromium	mg/L	<0.005	BDL		0.0005
Cobalt	mg/L	0.0007	BDL		0.0003
Copper	mg/L	<0.0005	BDL		0.0008
Iron	mg/L	<0.03	BDL		<0.005
Lead	mg/L	<0.0005	BDL		<0.0001
Lithium	mg/L		BDL		
Magnesium	mg/L	21.6	20.3		14.8
Manganese	mg/L	0.083	0.085		0.028
Molybdenum	mg/L	0.004	BDL		0.0011
Nickle	mg/L	<0.001	BDL		<0.0001
Potassium	mg/L	1.7	0.1		0.9
Selenium	mg/L	<0.002	BDL		<0.0004
Silicon	mg/L	3.02	3.3		
Silver	mg/L	<0.0001			<0.0002
Sodium	mg/L	85	87.8		62.6
Strontium	mg/L	0.100	0.120		0.0632
Tin	mg/L	<0.001	ENA		<0.0002
Titanium	mg/L	<0.005	BDL		<0.0003
Thallium	mg/L				<0.00005
Uranium	mg/L				0.0005
Vanadium	mg/L	<0.0005	BDL		0.0001
Zinc	mg/L	<0.005	0.028		0.009
Zirconium	mg/L		BDL		

PSC - Phillip Analytical Services

SCL - Syncrude Canada Ltd. Research Laboratory

UW - University of Waterloo Organic Geochemistry Lab

ETL - Envirotest Labs

*SCL - Note samples for nutrients and metals analyzed by SCL were not preserved

Sample ID	Unit	UW OW04-05B			
		PSC & UW	SCL*	UW	ETL & UW
Lab					
Date		15-Sep-04	15-Sep-04	22-Oct-04	28-Jun-05
Northing	m	53230.42	53230.42	53230.42	
Easting	m	54256.87	54256.87	54256.87	
Total Well Depth	mBTC	8.09	8.09	8.09	
Casing Elevation	mASL				
Dissolved Organic Carbon	mg/L	8.1			
Methane	ug/L	4.4			0.2
Total Naphthenic Acids	mg/L	1.8	1.2		<1.0
benzene	ug/L			ND	ND
toluene	ug/L			ND	ND
ethylbenzene	ug/L			ND	ND
p+m-xylene	ug/L			ND	ND
o-xylene	ug/L			ND	ND
1,3,5-trimethylbenzene	ug/L			ND	ND
1,2,4-trimethylbenzene	ug/L			ND	ND
1,2,3-trimethylbenzene	ug/L			ND	ND
naphthalene	ug/L			ND	ND
indole+2-methyl naphthalene	ug/L			ND	ND
1-methyl naphthalene	ug/L			ND	ND
biphenyl	ug/L			ND	ND
acenaphthylene	ug/L			ND	ND
acenaphthene	ug/L			ND	ND
dibenzofuran	ug/L			ND	ND
fluorene	ug/L			ND	ND
phenanthrene	ug/L			ND	ND
anthracene	ug/L			ND	ND
carbazole	ug/L			ND	ND
fluoranthene	ug/L			ND	ND
pyrene	ug/L			ND	ND
B(A)anthracene	ug/L			ND	ND
chrysene	ug/L			ND	ND
B(b+k)fluoranthene	ug/L			ND	ND
B(a)pyrene	ug/L			ND	ND
indeno(1,2,3,c,d)pyrene+dibenzo(a,h)anthracene	ug/L			ND	ND
benzo(g,h,i)perylene	ug/L			ND	ND

PSC - Phillip Analytical Services

SCL - Syncrude Canada Ltd. Research Laboratory

UW - University of Waterloo Organic Geochemistry Lab

ETL - Envirotest Labs

*SCL - Note samples for nutrients and metals analyzed by SCL were not preserved

Sample ID	Unit	UW OW04-05C			
		PSC & UW	SCL*	UW	ETL & UW
Lab					
Date		15-Sep-04	15-Sep-04	15-Sep-04	28-Jun-05
Northing	m	53230.42	53230.42	53230.42	
Easting	m	54256.87	54256.87	54256.87	
Charge Balance	RPD	-2.5	2.8		5.1
Conductivity (Lab)	mg/L	1056	1050		1090
Hardness	mg/L	360.9			372
pH (Lab)	pH units	7.88	7.58		8.1
Total Dissolved Solids (Lab)	mg/L	519			625
Total Ammonia-Nitrogen	mg/L	0.13	BDL		<0.05
Bicarbonate (Lab)	mg/L	256	302		345
Bromide	mg/L	<0.5			
Carbonate (Lab)	mg/L	1	0		<5
Chloride	mg/L	109	140		124
Fluoride	mg/L	<0.1	BDL		
Hydroxide	mg/L				<5
Nitrate-Nitrogen	mg/L	0.7	4.7		1.2
Nitrite-Nitrogen	mg/L	<0.2	BDL		<0.05
Ortho Phosphate	mg/L	<1	BDL		
Phosphorous	mg/L	<0.05	BDL		
Total Sulphur	mg/L		37.1		
Sulphate	mg/L	94	126		103
Aluminum	mg/L	0.006	BDL		<0.01
Antimony	mg/L	<0.0005	BDL		0.0006
Arsenic	mg/L	<0.002			<0.0004
Barium	mg/L	0.142	0.05		0.132
Beryllium	mg/L	<0.001			<0.0005
Bismuth	mg/L	<0.001			<0.00005
Boron	mg/L	<0.005	0.01		0.008
Cadmium	mg/L	<0.0001	BDL		<0.0001
Calcium	mg/L	107	127		107
Chromium	mg/L	<0.005	BDL		0.0009
Cobalt	mg/L	0.0019	BDL		0.0001
Copper	mg/L	<0.0005	BDL		<0.0006
Iron	mg/L	<0.03	BDL		<0.005
Lead	mg/L	<0.0005	BDL		<0.0001
Lithium	mg/L		BDL		
Magnesium	mg/L	22.5	26.8		22.1
Manganese	mg/L	0.337	0.334		<0.001
Molybdenum	mg/L	0.006	BDL		0.0011
Nickle	mg/L	0.003	BDL		<0.0001
Potassium	mg/L	2.4	0.1		0.8
Selenium	mg/L	<0.002	BDL		<0.0004
Silicon	mg/L	3.2	3.75		
Silver	mg/L	<0.0001			<0.0002
Sodium	mg/L	56	55		69.9
Strontium	mg/L	0.124	0.148		0.0902
Tin	mg/L	<0.001	ENA		0.0005
Titanium	mg/L	<0.005	BDL		0.0004
Thallium	mg/L				<0.00005
Uranium	mg/L				0.0007
Vanadium	mg/L	<0.0005	BDL		0.0001
Zinc	mg/L	<0.005	0.027		0.007
Zirconium	mg/L		BDL		

PSC - Phillip Analytical Services

SCL - Syncrude Canada Ltd. Research Laboratory

UW - University of Waterloo Organic Geochemistry Lab

ETL - Envirotest Labs

*SCL - Note samples for nutrients and metals analyzed by SCL were not preserved

Sample ID	Unit	UW OW04-05C			
		PSC & UW	SCL*	UW	ETL & UW
Lab					
Date		15-Sep-04	15-Sep-04	15-Sep-04	28-Jun-05
Northing	m	53230.42	53230.42	53230.42	
Easting	m	54256.87	54256.87	54256.87	
Total Well Depth	mBTC	9.10	9.10	9.10	
Casing Elevation	mASL				
Dissolved Organic Carbon	mg/L	6.4			
Methane	ug/L	100.6			0.9
Total Naphthenic Acids	mg/L	1.8	1.3		<1.0
benzene	ug/L			ND	ND
toluene	ug/L			ND	ND
ethylbenzene	ug/L			ND	ND
p+m-xylene	ug/L			ND	ND
o-xylene	ug/L			ND	ND
1,3,5-trimethylbenzene	ug/L			ND	ND
1,2,4-trimethylbenzene	ug/L			ND	ND
1,2,3-trimethylbenzene	ug/L			ND	ND
naphthalene	ug/L			ND	ND
indole+2-methyl naphthalene	ug/L			ND	ND
1-methyl naphthalene	ug/L			ND	ND
biphenyl	ug/L			ND	0.99
acenaphthylene	ug/L			ND	ND
acenaphthene	ug/L			ND	ND
dibenzofuran	ug/L			ND	ND
fluorene	ug/L			ND	ND
phenanthrene	ug/L			ND	ND
anthracene	ug/L			ND	ND
carbazole	ug/L			ND	ND
fluoranthene	ug/L			ND	ND
pyrene	ug/L			ND	ND
B(A)anthracene	ug/L			ND	ND
chrysene	ug/L			ND	ND
B(b+k)fluoranthene	ug/L			ND	ND
B(a)pyrene	ug/L			ND	ND
indeno(1,2,3,c,d)pyrene+dibenzo(a,h)anthracene	ug/L			ND	ND
benzo(g,h,i)perylene	ug/L			ND	ND

PSC - Phillip Analytical Services

SCL - Syncrude Canada Ltd. Research Laboratory

UW - University of Waterloo Organic Geochemistry Lab

ETL - Envirotest Labs

*SCL - Note samples for nutrients and metals analyzed by SCL were not preserved

Sample ID	Unit	OW01-04B
Lab		(sampled by Syncrude)
Date		5-Jul-04
Northing	m	
Easting	m	
Charge Balance	RPD	
Conductivity (Lab)	mg/L	497
Hardness	mg/L	
pH (Lab)	pH units	8.0
Total Dissolved Solids (Lab)	mg/L	300
Total Ammonia-Nitrogen	mg/L	
Bicarbonate (Lab)	mg/L	292
Bromide	mg/L	
Carbonate (Lab)	mg/L	
Chloride	mg/L	4
Fluoride	mg/L	
Hydroxide	mg/L	
Nitrate-Nitrogen	mg/L	
Nitrite-Nitrogen	mg/L	
Ortho Phosphate	mg/L	
Phosphorous	mg/L	
Total Sulphur	mg/L	
Sulphate	mg/L	25.3
Aluminum	mg/L	
Antimony	mg/L	
Arsenic	mg/L	
Barium	mg/L	
Beryllium	mg/L	
Bismuth	mg/L	
Boron	mg/L	
Cadmium	mg/L	
Calcium	mg/L	75.6
Chromium	mg/L	
Cobalt	mg/L	
Copper	mg/L	
Iron	mg/L	0.06
Lead	mg/L	
Lithium	mg/L	
Magnesium	mg/L	17
Manganese	mg/L	0.65
Molybdenum	mg/L	
Nickle	mg/L	
Potassium	mg/L	1.4
Selenium	mg/L	
Silicon	mg/L	
Silver	mg/L	
Sodium	mg/L	8
Strontium	mg/L	
Tin	mg/L	
Titanium	mg/L	
Thallium	mg/L	
Uranium	mg/L	
Vanadium	mg/L	
Zinc	mg/L	
Zirconium	mg/L	

PSC - Phillip Analytical Services

SCL - Syncrude Canada Ltd. Research Laboratory

UW - University of Waterloo Organic Geochemistry Lab

ETL - Envirotest Labs

*SCL - Note samples for nutrients and metals analyzed by SCL were not preserved

Sample ID	Unit	OW01-04B
Lab		
Date		
Northing	m	
Easting	m	
Total Well Depth	mBTOC	
Casing Elevation	mASL	
Dissolved Organic Carbon	mg/L	
Methane	ug/L	
Total Naphthenic Acids	mg/L	
benzene	ug/L	
toluene	ug/L	
ethylbenzene	ug/L	
p+m-xylene	ug/L	
o-xylene	ug/L	
1,3,5-trimethylbenzene	ug/L	
1,2,4-trimethylbenzene	ug/L	
1,2,3-trimethylbenzene	ug/L	
naphthalene	ug/L	
indole+2-methyl naphthalene	ug/L	
1-methyl naphthalene	ug/L	
biphenyl	ug/L	
acenaphthylene	ug/L	
acenaphthene	ug/L	
dibenzofuran	ug/L	
fluorene	ug/L	
phenanthrene	ug/L	
anthracene	ug/L	
carbazole	ug/L	
fluoranthene	ug/L	
pyrene	ug/L	
B(A)anthracene	ug/L	
chrysene	ug/L	
B(b+k)fluoranthene	ug/L	
B(a)pyrene	ug/L	
indeno(1,2,3,c,d)pyrene+dibenzo(a,h)anthracene	ug/L	
benzo(g,h,i)perylene	ug/L	

PSC - Phillip Analytical Services

SCL - Syncrude Canada Ltd. Research Laboratory

UW - University of Waterloo Organic Geochemistry Lab

ETL - Envirotest Labs

*SCL - Note samples for nutrients and metals analyzed by SCL were not preserved

Sample ID	Unit	UW OW04-06B			
		PSC & UW	SCL*	UW	ETL & UW
Lab					
Date		15-Sep-04	15-Sep-04	22-Oct-04	24-Jun-05
Northing	m	53154.13	53154.13	53154.13	
Easting	m	54573.32	54573.32	54573.32	
Charge Balance	RPD	1.7	2.2		1.7
Conductivity (Lab)	mg/L	606.1	489		510
Hardness	mg/L	211.7			254
pH (Lab)	pH units	8.08	7.69		8.0
Total Dissolved Solids (Lab)	mg/L	321			284
Total Ammonia-Nitrogen	mg/L	0.17	BDL		<0.05
Bicarbonate (Lab)	mg/L	321	316		303
Bromide	mg/L	<0.5			
Carbonate (Lab)	mg/L	1	0		<5
Chloride	mg/L	5	4.3		3
Fluoride	mg/L	0.1	BDL		
Hydioxide	mg/L				<5
Nitrate-Nitrogen	mg/L	<0.2	BDL		<0.1
Nitrite-Nitrogen	mg/L	<0.2	BDL		<0.05
Ortho Phosphate	mg/L	<1	BDL		
Phosphorous	mg/L	<0.05	BDL		
Total Sulphur	mg/L		9.7		
Sulphate	mg/L	40	33		31.5
Aluminum	mg/L	0.023	BDL		<0.01
Antimony	mg/L	<0.0005	BDL		0.0006
Arsenic	mg/L	<0.002			<0.0004
Barium	mg/L	0.064	BDL		0.0756
Beryllium	mg/L	<0.001			<0.0005
Bismuth	mg/L	<0.001			0.00050
Boron	mg/L	0.028	BDL		0.020
Cadmium	mg/L	<0.0001	BDL		<0.0001
Calcium	mg/L	61.2	64.7		75.4
Chromium	mg/L	<0.005	BDL		0.0024
Cobalt	mg/L	0.0007	BDL		0.0016
Copper	mg/L	0.0006	BDL		<0.0006
Iron	mg/L	0.08	BDL		0.021
Lead	mg/L	<0.0005	BDL		<0.0001
Lithium	mg/L		BDL		
Magnesium	mg/L	14.3	15.3		17.3
Manganese	mg/L	0.038	0.01		0.050
Molybdenum	mg/L	0.008	BDL		0.0015
Nickle	mg/L	<0.001	BDL		<0.0001
Potassium	mg/L	2.3	0.1		1.4
Selenium	mg/L	<0.002	BDL		<0.0004
Silicon	mg/L	3.74	4.32		
Silver	mg/L	<0.0001			<0.0002
Sodium	mg/L	39	28		6.6
Strontium	mg/L	0.139	0.116		0.144
Tin	mg/L	<0.001	EDA		0.0003
Titanium	mg/L	<0.005	BDL		0.0007
Thallium	mg/L				<0.00005
Uranium	mg/L				0.0005
Vanadium	mg/L	<0.0005	BDL		<0.0001
Zinc	mg/L	<0.005	0.027		0.006
Zirconium	mg/L		BDL		

PSC - Phillip Analytical Services

SCL - Syncrude Canada Ltd. Research Laboratory

UW - University of Waterloo Organic Geochemistry Lab

ETL - Envirotest Labs

*SCL - Note samples for nutrients and metals analyzed by SCL were not preserved

Sample ID	Unit	UW OW04-06B			
		PSC & UW	SCL*	UW	ETL & UW
Lab					
Date		15-Sep-04	15-Sep-04	22-Oct-04	24-Jun-05
Northing	m	53154.13	53154.13	53154.13	
Easting	m	54573.32	54573.32	54573.32	
Total Well Depth	mBTOC	5.35	5.35	5.35	
Casing Elevation	mASL				
Dissolved Organic Carbon	mg/L	5.3			
Methane	ug/L	0.8			0.2
Total Naphthenic Acids	mg/L	<0.5	0.7		<1.0
benzene	ug/L				ND
toluene	ug/L				ND
ethylbenzene	ug/L				ND
p+m-xylene	ug/L				ND
o-xylene	ug/L				ND
1,3,5-trimethylbenzene	ug/L				ND
1,2,4-trimethylbenzene	ug/L				ND
1,2,3-trimethylbenzene	ug/L				ND
naphthalene	ug/L				ND
indole+2-methyl naphthalene	ug/L				ND
1-methyl naphthalene	ug/L				ND
biphenyl	ug/L				0.66
acenaphthylene	ug/L				ND
acenaphthene	ug/L				ND
dibenzofuran	ug/L				ND
fluorene	ug/L				ND
phenanthrene	ug/L				ND
anthracene	ug/L				ND
carbazole	ug/L				ND
fluoranthene	ug/L				ND
pyrene	ug/L				ND
B(A)anthracene	ug/L				ND
chrysene	ug/L				ND
B(b+k)fluoranthene	ug/L				ND
B(a)pyrene	ug/L				ND
indeno(1,2,3,c,d)pyrene+dibenzo(a,h)anthracene	ug/L				ND
benzo(g,h,i)perylene	ug/L				ND

PSC - Phillip Analytical Services

SCL - Syncrude Canada Ltd. Research Laboratory

UW - University of Waterloo Organic Geochemistry Lab

ETL - Envirotest Labs

*SCL - Note samples for nutrients and metals analyzed by SCL were not preserved

Sample ID	Unit	UW OW04-07			
		PSC & UW	SCL*	UW	ETL & UW
Lab					
Date		17-Sep-04	17-Sep-04	23-Oct-04	23-Jun-05
Northing	m	55123.1	55123.1	55123.1	
Easting	m	53820.86	53820.86	53820.86	
Charge Balance	RPD	5.6	0.5		9.4
Conductivity (Lab)	mg/L	2750	2190		2210
Hardness	mg/L	167.5			146
pH (Lab)	pH units	8.06	7.59		8.1
Total Dissolved Solids (Lab)	mg/L	1467			1330
Total Ammonia-Nitrogen	mg/L	0.04	0.2		1.42
Bicarbonate (Lab)	mg/L	1000	985		877
Bromide	mg/L	<0.5			
Carbonate (Lab)	mg/L	1	0		<5
Chloride	mg/L	283	250		225
Fluoride	mg/L	1.5	0.76		
Hydioxide	mg/L				<5
Nitrate-Nitrogen	mg/L	<0.2	BDL		<0.1
Nitrite-Nitrogen	mg/L	<0.2	BDL		<0.05
Ortho Phosphate	mg/L	<1	BDL		
Phosphorous	mg/L	<0.05	BDL		
Total Sulphur	mg/L		39.3		
Sulphate	mg/L	144	137		137
Aluminum	mg/L	<0.005	BDL		<0.01
Antimony	mg/L	<0.0005	BDL		0.0007
Arsenic	mg/L	0.002			0.0019
Barium	mg/L	0.097	BDL		0.108
Beryllium	mg/L	<0.001			<0.0005
Bismuth	mg/L	<0.001			<0.00005
Boron	mg/L	1.22	1.07		1.26
Cadmium	mg/L	0.0002	BDL		<0.0001
Calcium	mg/L	46.5	39.4		39.4
Chromium	mg/L	<0.005	BDL		0.0008
Cobalt	mg/L	0.0008	BDL		0.0014
Copper	mg/L	<0.0005	BDL		<0.0006
Iron	mg/L	1.96	0.236		2.34
Lead	mg/L	<0.0005	BDL		<0.0001
Lithium	mg/L		BDL		
Magnesium	mg/L	12.5	11.1		10.5
Manganese	mg/L	0.815	0.72		0.601
Molybdenum	mg/L	0.015	BDL		0.013
Nickle	mg/L	0.005	BDL		0.0044
Potassium	mg/L	4.8	0.1		5.3
Selenium	mg/L	<0.002	BDL		<0.0004
Silicon	mg/L	4.92	4.54		
Silver	mg/L	<0.0001			<0.0002
Sodium	mg/L	482	526		376
Strontium	mg/L	0.137	0.147		0.123
Tin	mg/L	<0.001	ENA		0.0002
Titanium	mg/L	<0.005	BDL		0.0009
Thallium	mg/L				<0.00005
Uranium	mg/L				0.0025
Vanadium	mg/L	<0.0005	BDL		0.0005
Zinc	mg/L	0.035	0.028		0.004
Zirconium	mg/L		BDL		

PSC - Phillip Analytical Services

SCL - Syncrude Canada Ltd. Research Laboratory

UW - University of Waterloo Organic Geochemistry Lab

ETL - Envirotest Labs

*SCL - Note samples for nutrients and metals analyzed by SCL were not preserved

Sample ID	Unit	UW OW04-07			
		PSC & UW	SCL*	UW	ETL & UW
Lab		17-Sep-04	17-Sep-04	23-Oct-04	23-Jun-05
Date		55123.1	55123.1	55123.1	
Northing	m	53820.86	53820.86	53820.86	
Easting	m	7.58	7.58	7.58	
Total Well Depth	mBTC				
Casing Elevation	mASL				
Dissolved Organic Carbon	mg/L	47			
Methane	ug/L	2.1			2.5
Total Naphthenic Acids	mg/L	51.5	51.5		43
benzene	ug/L			ND	ND
toluene	ug/L			ND	ND
ethylbenzene	ug/L			ND	ND
p+m-xylene	ug/L			ND	ND
o-xylene	ug/L			ND	ND
1,3,5-trimethylbenzene	ug/L			ND	ND
1,2,4-trimethylbenzene	ug/L			ND	ND
1,2,3-trimethylbenzene	ug/L			ND	ND
naphthalene	ug/L			ND	ND
indole+2-methyl naphthalene	ug/L			ND	3.01
1-methyl naphthalene	ug/L			ND	2.31
biphenyl	ug/L			ND	1.34
acenaphthylene	ug/L			2.17	ND
acenaphthene	ug/L			ND	ND
dibenzofuran	ug/L			ND	ND
fluorene	ug/L			ND	ND
phenanthrene	ug/L			ND	ND
anthracene	ug/L			ND	ND
carbazole	ug/L			ND	ND
fluoranthene	ug/L			ND	ND
pyrene	ug/L			ND	ND
B(A)anthracene	ug/L			ND	ND
chrysene	ug/L			ND	ND
B(b+k)fluoranthene	ug/L			ND	ND
B(a)pyrene	ug/L			ND	ND
indeno(1,2,3,c,d)pyrene+dibenzo(a,h)anthracene	ug/L			ND	ND
benzo(g,h,i)perylene	ug/L			ND	ND

PSC - Phillip Analytical Services

SCL - Syncrude Canada Ltd. Research Laboratory

UW - University of Waterloo Organic Geochemistry Lab

ETL - Envirotest Labs

*SCL - Note samples for nutrients and metals analyzed by SCL were not preserved

Sample ID	Unit	Blank	Blank
Lab		PSC & UW	SCL*
Date		15-Sep-04	15-Sep-04
Northing	m		
Easting	m		
Charge Balance	RPD		
Conductivity (Lab)	mg/L	6.5	6.0
Hardness	mg/L	1.5	
pH (Lab)	pH units	6.75	8.61
Total Dissolved Solids (Lab)	mg/L	2	
Total Ammonia-Nitrogen	mg/L	0.03	
Bicarbonate (Lab)	mg/L	0	
Bromide	mg/L	<0.5	
Carbonate (Lab)	mg/L	1	
Chloride	mg/L	<0.5	
Fluoride	mg/L	<0.1	
Hydroxide	mg/L		
Nitrate-Nitrogen	mg/L	<0.2	
Nitrite-Nitrogen	mg/L	<0.2	
Ortho Phosphate	mg/L	<1	
Phosphorous	mg/L	<0.05	BDL
Total Sulphur	mg/L		BDL
Sulphate	mg/L	<0.5	
Aluminum	mg/L	<0.005	BDL
Antimony	mg/L	<0.0005	BDL
Arsenic	mg/L	<0.002	
Barium	mg/L	<0.005	BDL
Beryllium	mg/L	<0.001	
Bismuth	mg/L	<0.001	
Boron	mg/L	<0.005	BDL
Cadmium	mg/L	<0.0001	BDL
Calcium	mg/L	<0.5	0.164
Chromium	mg/L	<0.005	BDL
Cobalt	mg/L	<0.0001	BDL
Copper	mg/L	0.0036	BDL
Iron	mg/L	<0.03	BDL
Lead	mg/L	<0.0005	BDL
Lithium	mg/L		BDL
Magnesium	mg/L	<0.05	0.017
Manganese	mg/L	<0.005	BDL
Molybdenum	mg/L	<0.001	BDL
Nickle	mg/L	<0.001	BDL
Potassium	mg/L	<0.1	0.1
Selenium	mg/L	<0.002	BDL
Silicon	mg/L	<0.05	BDL
Silver	mg/L	<0.0001	
Sodium	mg/L	<0.1	1
Strontium	mg/L	<0.001	0.031
Tin	mg/L	<0.001	BDL
Titanium	mg/L	<0.005	BDL
Thallium	mg/L		
Uranium	mg/L		
Vanadium	mg/L	<0.0005	BDL
Zinc	mg/L	<0.005	0.027
Zirconium	mg/L		BDL

PSC - Phillip Analytical Services

SCL - Syncrude Canada Ltd. Research Laboratory

UW - University of Waterloo Organic Geochemistry Lab

ETL - Envirotest Labs

*SCL - Note samples for nutrients and metals analyzed by SCL were not preserved

Sample ID	Unit	Blank	Blank
Lab		PSC & UW	SCL*
Date		15-Sep-04	15-Sep-04
Northing	m		
Easting	m		
Total Well Depth	mBTOC		
Casing Elevation	mASL		
Dissolved Organic Carbon	mg/L	0.3	
Methane	ug/L	0.1	
Total Naphthenic Acids	mg/L	<0.5	
benzene	ug/L		
toluene	ug/L		
ethylbenzene	ug/L		
p+m-xylene	ug/L		
o-xylene	ug/L		
1,3,5-trimethylbenzene	ug/L		
1,2,4-trimethylbenzene	ug/L		
1,2,3-trimethylbenzene	ug/L		
naphthalene	ug/L		
indole+2-methyl naphthalene	ug/L		
1-methyl naphthalene	ug/L		
biphenyl	ug/L		
acenaphthylene	ug/L		
acenaphthene	ug/L		
dibenzofuran	ug/L		
fluorene	ug/L		
phenanthrene	ug/L		
anthracene	ug/L		
carbazole	ug/L		
fluoranthene	ug/L		
pyrene	ug/L		
B(A)anthracene	ug/L		
chrysene	ug/L		
B(b+k)fluoranthene	ug/L		
B(a)pyrene	ug/L		
indeno(1,2,3,c,d)pyrene+dibenzo(a,h)anthracene	ug/L		
benzo(g,h,i)perylene	ug/L		

PSC - Phillip Analytical Services

SCL - Syncrude Canada Ltd. Research Laboratory

UW - University of Waterloo Organic Geochemistry Lab

ETL - Envirotest Labs

*SCL - Note samples for nutrients and metals analyzed by SCL were not preserved

Sample ID	Unit	Blank	Blank
Lab		UW	ETL & UW
Date		24-Oct-04	24-Jun-05
Northing	m		
Easting	m		
Charge Balance	RPD		37.8
Conductivity (Lab)	mg/L		0.9
Hardness	mg/L		<1
pH (Lab)	pH units		6.2
Total Dissolved Solids (Lab)	mg/L		<1
Total Ammonia-Nitrogen	mg/L		<0.05
Bicarbonate (Lab)	mg/L		<5
Bromide	mg/L		
Carbonate (Lab)	mg/L		<5
Chloride	mg/L		<1
Fluoride	mg/L		
Hydroxide	mg/L		<5
Nitrate-Nitrogen	mg/L		<0.1
Nitrite-Nitrogen	mg/L		<0.05
Ortho Phosphate	mg/L		
Phosphorous	mg/L		
Total Sulphur	mg/L		
Sulphate	mg/L		<0.5
Aluminum	mg/L		<0.01
Antimony	mg/L		0.0005
Arsenic	mg/L		<0.0004
Barium	mg/L		<0.0001
Beryllium	mg/L		<0.0005
Bismuth	mg/L		0.00022
Boron	mg/L		<0.002
Cadmium	mg/L		<0.0001
Calcium	mg/L		<0.5
Chromium	mg/L		<0.0004
Cobalt	mg/L		<0.0001
Copper	mg/L		<0.0006
Iron	mg/L		<0.005
Lead	mg/L		<0.0001
Lithium	mg/L		
Magnesium	mg/L		0.02
Manganese	mg/L		<0.001
Molybdenum	mg/L		<0.0001
Nickle	mg/L		0.0002
Potassium	mg/L		<0.1
Selenium	mg/L		<0.0004
Silicon	mg/L		
Silver	mg/L		<0.0002
Sodium	mg/L		<0.5
Strontium	mg/L		<0.0001
Tin	mg/L		<0.0002
Titanium	mg/L		<0.0003
Thallium	mg/L		<0.00005
Uranium	mg/L		<0.0001
Vanadium	mg/L		<0.0001
Zinc	mg/L		<0.002
Zirconium	mg/L		

PSC - Phillip Analytical Services

SCL - Syncrude Canada Ltd. Research Laboratory

UW - University of Waterloo Organic Geochemistry Lab

ETL - Envirotest Labs

*SCL - Note samples for nutrients and metals analyzed by SCL were not preserved

Sample ID	Unit	Blank	Blank
Lab		UW	ETL & UW
Date		24-Oct-04	24-Jun-05
Northing	m		
Easting	m		
Total Well Depth	mBTOC		
Casing Elevation	mASL		
Dissolved Organic Carbon	mg/L		
Methane	ug/L		
Total Naphthenic Acids	mg/L		<1.0
benzene	ug/L	ND	ND
toluene	ug/L	4.15	ND
ethylbenzene	ug/L	ND	ND
p+m-xylene	ug/L	1.73	ND
o-xylene	ug/L	ND	ND
1,3,5-trimethylbenzene	ug/L	ND	ND
1,2,4-trimethylbenzene	ug/L	ND	ND
1,2,3-trimethylbenzene	ug/L	ND	ND
naphthalene	ug/L	ND	ND
indole+2-methyl naphthalene	ug/L	ND	ND
1-methyl naphthalene	ug/L	ND	ND
biphenyl	ug/L	ND	0.87
acenaphthylene	ug/L	ND	ND
acenaphthene	ug/L	ND	ND
dibenzofuran	ug/L	ND	ND
fluorene	ug/L	ND	ND
phenanthrene	ug/L	ND	ND
anthracene	ug/L	ND	ND
carbazole	ug/L	ND	ND
fluoranthene	ug/L	ND	ND
pyrene	ug/L	ND	ND
B(A)anthracene	ug/L	ND	ND
chrysene	ug/L	ND	ND
B(b+k)fluoranthene	ug/L	ND	ND
B(a)pyrene	ug/L	ND	ND
indeno(1,2,3,c,d)pyrene+dibenzo(a,h)anthracene	ug/L	ND	ND
benzo(g,h,i)perylene	ug/L	ND	ND

PSC - Phillip Analytical Services

SCL - Syncrude Canada Ltd. Research Laboratory

UW - University of Waterloo Organic Geochemistry Lab

ETL - Envirotest Labs

*SCL - Note samples for nutrients and metals analyzed by SCL were not preserved

Sample	Result (18O)	Repeat (18O)
04-01A	-13.71	
04-01B	-14.01	
04-02A	-19.53	-19.24
04-02B	-13.87	
04-02C	-13.73	
04-03A	-21.11	-21.38
04-03C	-15.11	
04-04A	-17.10	
04-04B	-14.06	
04-04C	-14.98	
04-05A	-19.55	
04-05B	-19.19	-19.20
04-05C	-18.61	
04-06B	-16.81	
04-08	-13.63	
04-09	-15.26	
Ditch	-15.30	

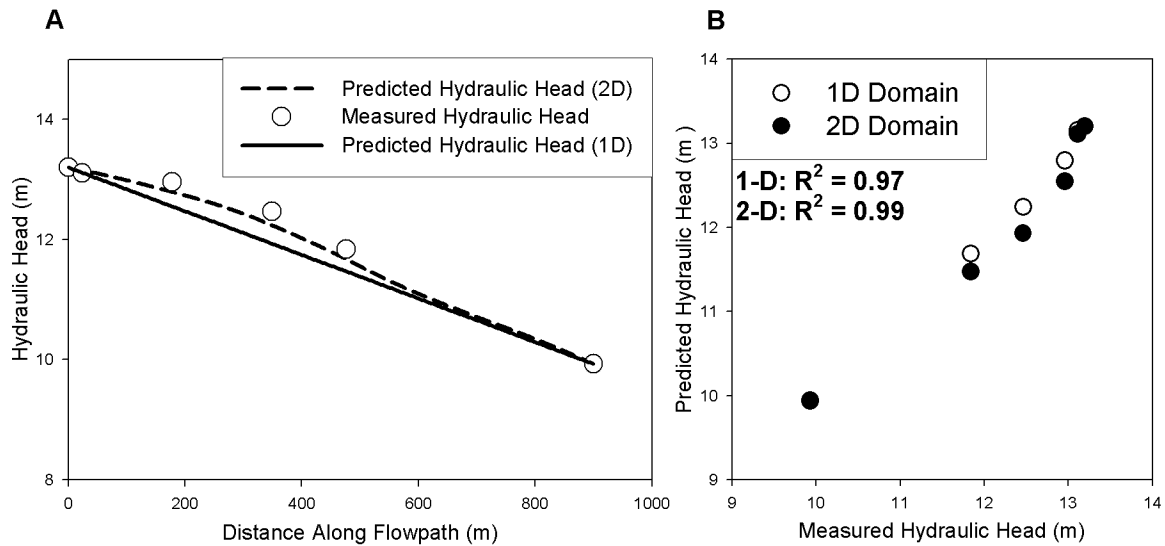
18O Analysis by University of Waterloo Environmental Isotope Laboratory
Samples collected by Author during June 2005

Appendix E
Evaluation of Physical Parameters of Reactive Transport Simulations

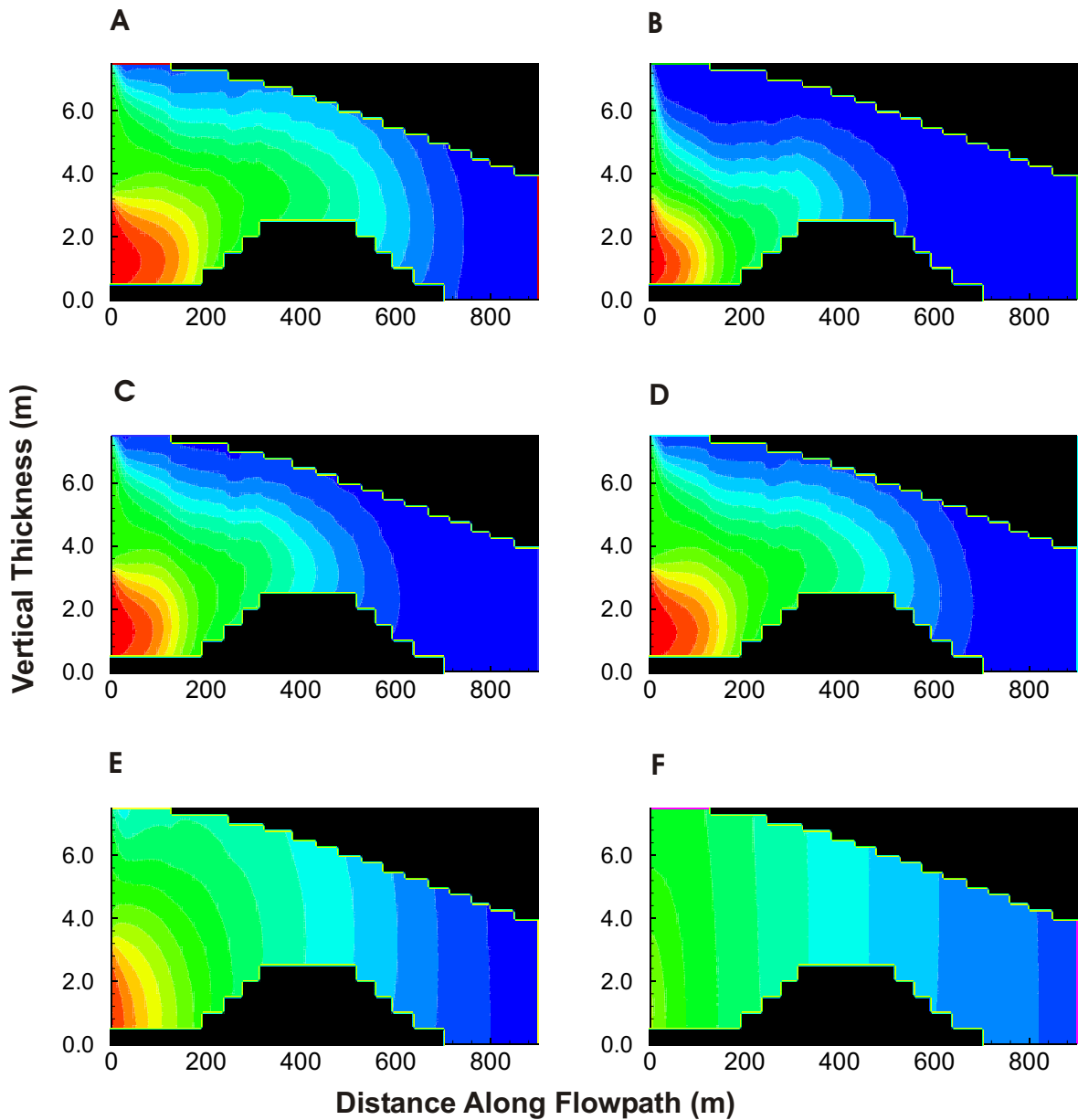
Predicted versus Measured Hydraulic Head

A comparison of hydraulic head (head) predicted using the 1D and 2D simulations to measured heads is shown in Figure 5-10a,b. Within the 2D domain, predicted heads were collected in horizontal transects along the top and bottom of the domain. However, similar to that observed in the field data (Section 4.1), the vertical gradient across the model domain is negligible, in all cases less than 1 cm separates predicted heads at the top of the domain from those at the bottom. Therefore only the heads collected from the top of the 2D domain are reported. Field measured heads represent measurements from monitoring wells installed along the transect shown in Fig 4-1. In the case of nested monitoring wells, the measurement from the monitoring well nearest the water table was used. A slightly better match was observed using the 2D simulations, since the geometry of the aquifer could be more accurately represented (Fig 5-10b). Overall the predicted hydraulic heads closely match those recently measured in the field, however the applicability of this head distribution to earlier times is unknown since data for these periods is unavailable.

Shown also in Appendix E are the calibration exercises for dispersivities and recharge.



Plot of Predicted and Measured Hydraulic Heads Along the Transect (A) and Comparison of predicted Hydraulic Heads to Measured Hydraulic Heads with Linear Regression Coefficients (B). Predicted hydraulic heads were extracted from horizontal transect extending along the top boundary of the domain. Water level measurements were collected during November 2005 and in the case of nested monitoring wells the measurement from the monitoring well nearest the water table was used.



Calibration Exercises for Physical Parameters: Recharge and Dispersivity. Plots shown are as follows: Base Case (A), Recharge in all areas doubled (B), Recharge only doubled in forested area, i.e. recharge area 3 from Figure 5-1 (C), Recharge increased by 1.5 times in forested area (D), Dispersivities increased by 1 order of magnitude (E) and Dispersivities increased by 2 orders of magnitude (F).